

**Mycobacterial adenylyl cyclases Rv1625c and Rv0386:  
orthodox vs. unorthodox catalysis**

**Die mycobakteriellen Adenylatcyclasen Rv1625c und  
Rv0386: Orthodoxe gegenüber unorthodoxer Katalyse**

**DISSERTATION**

**der Fakultät für Chemie und Pharmazie  
der Eberhard-Karls-Universität Tübingen**

**zur Erlangung des Grades eines Doktors  
der Naturwissenschaften**

**2004**

**vorgelegt von**

**Lucila Isabel Castro Pastrana**

Tag der mündlichen Prüfung: 27. Februar 2004  
Dekan: Prof. Dr. H. Probst  
Erster Berichterstatter: Prof. Dr. J. E. Schultz  
Zweiter Berichterstatter: PD Dr. J. Linder

Der experimentelle Teil der vorliegenden Arbeit wurde zwischen März 2001 und November 2003 am Institut für Pharmazeutische Chemie der Universität Tübingen unter der Leitung von Herrn Prof. Dr. J. E. Schultz angefertigt.

Herrn Prof. Dr. J. E. Schultz danke ich für das interessante Thema, die ständige Bereitschaft zur Diskussion und die Möglichkeit, diese Arbeit unter hervorragenden Arbeitsbedingungen in seiner Gruppe anzufertigen.

Herrn PD Dr. J. Linder danke ich für die Übernahme des Zweitgutachten und die kompetente Rate, Hilfe und Diskussionen.

Prof. Dr. Drews, G. und Prof. Dr. Heide, L. danke ich für die Übernahme der Nebenfachprüfungen.

Special thanks to the National Council for Science and Technology of México (CONACYT) for providing me the Ph.D. scholarship.

Der Deutscher Akademischer Austauschdienst (DAAD) danke ich für die Unterstützung im Rahmen des Abkommens CONACYT-DAAD.

Allen Mitgliedern der Arbeitsgruppe möchte ich für die gute Arbeitsatmosphäre und fachliche Hilfsbereitschaft Dank sagen aber vor allem danke ich diejenigen die mich emotionell unterstützt haben.

# Contents

<b>1 Introduction</b>	<b>1</b>
1.1 Adenylyl cyclases: function, classification and evolution	1
1.2 Mammalian adenylyl cyclases	4
1.3 Adenylyl cyclases of <i>Mycobacterium tuberculosis</i>	6
<b>2 Materials</b>	<b>9</b>
2.1 Chemicals and materials	9
2.2 Equipment	10
2.3 Buffers and solutions	11
2.3.1 Molecular biology	11
2.3.2 Protein chemistry	12
2.4 Oligonucleotides	16
2.5 Plasmids	19
<b>3 Methods</b>	<b>21</b>
3.1 Polymerase chain reaction (PCR)	21
3.2 Isolation and purification of DNA	21
3.2.1 General	21
3.2.2 Agarose electrophoresis	22
3.2.3 Photometric determination of DNA concentration	23
3.3 Enzymatic methods	23
3.3.1 General molecular biology methods	23
3.3.2 Generation of blunt ends	23
3.3.3 5'-Phosphorylation of PCR products	23
3.3.4 5'-Dephosphorylation of plasmid vectors	24
3.3.5 Ligation of DNA fragments	24
3.4 Transformation of recombinant DNA	24
3.4.1 Competent cells of <i>E. coli</i>	24
3.4.2 Rapid transformation	24

3.4.3	Standard transformation	24
3.4.4	Glycerol stock cultures	25
<b>3.5</b>	<b>DNA Sequencing</b>	<b>25</b>
<b>3.6</b>	<b>Cloning</b>	<b>27</b>
3.6.1	Mammalian and protozoan cyclases	27
3.6.2	<i>M. tuberculosis</i> Rv1625c	27
3.6.2.1	Site-directed mutagenesis	27
3.6.2.1.1	Mutants N372A and N372T	27
3.6.2.1.2	Mutant D300S	28
3.6.3	<i>Mycobacterium tuberculosis</i> Rv0386	29
3.6.3.1	Holoenzyme	29
3.6.3.2	Adenylyl cyclase domain	33
3.6.3.3	Putative AAA-ATPase domain	33
3.6.3.4	Putative transcription factor domain	34
3.6.3.5	Putative DNA-binding domain	35
3.6.3.6	Site-directed mutagenesis	36
3.6.3.6.1	Q57K and Q57A mutants	36
3.6.3.6.2	N106D and N106A mutants	37
3.6.3.6.3	Q57K/N106D mutant	38
3.6.3.6.4	N106S mutant	39
3.6.3.7	N-terminally elongated AC domain (N-His tag)	40
3.6.3.8	N-terminally elongated AC domain (C-His tag)	40
3.6.3.9	C-terminally His-tagged AC domain of Rv0386	40
3.6.3.10	AC domain mutant R7G	40
<b>3.7</b>	<b>Protein chemistry methods</b>	<b>41</b>
3.7.1	Expression of proteins in <i>E. coli</i>	41
3.7.1.1	Pre-cultures	41
3.7.1.2	Expression	41
3.7.2	Purification of soluble proteins from <i>E. coli</i>	42
3.7.3	Purification of insoluble proteins from <i>E. coli</i>	42
3.7.4	Protein concentration	43
3.7.4.1	Bio-Rad protein determination	43

3.7.4.2	Dialysis	43
3.7.4.3	Sample concentration	43
3.7.5	SDS-polyacrylamide gel electrophoresis (SDS-PAGE)	43
3.7.6	Anion exchange chromatography	45
3.7.7	Cyclase enzyme tests	45
3.7.7.1	Adenylyl cyclase test	46
3.7.7.2	Guanylyl cyclase test	47
3.7.8	Production of specific antibodies	47
3.7.8.1	Dot Blot	47
3.7.8.2	Western Blot	47
3.7.9	Crystallization	48
<b>4</b>	<b>Results</b>	<b>51</b>
<b>4.1</b>	<b>Chimeras of <i>M. tuberculosis</i> Rv1625c mutants with mammalian adenylyl and <i>Paramecium</i> guanylyl cyclases</b>	<b>51</b>
4.1.1	Introductory remarks	51
4.1.2	Expression and purification of mammalian, mycobacterial and <i>Paramecium</i> adenylyl cyclases	55
4.1.3	Mammalian/ <i>Mycobacterium</i> chimeras	57
4.1.4	<i>Paramecium</i> / <i>Mycobacterium</i> chimeras	58
4.1.4.1	Characterization of the chimera ParaGC-C2/D300A	59
4.1.5	<i>Mycobacterium</i> / <i>Mycobacterium</i> chimeras	61
4.1.5.1	Titration of N372A, N372T and R376A with D300A or D300S	62
<b>4.2</b>	<b>Expression and characterization of <i>M. tuberculosis</i> Rv0386</b>	<b>65</b>
4.2.1	Sequence features of Rv0386	65
4.2.2	Expression and characterization of the Rv0386 adenylyl cyclase domain	66
4.2.2.1	Expression and purification of the AC domain	66
4.2.2.2	Characterization of the AC activity	67
4.2.2.3	Characterization of the GC activity	76
4.2.2.4	Sensitivity of the antibodies anti-KD0386	80
4.2.2.5	Multimerization of the AC domain	81

4.2.2.6 Determination of cross-reactivity between anti-KD0386 and other ACs of <i>M. tuberculosis</i>	81
4.2.2.7 Expression, purification and characterization of the mutants Q57K, Q57A, N106D, N106A and Q57K/N106D	83
4.2.2.8 Expression and characterization of the mutant N106S	92
4.2.2.9 Expression and characterization of an N-terminally elongated AC domain	96
4.2.2.10 Expression and characterization of the C-terminally His-tagged Rv0386 AC domain	99
4.2.2.11 Expression and AC assay of the mutant R7G	103
4.2.2.12 Crystallization of the AC domain	103
4.2.3 Expression of the Rv0386 holoenzyme	105
4.2.3.1 Expression in BL21 (DE3) [pREP4] cells	105
4.2.3.2 Attempts of solubilization of the holoenzyme	108
4.2.3.3 Expression in BL21 STAR and ROSETTA cells	111
4.2.3.4 Anion exchange chromatography of the holoenzyme	115
4.2.3.6 Determination of Rv0386 orthologs in <i>M. bovis</i> BCG and <i>M. smegmatis</i>	116
4.2.4 Expression of the putative ATPase domain of Rv0386	117
4.2.5 Expression of the putative transcription factor domain of Rv0386	118
4.2.6 Expression of the putative DNA-binding domain of Rv0386	120
4.2.6.1 Sensitivity and specificity of the antibodies anti-DB0386	120
<b>5 Discussion</b>	<b>123</b>
<b>5.1 Chimeras of mycobacterial Rv1625c mutants with soluble mammalian         and <i>Paramecium</i> cyclases</b>	<b>123</b>
<b>5.2 Adenylyl cyclase catalytic domain of Rv0386</b>	<b>125</b>
<b>5.3 Holoenzyme Rv0386</b>	<b>130</b>
<b>5.4 Remaining questions</b>	<b>132</b>

<b>6 Summary</b>	<b>133</b>
<b>7 Zusammenfassung</b>	<b>134</b>
<b>8 Appendix</b>	<b>135</b>
<b>8.1 DNA and protein sequences of Rv0386</b>	<b>135</b>
<b>8.2 Results of the Protein-Protein BLAST Search</b>	<b>137</b>
8.2.1 Blastp of the full length Rv0386	138
8.2.2 Blastp of the adenylyl cyclase domain	138
8.2.3 Blastp of the ATPase domain	138
8.2.4 Blastp of the transcription factor domain	138
8.2.5 Blastp of the DNA-binding domain	138
<b>8.3 Sequence alignments of Rv0386</b>	<b>139</b>
<b>8.4 Crystal pictures</b>	<b>142</b>
8.4.1 Crystals of the AC domain of Rv0386 with N-terminal His-tag	142
8.4.2 Crystals of the AC domain of Rv0386 with C-terminal His-tag	143
<b>9 References</b>	<b>145</b>



## List of abbreviations

AC (s)	Adenylyl cyclase (s)
BSA	Bovine serum albumine
CHAPS	3-(3-Cholamidopropyl)- dimethylammonio-1- propane sulfonate
cpm	Counts per minute
dNTPs	Desoxynucleoside triphosphates
DTT	Dithiotreitol
FPLC	Fast performance liquid chromatography
GC (s)	Guanylyl cyclase (s)
HEPES	N-2-Hydroxyethyl piperazine-N'-2-ethanesulphonic acid
IPTG	Isopropyl thiogalactoside
LB-broth	Luria-Bertani bacterial growth medium
MCS	Multiple cloning site
MWCO	Molecular weight cut-off
Ni-NTA	Nickel-nitrilotriacetic acid-agarose
O/N	Overnight
PEG	Polyethylen glycol
PMSF	Phenylmethansulfonylchlorid
PVDF	Polyvinylidene difluoride
RT	Room temperature
TEMED	N,N,N',N'-Tetramethylethylene diamine
TLCK	N <sub>α</sub> -Tosyl-L-lysin-chlormethylketon-hydrochlorid
TPCK	Tosyl-L-phenylalanin-chlormethylketon
X-Gal	5-bromo-4-chloro-3-indolyl-β-D-galactoside

For amino acid residues the one-letter code was used.

# 1 Introduction

## 1.1 Adenylyl cyclases: function, classification and evolution

Adenylyl cyclases are responsible for the synthesis of cAMP (adenosine 3',5'-cyclic monophosphate) from adenosine triphosphate (ATP). Although they represent low abundance proteins in the cell, they produce a universal signalling molecule which mediates with high amplification diverse physiological processes in organisms as phylogenetically diverse as *Escherichia coli* and *Homo sapiens*. Transcription in bacteria and development in fungi and parasites are cAMP-regulated. In eukaryotes cellular functions like energy homeostasis, reproduction, brain function and cell differentiation are influenced by cAMP too. Cyclic AMP functions as a second messenger to relay extracellular signals to intracellular effectors such as protein kinase A. Regulation of intracellular concentrations of cyclic AMP are controlled primarily through modulation of AC activity and phosphodiesterases. The family of eukaryotic ACs consists of several membrane bound ACs and a single soluble AC with orthologs of the latter in rat, *Dictyostelium* and bacteria but absent from the genomes of *D. melanogaster*, *C. elegans*, *A. thaliana* and *S. cerevisiae* (Roelofs and Van Haastert, 2002).

Cyclases (ACs and GCs) have been classified according to their amino acid sequence similarities rather than their substrate specificities. The class I type comprises ACs which produce cAMP as a consequence of its phosphorylation and are found in *E. coli*, *Salmonella*, *Pasteurella*, *Haemophilus* and *Vibrio* as single copy genes (Danchin, 1993). The second class of ACs comprises those which are calmodulin-activated, secreted toxins like the enzymes produced by the pathogenic organisms *Bordetella pertussis* (Ladant and Ullman, 1999) and *Bacillus anthracis* (Baillie and Read, 2001). [For class III ACs see below]

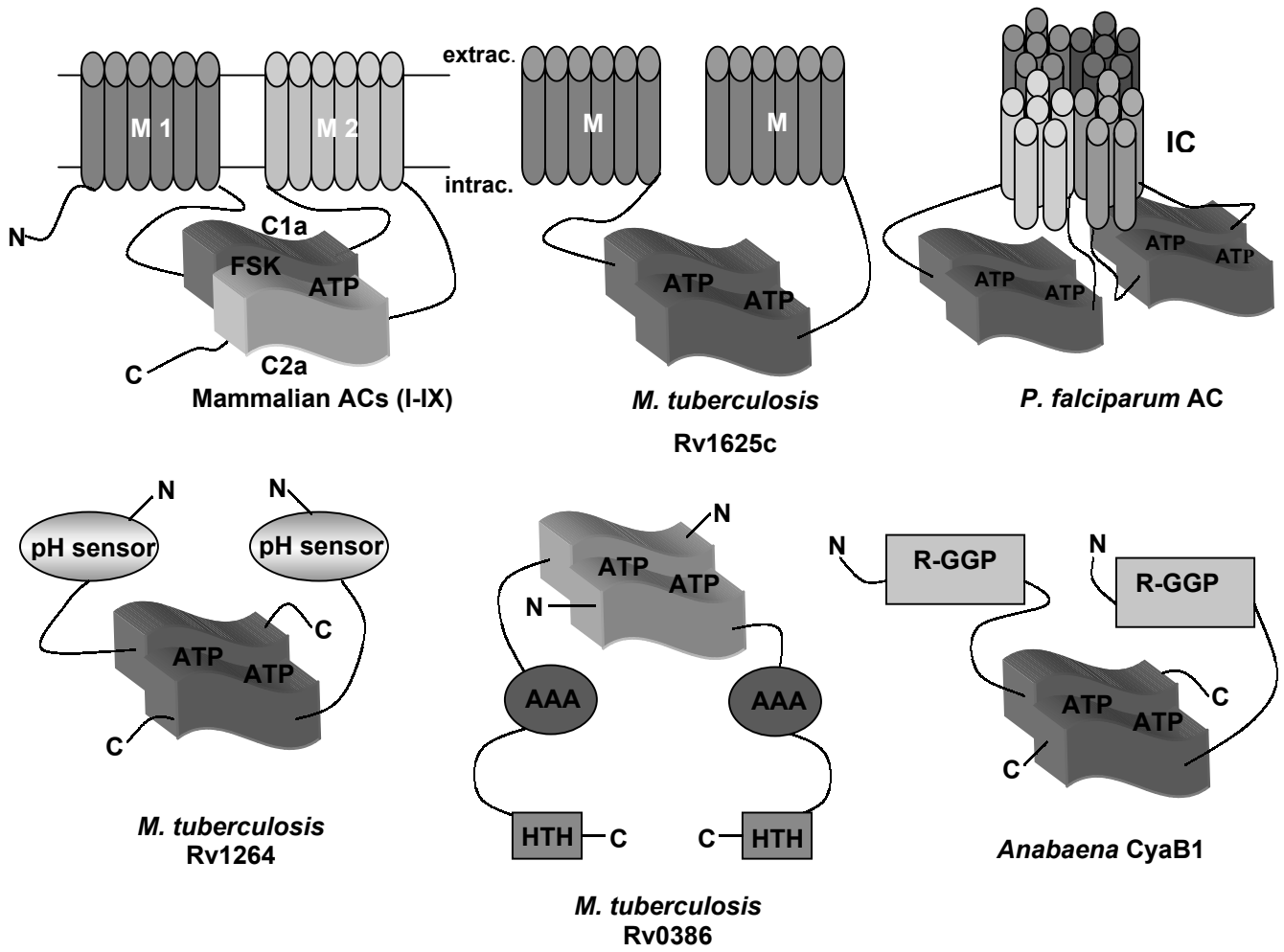
The fourth and fifth classes of ACs may be represented by cyclases with thermostable properties from *Aeromonas hydrophila* and from the ruminal anaerobe *Prevotella ruminicola*, respectively (Danchin, 1993).

The class III of nucleotide cyclases truly represents a conserved cyclase catalytic fold which are found in prokaryotes and in eukaryotes (Danchin, 1993). Recently, after analysis of amino acid sequence profiles, a division of the class III in to four subclasses,

class IIIa to III d was suggested. This subclassification is partly based on length differences of an “arm” region. This region was thought to be essential for dimerization (Tesmer et al., 1997) and comprises the sequence between a conserved glycine and the downstream adenine-specifying residue (D1018 in AC type II from rat) (Linder and Schultz, 2003). The arm region contains 14 residues in subclass a (mammalian ACs, mycobacterial Rv1625c), 15 residues in subclass b in conjunction with a highly characteristic D to T/S switch in a substrate defining position (*Anabaena* cya B1, mammalian soluble AC), 7 to 11 amino acids in subclass c (mycobacterial Rv1264, Rv0386, *Streptomyces coelicolor* AC acc. num. P40135) and 13-14 residues in subclass d (*U. maydis* AC acc. num. A55481, *L. donovani* cyaA acc. num. Q27675) in which also a special motif surrounding the substrate-defining lysine is highly conserved (Linder and Schultz, 2003). From an analysis based on the available genome sequence from over 80 bacteria and other pathogenic organisms, it is becoming clear that the majority of cells have at least one cyclase belonging to class III cyclases and that the other classes of cyclases are more restricted in their occurrence. That demonstrates the versatility of the class III catalytic domain which apparently can be incorporated as a distinct functional domain into a larger polypeptide in conjunction with other protein domains with diverse physiological functions. Furthermore, it appears that the same class III fold can adapt to utilize ATP or GTP as a substrate, given the sequence similarity between mammalian ACs and GCs (Shenoy et al., 2002). From recent phylogenetic studies it has been concluded that within the family of ACs, soluble ACs were poorly conserved during evolution, whereas membrane-bound ACs have expanded to form the subgroups of prevailing ACs and GCs (Roelofs and Van Haastert, 2002).

Most class III cyclases, from bacteria to higher vertebrates, are constructed in a modular fashion as evident from their rather large size. The variability in the block-building of cyclases makes possible a fine regulation of their activity (Linder and Schultz, 2003) [see figure 1.1].

## Adenylyl cyclases



## Guanylyl cyclases

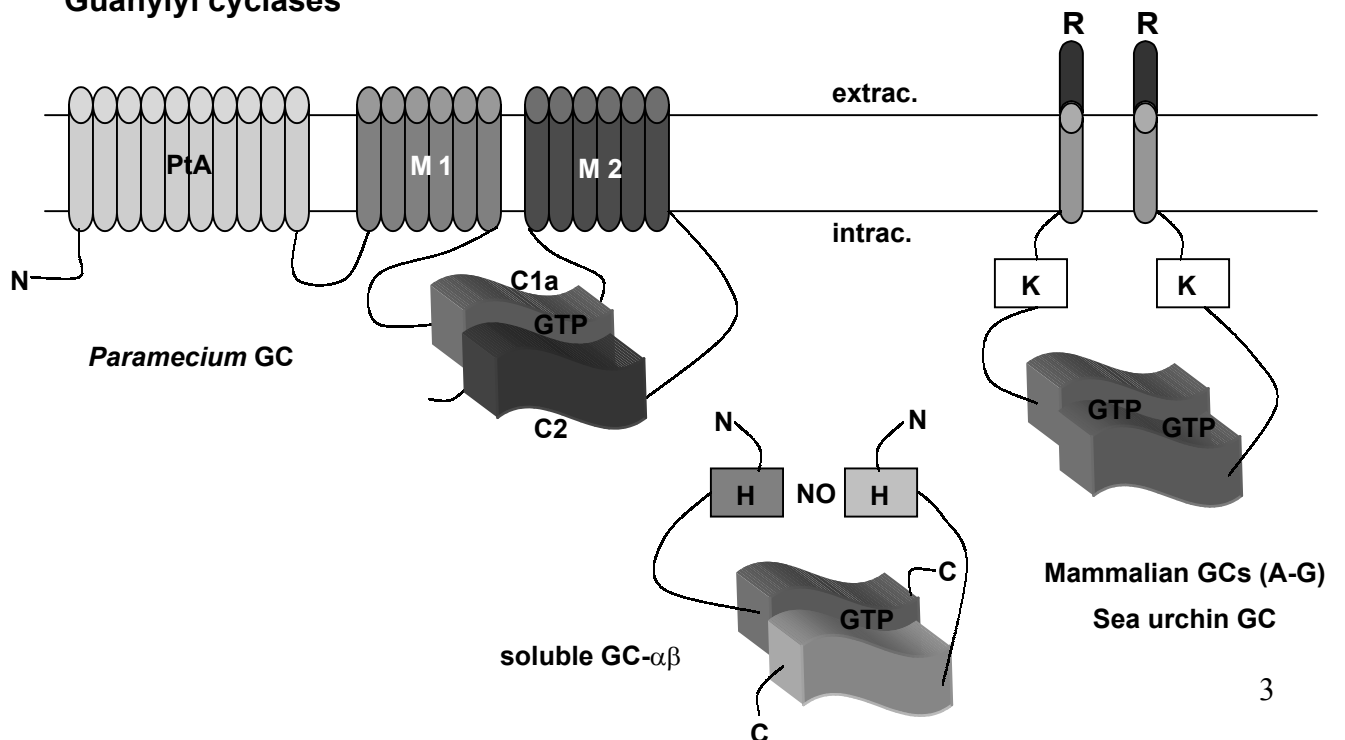


**Fig. 1.1:** Adenylyl and guanylyl cyclases (catalytic domain class III) are modular proteins. Drawn are the mammalian AC model (Tang and Hurley, 1998), the predicted topology for *M. tuberculosis* AC Rv1625c (Guo et al., 2001), Rv1264 (Linder et al., 2002), Rv0386, *Plasmodium falciparum* AC (Weber, 2003) and *Anabaena* CyaB1 (Kanacher, 2003). Predicted topology is also shown for mammalian GC's (isoforms A to G), soluble GC, sea urchin GC and for *Paramecium* GC (Linder et al., 2000). FSK=forskolin; IC=ion channel; AAA=AAA-ATPase; HTH=helix-turn-helix; R-GGP=regulator GAFA-GAFB-PAS; PtA=P-type ATPase; H=heme; NO=nitric oxide; R=receptor; K=kinase. The formation of homodimers is represented through identical colored catalytic domains, heterodimers show catalytic domains with different color intensity.

Evolutionarily, it has been shown that the 'palm' domain of the prokaryotic DNA polymerases I shares a common fold with the class III AC catalytic core, obviously both enzymes catalyse a phosphoryl transfer by a similar two-metal-ion mechanism suggesting a common ancestor. (Artymiuk et al., 1997; Tesmer et al., 1999). Interestingly, the catalytic domain of the  $\gamma$ -proteobacterial ACs (typified by *E. coli* CyaA) has similarity to the polymerase  $\beta$ -type nucleotidyl transferase superfamily, too. That emphasizes the general trend that cyclase signal transduction components evolved from enzymes involved in nucleotide processing (Aravind and Koonin, 1999).

In this work, an AC of *Mycobacterium tuberculosis* (Rv0386) with an N-terminal AC domain (class IIIc) and an attached C-terminal transcription factor domain is presented. Because here basically the AC function was studied, the meaning of combining a signal-transducing enzyme with a component of the basic nucleic acid processing is still an open question, the answer of which could be very useful for understanding evolution and maybe new regulatory mechanisms of ACs.

## 1.2 Mammalian adenylyl cyclases

Cyclic AMP is produced in mammals by nine isoforms of membrane-bound ACs and one soluble AC. The nine cloned ACs have a similar structure, with two hydrophobic domains comprising six predicted transmembrane helices each, and two cytoplasmic domains (Fig. 1.1). The cytosolic domains are similar to each other (roughly 30% identity), to the sequences within both bacterial and yeast ACs and even to those within GCs. Both together are responsible for catalytic activity (Taussig and Gilman, 1995; Sunahara et al., 1996). The nine isoforms share several regulatory features like activation by the  $\alpha$  subunit of the heterotrimeric G protein Gs, activation by the diterpene

forskolin (with exception of type IX) and inhibition by a class of adenosine analogs known as P-site inhibitors. Individual forms can also be regulated by other G protein subunits, Ca<sup>2+</sup>-calmodulin, Ca<sup>2+</sup> or phosphorylation (Sunahara et al., 1996; Tesmer et al., 1997).

The cytosolic domains are called C1 and C2 and are subdivided into C1a, C1b, and C2a, C2b respectively, where C1a and C2a contain all of the catalytic apparatus. These C1a and C2a domains heterodimerize with each other in solution but can also form homodimers or even chimeric heterodimers if derived from different isoforms (Tang and Gilman, 1995; Yan et al., 1996; Whisnant et al., 1996). The structure of the type II AC C2 region revealed a wreathlike dimer arrangement which is likely to exist in other enzymes including many similar ACs and GCs. In this arrangement the interface of C1a and C2a domains accommodate the catalytic site and the forskolin regulatory site. Recombinant C1 and C2 domains are capable of carrying out catalysis when they are mixed and activated by forskolin (Zhang et al., 1997; Tang and Hurley, 1998). The two metal ions required for catalysis bind to specific residues found in the C1 region, the nucleotide binding pocket and other catalytic residues are contributed primarily by the C2 region. Similarly, forskolin binds to a site on the C1-C2 heterodimer through hydrophobic interactions with residues of both, C1 and C2 domains contributing (Dessauer et al., 1997; Tesmer et al., 1997; Zhang et al., 1997).

From crystallographic and mutational studies those amino acid residues were determined which participate in catalysis in mammalian ACs (Tesmer et al., 1997, 1999; Zhang et al., 1997). For definition of substrate specificity all important amino acids are contributed from the C2 region, they are D1018 (AC type II from rat) which recognizes the exocyclic amine and K938 which recognizes the unprotonated N<sub>1</sub> of adenine. Both residues are capable to discriminate against O<sup>6</sup> and N<sup>2</sup>, and the protonated N<sub>1</sub> of guanine (Tesmer et al., 1997; Sunahara et al., 1998). The amino acids responsible for metal coordination are D396 and D440 (in canine AC type V). One Mg<sup>2+</sup> ion binds together with ATP, while the second one acts kinetically as a free ion (Tesmer et al., 1997). Residues N1025 and R1029 (in rat AC type II) stabilize the transition state by stabilizing the negative charge on the pyrophosphate leaving group (Yan et al., 1997; Hurley, 1998). For binding forskolin, amino acids T410 and S942 (in rat AC type II) are implicated (Tesmer et al., 1997).

In the present work, the possibility of formation of active heterodimeric chimeras between mammalian C1 or C2 monomers and inactive mutated monomers from *M. tuberculosis* (Rv1625c, catalytic domain) was studied. The possibility of creating a non-existing forskolin-binding site by mutation of the mycobacterial catalytic domain was examined. Chimeras between mammalian and *Paramecium* GC monomers, as well as between mycobacterial AC and *Paramecium* GC monomers were also studied.

Table 1.1 shows the amino acid residues that are essential for catalysis classified according to the catalytic function they realize. The mammalian AC amino acid positions are compared with respect to their equivalent positions in Rv1625c and Rv0386 of *M. tuberculosis*, as well as in *Paramecium* GC.

	Purine binding		Metal binding		Transition-state stabilization		Forskolin binding	
Mammalian AC	<b>K938</b> ACII C2 rat	<b>D1018</b> ACII C2 rat	<b>D396</b> ACV C1dog	<b>D440</b> ACV C1dog	<b>N1025</b> ACII C2 rat	<b>R1029</b> ACII C2 rat	<b>T410</b> ACII C1 rat	<b>S942</b> ACII C2 rat
<i>M. tuberculosis</i> Rv1625c	<b>K296</b>	<b>D365</b>	<b>D256</b>	<b>D300</b>	<b>N372</b>	<b>R376</b>	<i>N372</i>	<i>D300</i>
<i>M. tuberculosis</i> Rv0386	<b>Q57</b>	<b>N106</b>	<b>D16</b>	<b>D61</b>	<b>N113</b>	<b>R117</b>	<i>N113</i>	<i>D61</i>
<i>Paramecium</i> GC	<b>E1681</b> (C1)	<b>S1748</b> (C1)	<b>D2233</b> (C2)	<b>D2277</b> (C2)	<b>N1755</b> (C1)	<b>R1759</b> (C1)	<b>L2356</b> (C2)	<b>K1685</b> (C1)

**Table 1.1:** Summary of the canonical amino acid residues responsible for catalysis in mammalian ACs (Tesmer et al., 1997, 1999; Zhang et al., 1997) in comparison with their equivalent residues in Rv1625c (Guo et al., 2001) and Rv0386 (present work) of *M. tuberculosis* and with *Paramecium* GC (Linder et al., 2000). Residues of the mycobacterial and *Paramecium* cyclases which are positional but not functional equivalent to those of mammalian ACs are in italics.

### 1.3 Adenylyl cyclases of *Mycobacterium tuberculosis*

The complete sequence of *Mycobacterium tuberculosis* H37Rv was published in 1998 with the annotation of only five genes (Rv1625c, Rv1318c, Rv1319c, Rv1320c and Rv1264) as putative ACs (Cole et al., 1998). Later on, using computational methods 15 putative ACs were detected (McCue et al., 2000). *M. tuberculosis* encodes several more

putative nucleotide cyclases than other prokaryotic species with the presence of predicted cytoplasmic (9), receptor-type membrane bound (1) and integral membrane (5) cyclases. Two of them (Rv1625c and Rv2435c) are classified as class a ACs together with the mammalian ACs (Cole et al., 1998; McCue et al., 2000).

To date, nine gene products of *M. tuberculosis*, Rv1625c and Rv1264 (Guo et al., 2001; Reddy et al., 2001; Linder et al., 2002), Rv0386 (present work), Rv1318c, Rv1319c, Rv1320c, Rv3645, Rv2212 and Rv1900c (Hammer, Zeibig, Motaal, Wetterer; unpublished) have been shown to possess AC activity.

The gene Rv1625c encodes a six-transmembrane-helices membrane-anchored AC with a single C-terminal catalytic domain, representing exactly one-half of a mammalian AC (Tang and Hurley, 1998). Certainly, by alignment of the mycobacterial catalytic domain with C1 from canine type V and C2 from rat type II ACs, considerable sequence identities were found. The most important is the conservation of each of the amino acids that have been identified crystallographically as participating in catalysis. A soluble enzymatically active catalytic domain from Rv1625c was constructed, expressed in *E. coli* and characterized. The dimerization was substantiated with construction of linked monomers. Mutations of the amino acid residues indispensable for catalysis by the mammalian heterodimers inactivated the mycobacterial cyclase. Finally, it was possible to reconstitute productive heterodimers from inactive mutant monomers. These molecular and biochemical properties of Rv1625c made it likely that this cyclase is an evolutionary precursor of the mammalian AC family (Guo et al., 2001).

The gene product Rv1264, predicted to be composed of a C-terminal AC catalytic domain and a novel N-terminal protein domain, could also be expressed in *E. coli* (Linder et al., 2002). Rv1264 has the same modular composition as ACs from *Streptomyces* and *Brevibacterium liquefaciens* (Peters et al., 1991; Danchin et al., 1993). The catalytic domain expressed alone displayed high AC activity, homodimerization was demonstrated and the catalysis depended on the same amino acids previously identified as critical in mammalian ACs. Because of the notably lower AC activity of the holoenzyme, an autoinhibitory function of the N-terminal domain was suggested (Linder et al., 2002).

Until today, several anti-mycobacterial agents interfering with the synthesis and assembly of components of the mycobacterial cell wall have controlled a lot of infection



cases. But the control of global tuberculosis has so far failed and the number of multidrug-resistant isolates is rising. Therefore, it is required to advance our understanding of the complex biology of tuberculosis infection. The completed genome project is a major step toward this goal (Young, 2001).

From the genome sequence it is obvious that *M. tuberculosis* is equipped with a range of transcriptional regulators. These could confer a high capacity for adaptation as shown in several studies where a change in the pattern of gene expression occurred after transfer from laboratory conditions to the macrophage intracellular environment (Young, 2001). Also, the large number of putative cyclases in *M. tuberculosis* could point to the development of the ability to sense and respond to many intracellular and extracellular signals through this second messenger system (McCue et al., 2000). It is unknown if cyclase activity is necessary for pathogenesis, but it has been reported that macrophages with ingested mycobacteria increase cAMP levels which may inhibit the phagosome-lysosome fusion (Lowrie et al., 1975; McCue et al., 2000).

A recent computational study of genomic sequence comparison placed the gene Rv0386 between 19 genes in the genome of *M. tuberculosis* that may have been acquired by horizontal gene transfer from eukaryotes (Gamielidien et al., 2002), an event that could have conferred survival advantages to an ancient mycobacterium before becoming a pathogen of eukaryotes (McCue et al., 2000). On the basis of studies of the mycobacterial AC Rv1625c, in this thesis the enzyme Rv0386 was basically studied as an AC without paying much attention to its putative feature as a transcription factor. Investigation of this enzyme was of particular interest because of its deviation from the canonical amino acid residues participating in catalysis, specifically those involved in the definition of substrate specificity. The possibility of an AC catalysis by a novel mechanism lead to attempts of crystallization.

## 2 Materials

### 2.1 Chemicals and materials

**Amersham Pharmacia Biotech, Freiburg:** ECL Plus Western Blot Detection System, Hyperfilm ECL, Thermo Sequenase Fluorescent Labeled Primer Cycle Sequencing Kit with 7-deaza-dGTP, Formamide, [2,8-<sup>3</sup>H]-cAMP, [8-<sup>3</sup>H]-cGMP

**AppliChem, Darmstadt:** HEPES, Acrylamide 4K-Solution 30%

**Appligene, Heidelberg:** Taq DNA-Polymerase with 10X reaction buffer

**Bayer, Leverkusen:** Aprotinin

**BioGenes, Berlin:** Specific antibodies anti-KD0386 and anti-DB0386

**BIOLOG-Life Science Institute, Bremen:** (Rp)-ATP- $\alpha$ -S

**BIO-RAD, München:** BIO-RAD Protein-Assay Dye Reagent Concentrate

**Biozym Diagnostik, Hess. Oldendorf:** Sequagel XR, Sequagel Complete Buffer Reagent, Chill-Out 14 Liquid Wax von MJ Research

**Canberra PACKARD, Taunusstein:** Ultima Gold XR LSC Cocktail

**Dianova, Hamburg:** Goat anti-mouse antibodies horseradish peroxidase conjugated, Goat anti-rabbit antibodies horseradish peroxidase conjugated

**Fluka, Basel:** Trypsin inhibitor from lima beans, TLCK, TPCK, SDS, PMSF, PEG 5000 monomethyl ether, PEG 6000, Nonidet P 40

**Hampton Research, CA (USA):** Reagent Kits Crystal Screen, Crystal Screen 2 and Crystal Screen Lite for the crystallization screen for proteins and other molecules, PEG 400, PEG 3350, PEG 8000

**Hartmann Analytik, Braunschweig:** [ $\alpha$ -<sup>32</sup>P]-ATP and [ $\alpha$ -<sup>32</sup>P]-GTP

**ICN Biomedicals, Eschwege:** [ $\alpha$ -<sup>32</sup>P]-ATP

**Macherey-Nagel, Düren:** Nucleotrap

**Merck, Darmstadt:** Imidazole, Glycin, sodium citrate, potassium-sodium tartrate, sodium acetate, sodium chloride, PEG 4000

**Millipore, Bedford (USA):** Centricon YM-10 Centrifugal Filter Devices (MWCO 10000)

**MWG-Biotech, Ebersberg:** Oligonucleotides

**New England Biolabs, Schwalbach/Taunus:** Restriction Endonucleases, BSA, T4-Polynucleotide Kinase, 10X Kinase buffer

**Pall Corporation, Michigan (USA):** Nanosep 10K OMEGA centrifugal devices

**Peqlab, Erlangen:** Agarose, peqGOLD Protein Marker

**Promega, Madison (USA):** Wizard MiniPreps Plasmid Purification Kit

**Qiagen, Hilden:** Ni<sup>2+</sup>-NTA-Agarose, pQE-Expression vectors, *E. coli* M15 [pREP4],  
Purified mouse monoclonal RGS-His antibody (BSA-free)

**Roche (Boehringer), Mannheim:** Restriction endonucleases, Klenow-Polymerase, Alkaline Phosphatase, Rapid DNA Ligation Kit, dNTP's, ATP, GTP, CTP, Complete Protease Inhibitor Cocktail Tablets

**Sartorius, Göttingen:** Cellulose Acetate Filter with pore size 0.2 µm, Polycarbonate Filter Holder

**SERVA Electrophoresis, Heidelberg:** Coomassie-Brilliant-blue G250, VISKING Dialysis Tubing 8/32 and 27/32 with MWCO 12000-14000.

**Sigma, Deisenhofen:** Glycerol, MOPS, TRIS, EDTA, Xgal, IPTG, Ponceau S, Tween 20, TEMED, PMSF, BSA, ITP, UTP, αβ-CH<sub>2</sub>-ADP, Cordycepin 5'-triphosphate, 2'3' GMP, 2' GMP, 8-Br-cGMP, monobutyl cAMP, dibutyl cAMP, 2'd3'-AMP

**Spectrum Medical Instruments, Los Angeles (USA):** Spectrapor Membrane Tubing MWCO 3500

**Stratagene, Heidelberg:** Plasmid pBluescript II SK (-), *E. coli* XL1-Blue MRF'

## 2.2 Equipment

**Amersham Pharmacia Biotech, Freiburg:** ÄKTA™ FPLC with Fraction Collector Frac-950, Pump P-920, Monitor UPC-900, Valve INV-907, Mixer M-925 and Software Unicorn Version 4.00, general accessories for FPLC and Anion Exchange Column MonoQ HR 5/5.

**Biometra, Göttingen:** TRIO-Thermoblock thermocycler

**BIO-RAD, München:** Trans-Blot SD Semi Dry Transfer Cell

**Branson, Danbury, USA:** Sonifier B-12, Ultrasound Bath Bransonic B12

**Carl Zeiss, Göttingen:** Microscope Axioskop 40/40 FL with fixed Polarisator with Lambda plate and Canon PowerShot G2 high quality digital camera with 4.0 M pixel CCD sensor and 3X optical zoom.

**Eberhard-Karls-Universität, Tübingen:** Gel electrophoresis chambers

**Eppendorf, Hamburg:** Thermostat 3401, Table Centrifuges 5410 & 5414, Cooling centrifuge 5402, BioPhotometer

**Hampton Research, CA (USA):** VDX 24 well polystyrene pre-greased plates, 22 mm siliconized glass cover slides (squares)

**Heraeus, Osterode:** Megafuge 1.0 R (BS 4402/A)

**Idaho Technologies, Idaho Falls (USA):** Air Thermo Cycler 1605

**Kontron-Hermle, Gosheim:** Centrikon H401 & ZK401, Rotors A6.14 (SS34) and A8.24 (GSA)

**Macherey-Nagel, Düren:** Porablot PDVF-Blotting membrane (0.25 x 3 m)

**Millipore, Eschborn:** Water purification system MilliQ UF Plus

**MWG-Biotech, Ebersberg:** LI-COR DNA sequencer model 4000

**Sartorius, Göttingen:** Balance BP 2100 S, Analytic balance handy

**Savant, Farmingdale (USA):** Vacuum centrifuge speed vac concentrator SVC100H

**Schleicher & Schuell, Dassel:** Whatmanpaper 3MM, Protran BA 83 Cellulosenitrate 0.2  $\mu$ m (200 x 200 mm) Nucleic acid and protein transfer media

**SLM Instruments, Urbana (USA):** French Pressure Cell Press FA-078-E1, Manual Fill 20K Cell FA-073 (7.6 cm diam., 40 ml sample capacity)

**Stratagene, Austin (USA):** UV Stratalinker 2400

## 2.3 Buffers and solutions

### 2.3.1 Molecular biology

All solutions, buffers and culture media for molecular biology methods were sterilized 20 min at 120°C and 1 bar. pH was measured at room temperature.

#### Buffers for DNA

##### 10X TAE

400 mM	Tris/acetate pH 8.0
10 mM	Na <sub>2</sub> EDTA

##### 10X Klenow buffer

200 mM	Tris/HCl pH 7.5
60 mM	MgCl <sub>2</sub>
10 mM	DTT
1 mg/ml	BSA

##### TE-buffer

10 mM	Tris/HCl pH 7.5
1 mM	Na <sub>2</sub> EDTA

##### 10X TBE

1000 mM	Tris
890 mM	Boric acid
25 mM	Na <sub>2</sub> EDTA

**4X Loading sample buffer (agarose gel)**

0.05 %	Bromphenolblue
0.05 %	Xylenecyanol
50.0 %	Glycerol

**Loading sample buffer (sequencing gel)**

95 %	Formamide
20 mM	Na <sub>2</sub> EDTA
0.05 %	Bromphenolblue
0.05 %	Xylenecyanol

**10X CM buffer**

100 mM	CaCl <sub>2</sub>
100 mM	MgCl <sub>2</sub>

**10X Dephosphorylation buffer**

500 mM	Tris/HCl pH 8.5
1 mM	Na <sub>2</sub> EDTA

**Bacterial culture media****LB-broth**

1 %	Bacto Tryptone
0.5 %	Yeast extract
1 %	NaCl

**LB-agar**

1.5 %	Agar in LB-broth
-------	------------------

**LB-Amp-agar**

100 µg	Ampicilin / ml LB-agar
--------	------------------------

**2.3.2 Protein chemistry****Protein purification with Ni-NTA-agarose****Pellet wash buffer**

50 mM	Tris/HCl pH 8.0
1 mM	EDTA

**Cell Lysis buffer**

50 mM	Tris/HCl pH 8.0
10 mM	β-mercaptoethanol
50 mM	NaCl

**Wash buffer A**

50 mM	Tris/HCl pH 8.0
10 mM	β-mercaptoethanol
2 mM	MgCl <sub>2</sub>
400 mM	NaCl
5 mM	Imidazole

**Wash buffer B**

50 mM	Tris/HCl pH 8.0
10 mM	β-mercaptoethanol
2 mM	MgCl <sub>2</sub>
400 mM	NaCl
15 mM	Imidazole

Wash buffer C  
 50 mM Tris/HCl pH 8.0  
 10 mM  $\beta$ -mercaptoethanol  
 2 mM  $MgCl_2$   
 10 mM NaCl  
 15 mM Imidazole

Elution buffer  
 50 mM Tris/HCl pH 8.0  
 10 mM  $\beta$ -mercaptoethanol  
 2 mM  $MgCl_2$   
 10 mM NaCl  
 150 mM Imidazole

Glycerol dialysis buffer  
 10 mM NaCl  
 50 mM Tris/HCl pH 7.5  
 2 mM  $\beta$ -mercaptoethanol  
 20 % Glycerol

Phosphate dialysis buffer  
 50 mM  $Na_2HPO_4/NaH_2PO_4$   
 buffer (pH 7.5)  
 10 % Glycerol

Equilibration mixture for Ni-NTA-agarose  
 5 ml Cell lysis buffer  
 225 mM NaCl  
 13.5 mM Imidazole pH 8.0  
 4.5 mM  $MgCl_2$

Membrane Suspension Buffer  
 50 mM Tris/HCl pH 8.0  
 15 mM  $\beta$ -Mercaptoethanol  
 250 mM NaCl  
 20 % Glycerol  
 2 % CHAPS

High Saline Buffer  
 50 mM Tris/HCl pH 8.0  
 10 mM  $\beta$ -Mercaptoethanol  
 2 mM  $MgCl_2$   
 5 mM Imidazole pH 8.0  
 250 mM NaCl  
 20 % Glycerol  
 2 % CHAPS

Low Saline Buffer  
 50 mM Tris/HCl pH 8.0  
 10 mM  $\beta$ -Mercaptoethanol  
 2 mM  $MgCl_2$   
 15 mM Imidazole pH 8.0  
 10 mM NaCl  
 20 % Glycerol  
 2 % CHAPS

Elution Buffer with Detergent  
 50 mM Tris/HCl pH 8.0  
 10 mM  $\beta$ -Mercaptoethanol  
 2 mM  $MgCl_2$   
 300 mM Imidazole pH 8.0  
 10 mM NaCl  
 20 % Glycerol  
 2 % CHAPS

Tosyl-L-phenylalanin-chlormethylketon  
 (TPCK)  
 2.2 mg/ml in Ethanol (Stock)

$N_\alpha$ -Tosyl-L-lysin-chlormethylketon-  
 hydrochlorid (TLCK)  
 2.2 mg/ml in 1 mM HCl (Stock)

Phenylmethansulfonylchlorid (PMSF)  
2.2 mg/ml in Isopropanol (Stock)

Lima bean Trypsin Inhibitor  
3.2 mg/ml in H<sub>2</sub>O (Stock)

Aprotinin  
2.8 mg/ml in NaCl 0.9% (Stock)

### SDS-Polyacrylamide gel electrophoresis

Resolving Gel buffer  
1.5 M Tris/HCl pH 8.8  
0.4 % SDS

Stacking Gel buffer  
500 mM Tris/HCl pH 6.8  
0.4 % SDS

10X Running buffer  
250 mM Tris  
1.92 M Glycin  
1 % SDS

Staining solution  
0.2 % Coomassie Brilliant  
Blue G-250  
10 % Acetic acid  
40 % Methanol

4X Sample buffer  
130 mM Tris/HCl pH 6.8  
10 % SDS  
10 % β-mercaptoethanol  
20 % Glycerol  
0.06 % Bromphenolblue

Destaining solution  
10 % Acetic acid  
30 % Ethanol

Protein marker  
0.1 mg/ml BSA (66 kDa)  
0.1 mg/ml Ovoalbumine (45 kDa)  
0.1 mg/ml GAPDH (36 kDa)  
0.1 mg/ml Chymotrypsinogen A (25 kDa)  
0.1 mg/ml Trypsin inhibitor (20.1 kDa)  
0.1 mg/ml Cytochrom C (12.5 kDa)  
30 % 4X sample loading buffer

### Western blot

TBS buffer (Tris buffer saline) pH 7.6  
20 mM Tris  
150 mM NaCl

M-TBS  
5 % Milk powder non-fat  
in TBS

Towbin-Blot-buffer

25 mM Tris  
192 mM Glycin  
20 % Methanol

TBS-T  
0.1 % Tween 20 in TBS

Ponceau S Staining Solution

0.1 % (w/v) Ponceau S  
in 5% (v/v) acetic acid

**Cyclase enzyme test**

Creatine kinase

4 U /2.5 µl Creatine kinase in  
10 mM Tris/HCl pH 7.5

Creatine phosphate

120 mM in 10 mM Tris/HCl  
pH 7.5

ATP or GTP Stock solution

10 mM adjusted to pH 7.2-  
7.5 with NaOH

cAMP or cGMP Stock solutions

40 mM in H<sub>2</sub>O (adjust pH to  
7.5 with Tris buffer)

10X AC-Start Solution

0.75 to 10 mM ATP with  
2.5-4x10<sup>6</sup> Bq/ml  
[α-<sup>32</sup>P]-ATP

10X GC-Start Solution

0.75 to 10 mM GTP with  
2.5-4x10<sup>6</sup> Bq/ml  
[α-<sup>32</sup>P]-GTP

2X AC-Cocktail

43.5 % Glycerol  
100 mM Tris-HCl pH 7.5 or  
MOPS pH 7.5  
4 mM cAMP with  
2-4x10<sup>3</sup> Bq/ml  
[2,8-<sup>3</sup>H]-cAMP  
0.46 mg/2ml Creatine kinase  
6 mM Creatine phosphate  
2 to 5 mM MnCl<sub>2</sub> or  
5 to 10 mM MgCl<sub>2</sub>

2X GC-Cocktail

43.5 % Glycerol  
100 mM MOPS pH 7.5  
4 mM cGMP with  
2-4x10<sup>3</sup> Bq/ml  
[8-<sup>3</sup>H]-cGMP  
5 mM MnCl<sub>2</sub> or  
10 mM MgCl<sub>2</sub>



Adenylyl cyclase stop buffer (pH 7)  
 3 mM cAMP  
 3 mM ATP  
 1.5 % SDS

Guanylyl cyclase stop buffer  
 1.5 % SDS  
 Forskolin solution  
 10 mM Forskolin in DMSO

### Crystallization buffers

Self-produced crystallization buffers were made using deionized purified water (MilliQ®) and were filtrated through 0.2 µm size pore filters applying vacuum to a filter holder device.

## 2.4 Oligonucleotides

Restriction sites are underlined, mutations are in bold and mutations together with restriction sites are bold and underlined.

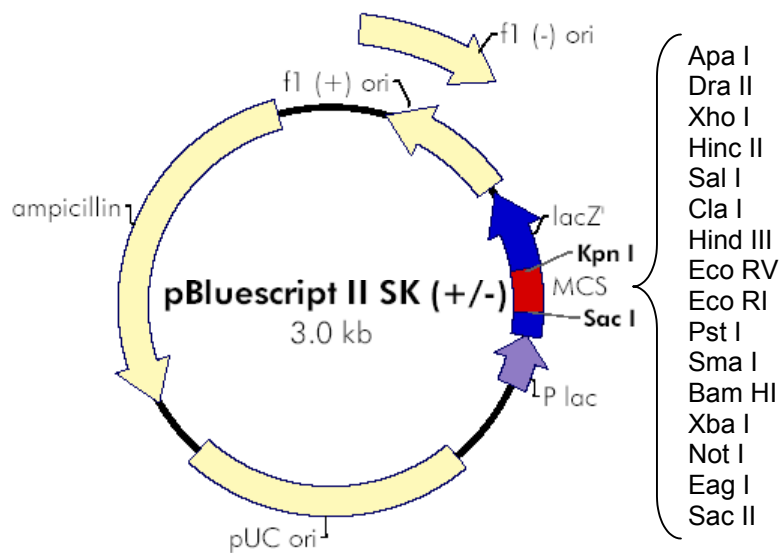
Name	Sense	Sequence (5' → 3')	Position	Comments
<b>Sequencing primers for plasmids</b>				
T7	s	GTA ATA CGA CTC ACT ATA GGG C	625-646	T7 pBluescript II SK(-)
T3	as	AAT TAA CCC TCA CTA AAG GG	772-791	T3 pBluescriptII SK(-)
U -pQE-IR	s	GAA TTC ATT AAA GAG GAG AAA	88-108	universal pQE30
R -pQE-IR	as	CAT TAC TGG ATC TAT CAA CAG G	212-233	reverse pQE30
<b>Cloning primers of Rv1625c mutants</b>				
myktub kat-s	s	AAA <u>GGA TCC</u> GAT ACT GCG CGT GCG GAG GCG	604-631	<u>Bam</u> HI Primer from Dr. Guo.
myktub 372A-1	as	CAT CCG <u>GCT AGC</u> GAC <b>AGC</b> GAC CGC GTC GCC	1102-1131	<u>Nhe</u> I
myktub 372A-2	s	GTC AAT GTC <u>GCT AGC</u> CGG ATG GAA TCC	1111-1137	<u>Nhe</u> I

myktub 1-as	as	AAA <u>GAG CTC</u> TCA GAC CCC TGC CGT GCG	1314-1338	<u>SacI</u> Primer from Dr. Guo.
myktub 372T-1	as	CAT CCG <u>GCT AGC</u> GAC <b>AGT</b> GAC CGC GTC GCC	1102-1131	<u>NheI</u>
myktub 300S-1	as	AAC CAT GTA <b>ACT CGA</b> <u>GCC</u> GCT GAC CTT GAT	883-912	<u>XhoI</u>
myktub 300S-2	s	GTC AGC <b>GGC TCG AGT</b> TAC ATG GTT GTC	889-916	<u>XhoI</u>
<b>Cloning primers of Rv0386 holoenzyme and AC catalytic domain</b>				
myco0386/B-C- Hforw	s	AAA <u>GGA TCC</u> ATG AGC AAG TTG CTG CCA CGG GGC ACA GTG ACA TTG CTG TTG GCC GAC GTC GAG <b>GGT</b> TCC ACC	1-63	<u>BamHI</u>
myco0386/B-C- H-rev	as	AAA <u>AGC TTT</u> <b>CAA</b> TCG ATA CGC AAT TCG GGA TG	505-534	<u>HindIII</u>
myco0386/C- Cforw	s	CGT <u>ATC GAT</u> TTC CCG CCG CTG	517-537	<u>Clal</u>
myco0386/C- Crev	as	GCC <u>ATC GAT</u> GAT CTC GTC AAG	1192-1212	<u>Clal</u>
myco0386/C- Sforw	s	ACG CTT GAC GAG ATC <u>ATC GAT</u> GGC	1189-1212	<u>Clal</u>
myco0386/C- Srev	as	CAG <u>GGC CTT</u> GTC <u>GGC</u> <u>CAA</u> TGC CCG	1855-1878	<u>SfiI</u>
myco0386/S- Sforw	s	CGG GCA <u>TTG GCC</u> GAC AAG <u>GCC</u> CTG	1855-1878	<u>SfiI</u>
myco0386/S- Srev	as	GGC <u>GGC CAA</u> CGC <u>GGC</u> <u>CGT</u> GGT CAA C	2460-2484	<u>SfiI</u>
myco0386/S- Hforw	s	TTG ACC <u>ACG GCC</u> GCG TTG <u>GCC</u> GCC	2461-2484	<u>SfiI</u>

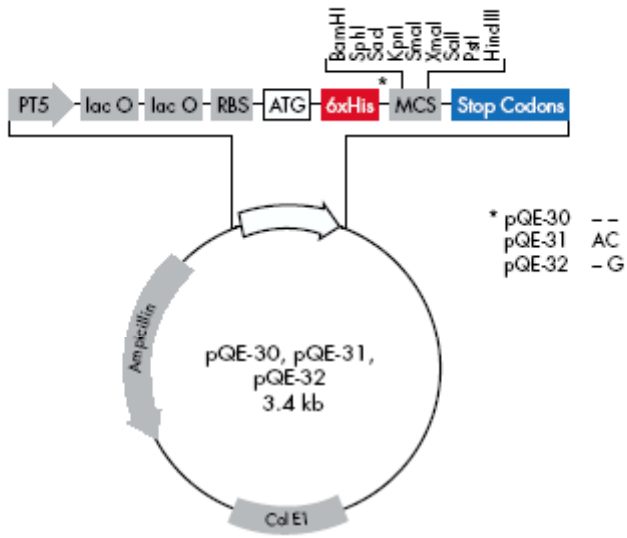
myco0386/S-Hrev	as	AAA <u>AGC TTT</u> CAG GTA CGG CGG GCG GCC GC	3238-3258	HindIII
<b>Cloning primers of Rv0386 mutants</b>				
myco0386/Q57Krev	as	ACC CTC ACC <b>CTT</b> CTC GAC <u>AGG CCT</u> TAC GCC	151-180	<u>StuI</u>
myco0386/Q57Kforw	s	GGC GTA <u>AGG CCT</u> GTC GAG AAG GGT GAG GGT	151-180	<u>StuI</u>
myco0386/Q57Arev	as	ACC CTC ACC <b>CGC</b> CTC GAC <u>AGG CCT</u> TAC GCC	151-180	<u>StuI</u>
myco0386/Q57Aforw	s	GGC GTA <u>AGG CCT</u> GTC GAG <b>CGC</b> GGT GAG GGT	151-180	<u>StuI</u>
myco0386/N106Drev	as	GTT GAT GGT <u>GGG CCC</u> GGC ATA <b>GTC</b> GCC TTC GTC	307-339	<u>ApaI</u>
myco0386/N106Dforw	s	GAC GAA GGC <b>GAC</b> TAT GCC <u>GGG CCC</u> ACC ATC AAC	307-339	<u>ApaI</u>
myco0386/N106Arev	as	GTT GAT GGT <u>GGG CCC</u> GGC ATA <b>GGC</b> GCC TTC GTC	307-339	<u>ApaI</u>
myco0386/N106Aforw	s	GAC GAA GGC <b>GCC</b> TAT GCC <u>GGG CCC</u> ACC ATC AAC	307-339	<u>ApaI</u>
myco0386/QKNDforw	s	AAG TGG CCG CCG CGT <u>TAG ATC TGC</u> AGC GAG CG	220-249	<u>Bgl II</u>
myco0386/QKNDrev	as	AAC CGC GCT CGC TGC <u>AGA TCT AAC</u> GCG GCG GC	222-252	<u>Bgl II</u>
myco0386/N106Sforw	s	GAC GAA GGC <b>TCA</b> TAT <u>GCC</u> GGT CCG ACC	307-333	<u>NdeI</u>

myco0386/ N106Srev	as	GGT CGG ACC GGC <u>ATA</u> <u>TGA</u> GCC TTC GTC	307-333	<u>NdeI</u>
<b>Primers for transcription factor-, ATPase- and DNA-binding domains of Rv0386</b>				
NHis/TF/ Rv0386forw	s	AAA <u>GGA TCC</u> TGT CAT CCC GAA TTG CGT ATC	502-522	<u>BamHI</u>
NHis/DBDom/ Rv0386	s	AAA <u>GGA TCC</u> GCA TGG GCC GAA GGT GCC GCG	2980-3000	<u>BamHI</u>
NHis/AADom/ Rv0386re	as	AAA <u>AAG CTT</u> GTG GCG CAT CGT CTC GCA	1501-1518	<u>HindIII</u>
<b>Primer for N-terminally elongated adenylyl cyclase domain</b>				
CDC1551ac- forw	s	AAA <u>GGA TCC ATG CGA</u> <b>CTG AGT GGA GCG GGG</b> ATG AGC AAG TTG CTG CCA CGG GGC ACA	1-27	<u>BamHI</u> and addition of <b>MRLSGAG</b>
myco0386/cata/ C-His	as	AAA <u>AGA TCT</u> ATC GAT ACG CAA TTC GGG ATG	505-525	<u>Bgl II</u>
<b>Primer for C-terminally His-tagged catalytic domain</b>				
myco0386/cata/C-His (see above)				

## 2.5 Plasmids

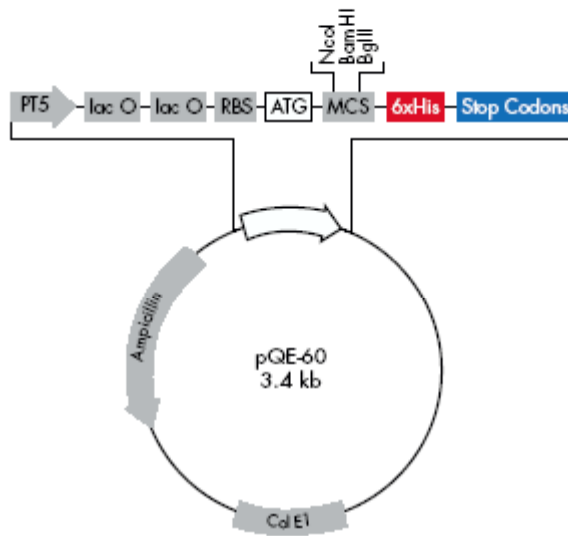
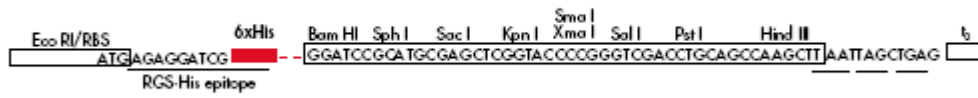


Source: Stratagene



Source: Qiagen

pQE-30



Source: Qiagen

pQE-60



## 3 Methods

### 3.1 Polymerase chain reaction (PCR)

The polymerase chain reaction was carried out with specific primers to amplify DNA fragments from plasmid or genomic DNA and for introduction of endonuclease restriction sites and point mutations. The annealing temperature was calculated with the formula:

$$T_a = 2 \times (AT) + 4 \times (GC) - 4$$

(AT) and (GC) represent the number of A+T and G+C respectively in the primer sequence. If the annealing temperatures for each primer were different the lower one was employed.

The reaction was run in 50 µl with a thermocycler with heatable lids to avoid volume and concentration changes through evaporation and condensation. The samples contained max. 1 ng plasmid or 800 ng genomic DNA, 5-10% DMSO, 200 µM dNTPs, 1 pmol/µl primers, 1U Taq-DNA-Polymerase and 1X of the corresponding reaction buffer. The temperature program applied is shown in Table 3.1.

Denaturation		95°C	5 min
20 - 40 cycles	Denaturation	95°C	1 min
	Primer annealing	$T_a$	1 min
	Extension	72°C	1 min
Fill up		72°C	10 min

**Table 3.1:** Program used for polymerase chain reaction.

### 3.2 Isolation and purification of DNA

#### 3.2.1 General

Plasmid DNA was isolated from bacterial cultures through a small-scale purification method, known as miniprep. The standard protocol of the Wizard Plus Minipreps DNA Purification System (PROMEGA) was carried out using 1-3 ml of O/N bacterial culture (12-16h by 37°C) and a vacuum manifold giving a yield of 1-10 ng DNA. DNA was

eluted with sterile water. The purified plasmid could be used directly for DNA sequencing and restriction digestion.

DNA fragments separated through electrophoresis were excised from the agarose gel with the help of a scalpel and extracted with the help of the Macherey-Nagel Nucleotrap-Gelextractions-Kit following the protocol of the manufacturers.

If a change in the buffer conditions was necessary in order to process the DNA samples, they were desalted following the corresponding protocol of the Nucleotrap-Gelextractions-Kit (Macherey-Nagel).

### 3.2.2 Agarose electrophoresis

To determine yield and purity of an isolated DNA or PCR reaction, to check digestion by a restriction enzyme and to determine the size of DNA molecules, agarose electrophoresis was carried out. Agarose was dissolved in TAE-buffer and melted in a microwave oven. The solution was poured into a mould in which a well-forming comb was fitted. The agarose content was chosen according to the expected size (bp) of DNA-fragments:

$\geq 2000$ bp	0.8 - 1 %
500 – 2000 bp	1 – 1.8 %
$\leq 500$ bp	2 %

TAE-buffer was used for electrophoresis, agarose gels were submerged in a horizontal electrophoresis apparatus. The DNA samples were mixed with loading sample buffer. Electrophoresis was performed at 80-100 V for 0.5-1 h at room temperature. The size markers EcoR I/Hind III-digested  $\lambda$ -DNA ( $\lambda$ -Marker: 21226, 5184, 4973, 4277, 3530, 2027, 1904, 1584, 1330, 983, 831, 564, 125 bp) and MspI/SspI-digested pBluescript II SK(-)-Vector ( $\pi$ -Marker: 489, 404, 312, 270, 242/241, 215, 190, 157, 147, 110, 67, 57, 34, 26 bp) were co-electrophoresed with DNA samples. For detection of the DNA, gels were submerged in a ethidium bromide bath (0.01 mg/ml) for 1-2 min. The gel was run 10 additional min and DNA fragments visualized on a UV light box (302 nm) and photographed.

### **3.2.3 Photometric determination of DNA concentration**

Nucleic acid content was measured at 260 nm. An OD of 1 corresponds to 50 µg/ml for double-stranded DNA. The ratio  $OD_{260}/OD_{280}$  was calculated to estimate purity. An OD ratio of >1.8 was desirable.

## **3.3 Enzymatic Methods**

### **3.3.1 General molecular biology methods**

Restriction enzyme digestions were performed by incubating double-stranded DNA molecules with the appropriate amount of restriction enzyme at the optimal temperature required and in the corresponding buffer as recommended by the supplier. In the case of simultaneous digestion with 2 or more enzymes, the more compatible buffer or the One-Phor-All-buffer was used. If no possible compatibility was found, digestions were performed sequentially with a desalting step in-between.

### **3.3.2 Generation of blunt ends**

After PCR or a restriction digest, the Klenow-fragment of the DNA-Polymerase I was used. For blunting, maximally 500 ng DNA, 1 µl of 10X Klenow-buffer and 0.8 µl of Klenow-Polymerase (1 U/µl) in a 10 µl reaction volume were mixed. The reaction mixture was incubated for 10 min at 37°C. Then 1 µl of dNTPs (25 mM) was added and the incubation continued for 30 min. The sample was heated to 70°C for 10 min for inactivation.

### **3.3.3 5'-Phosphorylation of PCR products**

This was necessary for blunt end ligation. The reaction was composed of 1-2 µg DNA or of the Klenow-treated DNA solution, 1 mM ATP, 10 U T4-Polynucleotide Kinase and 1X T4-PNK-buffer in 15 µl (37 °C, 1 h).



### **3.3.4 5'-Dephosphorylation of plasmid vectors**

To suppress circularization of plasmid DNA, the 5'-phosphates from both ends were removed with calf alkaline phosphatase. 500 ng DNA, 1 U/μmol of enzyme and 1X dephosphorylation buffer were mixed in 10 μl and incubated at 37°C for 1 h.

### **3.3.5 Ligation of DNA fragments**

DNA fragments were ligated with the Rapid DNA Ligation Kit according to the instructions of the manufacturer. The molar ratio of vector to DNA insert should be 1:3 for one insert and 1:1:1 in the case of two inserts.

## **3.4 Transformation of recombinant DNA**

### **3.4.1 Competent cells of *E. coli***

From a new plate of XL1-blue MRF<sup>-</sup>, BL21 (DE3) [pREP4], BL21 STAR (DE3) [pREP4] or BL21 Rosetta (DE3) [pREP4] cells, a single colony was picked and grown up in 5 ml LB broth (37°C, O/N). 1 ml was transferred into 50 ml LB and grown at 37°C to 0.3-0.4 OD<sub>600</sub> (approx. 2-3 h). The culture was cooled on ice (10 min) and transferred to Falcon tubes. Cells were recovered at 2500 x g (15-20 minutes, 4°C). Pellets were suspended in 10 ml of ice cold CaCl<sub>2</sub> (0.1 M) and centrifuged (2500 x g, 15 min, 4°C). This step was repeated with addition of 20 % glycerol. The suspended pellets were standing on ice for 2 hours, aliquoted (100 μl) and stored at -80°C.

### **3.4.2 Rapid transformation**

One aliquot of competent cells was thawed on ice. 100 ng plasmid DNA (max.) was added and mixed. After 5-15 min on ice the mixture was spread on LB agar plates containing the appropriate antibiotic and incubated at 37 °C O/N.

### **3.4.3 Standard transformation**

The entire DNA ligation reaction (21 μl from a Rapid Ligation Kit protocol) was diluted in 1X CM buffer to 50 μl. This was added to competent cells (100 μl), mixed gently and incubated on ice (30-45 min). Cells were then heat-shocked (1 to 2 min, 42°C) and incubated on ice (10 to 20 min). 400 μl of LB-broth were added and cells were incubated

at 37 °C for 45-60 min with agitation (210-230 rpm). 50 to 200 µl of the mixture were spread on LB agar plates with appropriate antibiotics. Plates were incubated in an inverted position for 12-16 h at 37 °C. For transformation with pBluescript II SK (-) vector it was possible to make a blue-white screen by spreading 40 µl of IPTG 0.1 M and 40 µl of X-Gal (2 %) over the LB agar plate prior to plating. Bacteria carrying recombinant DNA formed white colonies, those carrying plasmids without insert formed blue colonies.

### 3.4.4 Glycerol stock cultures

1-3 ml of a O/N bacterial culture was centrifuged (2 min, 10,000 x g). The pellet was suspended in 750 µl of a mixture of LB-broth/Glycerol 4:1, storage at -80 °C.

## 3.5 DNA Sequencing

Miniprep DNA was sequenced using sequenase and 7-deaza-dGTP (the latter to prevent band compression caused by DNA secondary structure). The Thermo Sequenase Primer Cycle Sequencing Kit was used. The DNA/Primer-Mix varied in its composition and volume depending on the type of vector used. DMSO was added to avoid primer-dimer formation. Primers used were fluorescent-labeled: for pBluescript T<sub>3</sub> and T<sub>7</sub> primers (T<sub>a</sub>= 56°C), and for pQE30 U-pQE-IR800 and R-pQE-IR800 primers (T<sub>a</sub>= 54 °C) were used.

DNA fragment cloned in pBluescript		DNA fragment cloned in pQE30	
DNA	1-2 pmol (~130 ng/kb) (8 µl)	DNA	1-2 pmol (~130 ng/kb) (10 µl)
Primer [2 pmol/µl]	1.5 µl	Primer [4 pmol/µl]	2 µl
DMSO	0.7 µl	DMSO	0.7 µl
Final volume (with H <sub>2</sub> O)	21 µl	Final volume	18 µl

**Table 3.2:** Components of the DNA/Primer-Mix used for DNA sequencing depended on the vector used for cloning.

4 - 5  $\mu$ l of DNA/Primer-Mix were added to 2  $\mu$ l of G, A, T or C-reagent mix of the corresponding kit following the instructions of the supplier. Each reaction was overlaid with one drop chill-out-wax and run in a Thermocycler using the following program:

Step	Temperature	Time	Cycles
First denaturation	95 °C	2 min	1
Denaturation	95 °C	20 s	25-30
Annealing	Ta of the primers used	20 s	
Extension	70 °C	20 s	
Termination	4 °C	$\infty$	1

**Table 3.3:** Program used for DNA sequencing.

At the end of the reaction 6  $\mu$ l of Formamide loading dye of the kit were added. 1  $\mu$ l of each sample was loaded onto a 6% polyacrylamide gel and electrophoresed with the help of a LI-COR Sequencing apparatus at 50 W (max. 1500 V or 37 mA, 50°C). Running buffer was TBE-buffer, DNA fragments were detected through Laser fluorescence at 800 nm. Data obtained was analyzed with the BasImageIR V. 4.0 Software.

## 3.6 Cloning

All constructs were cloned in the MCS of pBluescriptII (SK-) as a first cloning step and for sequencing. Finally, they were cloned for expression into pQE30 or pQE60. As a result, all proteins had either an N-terminal MRGSH<sub>6</sub>GS or a C-terminal RSH<sub>6</sub> extension.

### 3.6.1 Mammalian and protozoan cyclases

Clones of the mammalian and the *Paramecium* cyclases cytosolic regions were from Hoffmann (1999).

### 3.6.2 *M. tuberculosis* Rv1625c

#### 3.6.2.1 Site-directed mutagenesis

A DNA construct of Rv1625c (mycoAC<sub>204-443</sub>) with 5'-BamHI and 3'-Sacl sites in pQE30 was used as a template (Guo et al., 2001). Single amino acid mutations were introduced by site-directed mutagenesis using respective PCR.

##### 3.6.2.1.1 Mutants N372A and N372T

Table 3.4 and Figure 3.1 outline the cloning steps used for mycoAC<sub>204-443</sub> N372A and N372T, respectively.

Mutant	Fragment	Primers	Length of the PCR product (bp)
N372A	1	myktub kat-s myktub 372A-1	534
	2	myktub 372A-2 myktub 1-as	237
N372T	1	myktub kat-s myktub 372T-1	534
	2	myktub 372A-2 myktub 1-as	237

**Table 3.4:** Primers used for cloning the mutants N372A and N372T. See sequence of the primers in chapter 2.

Amplification conditions were: Ta= 52°C, 5 % DMSO, 20 cycles. Products were digested with BamHI/NheI to obtain fragment 1 and NheI/Sacl for fragment 2 of both N372A and

N372T. The fragments were 5' phosphorylated, purified by agarose gel electrophoresis and cloned into pQE30 plasmid digested with BamHI/SacI and dephosphorylated. Recombinants were isolated from *E. coli* XL-1 blue, and introduced into *E. coli* BL21(DE3)[pREP4] for protein expression with prior confirmation of the mutations by double-stranded sequencing.

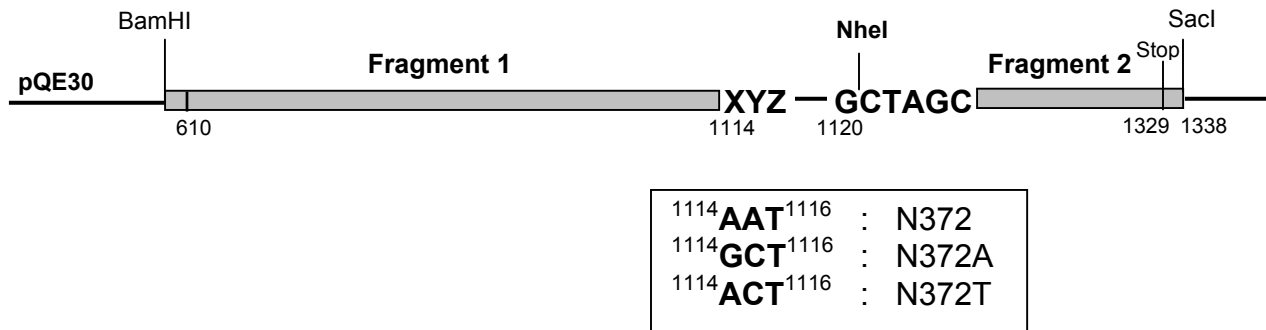


**Figure 3.1:** Restriction sites and sequence changes used for the mutants N372A and N372T. Numbering of the bases corresponds to positions in the holoenzyme. The silent insertion of an NheI restriction site and the codon changes corresponding to the respective mutations are in bold.

### 3.6.2.1.2 Mutant D300S

For cloning the mutant D300S two PCR products were amplified. For fragment 1 (312 bp) primers myktub kat-s and myktub 300S-1 with the insertion of a 5'-BamHI and a 3'-XhoI restriction sites were used. Fragment 2 (456 bp) was obtained with myktub 300S-2 and myktub 1-as with the insertion of a 5'-XhoI and a 3'-SacI site (figure 3.2). PCR conditions were: Ta= 52°C, 5 % DMSO, 20 cycles. PCR products were isolated, purified, digested with the respective enzymes and ligated to a dephosphorylated BamHI/SacI digested pQE30 vector. Recombinants were isolated from XL-1blue cells and introduced into BL21 cells for protein expression after sequencing.

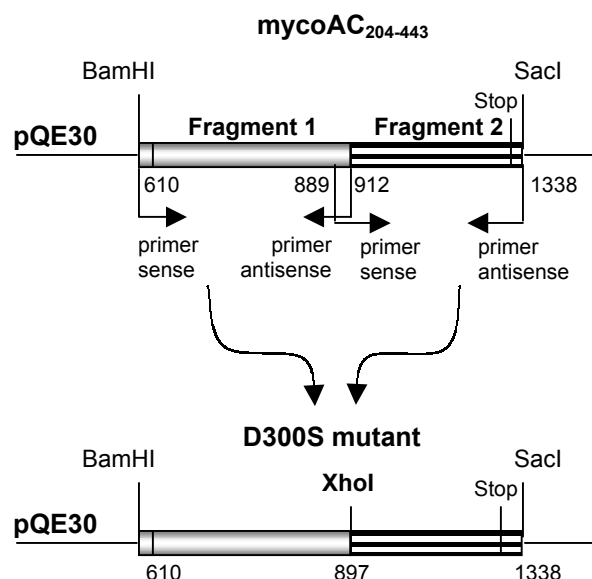


**Figure 3.2 :** Cloning of D300S in pQE30. Within the XhoI site the codon changes for the respective mutation were inserted by PCR (<sup>898</sup>TCG<sup>900</sup> to <sup>898</sup>GAC<sup>900</sup>). Numbering is according to the holoenzyme Rv1625c.

### 3.6.3 *Mycobacterium tuberculosis* Rv0386

#### 3.6.3.1 Holoenzyme

The *M. tuberculosis* genomic DNA was provided by Dr. Boettger (University of Zürich Medical School). The gene Rv0386 was obtained in 5 PCR reactions, i.e. in five different fragments which covered the entire ORF (3255 bp). For PCR conditions see Table 3.5. See appendix for Rv0386 DNA sequence (restriction sites used for cloning are outlined).

PCR fragment	Primers	Length (bp)	T <sub>annealing</sub> (°C)	Cycles	% DMSO
1	myco0386/B-C-Hforward myco0386/B-C-H-reverse	545	58	40	5
2	myco0386/C-Cforward myco0386/C-Creverse	696	60	40	5
3	myco0386/C-Sforward myco0386/C-Sreverse	690	62	40	5
4	myco0386/S-Sforward myco0386/S-Sreverse	630	62	40	5
5	myco0386/S-Hforward myco0386/S-Hreverse	806	70	40	5

**Table 3.5:** Primers used and PCR conditions for cloning Rv0386.

The primer myco0386/B-C-Hforward inserted a silent mutation at position 55 to eliminate a BamHI site. After PCR, the DNA products were purified by agarose gel electrophoresis, blunted, phosphorylated and ligated into different vectors (Table 3.6).

PCR fragment	Vector	Expected direction
1	pBSK(-), Clal digested, dephosphorylated and blunted	antisense
2,3 and 4	pBSK(-), EcoRV digested, dephosphorylated and blunted	sense
5	pBSK(-), EcoRV digested, dephosphorylated and blunted	antisense

**Table 3.6:** Vectors used for cloning the DNA fragments obtained by PCR (see Figures 3.3 and 3.4).

The ligation products were transformed into XL-1 blue cells. The recombinant DNA was analyzed by restriction. The direction of the five PCR products within vectors was controlled through digestion with BamHI and HindIII. To search for clones with fragment I in antisense direction, an additional control digestion with only BamHI was carried out. Similarly, for fragment V a digest with only HindIII identified the clones with antisense direction. All clones were verified through sequencing (Figures 3.3 and 3.4).

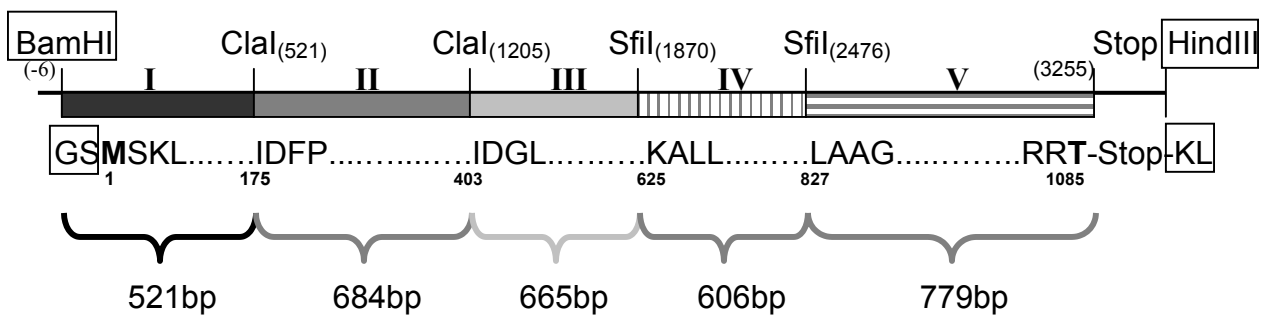
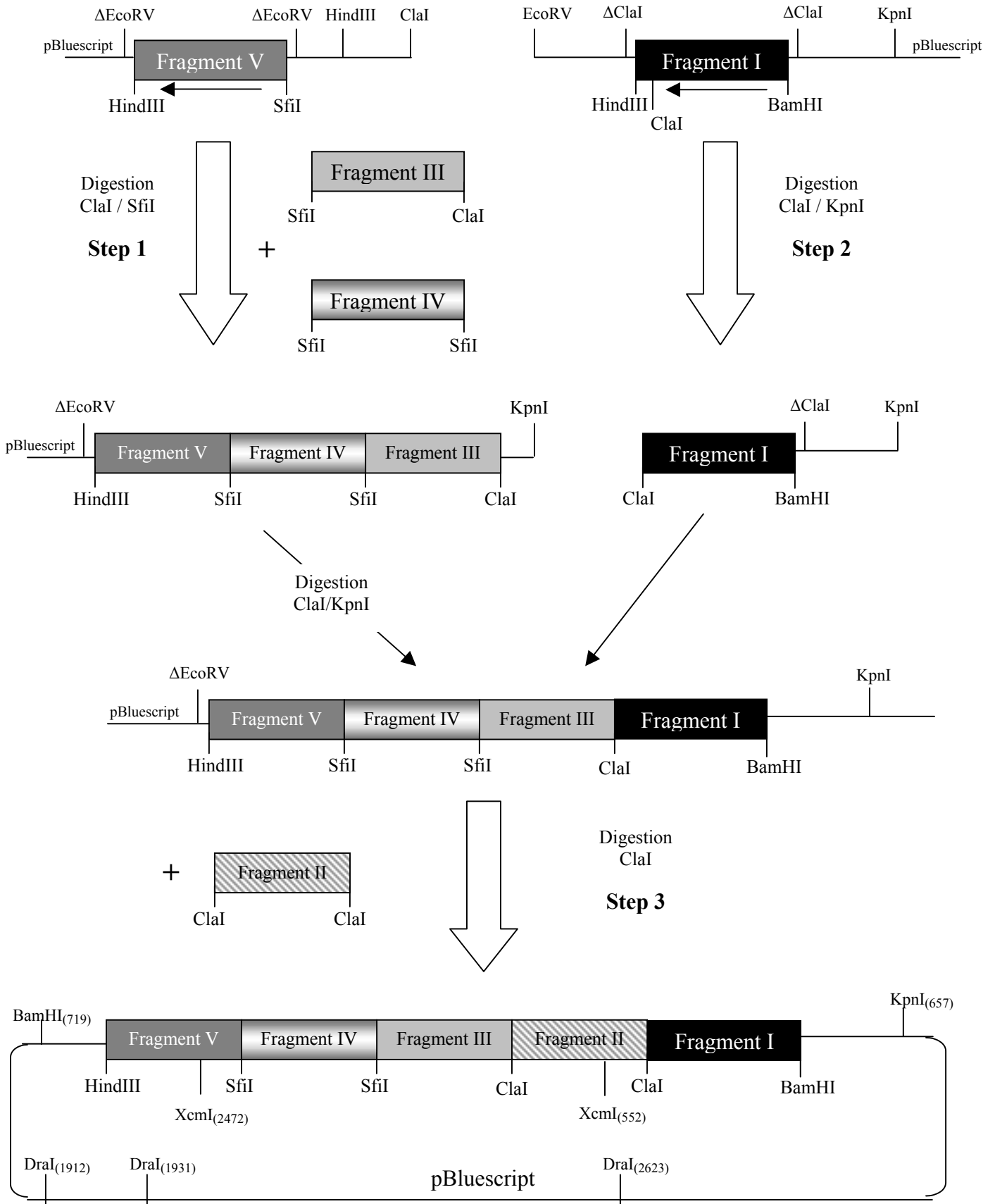


**Figure 3.3:** Overview of the sequence of Rv0386 to be expressed. Note the five fragments. The restriction sites BamHI and HindIII were introduced through primers. Clal and Sfil sites were from the original sequence.

**Figure 3.4:** Steps used for cloning Rv0386. Levels above correspond to vector positions and levels below to Rv0386 positions.





Step 1: DNA fragment V in pBluescript (in antisense direction) was digested with SfiI (2h, 50°C) and subsequently with ClaI (O/N, 37°C). The product was dephosphorylated and used as a vector. Simultaneously, fragments IV and III in pBluescript were digested with SfiI and fragment 3 additionally with ClaI. Both products were phosphorylated to function as inserts. Vector and the two inserts were triple ligated and transformed in XL-1 blue cells. Clones were first controlled by digestion with HindIII and ClaI. A second control digest was carried out with PstI (Figure 3.5). One of the correct clones was chosen.

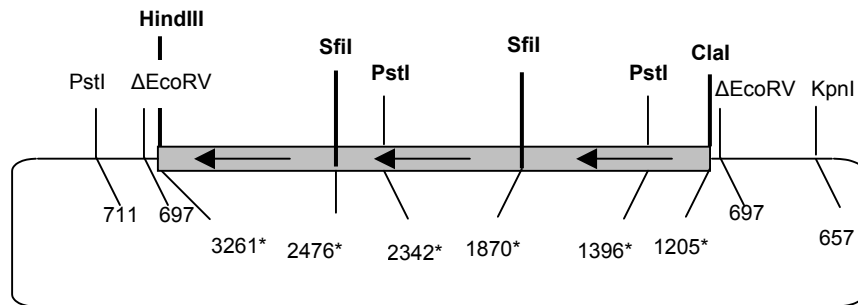


**Fig. 3.5:** Restriction sites used for controlling the insertion of fragment IV (SfiI/SfiI) in the correct direction between fragments III (ClaI/SfiI) and V (SfiI/HindIII). Names of the enzymes in bold correspond to restriction sites present in the holoenzyme sequence. \*Numbering corresponds to positions in Rv0386. The other restriction sites and numberings correspond to pBluescript.

Step 2: Fragment I cloned in pBluescript in antisense direction was digested with ClaI and KpnI (1h, 37°C). The product was the insert. Construct containing fragments III, IV and V cloned together in pBluescript (step 1) was digested with ClaI and KpnI and dephosphorylated to act as the vector (KpnI comes from pBluescript). Vector and insert were ligated and transformed in XL-1 blue cells. The obtained clones were controlled by digestion with BamHI and HindIII.

Step 3: Fragments I/III/IV/V (in pBluescript) were digested with ClaI and then dephosphorylated to be the vector. Fragment II in pBluescript was digested with ClaI to serve as a insert. Vector and insert were ligated and transformed in XL-1 blue cells. Clones were analyzed by digestion with BamHI, XcmI and HindIII to verify the direction of fragment II.

Step 4: The whole construct in pBluescript (in antisense direction) was digested with BamHI, HindIII and DraI to be the insert for the vector pQE30. DraI digests pBluescript into 3 fragments but does not cut the insert. This permitted the easy isolation of the insert from pBluescript because of the size difference. pQE30 was likewise digested with BamHI and HindIII and dephosphorylated. Insert and vector were ligated, transformed in XL-1 blue cells and clones were controlled by digestion with BamHI and HindIII. One of the correct clones was chosen for transformation into BL21 cells for expression and a glycerol stock culture was prepared.

### **3.6.3.2 Adenylyl cyclase domain**

Fragment I used for cloning the holoenzyme (figure 3.4) was digested with BamHI and HindIII from pBluescript and ligated into pQE30 digested correspondingly. Finally, it was transformed in BL21 cells for expression.

### **3.6.3.3 Putative AAA-ATPase domain**

Using the pQE30 cloned holoenzyme as a template, a PCR ( $T_a = 48^\circ\text{C}$ , 10 % DMSO, 30 cycles) with primers NHis/TF/Rv0386forw and NHis/AAADom/Rv0386rev was carried out. These primers inserted 5'-BamHI and 3'-HindIII sites. The DNA fragment between positions 502 and 1518 was amplified (Figure 3.6). The products were digested with BamHI and HindIII and phosphorylated. DNA of pQE30 was digested similarly and dephosphorylated. Insert and vector were ligated and transformed in XL-1 blue cells. Recombinant DNA from minipreps was sequenced to verify sequence fidelity. A correct clone was then transformed in BL21 cells and in BL21-STAR cells.

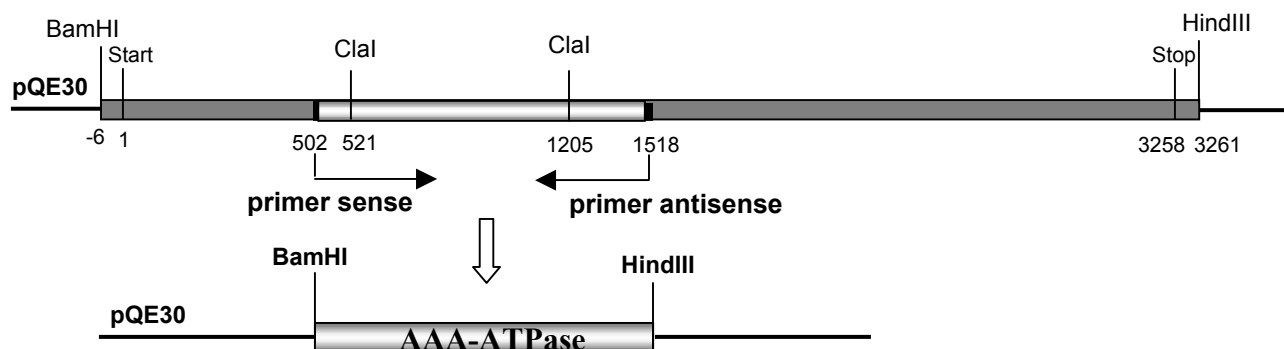


**Fig. 3.6:** Cloning steps of the AAA-ATPase domain of Rv0386 in expression vector pQE30. DNA from position 502 to 1518 was amplified. Numbering corresponds to positions in the holoenzyme sequence.

### 3.6.3.4 Putative Transcription factor domain

DNA between positions 502 and 1121 of Rv0386 was amplified by PCR ( $T_a = 54^\circ\text{C}$ , 5 % DMSO, 30 cycles) with primers NHis/TF/Rv0386forw and myco0386/C-Crev (Figure 3.7). The holoenzyme in pQE30 was used as a template. The primers introduced 5'-BamHI and 3'-BglIII restriction sites. PCR products were purified from agarose gel, blunted and phosphorylated. DNA of pBluescript was blunt digested with EcoRV and dephosphorylated. Insert and vector were ligated and transformed in XL-1 blue cells. Recombinant DNA of a correct clone was digested with BamHI and Bgl II and a 631 bp fragment was purified. The holoenzyme construct in pQE30 was digested with BamHI and BglIII, dephosphorylated and used as a vector. With this step the fragment between positions -6 and 1121 of the holoenzyme sequence was removed and replaced with the 631 bp fragment. The DNA of the obtained clones was analyzed by digestion with BamHI, Bgl II and HindIII (631, 2142 and 3460 bp fragments were expected). A correct clone was chosen for transformation into BL21 and BL21-STAR cells.

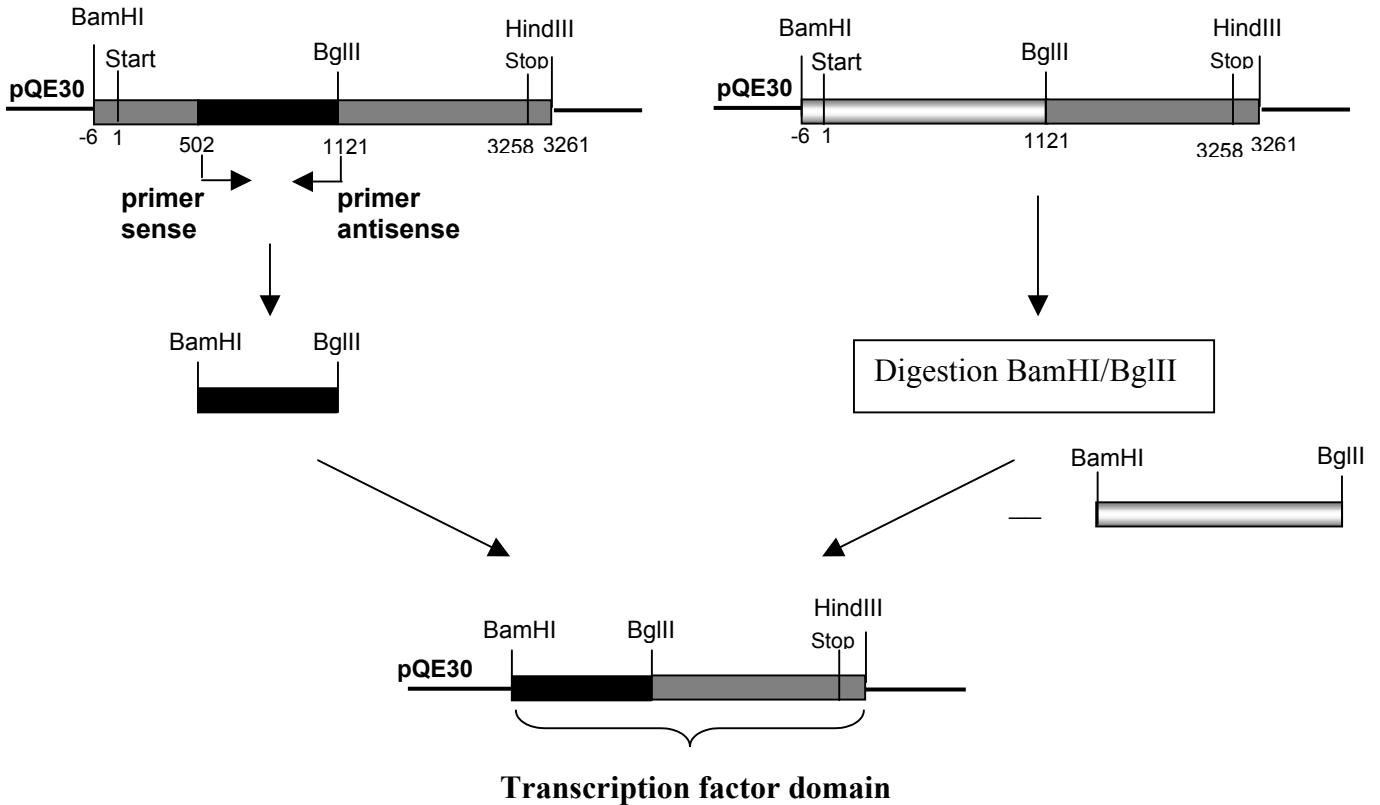


**Fig. 3.7:** Cloning steps for the transcription factor domain of Rv0386 into vector pQE30. Numbering is according to the holoenzyme.

### 3.6.3.5 Putative DNA-binding domain

Amplification of fragment 2980 to 3261 was performed with primers NHis/DBDom/Rv0386 and myco0386/S-Hrev ( $T_a = 64^\circ\text{C}$ , 5 % DMSO, 30 cycles). 5'-BamHI and 3'-HindIII sites were introduced (Figure 3.8). Fragment V used for cloning the holoenzyme (Sfil<sub>2476</sub> to HindIII<sub>3261</sub>) was used as a template. The product was isolated, purified and digested with BamHI and HindIII. pQE30 was cut similarly and dephosphorylated. Insert and vector were ligated and transformed in XL-1 blue cells. Recombinant DNA of the clones was sequenced and a correct one was used for transformation into BL21 cells.

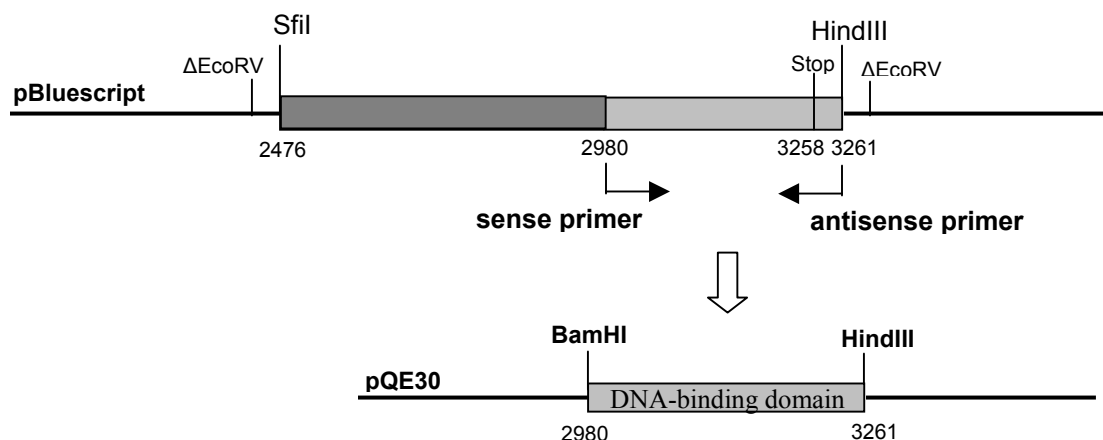


**Fig. 3.8:** Cloning steps of the DNA-binding domain of Rv0386 in pQE30. Numbering corresponds to the nucleotide positions in the holoenzyme.

### 3.6.3.6 Site-directed mutagenesis

Mutation primers were used to introduce the desired changes. See appendix for DNA sequence with outlined restriction and mutation sites.

#### 3.6.3.6.1 Q57K and Q57A mutants

In table 3.7 and figure 3.9 the primers and the strategy are delineated. PCR conditions: Ta= 60°C, 5 % DMSO, 40 cycles. The template was the construct of the AC domain in pQE30 vector.

Mutant	Fragment	Primers	Length of the PCR product (bp)
Q57K	1	myco0386/B-C-Hforw myco0386/Q57Krev	180
	2	myco0386/Q57Kforw myco0386/B-C-Hrev	390
Q57A	1	myco0386/B-C-Hforw myco0386/Q57Arev	180
	2	myco0386/Q57Aforw myco0386/B-C-Hrev	390

**Table 3.7:** Primers used for the cloning of Q57K and Q57A .

Fragments 1 and 2 were purified, blunted, ligated with dephosphorylated pBluescript vector  $\Delta$ EcoRV and transformed into XL-1 blue cells. Clones were verified through sequencing. Fragment 1 in pBluescript was digested with *Stu*I and *Hind*III and dephosphorylated to serve as a vector. Fragment 2 was obtained by a *Stu*I/*Hind*III digest. Vector and insert were ligated and transformed in XL-1 blue cells. Clones were controlled by a *Bam*HI/*Hind*III digestion. Then the mutated catalytic domain was cut out of pBluescript, inserted in a dephosphorylated pQE30 vector  $\Delta$ (*Bam*HI/*Hind*III) and transformed into BL21 cells.

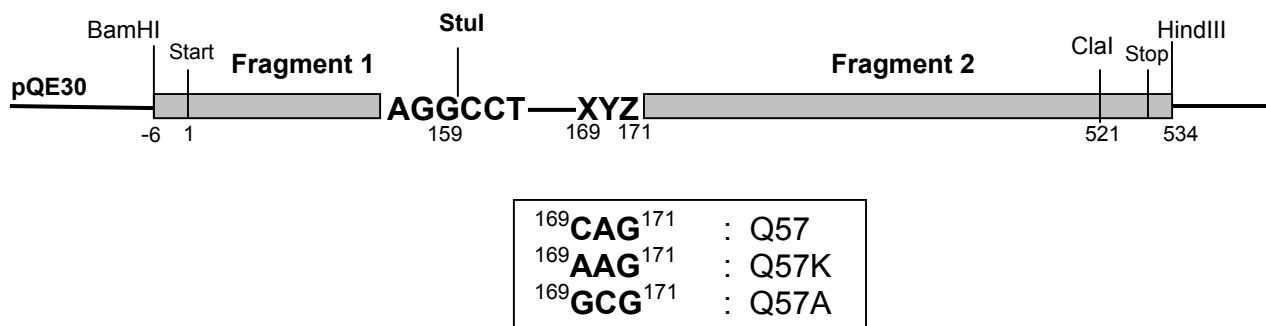


**Fig. 3.9:** Site-directed mutagenesis for cloning Q57K and Q57A in pQE30. A silent restriction site for *Stu*I and the corresponding nucleotide changes for each mutation were inserted by PCR. Numbering is according to the holoenzyme.

### 3.6.3.6.2 N106D and N106A mutants

In table 3.8 and figure 3.10 the primers and the strategy are delineated. PCR conditions:  $T_a = 60^\circ\text{C}$ , 5 % DMSO, 40 cycles. Template was the AC domain in pQE30.

Mutant	Fragment	Primers	Length of the PCR product (BP)
N106D	1	myco0386/B-C-Hforw myco0386/N106Drev	339
	2	myco0386/N106Dforw myco0386/B-C-Hrev	234
N106A	1	myco0386/B-C-Hforw myco0386/N106Arev	339
	2	myco0386/N106Aforw myco0386/B-C-Hrev	234

**Table 3.8:** Primers used for cloning of N106D and N106A.

Each fragment was purified, blunted, phosphorylated, ligated with a blunt dephosphorylated pBluescript  $\Delta$ Apal and transformed in XL-1 blue cells. Clones were verified through sequencing. Correct clones were digested with BamHI/ApaI and ApaI/HindIII to cut out fragments 1 and 2, respectively. Both fragments were ligated with dephosphorylated pQE30  $\Delta$ (BamHI/HindIII) and transformed in XL-1 cells. Clones were controlled by digestion with BamHI and HindIII and a correct one was transformed in BL21 cells.

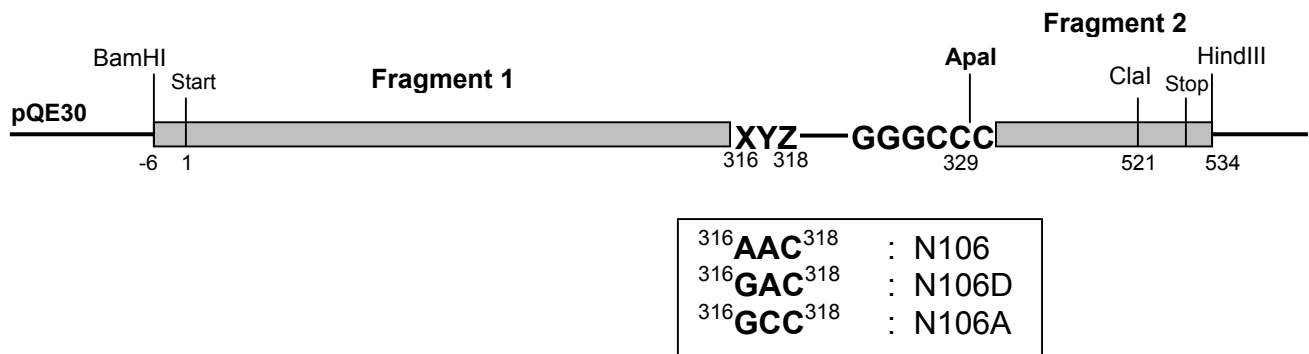


**Fig. 3.10:** Cloning of N106A and N106D in pQE30. Silent restriction site for Apal and nucleotide changes for each mutant were inserted by PCR. Numbering is according to the holoenzyme.

### 3.6.3.6.3 Q57K/N106D mutant

Two PCR products were amplified with primers myco0386/B-C-Hforw and myco0386/QKNDrev for fragment 1, and myco0386/QKNDforw and myco0386/B-C-Hrev for fragment 2. PCR conditions: Ta= 56°C, 5 % DMSO and 20 cycles. Template for fragment 1 (258 bp) was the mutant Q57K in pQE30 vector and for fragment 2 (312 bp) mutant N106D in pQE30. 5'-BamHI and 3'-BglII sites for fragment 1 and 5'-BglII and 3'-HindIII sites for fragment 2 were inserted. PCR products were purified, blunted, phosphorylated and ligated to a blunt dephosphorylated pBluescript SK(-) vector  $\Delta$ EcoRV. DNA of the clones was sequenced. Fragment 1 was cut from pBluescript with BamHI/BglII and fragment 2 with BglII/HindIII. Both fragments were simultaneously ligated into a dephosphorylated pQE30 vector  $\Delta$ (BamHI/HindIII). The final construct was controlled by BamHI/Bgl II/HindIII digestion and transformed into BL21 cells (figure 3.11).

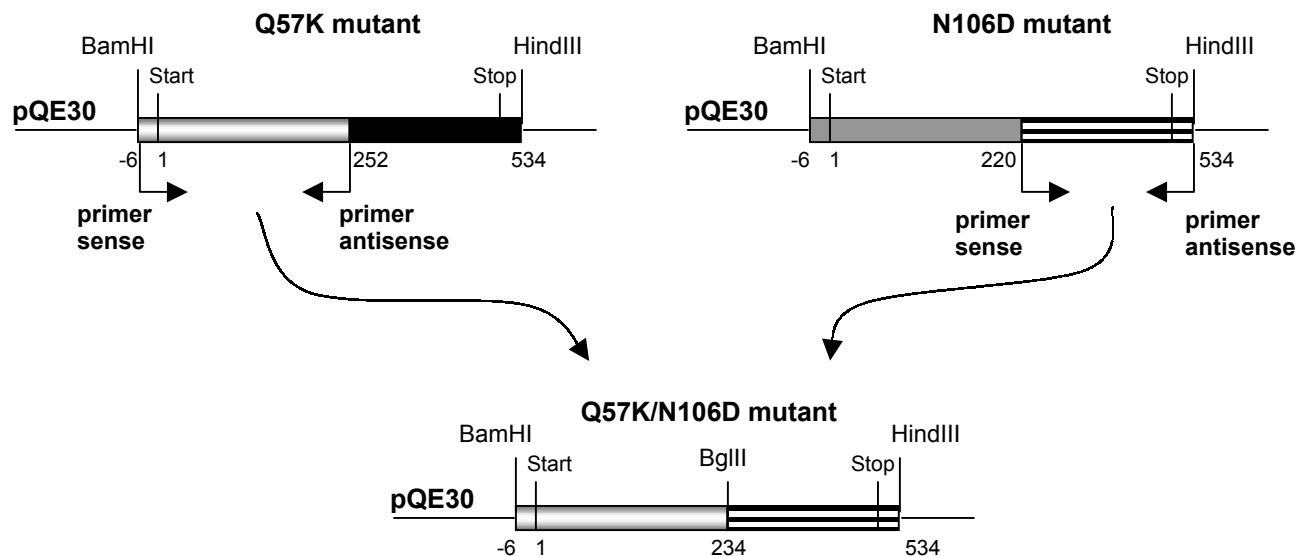


**Fig. 3.11:** Cloning of Q57K/N106D in pQE30. Silent restriction site for BglIII was inserted by PCR. Numbering is according to the holoenzyme.

#### 3.6.3.6.4 N106S mutant

Mutant	Fragment	Primers	Length of the PCR product (bp)
N106S	1	myco0386/B-C-Hforw myco0386/N106Srev	342
	2	myco0386/N106Sforw myco0386/B-C-Hrev	228

**Table 3.9:** Primers used for cloning of mutant N106S.

PCR conditions:  $T_a = 58^\circ\text{C}$  for fragment 1 and  $54^\circ\text{C}$  for fragment 2, 5 % DMSO and 30 cycles. The AC domain in pQE30 was the template. Cloning strategy was similar as for mutant D300S of Rv1625c (see above). Products were purified, digested with BamHI/NdeI (fragment 1) or NdeI/HindIII (fragment 2), desalted and ligated into dephosphorylated pQE30  $\Delta$ (BamHI/HindIII) in a triple ligation. Recombinants were isolated from XL-1 blue cells and introduced into BL21 for expression with prior sequence confirmation.



### **3.6.3.7 N-terminally elongated AC domain (with N-terminal His-tag)**

By comparison of Rv0386 with its homologue MT0399 from *Mycobacterium tuberculosis* CDC1551 (Fleischmann et al., 2002), an almost total identity was observed with the exception of 7 extra N-terminal amino acids in MT0399 (MRLSGAG). These amino acids are just ahead of the START codon of Rv0386. To determine the potential influence of this addition they were inserted through PCR. The original 'gtg' START of MT0399 was changed to 'atg'.

Primers CDC1551ac-forw and myco0386/B-C-Hrev were used. PCR conditions: Ta= 58°C, 5% DMSO and 30 cycles. The AC domain in pQE30 was the template. The 564 bp PCR product obtained was purified from agarose gel, digested with BamHI and HindIII and directly ligated with suitably prepared pQE30 vector. After transformation into XL-1 blue cells, it was controlled by sequencing. Finally, it was transformed into BL21 cells for expression.

### **3.6.3.8 N-terminally elongated AC domain (with C-terminal His-tag)**

The PCR product was amplified with primers CDC1551ac-forw and myco0386/cata/C-His. PCR conditions: Ta= 58°C, 5 % DMSO, 30 cycles and AC domain in pQE30 as template. The product (564 bp) was purified, digested with BamHI and BglII and ligated into a dephosphorylated pQE60 vector  $\Delta$ (BamHI/BglII). After transformation into XL-1 blue cells clones were sequenced. Finally, it was transformed into BL21 cells for expression.

### **3.6.3.9 C-terminally His-tagged AC catalytic domain of Rv0386**

With primers myco0386/B-C-Hforw and myco0386/cata/C-His the AC catalytic domain was amplified. PCR conditions: Ta= 58°C, 5% DMSO and 30 cycles. The AC domain in pQE30 was the template. The 543 bp PCR product was purified from agarose gel, digested with BamHI and BglII and directly ligated into suitably prepared pQE60. After transformation into XL-1 blue cells, it was controlled by sequencing. Finally, it was transformed into BL21 cells for expression.

### **3.6.3.10 AC domain mutant R7G**

This mutant was unintentionally constructed due to a wrong nucleotide in the primer myco0386/B-C-Hforw. This changed nucleotide introduced a mutation by changing a C

in the codon **CGG** (codes for arginine) into a G forming the wrong codon **GGG** (codes for glycine). This mutant was cloned presuming that it was the catalytic domain wild type (see above).

## **3.7 Protein chemistry methods**

### **3.7.1 Expression of proteins in *E. coli***

Most proteins were expressed in *E. coli* BL21 (DE3) [pREP4]. Rv0386 holoenzyme and its transcription factor as well as its ATPase domain were also expressed in *E. coli* BL21 STAR (DE3) [pREP4]. In *E. coli* Rosetta [pREP4] cells only the holoenzyme Rv0386 was expressed.

#### **3.7.1.1 Pre-cultures**

For expression in BL21 [pREP4], BL21 STAR [pREP4] and Rosetta [pREP4] cells, 5 ml of LB-broth with 50 µg/ml kanamycin and 100 µg/ml ampicillin were inoculated. With a sterile tip a small amount of the frozen glycerol stock culture was inoculated and incubated O/N at 37 °C (210-230 rpm).

#### **3.7.1.2 Expression**

All mammalian, protozoan and mycobacterial constructs were expressed in *E. coli* BL21 [pREP4] from frozen stocks. Mycobacterial Rv0386 constructs were also expressed in *E. coli* BL21 STAR and ROSETTA. 5 ml pre-culture were inoculated and grown in 200 ml LB broth containing 100 µg/ml ampicillin and 50 µg/ml kanamycin (30°C, 220 rpm) to  $A_{600}$  0.4-0.6 (approx. after 1.5-3 h). Expression of the mammalian, protozoan and Rv1625c mycobacterial proteins was induced with 30 µM IPTG and Rv0386 proteins with 60 µM IPTG (22-25°C for BL21 or 12-16°C for STAR and ROSETTA, 220 rpm). Cells were harvested after 3-5 h for constructs in BL21 cells or after 16-18 h for constructs in BL21 STAR and ROSETTA cells (10 min, 5000 x g, 4°C). Supernatant was discarded and the pellet washed with 30 ml Pellet Wash Buffer and centrifuged again (6000 x g, 15-20 min, 4 °C). Cell pellets were then stored at -80°C.

### **3.7.2 Purification of soluble proteins from *E. coli***

Frozen -80°C pellets were thawed on ice (10 min), suspended in 25 ml of Cell Lysis buffer and sonificated for lysis (microtip setting 4, on ice, 3 x 10 s). These suspensions were called cell homogenate. For mammalian ACs lysis buffer contained protease inhibitors (76 nM aprotinin, 62.5 µM TPCK, 59.6 µM TLCK, 126.3 µM PMSF and 0.16 µM lima bean trypsin inhibitor). The cell homogenate was centrifuged (16,000 x g, 30 min, 4°C). Occasionally, lysozyme (0.2 mg/ml, on ice, 30 min) and DNase (0.02 mg/ml with 5 mM MgCl<sub>2</sub>, on ice, 30 min) were added prior to centrifugation. The supernatant and the pellet were separately tested for AC activity.

Supernatants were mixed with 250 mM NaCl and 15 mM imidazole. Then 250 µl of pre-equilibrated Ni<sup>2+</sup>-NTA-Agarose were added (rocking for at least 1 h on ice). Samples were centrifuged (5 min, 2500 x g). Supernatant was transferred into a 10 ml syringe with a Wizard mini-column attached. The solution was let through and the resin was then washed with 3 ml of each of Washing buffers A, B and C. Elution was performed with 400 µl Elution Buffer.

### **3.7.3 Purification of insoluble proteins from *E. coli***

Frozen -80°C pellets were thawed on ice (10 min), suspended in 25 ml cell lysis buffer containing Complete<sup>®</sup> protease inhibitors (1/2 tablet) and passed twice through the french press for cell lysis (20,000 psi). The homogenate was centrifuged (4°C, 3000 x g, 30 min). The pellet from this step was suspended in 500 µl lysis buffer to be analysed later. The supernatant was centrifuged (4°C, 100,000 x g, 1 h). Supernatant was discarded and the pellet was suspended in 25 ml of membrane suspension buffer containing 2 % CHAPS (or other detergent) and incubated on ice for 1 h with gentle agitation. The membrane suspension was centrifuged (4°C, 100,000 x g, 1 h). The pellet was suspended in 500 µl of membrane suspension buffer. Supernatant was mixed with 15 mM imidazole pH 8.0 and incubated O/N with gentle agitation with 200 µl Ni-NTA-agarose (pre-equilibrated with 2 % CHAPS). Ni-NTA bound protein was washed and eluted. Two washing steps were made, the first with 6 ml of High Saline Buffer and the second one with 6 ml of Low Saline Buffer. Finally, the protein was eluted with 400 µl of Elution Buffer. Each washing fraction was stored and analysed later.

### **3.7.4 Protein concentration**

#### **3.7.4.1 Bio-Rad protein determination**

1 mg/ml of BSA was used as a standard. 1-10 µg of protein were pipetted to 800 µl distilled water and mixed. 200 µl of Dye Reagent Concentrate (5X) were added and mixed. Samples were measured at OD<sub>595</sub>. The presence of ≤ 2% of the detergent CHAPS did not interfere.

#### **3.7.4.2 Dialysis**

To eliminate imidazole from the eluate and change buffer samples were dialyzed (VISKING Dialysis Tubing, MWCO12000-14000). The DNA-binding domain of Rv0386 (~12000 Da) was dialyzed with a SPECTRAPOR membrane (MWCO 3500). Samples were dialyzed at least for 3 hours at 4°C.

#### **3.7.4.3 Sample Concentration**

To produce antibodies against the Rv0386 DNA-binding domain (made by BioGenes) and to carry out the crystallization experiments with the Rv0386 AC domain, concentration of proteins was required. Samples were centrifuged until the desirable protein concentration was achieved (4 °C, 2500-3500 x g, 2-4 h, CENTRICON Centrifugal Filter Devices MWCO 10000). For crystallization, samples were centrifuged with the Nanosep 10K Omega centrifugal devices MWCO 10000 (14,000 x g, 4°C, 10-30 min).

### **3.7.5 SDS-polyacrylamide gel electrophoresis (SDS-PAGE)**

An electrophoresis apparatus from HOEFER was used. In Tables 3.10 a and b the recipe for polyacrylamide gels and the effective separation range of proteins are shown:

**a**

<b>Resolving Gel (pH 8.8)</b>	<b>7.5 %</b>	<b>10 %</b>	<b>12.5 %</b>	<b>15 %</b>
Resolving Gel buffer	3 ml	3 ml	3 ml	3 ml
H <sub>2</sub> O	6 ml	5 ml	4 ml	3 ml
Acrylamide/Bisacrylamide 37.5 : 1	3 ml	4 ml	5 ml	6 ml
TEMED	10 µl	10 µl	10 µl	10 µl
APS 10 %	80 µl	80 µl	80 µl	80 µl
<b>Effective Separation Range (kDa)</b>	<b>45 - 200</b>	<b>20 - 200</b>	<b>14 - 70</b>	<b>5 - 70</b>

**b**

<b>Stacking Gel (pH 6.8)</b>	<b>4 %</b>
Stacking Gel buffer	1 ml
H <sub>2</sub> O	2.4 ml
Acrylamide / Bisacrylamide 37.5 : 1	0.6 ml
TEMED	10 µl
APS 10 %	40 µl

**Table 3.10:** (a) Components required for different concentrations (%) of resolving gels for SDS-PAGE; (b) components of the stacking gel.

Soluble protein samples were mixed with 1X sample buffer and pellets and cell homogenates with 4X sample buffer. Usually, they were heated at 95 °C for 5 minutes before loading. Gels were run at a constant current: 20 mA, 200 V for 50-65 minutes. Gels were stained with Coomassie Blue for 30 min with gentle agitation. After destaining 0.1 to 0.5 µg protein/band was detectable.

Usually, SDS-PAGE was performed simultaneously with pellets and supernatants of *E. coli* containing an empty vector (pQE30) as a control. Protein Marker components (10 µl contained 1 µg of each protein) are listed below.

Protein Marker	MW (kDa)	peqGold Marker	MW (kDa)
Cytochrom C	12.5	Lysozyme	14.4
Trypsin Inhibitor	20.1	$\beta$ -Lactoglobulin	18.4
Chymotrypsinogen A	25	RE Bsp981	25
GAPDH	36	Lactate dehydrogenase	35
Ovalbumin	45	Ovalbumin	45
BSA	66	Bovine Serum Albumin	66
		$\beta$ -Galactosidase	116

### 3.7.6 Anion exchange chromatography

The holoenzyme Rv0386 and its catalytic domain were additionally purified with anion exchange chromatography with an ÄKTA FPLC at 4 °C. All buffers were made with MilliQ water, filtrated and degassed. Protein was measured at 280 nm. All fractions were tested for AC activity. About 1.4 mg (800  $\mu$ l) catalytic domain protein or 0.3 mg (800  $\mu$ l) holoenzyme diluted to 10 ml with respective “A” buffers (see Table 3.11), were applied through a 10 ml loop to a pre-equilibrated column (Mono Q).

Protein	pI	Buffer A	Buffer B
Catalytic domain Rv0386	6.6	50 mM Tris pH 8.0 2 mM $\beta$ -mercapto ethanol 10 % glycerol	Buffer A + 1 M NaCl
Holoenzyme Rv0386	5.8	50 mM Tris pH 7.0 10 mM $\beta$ -mercapto ethanol 2 mM MgCl <sub>2</sub> 20 % Glycerol	1 M NaCl

**Table 3.11:** Compositions of buffer A and buffer B used for anion exchange chromatography of the catalytic domain and the holoenzyme Rv0386. pI= isoelectrical point.

Columns were developed with a stepwise NaCl gradient. Flow rate was 1 ml/min. Elution began at 0% NaCl (only buffer A) for 3 fractions of 5 ml. After that fractions were 1 ml. After 10 fractions the NaCl concentration was increased (100, 200, 300, 400, 500 mM and 1 M NaCl steps). 70 fractions were collected.

### 3.7.7 Cyclase enzyme tests

They were carried out according to Salomon et al., 1974, and Steinlen, 1988.

### 3.7.7.1 Adenylyl cyclase test

A standard test contained in 100  $\mu\text{l}$  75  $\mu\text{M}$  [ $\alpha$ - $^{32}\text{P}$ ]-ATP (25 kBq, 30 °C, 10 min). 40  $\mu\text{l}$  of protein sample including reagents like forskolin, inhibitors or detergents was mixed with 50  $\mu\text{l}$  of AC Test Cocktail. The assay was started with 10  $\mu\text{l}$  of AC-Start solution. Final concentrations were: 50 mM buffer (Tris-HCl pH 7.5 or MOPS pH 7.5), 22 % glycerol, 2-5 mM  $\text{MnCl}_2$  or 5-10 mM  $\text{MgCl}_2$ , 2 mM [2,8- $^3\text{H}$ ]-cAMP (100 Bq), 3 mM creatine phosphate and 1 U creatine kinase (the latter as an ATP-regenerating system when testing impure protein samples). [2,8- $^3\text{H}$ ]-cAMP was used as an internal standard.

The reaction was stopped by addition of 150  $\mu\text{l}$  stop buffer. Water was added to 1 ml and the mixture was applied to a Dowex column (9 x 1 cm glass column with 1.2 g Dowex 50). After washing with 3 ml water the samples were eluted with 5 ml water on  $\text{Al}_2\text{O}_3$  columns (10 x 0.5 cm plastic column with 1 g active, neutral  $\text{Al}_2\text{O}_3$  90). Samples were immediately eluted with 4.5 mL 0.1 M Tris-HCl pH 7.5, mixed with 4 ml Ultima Gold XR Scintillator Solution and counted. Dowex columns were regenerated with 1 x 5 ml HCl (2N), 1 x 10 ml and 1 x 5 ml water, and  $\text{Al}_2\text{O}_3$  columns with 2 x 5 ml Tris-HCl pH 7.5 (0.1 M). Specific activity ( $A = \text{pmol}\cdot\text{mg}^{-1}\cdot\text{min}^{-1}$ ) was calculated with the following formula:

$$A = \frac{\text{Substrate } (\mu\text{M}) \times 100 \mu\text{l}}{\text{Time (min)}} \times \frac{1000}{\text{Protein } (\mu\text{g})} \times \frac{\text{cpm } [^3\text{H}]_{\text{total}}}{\text{cpm } [^3\text{H}]_{\text{sample}} - 3\% [^{32}\text{P}]_{\text{sample}}} \times \frac{\text{cpm } [^{32}\text{P}]_{\text{sample}} - \text{cpm } [^{32}\text{P}]_{\text{blanc}}}{\text{cpm } [^{32}\text{P}]_{\text{total}}}$$

The subtraction of 3 % of the phosphorous counts from the tritium value for each sample was made because of spillover of  $^{32}\text{P}$  into the tritium channel. For AC reconstitution assays where proteins were mixed at different concentrations the lowest one was used for calculations. Activities lower than double background (in cpm) were considered zero.

### **3.7.7.2 Guanylyl cyclase test**

Assays were carried out simultaneously with an AC test for comparison. The same protocol used for AC tests was used with [8-<sup>3</sup>H]-cGMP (100 Bq) contained in the GC Test Cocktail and 75 μM [α-<sup>32</sup>P]-GTP (25 kBq) as a substrate. The Dowex columns for GC test contained 4 g of this material, and the Al<sub>2</sub>O<sub>3</sub> columns 0.8 g. The elution of the Dowex columns was with 2 ml water (after a washing step with 3 ml water) and of the Al<sub>2</sub>O<sub>3</sub> columns with 4 ml 0.1 M Tris-HCl pH 7.5. Regeneration of the Dowex columns was with 1 x 5 ml 2 N HCl, 1 x 10 ml water and 1 x 5 ml with water, the Al<sub>2</sub>O<sub>3</sub> columns were washed with 2 x 4 ml 0.1 M Tris-HCl pH 7.5. The calculation of the enzymatic activity was carried out as above.

### **3.7.8 Production of specific antibodies**

Production of antibodies against the AC domain (KD0386) and the DNA-binding domain (DB0386) of Rv0386 was done by BioGenes (Berlin) using purified proteins dialyzed against 50 mM phosphate buffer (10 % glycerol, filtered). Specific IgG anti-KD0386 were delivered in Tris-Glycin-Buffer pH 7.5 containing 0.02% Thimerosal. Specific IgG anti DB0386 were delivered in Tris-Glycin-Buffer pH 7.5, 250 mM NaCl and 0.02% Thimerosal. The sensitivity and specificity of the antibodies were tested through Dot-Blot and Western-Blot, respectively.

#### **3.7.8.1 Dot Blot**

This was used to determine the optimal concentrations for subsequent binding assays. A set of serial dilutions of the purified protein (concentrations of 0.1 ng to 1 μg pro spot) were applied to a Protran nitrocellulose membrane. The membrane was then incubated with different dilutions in M-TBS of the antibodies and developed as described for Western blotting.

#### **3.7.8.2 Western Blot**

Samples were separated by SDS-PAGE. The Semi-Dry-Electrotransfer method of Towbin et al. (1979) was used. At the end of the electrophoresis the gel was removed and attached to a PVDF membrane, which were soaked for 10 min in methanol, 10 min in water and 10 min in Towbin buffer. Gel and membrane were sandwiched between



pieces of Whatman 3 MM paper soaked in Towbin buffer. The sandwich was then placed between graphite plate electrodes with the transfer membrane on the anodic side. A current of 2-3 mA/cm<sup>2</sup> of gel (20 V) was applied for 2-3 hours. The gel was stained with Coomassie Brilliant Blue. The transfer membrane was stained with Ponceau S for no longer than 5 minutes. When protein was visible the membrane was destained by washing with deionized water and the positions of proteins were marked with a pencil. The membrane was then incubated for 1 hour at RT in M-TBS blocking solution. The membrane was rinsed twice for 5 min with TBS-T buffer and then incubated for 1 h with the primary antibody solution (mouse monoclonal RGS-His antibodies, antibodies anti-KD0386 or antibodies anti-DB0386, in M-TBS diluted). The primary antibody was then discarded and the membrane rinsed once for 15 minutes and twice for 5 minutes with TBS-T. The membrane was incubated immediately with the secondary antibody solution (goat anti-mouse or goat anti-rabbit horseradish peroxidase conjugated antibodies, in M-TBS diluted). After 1 hour the secondary antibody was discarded and the membrane washed with TBS-T (see above). For chemiluminescence a mixture of 2 ml solution A and 50 µl solution B of the ECL-Plus Western Blotting Detection Kit was prepared. The mixture was uniformly distributed over the whole surface of the membrane. After a 5 min reaction a film exposure with Hyperfilm-ECL was taken. Exposure periods varied from 10 seconds to 10 minutes.

### **3.7.9 Crystallization**

Within the scope of this study conditions for crystallization and first attempts to optimize the obtained crystals of the Rv0386 catalytic domain were made. The hanging drop vapor diffusion technique (Figure 3.12) and the 24 well plates of Hampton Research were used.

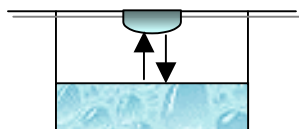


**Fig. 3.12:** Scheme of the hanging drop method where drops are prepared on a siliconized microscope glass cover slip by mixing the protein sample and the precipitant solution. The cover slip is placed over a small well (reservoir) containing the precipitating solution. The drop and the liquid reservoir of reagent are placed in vapor equilibration.

The reagent kits Crystal Screen, Crystal Screen 2 and Crystal Screen Lite of Hampton Research were used. For crystallization of Rv0386<sub>(1-175)</sub> with N-terminal His-tag the set of Crystal Screen buffers 4-6, 8-20, 22, 25, 27, 29-41, 43, 45, and 47-50 were used. The buffers 1-3, 6-11, 14, 16, 19, 22, 23, 28-30 and 39-46 of the set Crystal Screen 2 were also used. Finally the buffers 4-10, 13, 14, 16, 17, 19, 22, 23, 25-29, 31, 36, 41, 43, and 47-50 of the set Crystal Screen Lite were utilized. In the case of Rv0386<sub>(1-175)</sub> with C-terminal His-tag, all buffers of the three screening sets were examined with the protein dialyzed after Ni-NTA purification in glycerol dialysis buffer. All further optimization steps were performed only with the protein Rv0386<sub>(1-175)</sub> with N-terminal His-tag.

The crystallization variables that were examined for optimization were: glycerol, buffer system in the sample solution and its pH, protein concentration, composition of the precipitant solution, temperature of incubation, proportions of the components in the drop mixture, protein sample purification steps and addition of substrates, inhibitors, cofactors and other substances.

Protein sample solutions were dialyzed against glycerol dialysis buffer (10 and 20% glycerol) containing different buffer systems like MOPS, Tris-HCl and HEPES with pH's 7.5 and 8.5 and then stored at  $-20^{\circ}\text{C}$ ,  $15^{\circ}\text{C}$ ,  $4^{\circ}\text{C}$  and RT. All these conditions were examined for stability tests by testing the AC activity. Conditions where the protein showed no aggregation and less lost of AC activity were examined in the crystallization screens. Protein samples were centrifuged by 14,000 rpm at  $4^{\circ}\text{C}$  for 30 min before setting the crystallization experiments to remove aggregates and amorphous debris. For the first screenings 1  $\mu\text{l}$  of protein sample (protein concentration between 5 and 11  $\mu\text{g}/\mu\text{l}$ ) was mixed with 1  $\mu\text{l}$  of each screening buffer (drop mixture 1:1). In the reagent reservoir 0.5 ml of the precipitant solution were mixed with glycerol until obtaining a

concentration of about 2-5% more than the glycerol present in the drop mixture. The 24 well plates were incubated at 12 and 16°C and examined under a polarization microscope.

After obtaining the first crystals the components of the successful precipitant solutions were varied to optimize form, amount and size of the crystals. The protein concentration of the sample was also varied (increased upto 30 µg/µl) and the composition of the drop mixture (proportions 2:1, 1:2, 3:1, 1:3 of protein:precipitant were examined). Ni-NTA purified protein further purified with anion exchange chromatography was also examined for crystal formation. Additions of Mn<sup>2+</sup> or Mg<sup>2+</sup>, nucleotides like ATP (substrate), GTP (substrate) or CTP, P-site inhibitors, cGMP and cAMP analogs were examined for optimization.

## 4 Results

### 4.1 Chimeras of *M. tuberculosis* Rv1625c mutants with mammalian adenylyl and *Paramecium* guanylyl cyclases

#### 4.1.1 Introductory remarks

Biochemical and mutational studies showed that the mycobacterial AC Rv1625c forms a homodimer where two identical and equivalent catalytic sites are generated (Guo et al., 2001). The possibility to make reconstitutions between mutated mycobacterial and mammalian cytosolic monomers as well as with *Paramecium* GC (ParaGC) monomers was examined (Fig. 4.1 and 4.2). From *M. tuberculosis* the mutants Rv1625<sub>C204-443</sub>R376A and D300A from Dr. Guo and Rv1625<sub>C204-443</sub>N372A, N372T and D300S (generated here) were used. The mammalian cytosolic domains, the C2 region of ParaGC and its triple mutant ParaGC-C2 KWQ were from Hoffmann, 1999 (Table 4.1).

Name	Domain (function)	Amino acid position	Origin
AC I	C1 (C1)	304-519	Bovine
AC II	C2 (C2)	848-1114	Rat
AC V	C1 (C1)	403-647	Rabbit
AC VII	C1 (C1)	220-486	Bovine
AC IX	C1 (C1) C2 (C2)	323-570 1012-1355	Mouse
Rv1625c wild type D300A* D300S* R376A* N372A* N372T*	C (C1+C2) C (C2) C (C2) C (C1) C (C1) C (C1)	204-443	<i>M. tuberculosis</i>
ParaGC-C2 ParaGC-C2-KWQ**	C2 (C1) C2 (C1)	2178-2415	<i>Paramecium</i>
*Point mutants of <i>M. tuberculosis</i> Rv1625c AC domain.			
* **Triple mutant <sub>2345</sub> LVR <sub>2347</sub> to <sub>2345</sub> KWQ <sub>2347</sub> of <i>Paramecium tetraurelia</i> guanylyl cyclase.			

**Table 4.1:** Cytoplasmic domains used in this work (Hoffmann T.R., 1999; Guo et al., 2001).

**a**

```
                                     Me
                                     ↓
Rv1625c    231 : IAERLKEPE-----RNIIADKYDEASVLFADIVGFTERASSTAPA
IC1_BOV    304 : -----VSILFADIVGFTGLASQCTAQ
VC1_RABBIT 451 : INAKQEDM-----MFHKIYIQKHDNVSILFADIEGFTSLASQCTAQ
VIIC1_BOV  249 : IIERLKERGDRRYLPDNNFHNLVYKRHNVSILYADIVGFTRLASDCSPK
IXC1_MOU   368 : --NRKKSSIQK--APIAFRPFKMQQIEEVSILFADIVGFTKMSANKSAH
ParaGC-C2  2207 : -----LEEFFRPNEEKRVLREQADEVTLLFADIAGFTEYSKVKQPE
```

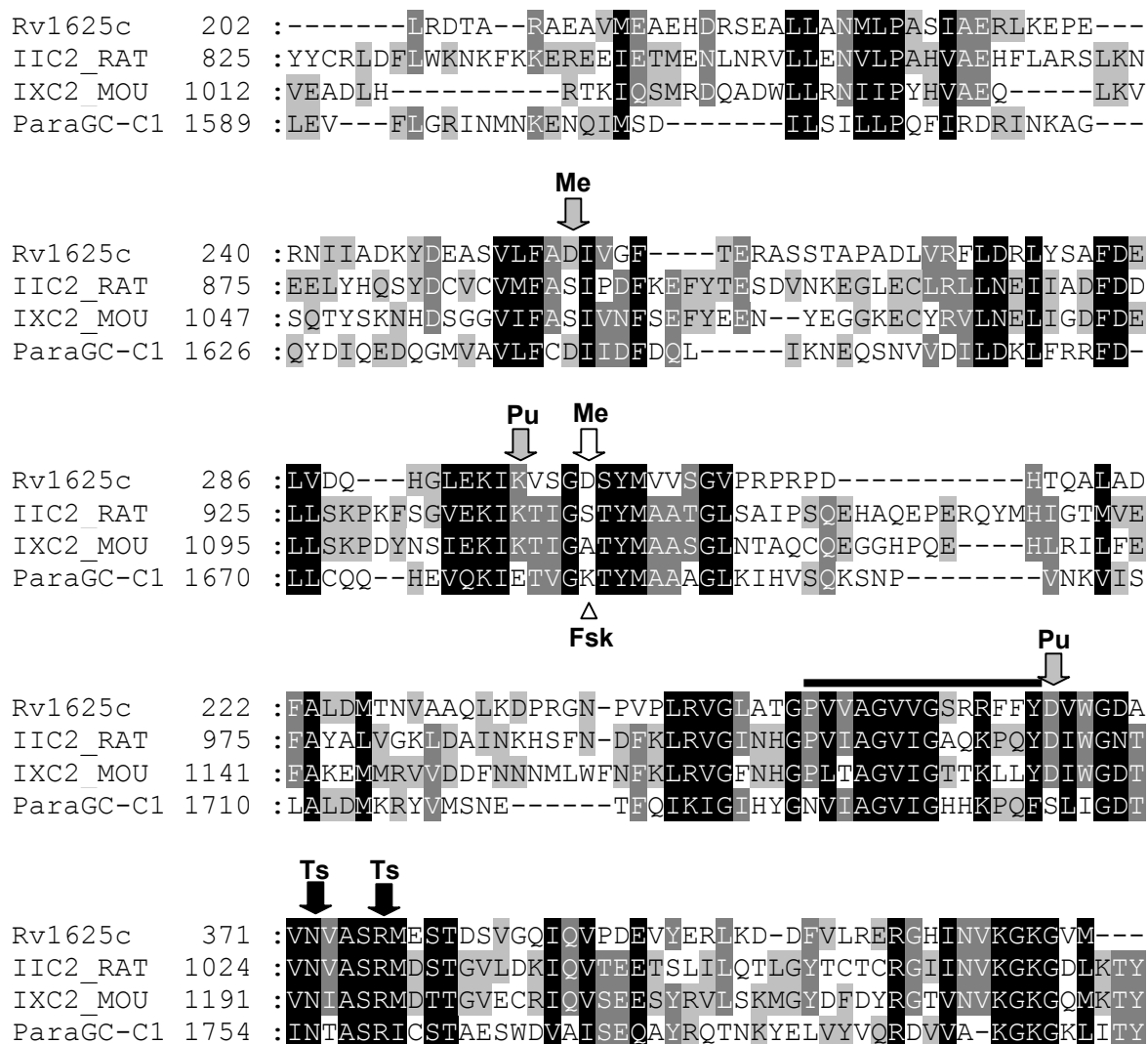
```
                                     Pu  Me
                                     ↓   ↓
Rv1625c    271 : DLVRFLDRLYSADFDELVDQHGLEKIKVSGDSYMVVS-----GVPRPRPD
IC1_BOV    325 : ELVKLLNELFGKFDELATENHCRRIKILGDCYCVS-----GLTQPKTD
VC1_RABBIT 492 : ELVMTLNELEFARFDKLAENHCLRIKILGDCYCVS-----GLPEARAD
VIIC1_BOV  299 : ELVVVLNELEFGKFDQIAKANECMRIKILGDCYCVS-----GLPVSLPN
IXC1_MOU   414 : ALVGLLNDLEGRFDRLECEQTKCEKISTLGDCYCVVA-----GCPEPRAD
ParaGC-C2  2248 : QVNMRLRNLETFEDKNSLLHNVFKLYTIGDCYVVMGMVDYGKGIQRNPSQ
```

```

Rv1625c    315 : HTQALADFALDMTNVAAQLKDPRGNP-VPLRVGLATGPPVAVGVGSRRF
IC1_BOV    369 : HAHCCVEMGLDMIDTITSVAEATEVD-LNMRVGLHTGRVLCGVLGLRQW
VC1_RABBIT 536 : HAHCCVEMGMDMIEAISLVREVTGVN-VNMRVGIHSGRVHCGVLGLRQW
VIIC1_BOV  343 : HARNCVKMGLDMCEAIKQVREATGVD-ISMVGIHSGNVLCGVIGLRQW
IXC1_MOU   458 : HAYCCIEMGLGMIKAIQFCQEKEM-VNMRVGVHTGTVLCGILGMRRFK
ParaGC-C2  2298 : EAVNVVRMGFAMIDAIRRVRAHINHPTLDMRIGVHTGSIIGVVLGTELV
```

```
                                     Pu  Ts  Ts
                                     ↓   ↓   ↓
Rv1625c    364 : YDVWGDVNVASRMESTDSVGOIQVPDEVYERLKDDFVLRERGHINVK-G
IC1_BOV    418 : YDVWSNDVTLANVMEAGLPGKVHITKTTLACLNGDYEV-EPGHGHER--
VC1_RABBIT 585 : FDVWSNDVTLANHMEAGGKAGRIHITKATLNYLNGDYEV-EPGCGGER--
VIIC1_BOV  392 : YDVWSDVSLANRMEAGVPGRVHITEATLKHLDKAYEV-EDGHGQQR--
IXC1_MOU   507 : FDVWSNDVNLANLMEQLGVAGKVHISEATAKYLDREYEM-EDGRVIERLG
ParaGC-C2  2348 : YDIYGPDVLIANKMESKGAKGFVQVSQETKDIIFERE-----
                                     Δ
                                     Fsk
```

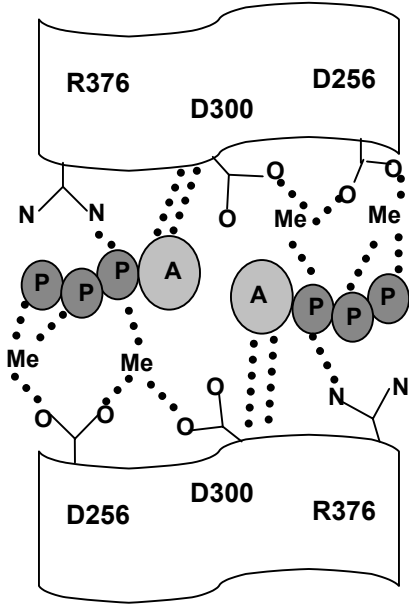
**b**



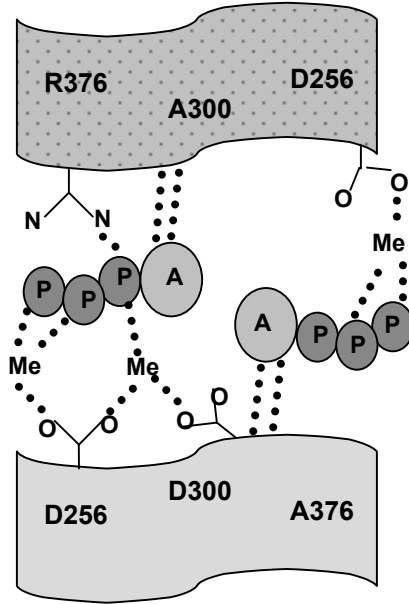
**Fig 4.1: a)** Alignment of the catalytic domain of Rv1625c with the cytosolic C1 loop from bovine AC type I (IC1), rabbit AC type V (VC1), bovine type VII (VIIC1), mouse type IX (IXC1) and with the cytosolic C2 loop from the *Paramecium* GC. **b)** Alignment of the catalytic domain of Rv1625c with the cytosolic C2 loops from rat AC type II (IIC2), mouse type IX (IXC2) and the C1 domain from the *Paramecium* GC. Me= metal-cofactor binding; Pu= purine-specifying; Ts= transition state stabilizing; Fsk= forskolin-binding. Conservation scale: inverted (80-100%), dark gray (60-80%), gray (40-60%). The top bar specifies the “arm region” (sequence between a conserved G and the downstream adenine-specifying residue in ACs). Boxed residues are the AC-specific dimer-formation stabilizing motif (KWQ) and its corresponding motif in *Paramecium* and *Mycobacterium*.

**A**

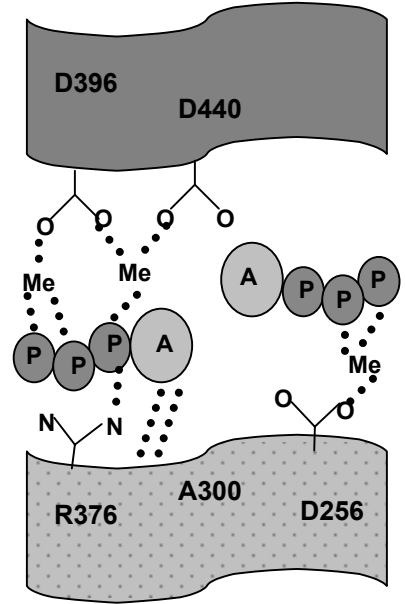
Rv1625c  
wild type homodimer

**B**

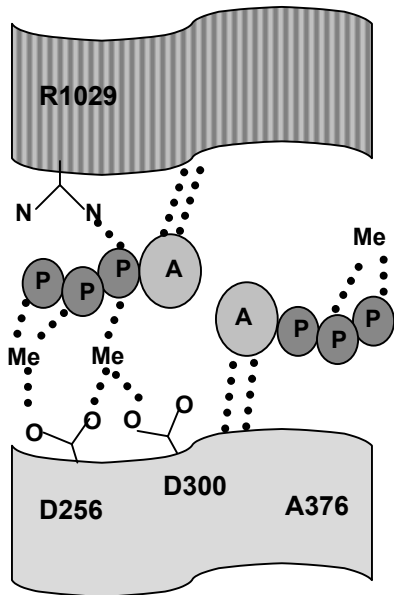
D300A + R376A

**C**

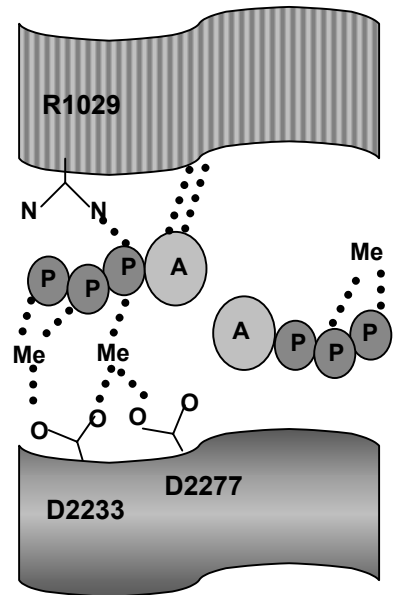
ACV C1 + D300A

**D**

ACII C2 + R376A

**E**

ACII C2 + ParaGC C2

**F**

D300A + ParaGC C2

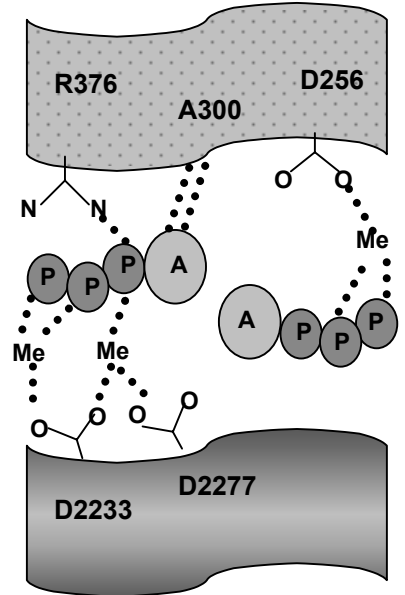


**Fig. 4.2:** (A) Graphic representation of the homodimeric catalytic center of the mycobacterial Rv1625c AC forming two catalytic sites (adapted from Guo et al., 2001). Residues D256, D300 and R376 are outlined; binding of the adenine ring A is indicated by dotted lines. (B) Heterodimer with only one catalytic site from the reconstitution of Rv1625c mutant monomers D300A with R376A. (C to F) Symbolized heterodimers between mycobacterial D300A and the C1 domain from canine type V; mycobacterial R376A reconstituted with C2 from rat type II; *Paramecium* GC C2 domain reconstituted with mycobacterial D300A and with the C2 domain from rat type II. P= phosphate; Me= divalent metal cation.

#### 4.1.2 Expression and purification of mammalian, mycobacterial and *Paramecium* ACs

The cytosolic domain constructs of the mammalian AC's IC1, VC1, VIIC1, IXC1, IIC2 and *Paramecium* GC (Hoffmann, 1999) as well as the mycobacterial Rv1625c cytosolic domain mutants D300A and R376A (Guo et al., 2001) were available as glycerol stock in BL21 cells. Total amount of protein obtained after purification based on 600 ml culture were: 200 µg of IC1, VC1 and IXC1; 300 µg of VIIC1, IIC2 and ParaGC-C2; 500 µg of ParaGC-C2 KWQ mutant; and 3 mg of D300A and R376A (Fig. 4.3).

The mammalian monomers considerably lost activity after 3 days of storage with 50% glycerol. An example is the chimera VIIC1/IIC2 which had only a residual specific activity of 0.14 nmol·mg<sup>-1</sup>·min<sup>-1</sup> (about 6%) [Table 4.2]. Therefore assays were carried out within hours after elution from the affinity resin. Mycobacterial mutants D300A and R376A were stable at -20°C with 50% glycerol. *Paramecium* ParaGC-C2 and ParaGC-C2-KWQ mutant also lost most of their activity after only 4 days of storage with 50% glycerol. The chimera ParaGC-C2/D300A retained only 11% from its activity after 4 days (6.5 nmol·mg<sup>-1</sup>·min<sup>-1</sup>; Table 4.3).

The three point mutants Rv1625C<sub>204-443</sub>N372T, N372A and D300S were expressed in BL21 cells. After Ni<sup>2+</sup>-NTA purification (addition of 20 µg/ml DnaseI after sonification was omitted) and dialysis with glycerol dialysis buffer (to remove excess imidazole) pure proteins were obtained. All mutants were expressed in good quantities, after purification about 1 mg protein was purified from 600 ml culture (Fig. 4.4).

They were stable at -20°C with 20% glycerol.



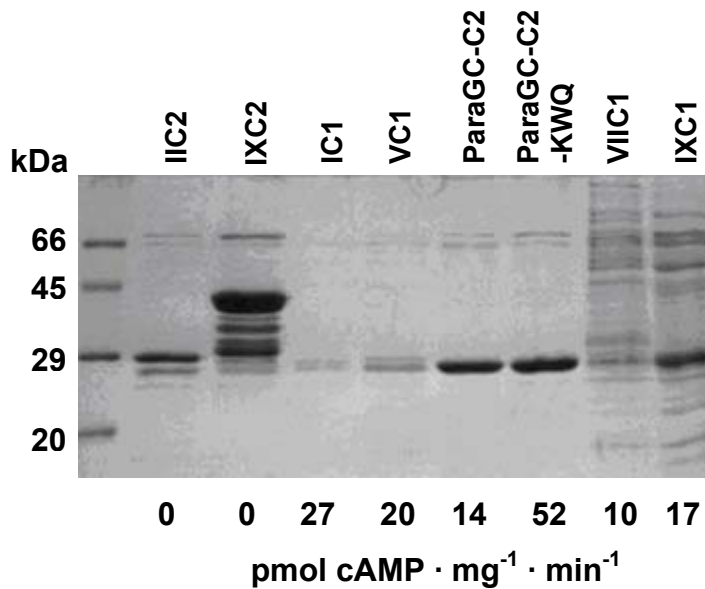


**Fig. 4.3:** 15% SDS-PAGE analysis of the purified mammalian and *Paramecium* soluble cyclases (Coomassie blue staining). Applied were: about 7-9  $\mu$ g of IIC2 (29kDa), ParaGC-C2 (29kDa) and ParaGC-C2-KWQ (29kDa); 12-16  $\mu$ g of IXC2 (36kDa), IC1 (27kDa), VC1 (27kDa), VIIC1 (29kDa) and IXC1 (29kDa). Molecular mass standards are on the left. The specific activities indicated below each lane were determined with 75  $\mu$ M ATP at 4  $\mu$ g IC1 (1.5  $\mu$ M), 8  $\mu$ g VC1, ParaGC-C2 and C2-KWQ (3  $\mu$ M), 7  $\mu$ g IIC2 and IXC2 (2.5 and 2  $\mu$ M), 11  $\mu$ g IXC1 (4  $\mu$ M) and 15  $\mu$ g VIIC1 (5  $\mu$ M) protein/assay.

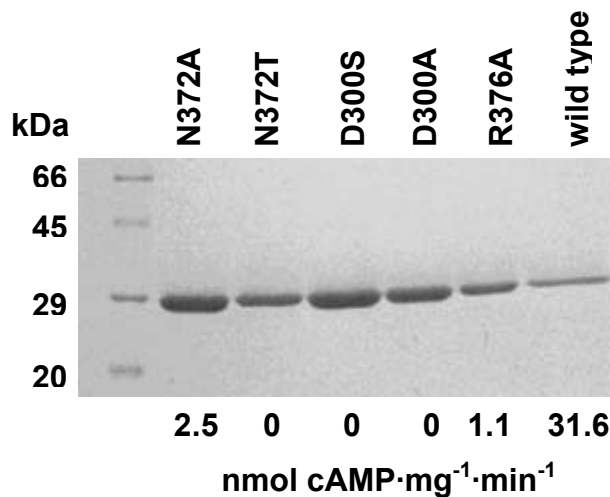


**Fig. 4.4 :** Purification and activity of all mutants of *Mycobacterium* Rv1625<sub>C204-443</sub> used in this work (SDS-PAGE analysis, Coomassie blue staining). The catalytic domain wild type is also present on the gel. All proteins were Ni<sup>2+</sup>-NTA purified and dialyzed. About 1-2  $\mu$ g of each protein were applied. Molecular weight marker is shown on the left. All mutants have a molecular weight of about 27 kDa like the wild type. The specific activities indicated below each lane were determined with 75  $\mu$ M ATP (30°C, 10 min) at a protein concentration of 0.1  $\mu$ g/assay (40 nM).

### 4.1.3 Mammalian/*Mycobacterium* chimeras

The reconstitution of mammalian/mammalian monomers and of R376A with D300A (Guo et al., 2001) were used as a control. In most cases it was not possible to reconstitute robustly active heterodimeric catalytic complexes from mammalian monomers with the mycobacterial mutants. The low activities obtained were  $\ll 1\%$  in comparison to that of the mycobacterial R376A/D300A chimera. Mutants D300S and N372T (generated to investigate the lack of forskolin stimulation of Rv1625c) in conjunction with mammalian monomers could not be stimulated by forskolin. Forskolin stimulation and cofactor dependence of chimera R376A/IIC2 were further investigated (not shown). Activity of this chimera was not detectable with  $Mg^{2+}$  as a cofactor and an insignificant stimulation with forskolin was observed.

Chimeras	$\mu M$ in the assay ( $\mu g$ )	specific activity $nmol \cdot mg^{-1} \cdot min^{-1}$ (cpm)	specific activity with forskolin $nmol \cdot mg^{-1} \cdot min^{-1}$ (cpm)
IC1 / IIC2 <sup>a</sup>	1.5 / 2.5 (4 / 7)	0.1 (629)	0.5 (2051)
VC1 / IIC2 <sup>c</sup>	3 / 2.5 (8 / 7)	0.1 (813)	0.5 (3500)
VIIC1 / IIC2 <sup>c</sup>	5 / 2.5 (15 / 7)	2.5 (12672)	2.7 (26731)
IXC1 / IIC2 <sup>a</sup>	3.7 / 3.7 (11 / 11)	0.04 (563)	0.03 (366)
IC1 / D300A(C2) <sup>b</sup>	5 / 1.6 (13 / 4)	0.2 (1116)	not done
VC1 / D300A(C2) <sup>b</sup>	5 / 1.6 (14 / 4)	0.1 (526)	not done
VIIC1 / D300A(C2) <sup>b</sup>	5 / 1.6 (15 / 4)	0.1 (596)	not done
IXC1 / D300A(C2) <sup>b</sup>	3.8 / 1.6 (11 / 4)	0.8 (643)	not done
IC1 / D300S (C2) <sup>b</sup>	3 / 1.6 (9 / 4)	not detectable	not detectable
VC1 / D300S (C2) <sup>b</sup>	3 / 1.6 (9 / 4)	not detectable	not detectable
R376A(C1) / IIC2 <sup>a</sup>	0.4 / 5 (1 / 14)	9.4 (14432)	not done
N372A (C1) / IIC2 <sup>b</sup>	0.16 / 2.5 (0.4 / 7)	1.6 (711)	1.3 (538)
N372A (C1) / IXC2 <sup>b</sup>	0.16 / 1.9 (0.4 / 7)	2 (713)	1.6 (604)
N372T (C1) / IIC2 <sup>b</sup>	0.16 / 2.5 (0.4 / 7)	0.6 (311)	0.9 (423)
N372T (C1) / IXC2 <sup>b</sup>	0.16 / 1.9 (0.4 / 7)	0.5 (237)	1.2 (390)
R376A / D300A <sup>a</sup> (C1) / (C2)	0.4 / 1.6 (1 / 4)	351 (498939)	not done

Basal activities of R376A and N376A were 6.3 and 0.4  $nmol \cdot mg^{-1} \cdot min^{-1}$ , respectively. Basal activities for IC1, VC1, IXC1, VIIC1 were 27, 20, 17 and 10  $pmol/mg/min$ , respectively, and for the other monomers zero. DMSO (used for forskolin dilution) controls were not made.

**Table 4.2:** Reconstitution of mammalian/mammalian and mammalian/mycobacterial heterodimers. The functional analogies of the mutant mycobacterial catalytic loops to the C<sub>1</sub> and C<sub>2</sub> catalytic domains of mammalian AC's are in parentheses. The reconstituted activity of the mycobacterial chimera R376A/D300A was used as control for the mycobacterial monomers. Assay conditions: 75  $\mu$ M ATP, 30°C, 10 min, 2 mM MnCl<sub>2</sub>, forskolin 120  $\mu$ M. Data are from single representative experiments (n=2<sup>a</sup> reproducible; n=1<sup>b</sup> and n=2<sup>c</sup> bad reproducible, experiments). The detection limit of the assays (double background) was 10 pmol·mg<sup>-1</sup>·min<sup>-1</sup>.

#### 4.1.4 *Paramecium*/*Mycobacterium* chimeras

Reconstitution of AC activity by chimeras between *Paramecium* GC C1 monomer and mammalian C1- and C2-monomers (IC1, IIC2, VC1, VC2, VIIC1, VIIC2, IXC2) failed, all chimeras were inactive (Hoffmann, 1999). Therefore, in this work only ParaGC-C2 and C2-KWQ were used for reconstitution with IIC2 and this was used as a control for the reconstitution with D300A, N372T, N372A and D300S. The reconstitution of IIC2 with the mutant ParaGC-C2-KWQ was in this study 3-fold more active in comparison with ParaGC-C2/IIC2 (Table 4.3), as reported by Hoffmann, 1999. The chimeras ParaGC-C2/D300A and ParaGC-C2-KWQ/D300A had comparable activity as ParaGC-C2/IIC2. Since in the mixtures of *Paramecium* monomers with N372A and N372T only C1 domains were mixed, no significant reconstitution was observed, as expected.

Chimera	$\mu$ M in the assay ( $\mu$ g)	specific activity nmol·mg <sup>-1</sup> ·min <sup>-1</sup> (cpm)
ParaGC-C2 / IIC2 <sup>b</sup>	5.1 / 3.7 (15 / 11)	50.3 (77741)
ParaGC-C2KWQ / IIC2 <sup>b</sup> C1 / C2	9.2 / 3.7 (27 / 11)	148.3 (221496)
ParaGC-C2 / D300A <sup>a</sup>	5.1 / 1.6 (15 / 4.4)	57.5 (40617)
ParaGC-C2KWQ / D300A <sup>a</sup> C1 / C2	9.2 / 1.6 (27 / 4.4)	54.9 (34137)
ParaGC-C2 / D300S <sup>b</sup>	3.4 / 1.6 (10 / 4)	2.2 (7739)
ParaGC-C2KWQ / D300S <sup>b</sup> C1 / C2	3.4 / 1.6 (10 / 4)	2.6 (9777)
ParaGC-C2 / N372T <sup>b</sup>	3.4 / 0.16 (10 / 0.4)	0.4 (210)
ParaGC-C2KWQ / N372T <sup>b</sup> C1 / C1	3.4 / 0.16 (10 / 0.4)	0.6 (290)
ParaGC-C2 / N372A <sup>b</sup>	3.4 / 0.16 (10 / 0.4)	0.6 (274)
ParaGC-C2KWQ / N372A <sup>b</sup> C1 / C1	3.4 / 0.16 (10 / 0.4)	0.7 (306)
Basal activities of ParaGC-C2, ParaGC-C2-KWQ and N372A were 0.02, 0.03 and 0.4 nmol/mg/min, respectively. Basal activities of the other monomers were zero.		

**Table 4.3:** Reconstitution of C1-C2-like catalytic sites between IIC2, D300A and *Paramecium* GC-C2 and C2-KWQ. Assay conditions: 75  $\mu\text{M}$  ATP, 30°C, 10 min, 2 mM  $\text{MnCl}_2$ . Data from a representative experiment are shown ( $n=2^a$ ;  $n=1^b$ ). Detection limit (double background) was 16  $\text{pmol}\cdot\text{mg}^{-1}\cdot\text{min}^{-1}$ .

#### 4.1.4.1 Characterization of the chimera ParaGC-C2/D300A

This chimera was 200-fold more active with  $\text{Mn}^{2+}$  compared to  $\text{Mg}^{2+}$  (Table 4.4).

Protein(s)	$\mu\text{M}$ in the assay ( $\mu\text{g}$ )	specific activity with 2 mM $\text{Mn}^{2+}$ $\text{nmol}\cdot\text{mg}^{-1}\cdot\text{min}^{-1}$ (cpm)	specific activity with 5 mM $\text{Mg}^{2+}$ $\text{nmol}\cdot\text{mg}^{-1}\cdot\text{min}^{-1}$ (cpm)
ParaGC-C2	3 (8.5)	0.01 (200)	0 (51)
D300A	3 (8.5)	0.01 (170)	0 (52)
ParaGC-C2 / D300A	3/3 (8.5/8.5)	6.77 (70000)	0.03 (279)

**Table 4.4:** Cofactor dependence of the AC activity of the chimera ParaGC-C2/D300A. Test conditions: 75  $\mu\text{M}$  ATP, 30°C, 10 min, Tris-HCl pH 7.5, 8.5  $\mu\text{g}$  protein. Detection limit: 12  $\text{pmol}\cdot\text{mg}^{-1}\cdot\text{min}^{-1}$ . Data from  $n=1$  experiment are shown.

ParaGC-C2 was titrated with increasing amounts of D300A to determine the  $K_d$  value (Fig. 4.5). Within the experimental conditions no saturation was observed, i.e. the  $K_d$  probably is rather high ( $>100 \mu\text{M}$ ).

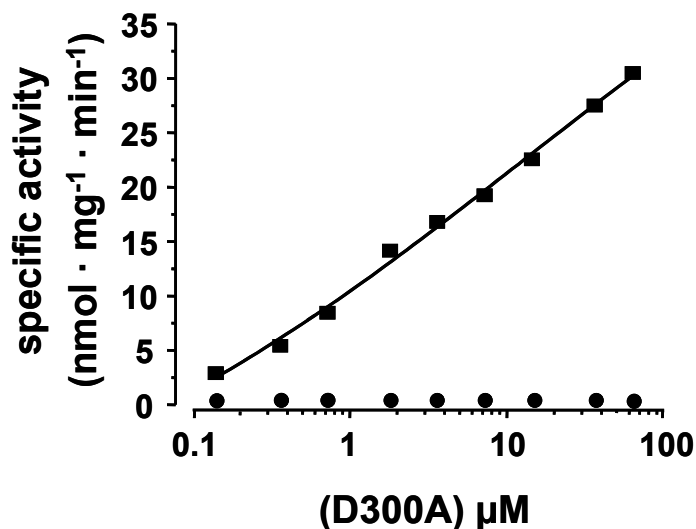


**Fig. 4.5:** Titration of 155 nM ParaGC-C2 with D300A (0.144-63  $\mu\text{M}$ ). Assay was with 75  $\mu\text{M}$  ATP, 10 min, 30°C, 2 mM  $\text{MnCl}_2$ . Circles show D300A alone.

The kinetic characterization was carried out with 40 nM ParaGC-C2 and 9  $\mu\text{M}$  D300A. Basal activities were zero for both monomers. By increasing ATP (10  $\mu\text{M}$  to 1 mM) the

chimera showed a substrate dependence according to the Michaelis-Menten model. Lineweaver-Burk treatment yielded a  $K_M$  of 201  $\mu\text{M}$  and a  $V_{\text{max}}$  of 29.5  $\text{nmol}\cdot\text{mg}^{-1}\cdot\text{min}^{-1}$  (Fig. 4.6).

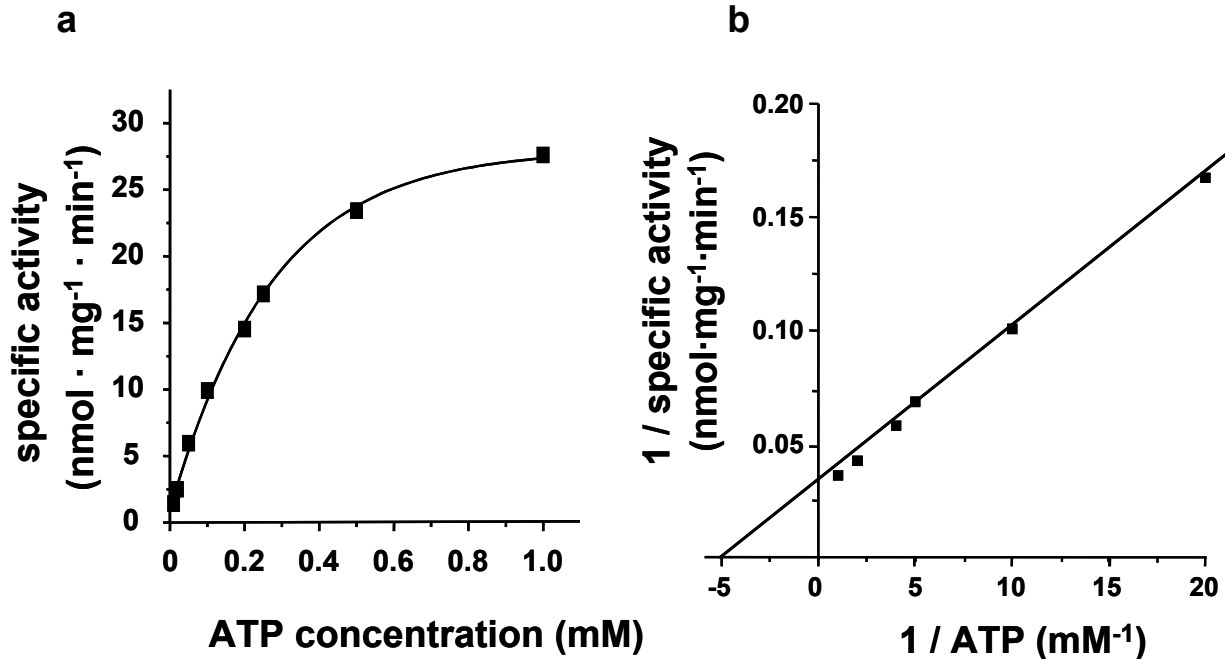


**Fig. 4.6:** Substrate dependence of the chimera ParaGC-C2/D300A (30°C, 10 min, Tris-HCl pH 7.5, 2 mM MnCl<sub>2</sub>). (a) Michaelis-Menten graphic; (b) Lineweaver-Burk graph (values of the two smallest ATP concentrations were not drawn for graph clarity but used for calculation of  $K_M$  and  $V_{\text{max}}$ ).

The effects of mammalian AC activators/inhibitors on the activity of ParaGC-C2/D300A were similar to those observed for *Paramecium* GC and Rv1625c separately (Table 4.5; Linder et al., 2000; Guo et al., 2001).

Substance	specific activity (nmol · mg <sup>-1</sup> · min <sup>-1</sup> )	residual activity (%)
<b>Chimera alone</b>	<b>10.08</b>	<b>100%</b>
Forskolin (0.1 mM)	9.41	93.3
2'd, 3'-AMP (1 mM)	8.28	82.1
2' d, 3'-GMP (1mM)	7.96	78.9
GTP <sub>γ</sub> s (1mM)	3.02	30

**Table 4.5:** Influence of forskolin and P-site inhibitors on the chimera 860 nM ParaGC-C2/ 9  $\mu\text{M}$  D300A. Assay conditions were 75  $\mu\text{M}$  ATP, 30°C, 10 min, Tris-HCl pH 7.5.

### 4.1.5 Mycobacterium/Mycobacterium chimeras

Essentially inactive C1 and C2-like mutant monomers could reconstitute each other with  $Mn^{2+}$  as a cofactor (Table 4.6).  $Mg^{2+}$ -mediated catalysis either was rather poor ( $0.3 \text{ nmol cAMP} \cdot \text{mg}^{-1} \cdot \text{min}^{-1}$  for N372T[ $0.2 \mu\text{M}$ ]/D300S[ $4 \mu\text{M}$ ]) and  $2.5 \text{ nmol} \cdot \text{mg}^{-1} \cdot \text{min}^{-1}$  for R376A[ $0.2 \mu\text{M}$ ]/D300S[ $4 \mu\text{M}$ ]) or was not detectable for other chimeras.

Protein concentration		Specific activity
40 nM	40 nM	( $\text{nmol cAMP} \cdot \text{mg}^{-1} \cdot \text{min}^{-1}$ )
R376A (C1)		1.1
	+ D300A (C2)	24.8
	+ D300S (C2)	31.7
N372A (C1)		2.5
	+ D300A (C2)	14.9
	+ D300S (C2)	4.2
N372T (C1)		0
	+ D300A (C2)	5.3
	+ D300S (C2)	1.6

**Table 4.6:** AC reconstitution in pairs from point-mutated Rv1625c monomers. The functional analogies to the C1 and C2 domains are in parentheses. Assay conditions:  $75 \mu\text{M}$  ATP,  $30^\circ\text{C}$ , 10 min, Tris-HCl pH 7.5, 2 mM  $MnCl_2$ . Basal activities of monomers D300A and D300S were zero.

Forskolin stimulation assays with the catalytic domain wild type and the chimera N372T/D300S were carried out. Since forskolin was diluted in DMSO, controls with addition of DMSO alone and DMSO/Forskolin were tested (Table 4.7). It was concluded that the stimulation observed with DMSO/Forskolin was due to DMSO.

Protein (s)	$\mu\text{M}$ in the assay ( $\mu\text{g}$ protein)	Specific activity ( $\text{nmol} \cdot \text{mg}^{-1} \cdot \text{min}^{-1}$ )		
		alone	With 1 $\mu\text{l}$ DMSO	With 1 $\mu\text{l}$ 50 $\mu\text{M}$ Forskolin (0.5 $\mu\text{M}$ in the assay)
Rv1625 <sub>C204-443</sub>	0.144 (0.4)	16.6	22.4	22.9
N372T/D300S	1.6/1.6 (4.4/4.4)	3.7	4.1	4.0

**Table 4.7:** DMSO stimulation in forskolin assays of Rv1625<sub>C204-443</sub> and chimera N372T/D300S. Assay conditions:  $75 \mu\text{M}$  ATP, 10 min,  $30^\circ\text{C}$ , 2 mM  $MnCl_2$ , Tris-HCl pH 7.5.

#### 4.1.5.1 Titration of N372A, N372T and R376A with D300A or D300S

For each chimera curves with 85 and 850  $\mu\text{M}$  ATP were established to determine if the association of the monomers might be substrate-dependent. Mutants N372A, N372T and R376A (an inactive protein concentration was used) were titrated with increasing amounts of D300A and D300S (Fig. 4.7 to 4.12). The apparent  $K_d$  values were derived graphically. The high specific activities obtained were due to an unusual high radioactive substrate used (from ICN Biochemicals).

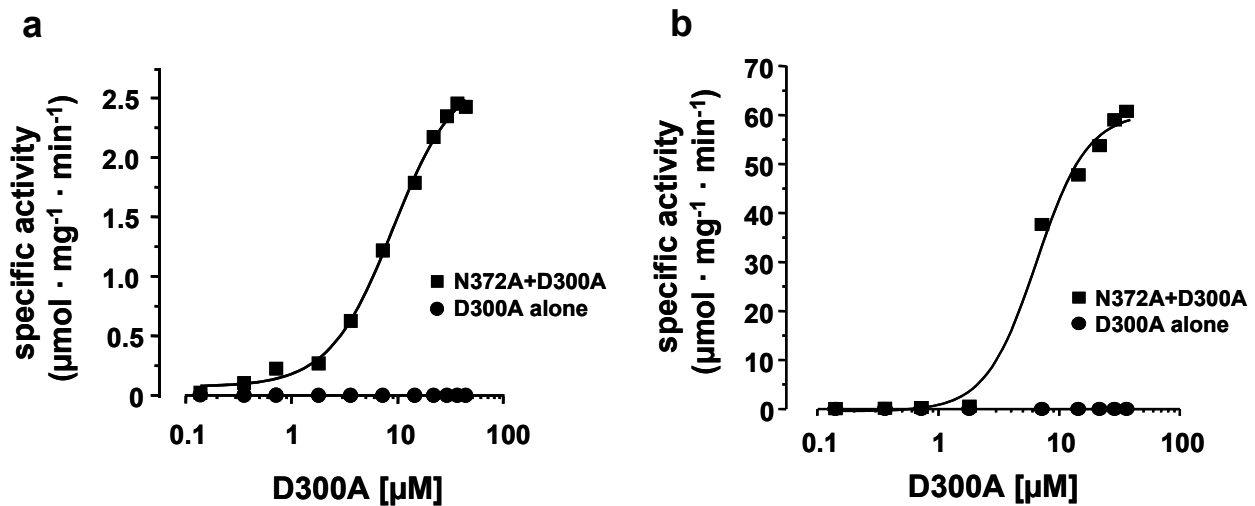


Fig. 4.7: Reconstitution of AC activity of 45 nM **N372A** with increasing amounts of **D300A**. Assay conditions were 30 °C, Tris-HCl pH 7.5, 2 mM  $\text{MnCl}_2$  and (a) 85  $\mu\text{M}$  ATP for 10 min; or (b) 850  $\mu\text{M}$  ATP for 4 min. (a)  $K_d$ = 7  $\mu\text{M}$ ; (b)  $K_d$ = 6  $\mu\text{M}$ .

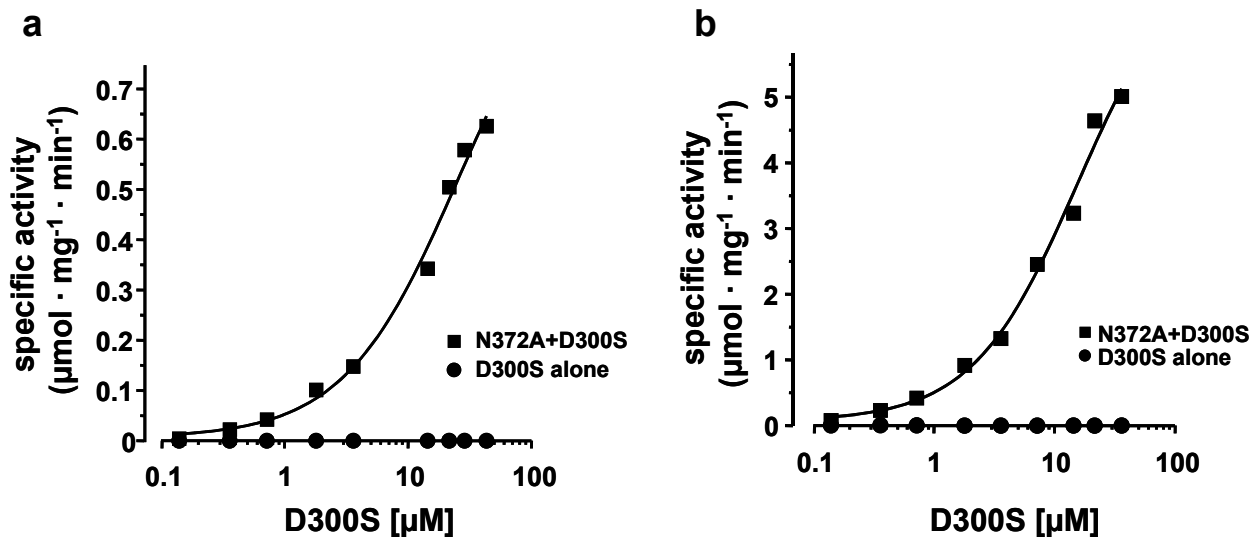
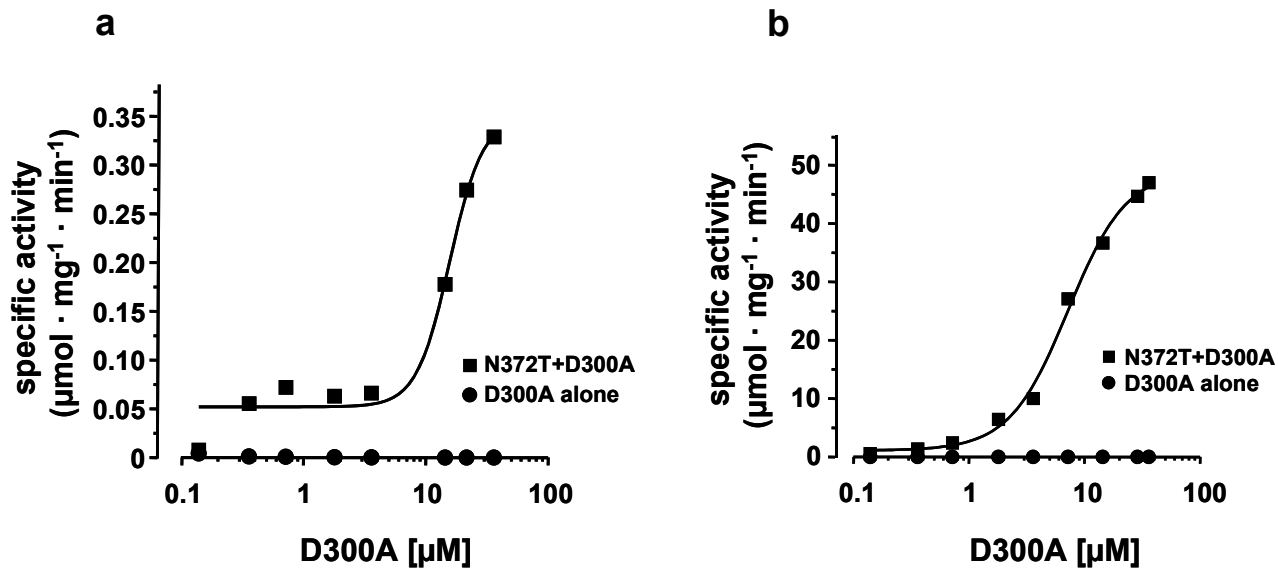
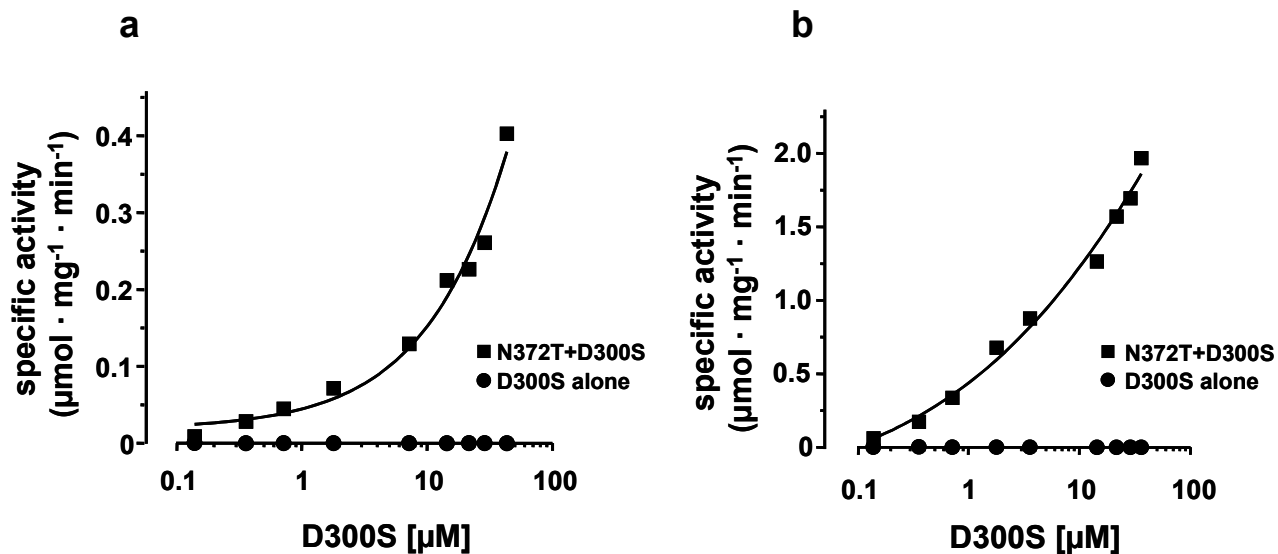


Fig. 4.8: Reconstitution of AC activity of 45 nM **N372A** with increasing amounts of **D300S**. Assay conditions were 30 °C, Tris-HCl pH 7.5, 2 mM  $\text{MnCl}_2$  and (a) 85  $\mu\text{M}$  ATP for 10 min; or (b) 850  $\mu\text{M}$  ATP for 4 min. (a)  $K_d$ = 14  $\mu\text{M}$ ; (b)  $K_d$ = 8  $\mu\text{M}$ .



**Fig. 4.9:** Reconstitution of AC activity of 45 nM **N372T** with increasing amounts of **D300A**. Assay conditions were 30 °C, Tris-HCl pH 7.5, 2 mM MnCl<sub>2</sub> and (a) 85 μM ATP for 10 min; or (b) 850 μM ATP for 4 min. (a) K<sub>d</sub>= 12-14 μM; (b) K<sub>d</sub>= 6-7 μM.



**Fig. 4.10:** Reconstitution of AC activity of 45 nM **N372T** with increasing amounts of **D300S**. Assay conditions were 30 °C, Tris-HCl pH 7.5, 2 mM MnCl<sub>2</sub> and (a) 85 μM ATP for 10 min; or (b) 850 μM ATP for 4 min. (a) and (b) K<sub>d</sub>= not determinable.



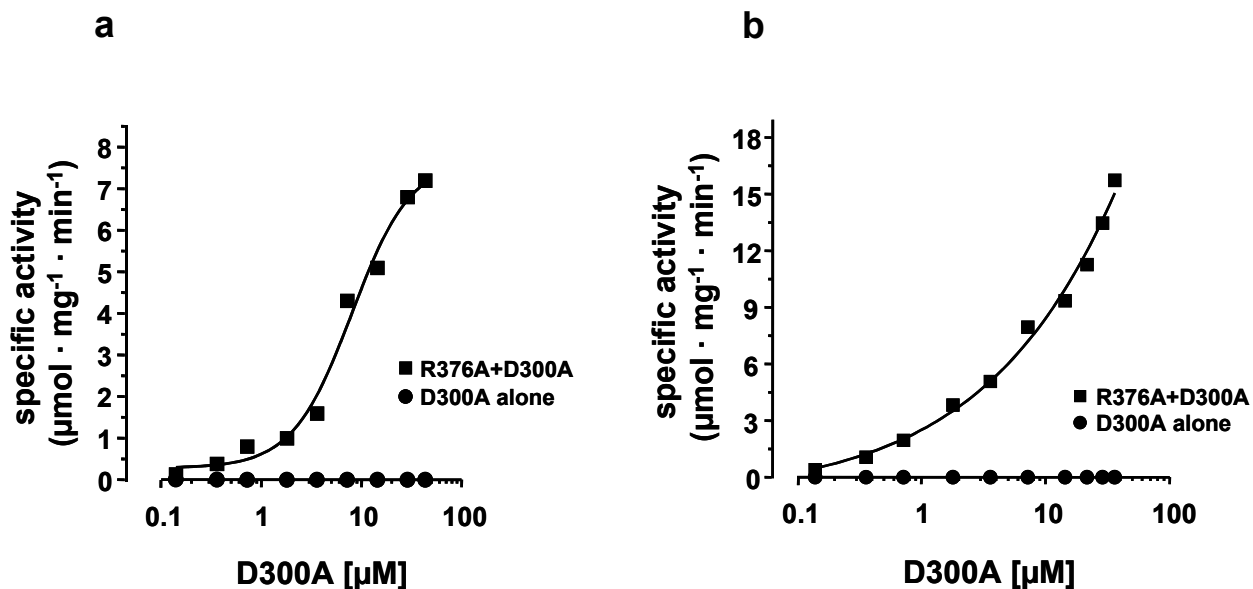


**Fig. 4.11:** Reconstitution of AC activity of 45 nM **R376A** with increasing amounts of **D300A**. Assay conditions were 30 °C, Tris-HCl pH 7.5, 2 mM  $\text{MnCl}_2$  and (a) 85  $\mu\text{M}$  ATP for 10 min; or (b) 850  $\mu\text{M}$  ATP for 4 min. (a)  $K_d = 6\text{-}8 \mu\text{M}$ ; (b)  $K_d$  not determinable.

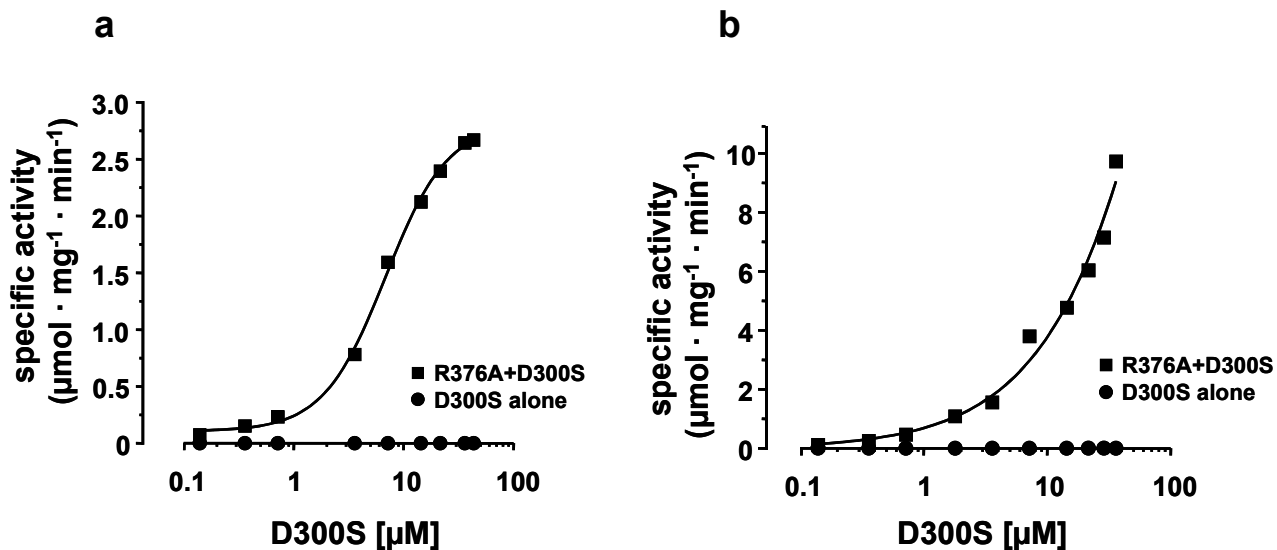


**Fig. 4.12:** Reconstitution of AC activity of 45 nM **R376A** with increasing amounts of **D300S**. Assay conditions were 30 °C, Tris-HCl pH 7.5, 2 mM  $\text{MnCl}_2$  and (a) 85  $\mu\text{M}$  ATP for 10 min; or (b) 850  $\mu\text{M}$  ATP for 4 min. (a)  $K_d = 6 \mu\text{M}$ ; (b)  $K_d$  not determinable.

The high activities reached for all chimeras could be explained by the formation of large amounts of productive heterodimers by the excess of D300A or D300S over N372A, N372T and R376A. Apparently, the association of the monomers of chimeras N372A/D300A, N372T/D300A and N372A/D300S was improved when using high ATP

concentration (850  $\mu\text{M}$ ) since their respective apparent  $K_d$  values decrease with respect of titration using 85  $\mu\text{M}$  ATP. On the contrary, a  $K_d$  for chimeras R376A/D300A and R376A/D300S could not be determined by testing with 850  $\mu\text{M}$  but with 85  $\mu\text{M}$  ATP (possibly because of presence of limiting substrate concentrations). Affinity of the monomers of chimera N372T/D300S showed to be very low since no  $K_d$  value was determinable. These reconstitution assays with the new mutants are further evidence for the catalysis of the mycobacterial Rv1625c adenylyl cyclase through dimerization. The  $K_d$  values obtained for all chimeras is higher than the  $K_d$  of the wild type monomers (Guo et al., 2001), presumably indicating conformational changes due to mutations that had affected the dimerization process.

## **Expression and characterization of the adenylyl cyclase Rv0386 of *Mycobacterium tuberculosis***

### **Sequence features of Rv0386**

At the Sanger Institute Website, the *M. tuberculosis* gene product Rv0386 is annotated as a probable transcriptional regulator (LuxR/UhpA family) with some similarity to AFSR\_STRCO P25941 regulatory protein afsr and many putative *M. tuberculosis* regulatory proteins. It has been reported to contain an ATP/GTP-binding motif A (P-loop) and a probable helix-turn-helix motif. AC Rv0386 was analyzed by several programs to collect information about sequence features and similarities to other proteins of *M. tuberculosis* and other organisms. Rv0386 was analyzed as entity as well as in separated domains (AC, ATPase-, DNA-binding and transcription factor) with the program Protein-Protein-BLAST (NCBI; Nov-26-2003; see 8.2 in appendix). Most similarities were found with *M. tuberculosis* hypothetical proteins Rv2488c and Rv0890c and with transcriptional regulators of Bradyrhizobium, Mesorhizobium and Streptomyces sp.. Analysis with the program DNA-STAR did not detect neither significant hydrophobic nor transmembrane segments in the sequence of Rv0386. Also with this program protein sequence alignments of Rv0386 with other ACs (e.g. Rv1625c, AC type II from rat), GCs (e.g. *Paramecium* GC), proteins containing the ATPase P-loop motif (e.g. AfsR and L6tr) and DNA-binding proteins (e.g. *B. pertussis* BVGA, *S. coelicolor* SCO3008 and *M. tuberculosis* Rv0890c) were made (see 8.3 in appendix). Additionally, an analysis

with the program PESTfind (Rechsteiner and Rogers, 1996) did not detect potential proteolytic signals in Rv0386.

## 4.2.2 Expression and characterization of the Rv0386 adenylyl cyclase catalytic domain

### 4.2.2.1 Expression and purification

The protein was expressed for 4 h with 60  $\mu\text{M}$  IPTG with a protein yield of approximately 2.7 mg/600 ml culture after  $\text{Ni}^{2+}$ -NTA-agarose purification. The protein was dialyzed with glycerol dialysis buffer (20%) and stored at  $-20^\circ\text{C}$ . Pellet, supernatant and purified AC domain were analyzed by SDS-PAGE (20 kDa including N-terminal His-tag) and tested (Fig. 4.13).

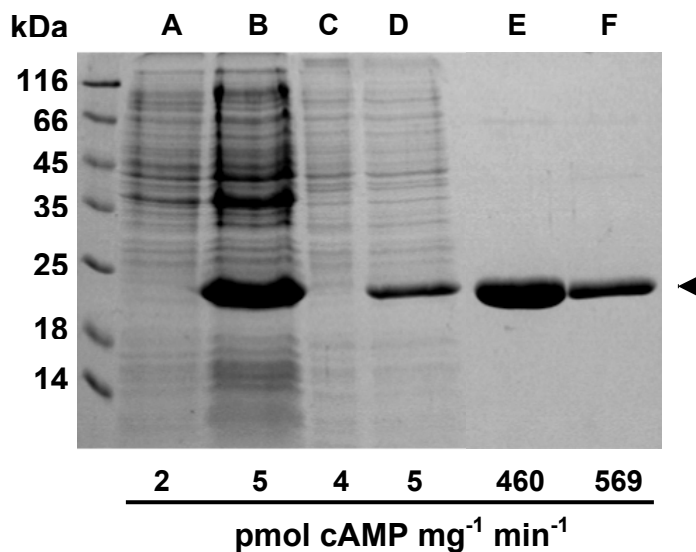


**Fig. 4.13:** 15% SDS-PAGE. Lanes A (control) and B (construct), pellets of pQE30 in BL21 cells. Lanes C and D, supernatants from A and B. Lane E, AC domain after Ni-NTA purification. Lane F, AC domain after dialysis. The specific activities indicated below each lane were determined for lanes A to E with 75  $\mu\text{M}$  ATP ( $30^\circ\text{C}$ , 2 mM  $\text{MnCl}_2$ , buffer Tris-HCl pH 7.5, 10 min assay) and 7, 26, 62, 5 and 9  $\mu\text{g}$  protein, respectively. Specific activity in lane F was determined with 75  $\mu\text{M}$  ATP ( $30^\circ\text{C}$ , 5 mM  $\text{MnCl}_2$ , MOPS pH 7.5, 10 min assay) and 4  $\mu\text{g}$  protein (1.9  $\mu\text{M}$ ). Same protein amounts tested were correspondingly applied at each lane.

#### 4.2.2.2 Characterization of the AC activity

##### 4.2.2.2.1 Optimal temperature

The temperature optimum was around 30-37°C (Fig. 4.14a). The activation energy of 76.1 kJ/mol was derived by an Arrhenius plot (Fig. 4.14b). This value is within the range reported for other mycobacterial ACs (Guo et al., 2001; Linder et al., 2002).

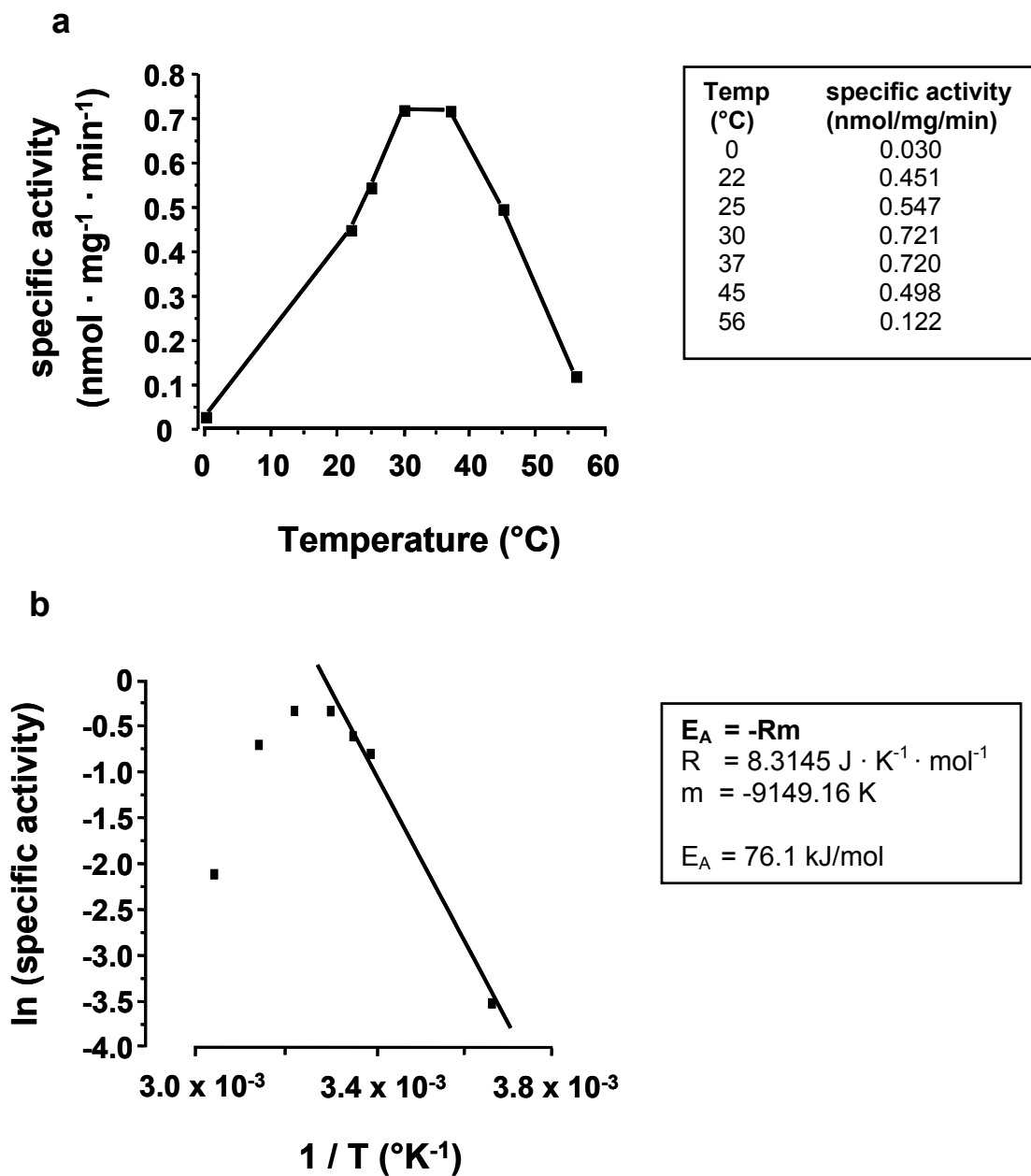


**Fig. 4.14:** a) Temperature dependence. Assay conditions: 75  $\mu\text{M}$  ATP, 10 min, 11.6  $\mu\text{g}$  protein (5.6  $\mu\text{M}$ ), MOPS pH 7.5. b) Arrhenius plot. An activation energy of 76.1 kJ/mol is

necessary for Rv0386 catalytic domain in order to convert ATP into cAMP.  $y = -9149.16x + 30.03$

#### 4.2.2.2.2 $Mn^{2+}/Mg^{2+}$ dependence

ACs use predominantly  $Mn^{2+}$  as divalent cation although  $Mg^{2+}$  probably will be the physiologically more important divalent cation. In most class III ACs,  $Mg^{2+}$ -supported activity is rather low (Kasahara et al., 1997; Hurley, 1999; Guo et al., 2001; Linder et al., 2002). The *in vitro* activity of the Rv0386 catalytic domain is absolutely  $Mn^{2+}$  dependent (Fig. 4.15).

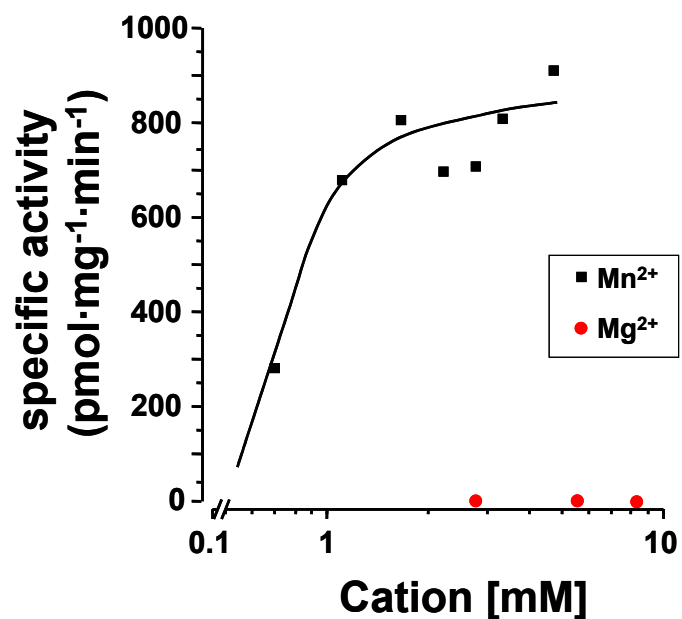


**Fig. 4.15:** Cofactor dependence of the AC activity.  $Mn^{2+}$  was tested from 0.7 mM to 4.7 mM and  $Mg^{2+}$  from 2.7 mM to 8.3 mM. Assay conditions: 75  $\mu$ M ATP, 10 min, 2.3  $\mu$ M protein.

#### 4.2.2.2.3 pH dependence

The activity of the catalytic domain was strongly affected by the pH and dependent on the buffer system. A pH range from 3.1 to 9.9 was tested using 10 different buffer systems (Fig. 4.16) pH 8.3 was the best for the activity corresponding to Tris/HCl pH 8.5. Because at this value  $Mn^{2+}$  is oxidized, pH 7.4 corresponding to MOPS pH 7.5 was used in assays.

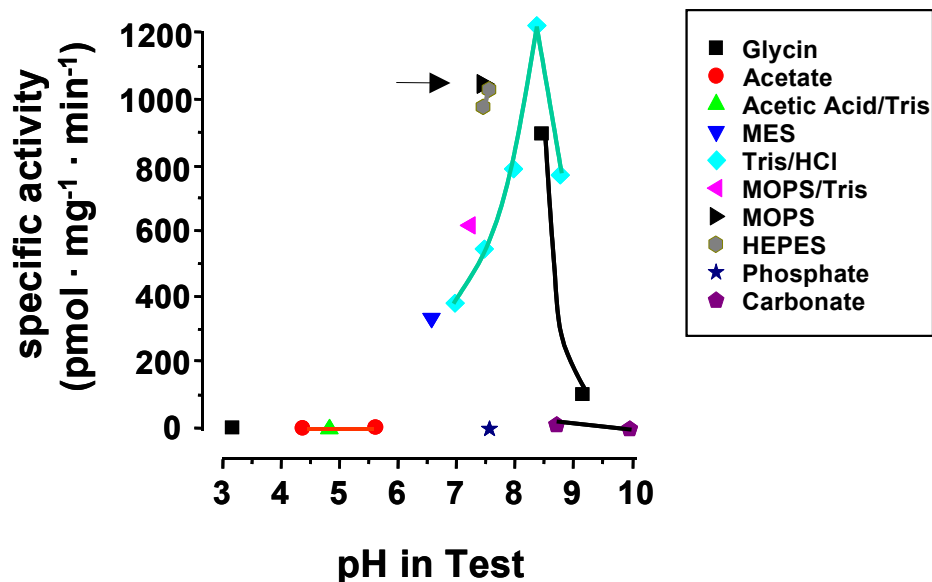
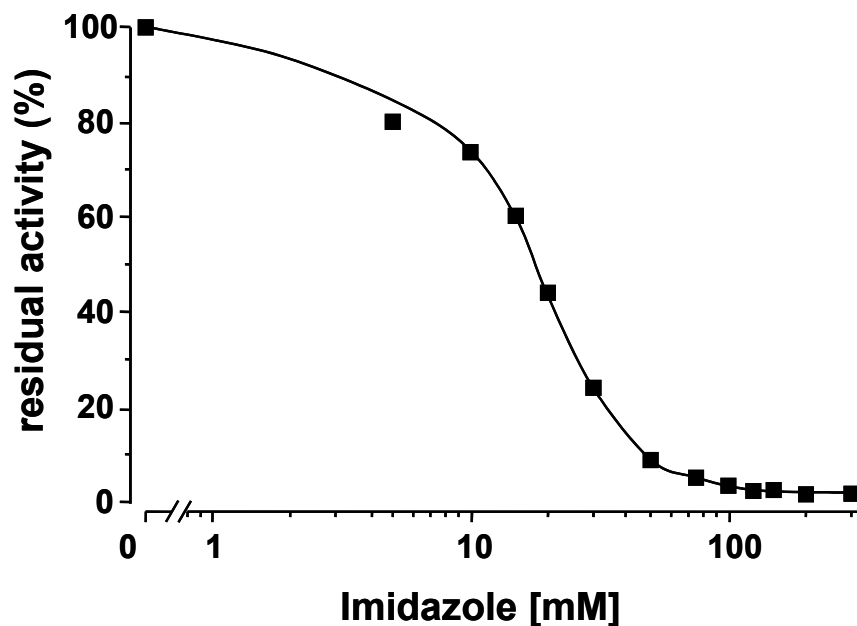


Fig. 4.16: pH dependence. Assay conditions: 75  $\mu$ M ATP, 4.38  $\mu$ M protein, 10 min.

#### 4.2.2.2.4 Effect of imidazole

Elution buffer of Ni-NTA-agarose purification contains 150 mM imidazole. That corresponds to a maximal final concentration in the usual AC assay of 60 mM. On the other hand, imidazole was shown to inhibit Rv1625c (personal communication Dr. Guo). Therefore its effect on Rv0386 was examined (Fig. 4.17). Surprisingly, it was observed that at 60 mM AC activity is inhibited >>90%. Therefore the protein was always dialyzed after purification (glycerol dialysis buffer) to remove rest of the imidazole.



**Fig. 4.17:** Inhibition of the AC activity through imidazole (5-300 mM). Assay conditions were 75  $\mu$ M ATP, 10 min, 30°C and 2.2  $\mu$ M protein concentration.

#### 4.2.2.2.5 Effect of detergents

A set of detergents used for purification of insoluble proteins was tested. A slight activation with Triton X-100, Polidocanol (dodecyl polyethylene glycolether) and Nonidet P-40 was observed. The addition of SDS (anionic detergent) ablated the activity completely. The detergent CHAPS (zwitterionic steroid detergent) reduced but did not completely abolished it (Table 4.8).

Detergent	% in test	AC-activity (%)
Triton X-100	1	124
Polidocanol	1	130
Nonidet P-40	1	144
CHAPS	1	33
	2	9
	3	6
	4	9
SDS	1	1

**Table 4.8:** Influence of detergents on the AC activity. Assay conditions: 2.2  $\mu$ M (4.5  $\mu$ g) protein, 75  $\mu$ M ATP, 3 mM  $Mn^{2+}$ , 30°C, MOPS pH 7.5, 10 min.

#### 4.2.2.2.6 Stability tests

The best storage temperature was  $-20^{\circ}\text{C}$  (with 20% glycerol). The best buffer system that maintained protein stability was Tris/HCl pH 7.5, which retained 90% of activity after 1 month and 50% after 2.5 months. In Tris/HCl pH 8.5, the protein was fully active after 2 weeks. At  $4^{\circ}\text{C}$  and  $25^{\circ}\text{C}$  a residual activity of 85% and 51% was present after 2 weeks, respectively (data not shown). For crystallization purposes the stability of the protein with 10 % glycerol stored at  $-20^{\circ}\text{C}$  was also tested. After one day full activity was retained in Tris/HCl pH 7.5, and after 2 weeks residual activity was 81%.

#### 4.2.2.2.7 Protein dependence

From 46.5 to 465 nM protein specific activity increased 4.5-folds but further increments resulted in a slight decrement of activity (Fig. 4.18). These results suggested rapid formation of a homodimer with further formation of less active oligomers upon increasing protein concentrations. Half maximal activity was attained at 140 nM protein, indicating a high affinity of the catalytic domains for each other.



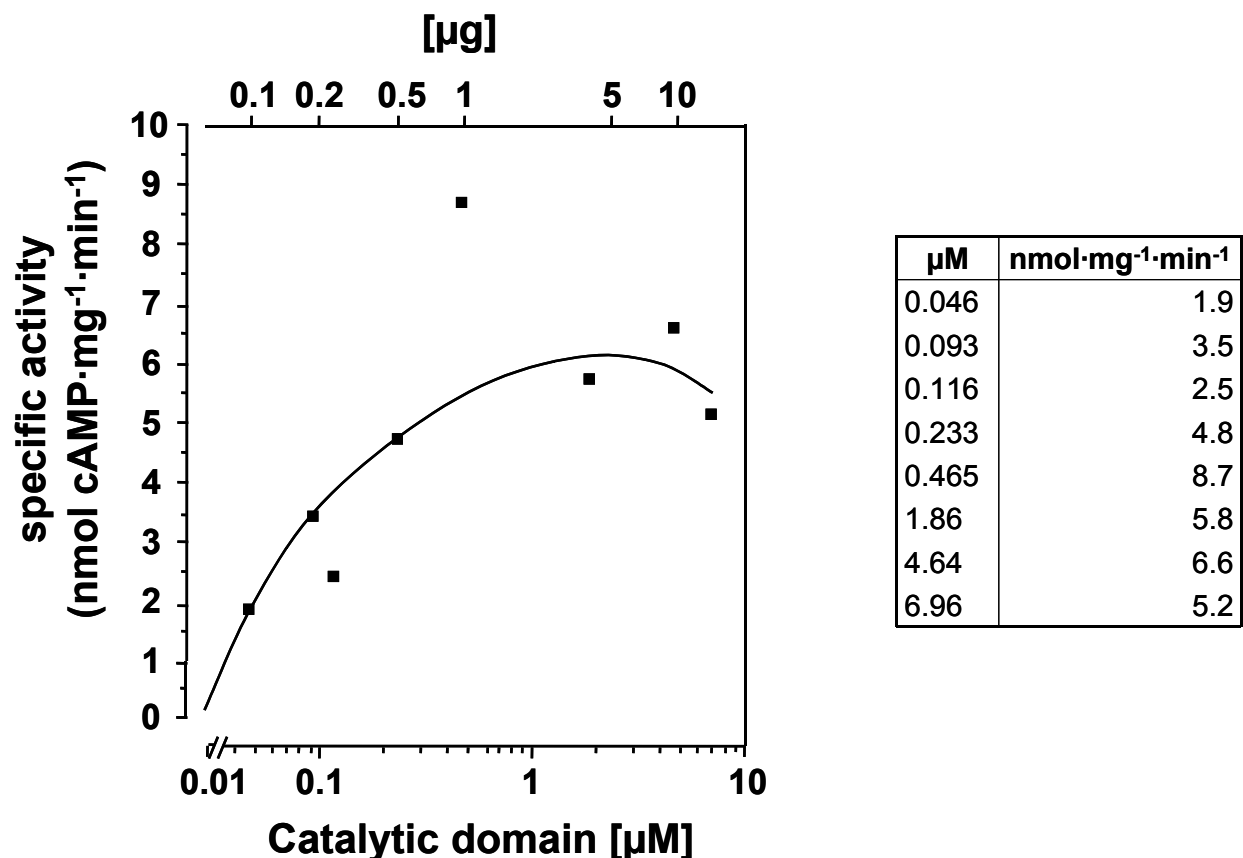
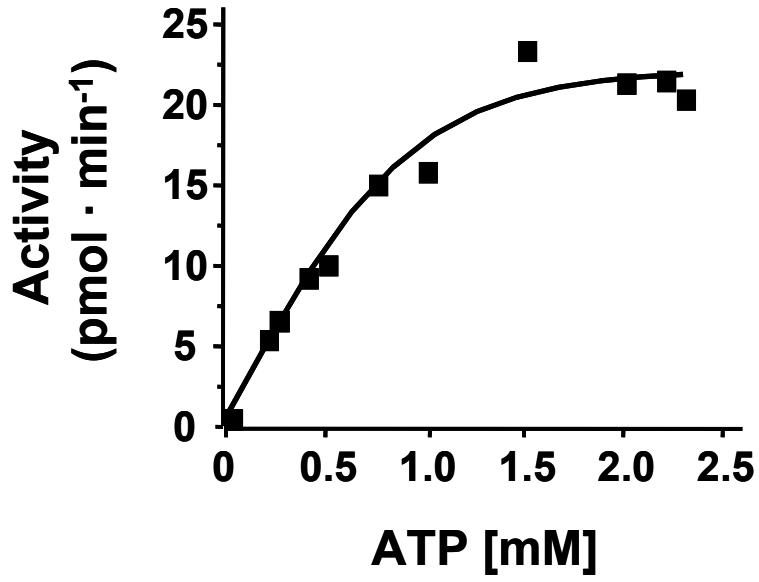


**Fig. 4.18:** Protein dependence of Rv0386 catalytic domain. Assay conditions were 850  $\mu\text{M}$  ATP, 5 mM  $\text{Mn}^{2+}$ , MOPS buffer pH 7.5, 30 °C and 20 min. Protein concentrations tested were from 46.5 nM to 6.9  $\mu\text{M}$  (96 ng to 14  $\mu\text{g}$ ).

#### 4.2.2.2.8 Enzyme kinetics

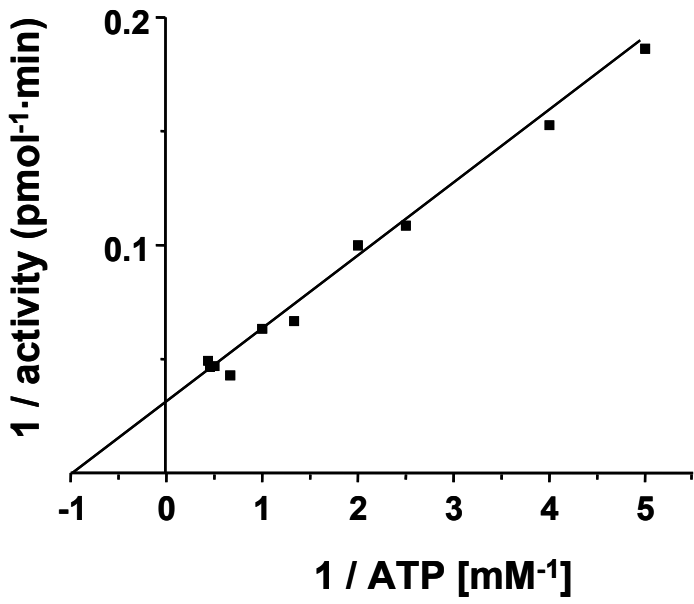
The kinetic properties were analyzed using 5 mM  $\text{Mn}^{2+}$  and substrate concentrations from 10  $\mu\text{M}$  to 2.3 mM. The  $K_M$  for Mn-ATP was 417  $\mu\text{M}$ , the  $V_{\text{max}}$  was 14.4 pmol/min (4.8 nmol/mg/min). The  $K_M$  value obtained is within the range of 30-400  $\mu\text{M}$  observed for purified membrane-bound and soluble ACs (Tang and Hurley, 1998).  $V_{\text{max}}$  is rather low compared with that of the catalytic domain of other ACs, e.g. Rv1625c (2.1  $\mu\text{mol}\cdot\text{mg}^{-1}\cdot\text{min}^{-1}$ ; Guo et al., 2001), Rv1264 (1.25  $\mu\text{mol}\cdot\text{mg}^{-1}\cdot\text{min}^{-1}$ ; Linder et al., 2002) and cyaB1 (309 nmol·mg<sup>-1</sup>·min<sup>-1</sup>; Kanacher et al., 2002). The Hill coefficient was 1.0 which indicated no cooperativity (Fig. 4.19a,b,c).

a



mM	pmol·min <sup>-1</sup>
0.01	0.4
0.02	0.4
0.2	5.4
0.25	6.5
0.4	9.2
0.5	10
0.75	15
1	15.8
1.5	23.3
2	21.3
2.2	21.5
2.3	20.3

b



1/activity	1/ATP
100	2.63
50	2.22
5	0.19
4	0.15
2.5	0.11
2	0.1
1.3	0.06
1	0.06
0.66	0.04
0.5	0.05
0.45	0.05
0.43	0.05

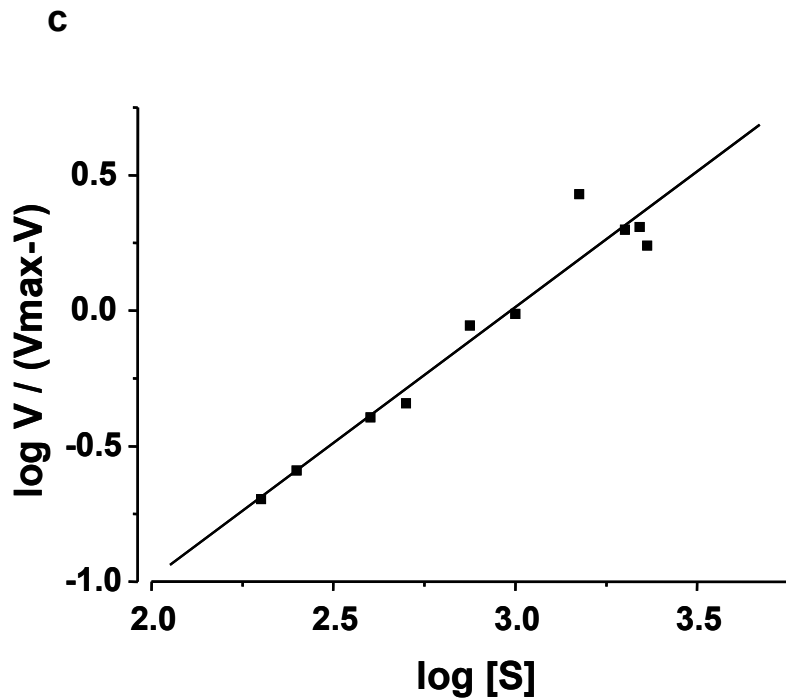


**Fig. 4.19:** **a)** Michaelis-Menten kinetic of the catalytic domain. Assays were conducted at 1.45  $\mu\text{M}$  (3  $\mu\text{g}$ ) protein, MOPS pH 7.5, 30°C and 10 min; **b)** corresponding Lineweaver-Burk linear fit; **c)** corresponding Hill-Plot ( $R^2 = 0.9835$ ;  $y = 1.0148x - 3.0329$ ). **b** and **c)** the two smallest values were not drawn for graph clarity but taken for  $K_M$  and  $V_{\text{max}}$  calculation.  $V =$  activity ( $\text{pmol}\cdot\text{min}^{-1}$ );  $[S] = \text{ATP}$ .

#### 4.2.2.2.9 Influence of inhibitors, substrate analogs and other substances

Activity was tested in presence of forskolin, 2'-deoxy-3'-adenosine monophosphate (2'd3'-AMP) [P-site inhibitor], cyclic AMP (cAMP), guanosine 2'&3'-monophosphoric acid (2'3' GMP; mixed isomers), guanosine 2'-monophosphoric acid (2'-GMP); 8-bromoguanosine 3',5'-cyclic monophosphate (8-Br-cGMP);  $O^2$ -monobutyryl adenosine-3',5'-cyclic monophosphoric acid (monobutyryl cAMP);  $N^6, O^2$ - dibutyryl adenosine 3',5'-cyclic monophosphoric acid (dibutyryl cAMP); 3'-deoxyadenosine 5'-triphosphate (Cordycepin 5'-triphosphate; ATP-analog);  $\alpha, \beta$ -methylene adenosine diphosphate ( $\alpha\beta$ - $\text{CH}_2$ -ADP; ADP-analog) and adenosine-5'-O-(1-thiotriphosphate), Rp-diastereomer (Rp-ATP- $\alpha$ -S, ATP-analog).

Substance tested [mM]	% activity of corresponding basal	Specific activity nmol·mg <sup>-1</sup> ·min <sup>-1</sup> (control with no addition)
Forskolin [0.1]	114	6.3 (5.5)
2'd3' AMP [1]	102	5.6 (5.5)
2'3' GMP [1]	119	6.6 (5.5)
2' GMP [1]	129	7.1 (5.5)
8-Br-cGMP [1]	131	7.2 (5.5)
cAMP [1]	103	6.4 (6.2)
(Rp) ATP $\alpha$ S [1]	119	7.4 (6.2)
Monobutyryl cAMP [1]	29	1.8 (6.2)
Dibutyryl cAMP [1]	58	3.2 (5.5)
$\alpha\beta$ CH <sub>2</sub> ADP [1]	13	0.8 (6.2)
Cordycepin 5' triphosphate [1]	23	1.4 (6.2)

**Table 4.9:** Effect of inhibitors, substrate analogs and other substances on AC activity. Assay conditions: 850  $\mu$ M ATP, 30°C, 10 min, MOPS pH 7.5. Substances were tested in two separate assays.

Only  $\alpha\beta$ -CH<sub>2</sub>-ADP, cordycepin and monobutyryl cAMP showed a significant inhibitory effect on Rv0386. Dibutyryl cAMP could be also considered as an inhibitor. Neither forskolin nor the P-site inhibitor did show considerable activation or inhibition, respectively.

#### 4.2.2.2.10 Influence of purine and pyrimidine nucleotides

ITP and CTP had no significant effect (Fig. 4.20). The activation showed by addition of GTP and UTP may be explained as an allosteric effect. It is possible that GTP or UTP bound to one of the catalytic sites and activated the enzyme allosterically.

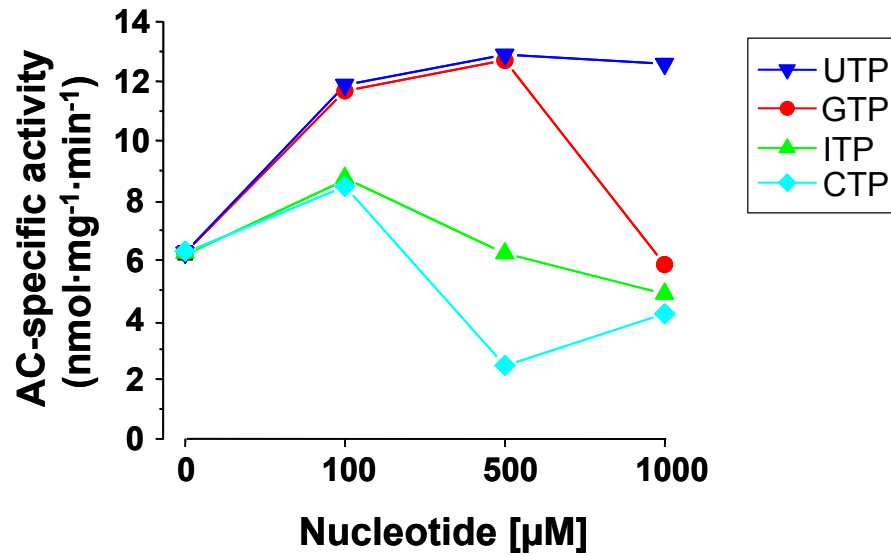


**Fig. 4.20:** Influence of nucleotides on the AC activity. Assay conditions were: 850  $\mu\text{M}$  ATP, 30  $^{\circ}\text{C}$ , 5 mM  $\text{MnCl}_2$ , MOPS pH 7.5, 10 min. Protein concentration tested was 465 nM (0.96  $\mu\text{g}$ ) showing a specific activity of 6.2 nmol cAMP  $\text{mg}^{-1} \text{min}^{-1}$ .

#### 4.2.2.3 Characterization of the GC activity

The catalytic domain was tested for GC activity at a GTP concentration of 75  $\mu\text{M}$  in MOPS buffer pH 7.5 at 30 $^{\circ}\text{C}$ , 5 mM  $\text{Mn}^{2+}$ . Simultaneously an AC assay was carried out for comparison. The catalytic domain has a GC activity of 30% of the AC activity. That resulted surprising since it is not reported about other ACs with any GC side activity. No GC activity was detectable with  $\text{Mg}^{2+}$  (Table 4.10).

Protein ( $\mu\text{M}$ )	AC activity $\text{pmol} \cdot \text{mg}^{-1} \cdot \text{min}^{-1}$		GC activity $\text{pmol} \cdot \text{mg}^{-1} \cdot \text{min}^{-1}$		% GC to AC activity
	5 mM $\text{Mn}^{2+}$	10 mM $\text{Mg}^{2+}$	5 mM $\text{Mn}^{2+}$	10 mM $\text{Mg}^{2+}$	
1.94	226	0	68	0	30
2.15	308	0	85	0	27.6
4.84	435	0	142	0	32.6

**Table 4.10:** Determination of the guanylyl cyclase side activity of Rv0386.

The process of dimerization occurred slower than with ATP as a substrate (see Fig. 4.19 and 4.21 for comparison). The specific activity increased only 3-folds from 665 nM to 14.5  $\mu\text{M}$  protein. An  $\text{EC}_{50}$  value of 0.88  $\mu\text{M}$  was derived graphically.

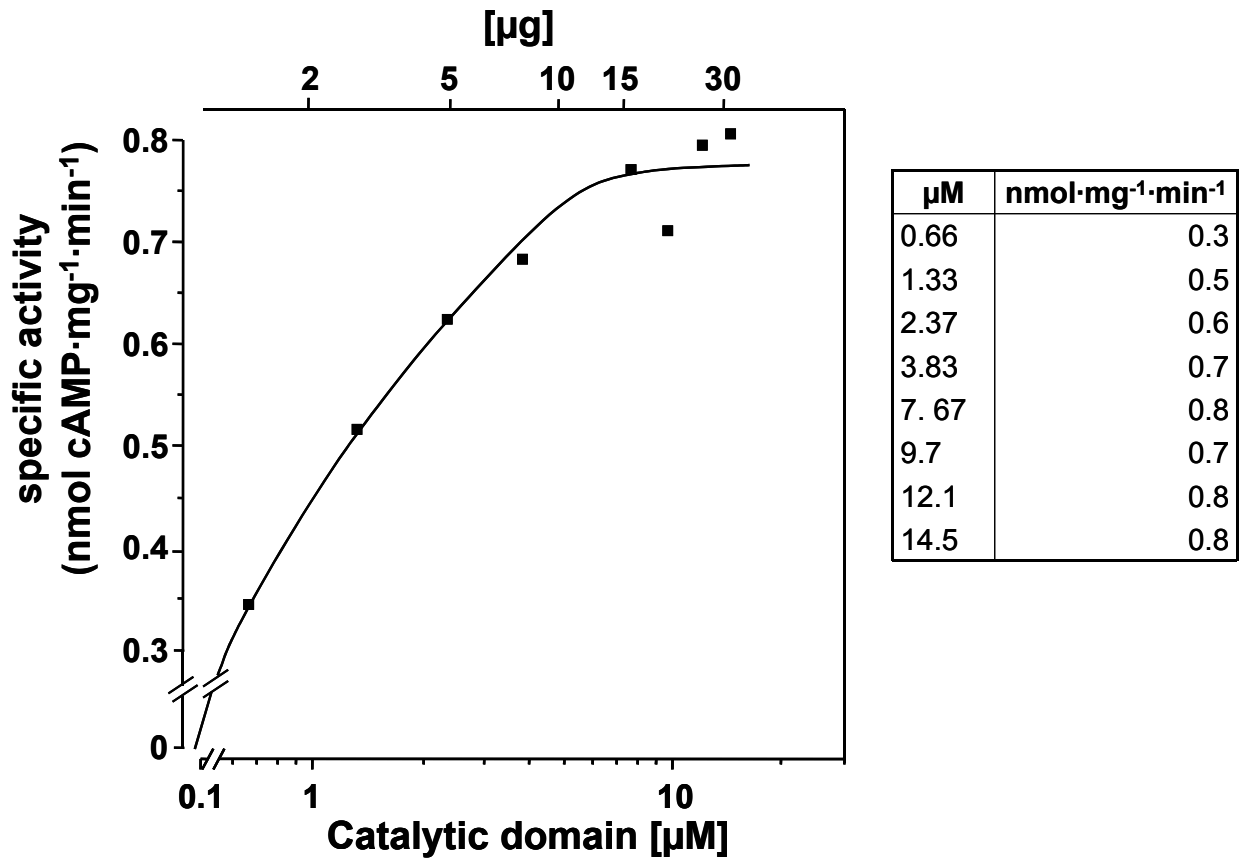
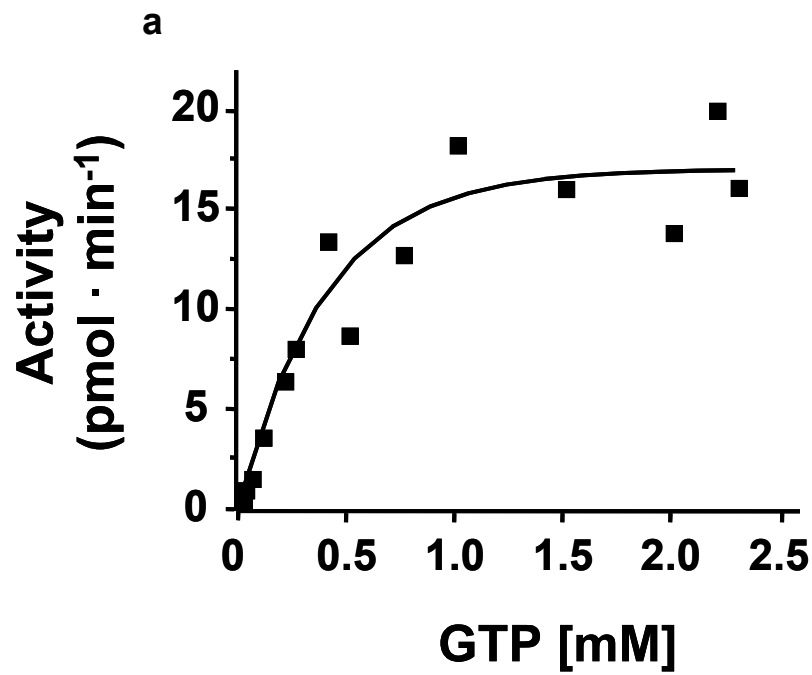


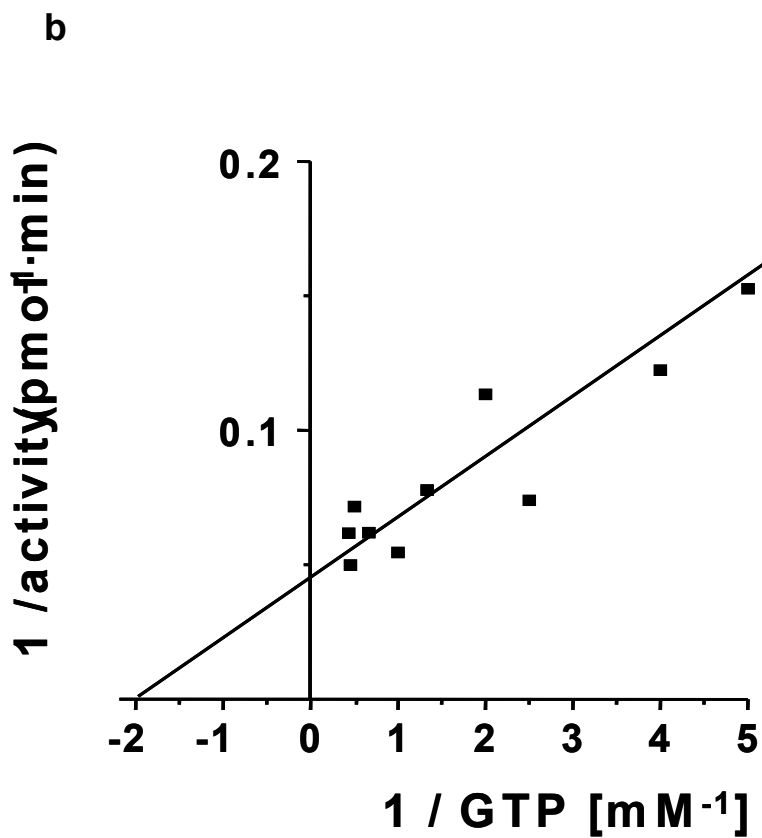
**Fig. 4.21:** Protein dependence with GTP as a substrate. Assay conditions: 850  $\mu\text{M}$  GTP, 5 mM  $\text{Mn}^{2+}$ , MOPS pH 7.5, 30 °C and 20 min.

#### 4.2.2.3.8 Enzyme kinetics

The substrate dependency was assayed with 5 mM  $\text{Mn}^{2+}$  as a cofactor (Fig. 4.22a). The  $K_m$  was 299  $\mu\text{M}$ , the  $V_{\text{max}}$  was 16.1 pmol/min. The Hill coefficient of 0.8 indicates no cooperativity.



mM	pmol·min <sup>-1</sup>
0.01	0.5
0.02	1.1
0.05	1.7
0.1	3.7
0.2	6.5
0.25	8.2
0.4	13.5
0.5	8.8
0.75	12.8
1	18.3
1.5	16.1
2	13.9
2.2	20
2.3	16.2



1/activity	1/ATP
100	1.9
50	0.9
20	0.6
10	0.3
5	0.15
4	0.12
2.5	0.07
2	0.11
1.3	0.08
1	0.05
0.66	0.06
0.5	0.07
0.45	0.05
0.43	0.06

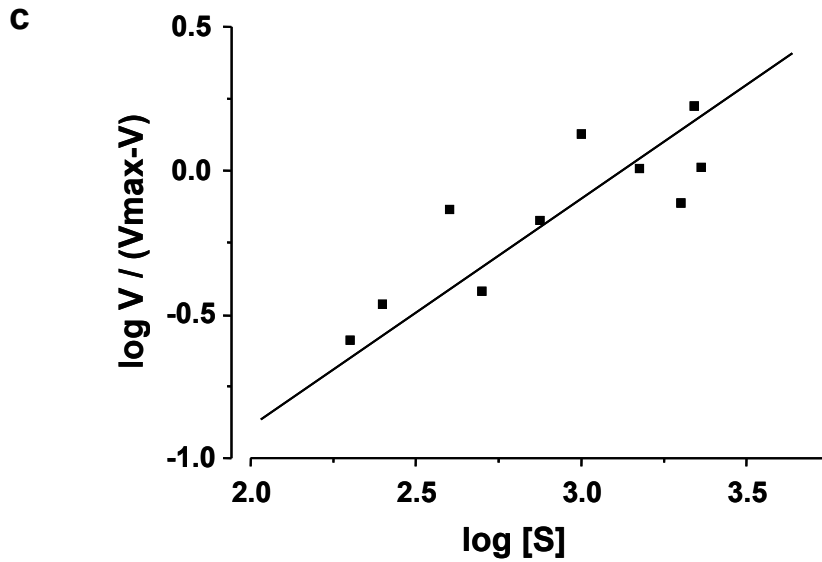


**Fig. 4.22:** a) Michaelis-Menten kinetic for GTP as a substrate. Assays were conducted at 4.85  $\mu\text{M}$  of protein, MOPS pH 7.5, 30°C, 5 mM  $\text{Mn}^{2+}$  and 10 min; b) corresponding Lineweaver-Burk linear fit; c) corresponding Hill-Plot ( $R^2= 0.9456$ ;  $y= 0.7953x - 2.4837$ ). b and c) the four smallest values were not drawn for graph clarity but taken for calculation of  $K_M$  and  $V_{\text{max}}$ . V= activity ( $\text{pmol}\cdot\text{min}^{-1}$ ); [S]= GTP.

UTP did not affect GC activity but other nucleotides did, presumably because of allosterical interactions or because they were used as substrates, e.g. ATP inhibited the GC activity as expected, since the enzyme uses it as a substrate (Fig. 4.23).

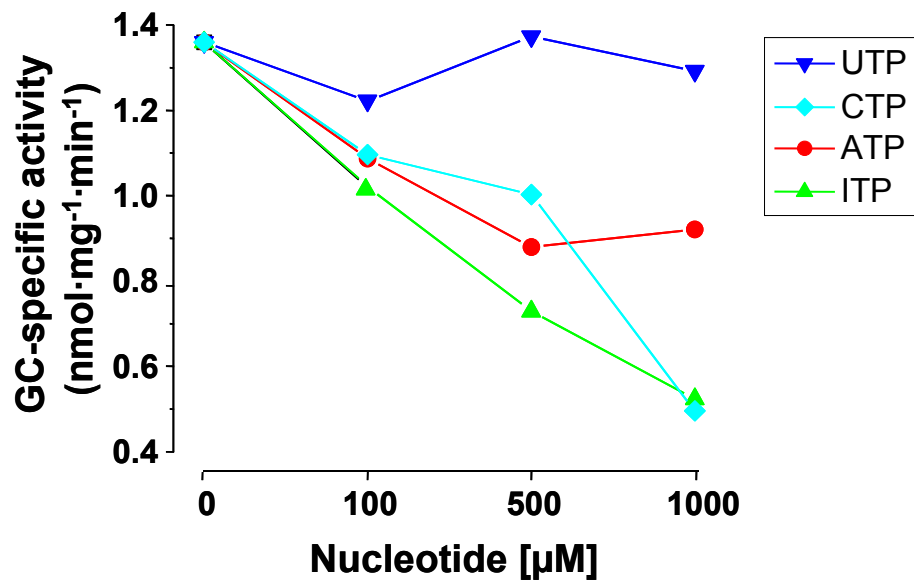


**Fig. 4.23:** Influence of nucleotides on the GC activity. Assay conditions: 850  $\mu\text{M}$  GTP, 30 °C, 5 mM  $\text{MnCl}_2$ , MOPS pH 7.5, 20 min, 4.6  $\mu\text{M}$  (9.6  $\mu\text{g}$ ) protein.



#### 4.2.2.4 Sensitivity of the antibodies anti-KD0386

BioGenes GmbH Berlin produced antibodies against the catalytic domain (KD0386; see chapter 3). The immune reactivity of the antigen-affinity purified antibodies from two immunized rabbits was tested individually against different protein concentrations by Dot Blotting (Fig. 4.24). With an antibody dilution of 1:10 000 it was possible to detect 10 ng protein (rabbit 4555). Effect of addition of anti-KD0386 on the AC activity of the catalytic domain was tested (Table 4.11). Inhibition of the enzyme activity results obvious since antibody bound to the protein brings it to precipitation.

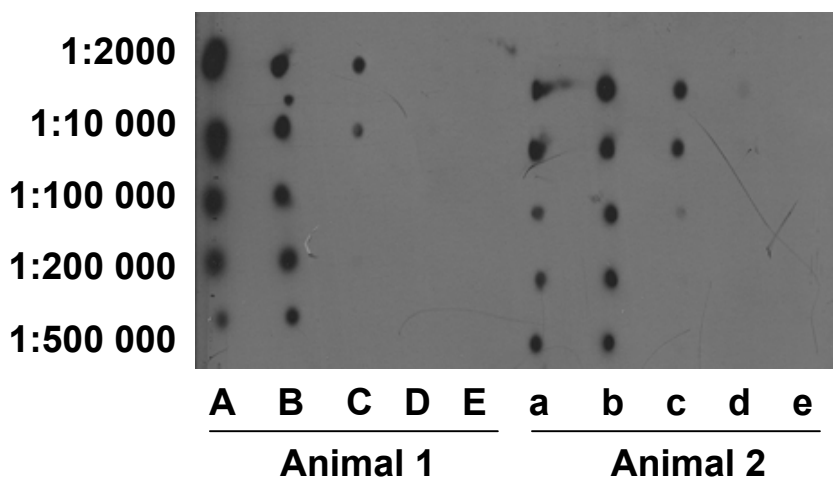


**Fig. 4.24:** Control of the KD0386 antibodies by Dot Blot. 5 different antibody dilutions (1:2000 to 1:500,000) as well as protein concentrations were used (rabbits 4554: animal 1; and 4555: animal 2). Protein concentrations were 1 µg (A), 100 ng (B), 10 ng (C), 1 ng (D) and 0.1 ng (E).

Anti-KD0386 [µg]	specific activity (nmol·mg <sup>-1</sup> ·min <sup>-1</sup> )	% residual activity
No addition	5.2	100
0.8	4.5	86
1.6	4.5	86
2.4	4.1	77
3.2	3.7	71
5	1	20

**Table 4.11:** Inhibition of the AC activity by addition of antibody anti-KD0386. Assay conditions: 500 µM ATP, 30°C, 20 min, 5 mM Mn<sup>2+</sup>, MOPS pH 7.5, 8.5 µg (4.1 µM) protein.

#### 4.2.2.5 Multimerization of the catalytic domain

On a Coomassie-stained SDS-PAGE the Ni<sup>2+</sup>-NTA purified protein was visible as a single band (Fig. 4.13). Using 3 µg protein/lane it was tested whether multimerization could be detected in a Western blot (Fig. 4.25). The protein sample (3 µg, 1.45 µmol, purified, dialyzed, 20% glycerol, at -20°C for about 2 months) was blotted from a 15% SDS-PAGE gel following the standard Western Blot method described in chapter 3. AC and GC activities of the sample were 3.7 and 1.1 nmol/mg/min, respectively (tested with 500 µM ATP or GTP; 10 min; MOPS pH 7.5; 5 mM Mn<sup>2+</sup>). The formation of oligomers presumed from the protein dependence curve (Fig. 4.21) was proved as well as the difference in sensitivity between anti-KD0386 and Coomassie blue.

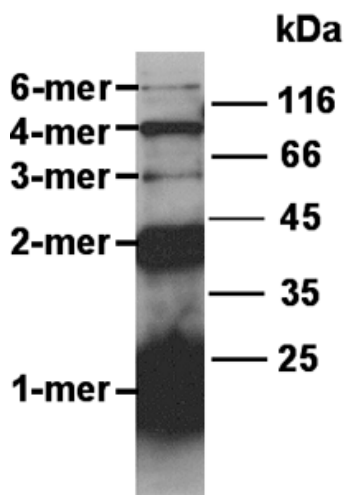


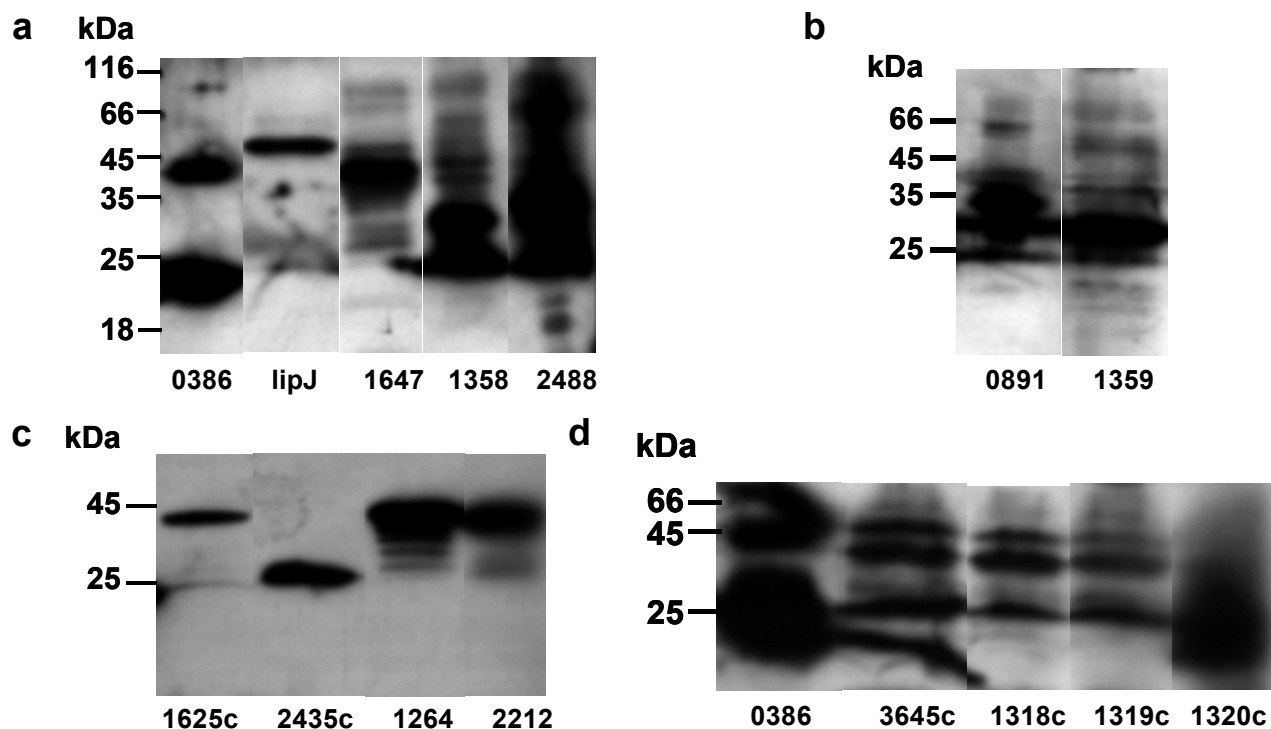
**Fig. 4.25:** Western blot analysis of the AC domain. Primary antibody diluted 1:200 000 and secondary antibody (Goat anti-rabbit antibodies conjugated with horseradish peroxidase) 1:5000. Exposure time was 15 s.

#### 4.2.2.6 Determination of cross-reactivity between anti-KD0386 and other ACs

The 15 mycobacterial ACs (present work; Guo et al., 2001; Linder et al., 2002; Wetterer, Hammer, Motaal, Zeibig, Weber, Luban unpublished data) were analyzed with the specific antibodies anti-KD0386 for determination of possible cross-reactivity (see Table 4.12 and Fig. 4.26 a to d). At a dilution of 1:10000 of the antibodies all ACs with exception of Rv3645c, Rv1318c, Rv1319c and Rv1320 showed crossreactivity after a 15 s exposure. Based on these results, this antibody will not be a suitable tool for immunodetection studies of Rv0386.

Adenylyl cyclase	Construct	Sample type	Molecular weight (kDa)	Protein amount applied ( $\mu\text{g}$ )
Rv1625c	Holoenzyme	Purified	47	2
Rv2435c	Catalytic domain	Purified	26	4
Rv1264	Holoenzyme	Purified	43	5
Rv2212	Holoenzyme	Purified	40	3
Rv1900 (LipJ)	Holoenzyme	Purified	51	6
Rv0891	Holoenzyme	Cell homogenate	33	16
Rv1647	Holoenzyme	Cell homogenate	37	30
Rv1358	Catalytic domain	Cell homogenate	29	16
Rv1359	Holoenzyme	Cell homogenate	28	22
Rv2488	Catalytic domain	Cell homogenate	29	16
Rv3645c	Holoenzyme	Cell homogenate	60	19
Rv1318c	Holoenzyme	Cell homogenate	60	17
Rv1319c	Holoenzyme	Cell homogenate	60	20
Rv1320c	Holoenzyme	Cell homogenate	60	20

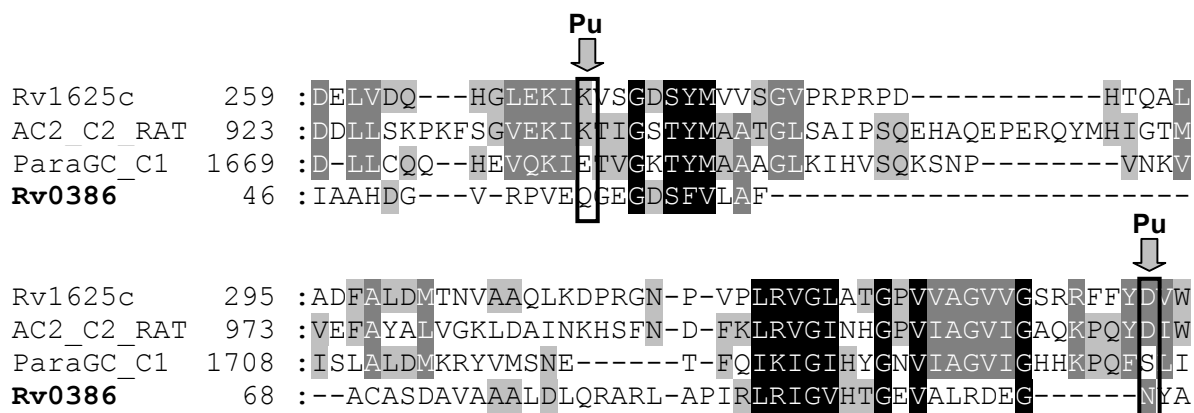
**Table 4.12:** Samples of the mycobacterial ACs used for a Western blot with antibodies anti-KD0386.



**Fig. 4.26 a to d:** Western blot of the 15 ACs of *M. tuberculosis* with antibodies anti-KD0386. According to the molecular weight of each protein (see table 4.21), only ACs of figure d did not show cross-reactivity with anti-KD0386.

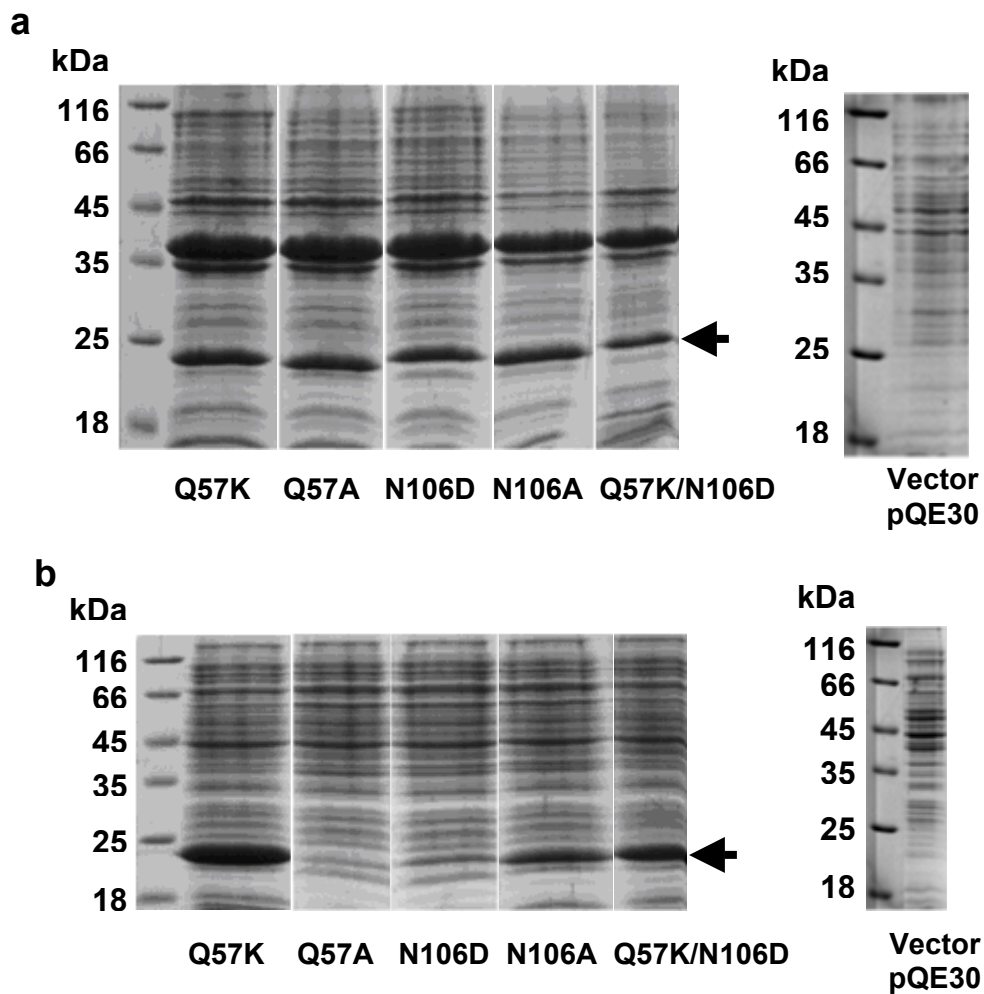
#### 4.2.2.7 Expression, purification and characterization of mutants Q57K, Q57A, N106D, N106A and Q57K/N106D

These mutants were generated to study the importance of residues Q<sub>57</sub> and N<sub>106</sub> for the AC activity of Rv0386 on the basis of the alignment with mammalian cyclases and with Rv1625c (Fig. 4.27).



**Fig. 4.27:** Alignment of Rv0386 AC domain with the cytosolic domains of mammalian AC type 2, *Paramecium* GC and Rv1625c. Marked in boxes: purine-specifying residues.

All mutants were expressed in BL21 cells (60  $\mu$ M IPTG, RT, 4 h). They were purified with Ni-NTA-agarose and dialyzed (20% glycerol; Fig. 4.28a,b,c). Mutants Q57K, N106A and Q57K/N106D were well purified. From 400 ml culture the recoveries of Q57K and N106A were 3 and 0.7 mg protein, respectively. From 600 ml culture the recovery of Q57K/N106D was 0.8 mg protein. Purification of mutants N106D and Q57A was incomplete. The presence of a 25 kDa protein after purification and dialysis could not be avoided. From 600 ml culture the recovery of N106D was only 80  $\mu$ g protein. Recovery of mutant Q57A was 0.1 mg protein from 400 ml culture. No further purification was attempted with these proteins. Western blot analysis with antibodies anti-KD0386 was more sensitive than Coomassie blue showing dimerization of all mutants and degradation of N106D (Fig. 4.28d).



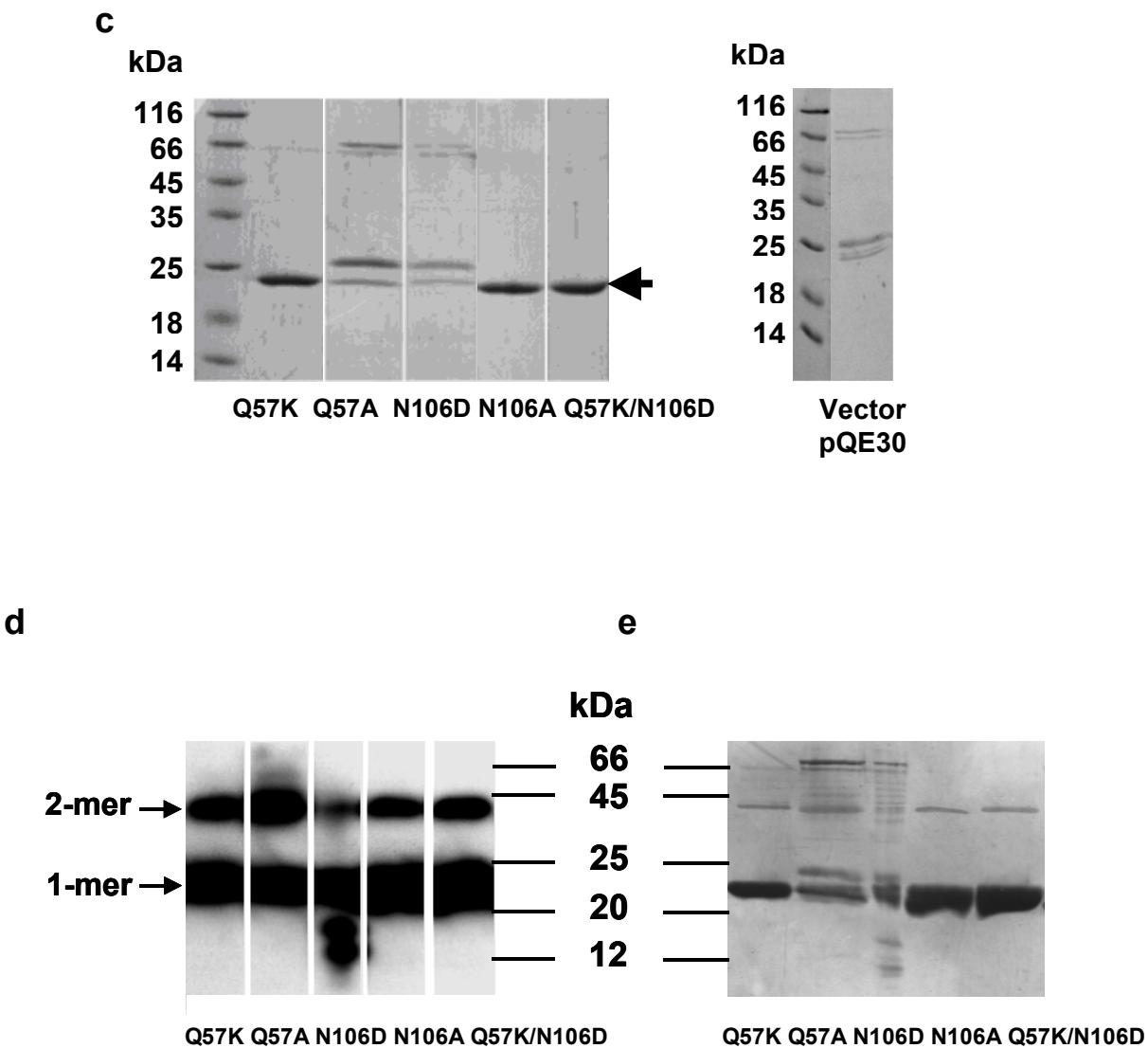


**Fig. 4.28:** 15% SDS-PAGE analysis of five mutants in pellet and supernatant fractions and after Ni-NTA purification with further dialysis (Coomassie staining). About 20 µg protein were applied in each lane from the pellets (**a**) and supernatants (**b**). Purified and dialyzed proteins (**c**) were applied in amounts of about 1-1.5 µg. Controls of vector pQE30 also in pellet, supernatant and purification's eluate are shown. Note proteins of the vector control that could also bind to Ni-NTA-agarose (**c**). (**d**) Western blot from 15% SDS-PAGE of 2 µg/lane of each mutant. Antibodies anti-KD0386 were used (5 s exposure time).

#### 4.2.2.7.1 AC activity of the mutants

Substrate specificity in class III ACs is determined by a lysine and aspartic acid residues (e.g. K296 and D365 in Rv1625c), in Rv0386, these residues are glutamine and asparagine. Therefore, it was already surprising, that Rv0386 had AC activity at all. Now I investigated by a mutational approach the importance of the substrate-defining amino acids for catalysis in Rv0386. In all mutants, activity was below 10% of the wild-type level (Table 4.13) indicating the critical role of Q57 and N106 for substrate recognition in Rv0386 which could not be improved or replaced when mutating to the canonical corresponding amino acids.

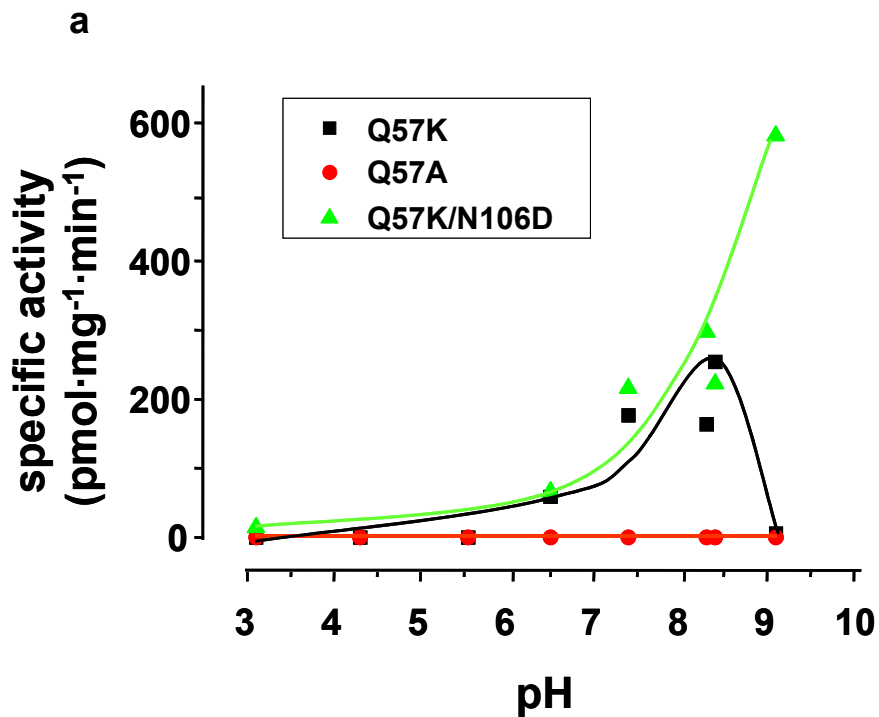
Mutant	[ $\mu$ M]	cpm	Specific activity ( $\text{pmol}\cdot\text{mg}^{-1}\cdot\text{min}^{-1}$ )	(%) activity of corresponding basal	[ATP] in assay ( $\mu$ M)
<b>Q57K</b>	2	182	18 (363)	<b>5</b>	75
	5	294	16 (289)		
	9.5	562	16 (433)		
<b>Q57A</b>	3.9	145	66 (3905)	<b>1.4</b>	1000
	5.8	120	35 (3281)		
<b>N106D</b>	1.9	62	0 (569)	<b>0</b>	75
	4.9	68	0 (538)		
	9.7	76	0 (381)		
<b>N106A</b>	1.9	125	13 (569)	<b>1.5</b>	75
	4.9	121	5 (538)		
	9.7	245	6.4 (381)		
<b>Q57K/N106D</b>	2.4	290	136 (1830)	<b>6</b>	500
	4.8	397	95 (2080)		

**Table 4.13:** AC activities of the five mutants. Specific activities in parenthesis correspond to the catalytic domain wild type under the same assay conditions (MOPS pH7.5, 10 min, 30°C, 5 mM  $\text{Mn}^{2+}$ ). Detection limit was 5  $\text{pmol}\cdot\text{mg}^{-1}\cdot\text{min}^{-1}$ .

#### 4.2.2.7.2 pH dependence

Each mutant was tested with different buffer systems from pH 3 to 9 (Fig. 4.29 a and b). Activity was strongly affected by the pH. Optimal buffers were: for Q57K and N106A Glycin/NaOH buffer pH 8.4 and for N106D and Q57K/N106D Glycin/NaOH pH 9.1.

Q57A did not show activity under these assay conditions. Activity of Q57A was actually only detectable with Tris/HCl pH 8.3 and MOPS pH 7.5 when testing at higher ATP concentrations (Tables 4.13 and 4.14). Since activities of Q57A and N106D are rather low it resulted not clear if they show a large buffer effect or the observations are due only to the substrate concentration in the different assays (see Tables 4.13 and 4.14, Fig. 4.29a and b for comparison). A slight displacement of the pH optimum compared with the catalytic domain wild type was observed only for N106D and Q57K/N106D (Fig. 4.17 and 4.29).





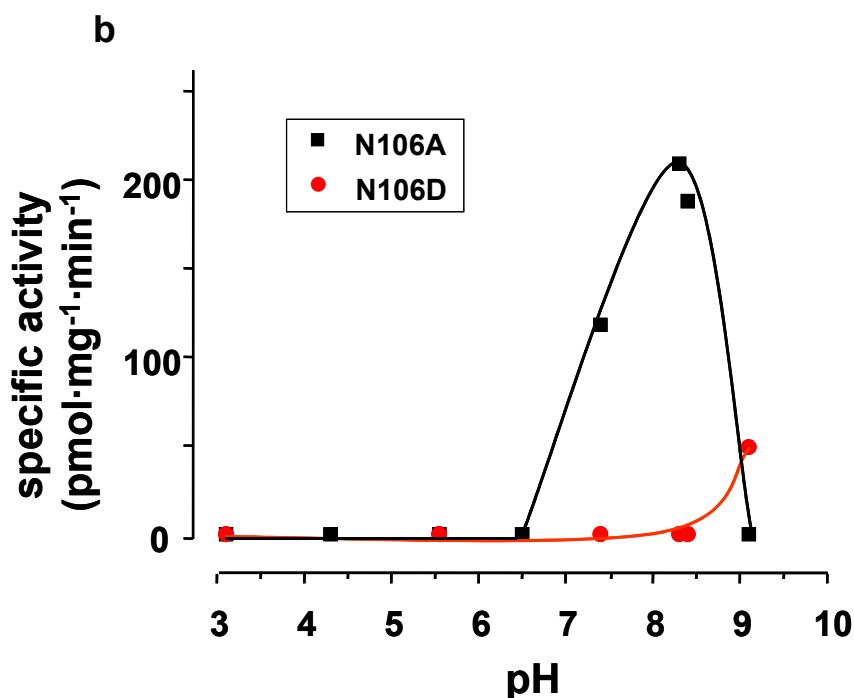


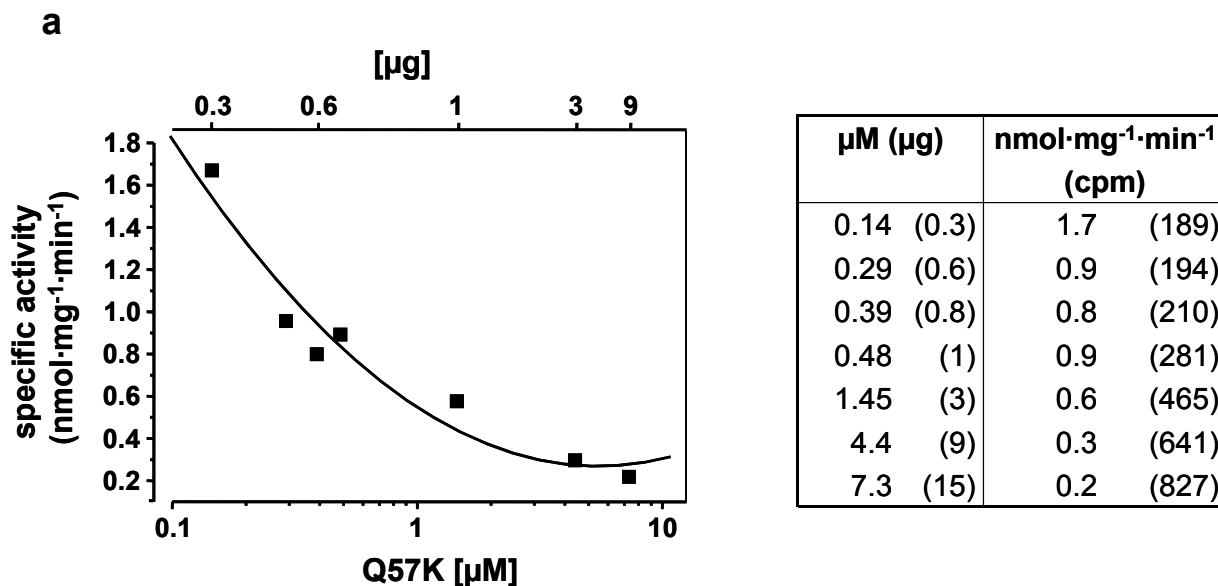
**Fig. 4.29:** Dependence on pH of the mutants. Assay conditions: 500  $\mu\text{M}$  ATP, 10 min, 30°C, 5 mM  $\text{Mn}^{2+}$ , 6  $\mu\text{M}$  Q57K, 4  $\mu\text{M}$  Q57A, 5  $\mu\text{M}$  Q57K/N106D (a), 3  $\mu\text{M}$  N106D and 9  $\mu\text{M}$  N106A (b).

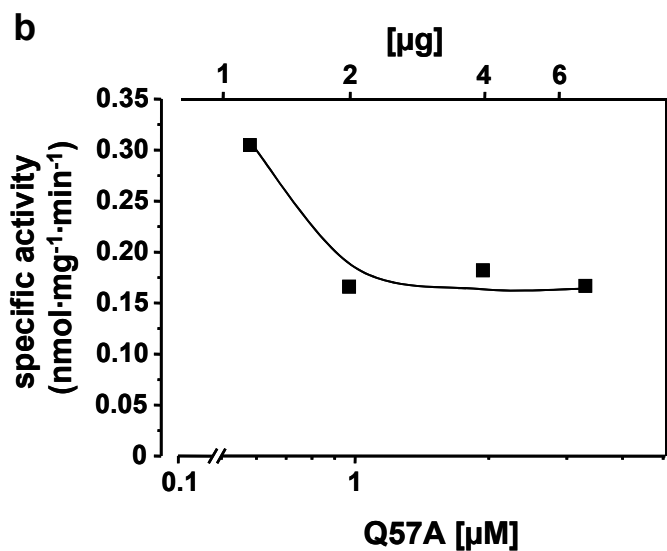
Mutant	[ $\mu\text{M}$ ]	cpm	Specific activity ( $\text{pmol}\cdot\text{mg}^{-1}\cdot\text{min}^{-1}$ )	% activity of corresponding basal	ATP in assay [ $\mu\text{M}$ ]	pH
Q57K	1.9	634	512 (7787)	<b>6.5</b>	850	8.4
Q57A	1.9	290	182 (4577)	<b>4</b>	850	8.3
N106D	3.9	155	45 (1872)	<b>2.4</b>	850	9.1
N106A	2.4	176	161 (3168)	<b>5</b>	500	8.4
Q57K/N106D	2.9	648	399 (6437)	<b>6</b>	850	9.1

**Table 4.14:** AC activities of the mutants measured at their pH optimum. The pH values correspond to the final pH measured after mixing all components of the AC-test mixture. Assays conditions: 30°C, 20 min, 5 mM  $\text{Mn}^{2+}$ . Data are from separate tests. Specific activities in parentheses correspond to the catalytic domain wild type under the same assay conditions.

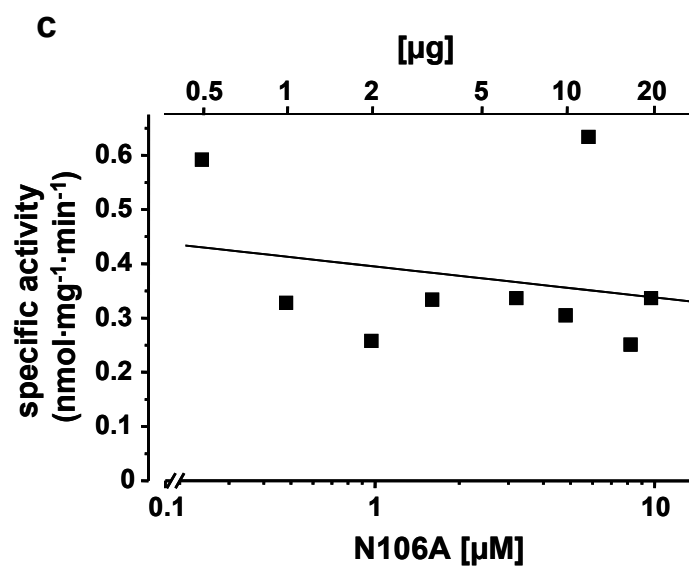
#### 4.2.2.7.3 Protein dependence

Mutants Q57K, Q57A and Q57K/N106D showed a notable decrease in activity at increasing protein concentration (Fig. 4.30a,b,d). The  $K_d$  values could not be calculated because at lower concentrations AC activity was reliably unmeasurable. It is possible that the mutants have a  $K_d$  similar or lower than that calculated for the wild type (0.14  $\mu\text{M}$ ) and that less active multimers are formed upon increasing protein concentrations. Activity of N106A was relatively constant at increasing protein concentrations (Fig. 4.30c). For mutant N106D it was impossible to determine protein dependency because of its lack of activity at concentrations lower than 1.9  $\mu\text{M}$ , and its low recovery after purification made it impossible to test it at concentrations higher than 5  $\mu\text{M}$  (Fig. 4.30e).

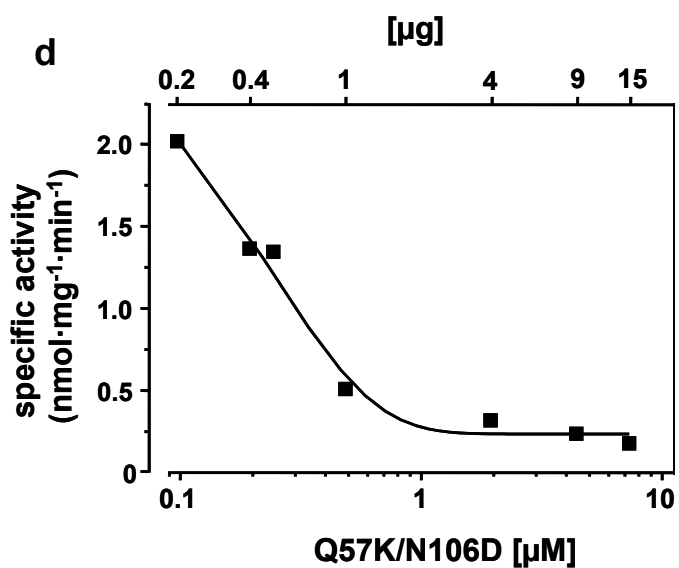




$\mu\text{M}$ ( $\mu\text{g}$ )	$\text{nmol}\cdot\text{mg}^{-1}\cdot\text{min}^{-1}$ (cpm)
0.58 (1.2)	0.30 (191)
0.97 (2)	0.17 (189)
1.94 (4)	0.18 (290)
3.3 (6.8)	0.17 (419)



$\mu\text{M}$ ( $\mu\text{g}$ )	$\text{nmol}\cdot\text{mg}^{-1}\cdot\text{min}^{-1}$ (cpm)
0.24 (0.5)	0.6 (102)
0.48 (1)	0.3 (111)
0.97 (2)	0.2 (136)
1.6 (3.3)	0.3 (243)
3.2 (6.7)	0.3 (453)
4.8 (10)	0.3 (618)
5.8 (12)	0.6 (1430)
8.2 (17)	0.2 (859)
9.7 (20)	0.3 (1216)



$\mu\text{M}$ ( $\mu\text{g}$ )	$\text{nmol}\cdot\text{mg}^{-1}\cdot\text{min}^{-1}$ (cpm)
0.097 (0.2)	2 (164)
0.194 (0.4)	1.4 (178)
0.243 (0.5)	1.3 (226)
0.485 (1)	0.5 (174)
1.94 (4)	0.3 (303)
4.4 (9)	0.2 (400)
7.3 (15)	0.2 (622)

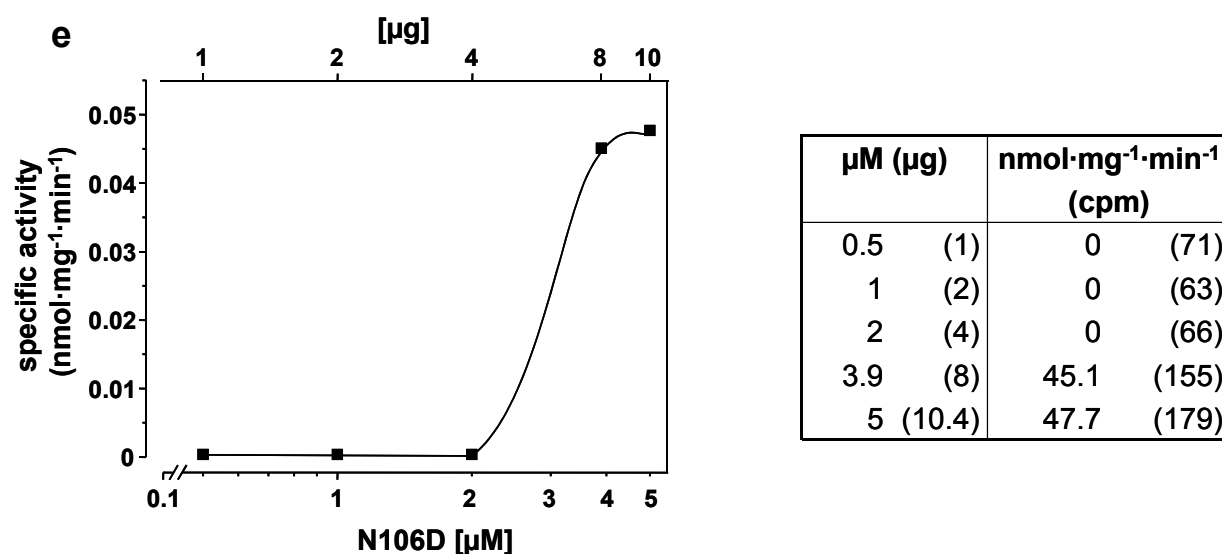


**Fig. 4.30:** Protein dependence of the Rv0386 catalytic domain mutants. For the curves of Q57K (a), Q57A (b), Q57K/N106D (d) and N106D (e) conditions were 850  $\mu\text{M}$  ATP, 5 mM  $\text{Mn}^{2+}$ , 30°C, 20 min. Assay conditions for N106A (c) were 500  $\mu\text{M}$  ATP, 5 mM  $\text{Mn}^{2+}$ , 30°C, 10 min. Each mutant was tested at the optimal pH. Data are from a single representative experiment (n=2 with similar results).

#### 4.2.2.7.4 GC activity of the mutants

Direct comparison of AC and GC activities of the mutants showed a considerably attenuation in the substrate discrimination for mutants Q57K/N106D and N106A (Table 4.15). Mutant Q57K discriminate the substrate in the same proportion that the wild type did (30% residual activity). No GC activity was detectable for mutants N106D and Q57A. Activity of lower or higher protein concentrations of these mutants was impossible to be detected. It is possible that residues Q57 and N106D in conjunction are responsible for preferring ATP as a substrate.

Mutant	$\mu\text{M}$ Protein ( $\mu\text{g}$ )	AC activity $\text{pmol}\cdot\text{mg}^{-1}\cdot\text{min}^{-1}$ (cpm)	GC activity $\text{pmol}\cdot\text{mg}^{-1}\cdot\text{min}^{-1}$ (cpm)	% GC residual activity	GTP in assay [ $\mu\text{M}$ ]
Q57K	1.9 (4)	512 (634)	154 (245)	30	850
Q57A	1.9 (4)	182 (290)	0 (184)	0	850
N106D	3.9 (8)	45.1 (155)	0 (161)	0	850
N106A	2.4 (5)	161 (176)	109 (176)	67.7	500
Q57K/N106D	4.4 (9)	357 (918)	331 (801)	92.7	850

**Table 4.15:** GC activities of the mutants of the catalytic domain. Assay conditions: 30°C, 20 min for Q57A, Q57K, N106D and Q57K/N106D and 10 min for N106A. Each mutant was tested at its pH.

#### 4.2.2.8 Expression and characterization of the mutant N106S

Mutant N106S was generated to turn the substrate specificity of the catalytic domain toward GTP, according to the alignment of the sequences of the AC domain of Rv0386 and the C1 domain of the *Paramecium* GC (Fig. 4.31). It was assumed that residue E56 (next neighbor to Q57) in Rv0386 could bind the purine corresponding to E1681 in ParaGC. Therefore only N106 was mutated to S.

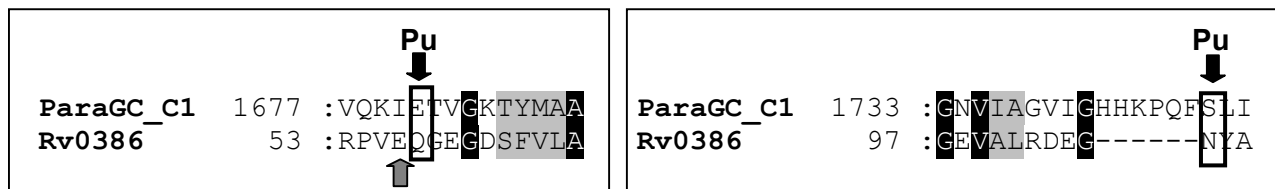


**Fig. 4.31:** Short alignment of Rv0386 with *Paramecium* GC showing their corresponding purine-specifying residues. Residues E<sub>1681</sub> and S<sub>1748</sub> confer ParaGC its GTP-specificity (Linder et al., 2000).

N106S was expressed in BL21 cells (5 h, 60  $\mu$ M IPTG, RT), purified and dialyzed as usual and stored at  $-20^{\circ}\text{C}$  with 20% glycerol. From 3 x 600 ml bacterial culture approx. 1 mg of purified and dialyzed protein was obtained. Expression and purification grade of N106S were analyzed by SDS-PAGE (Fig. 4.32a). Dimerization of the mutant was shown with a Western blot with anti-KD0386 (Fig. 4.32b).

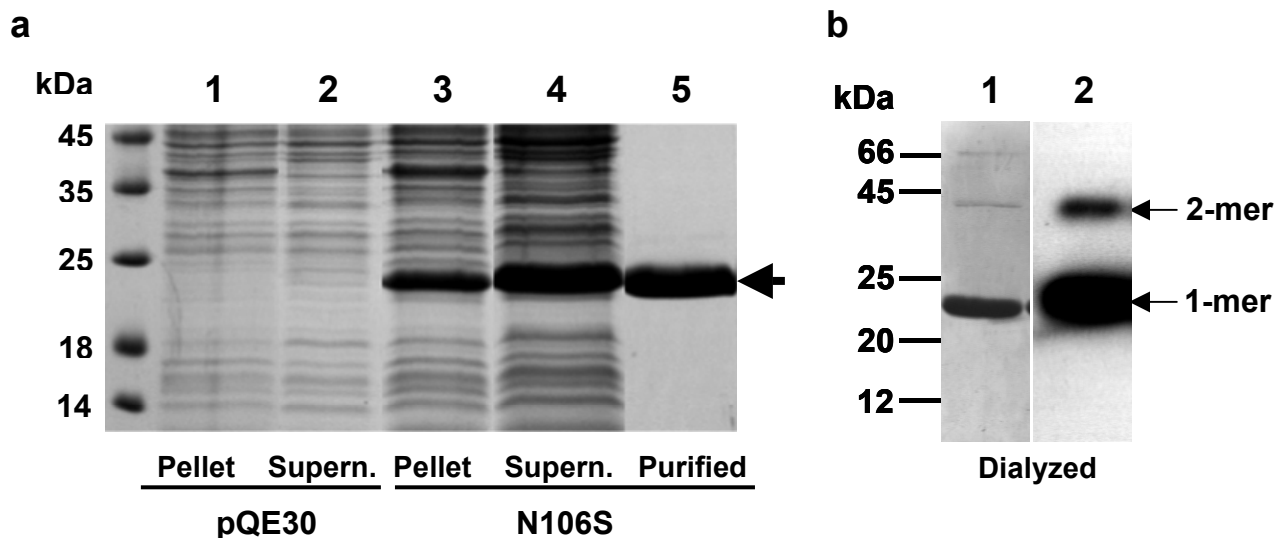


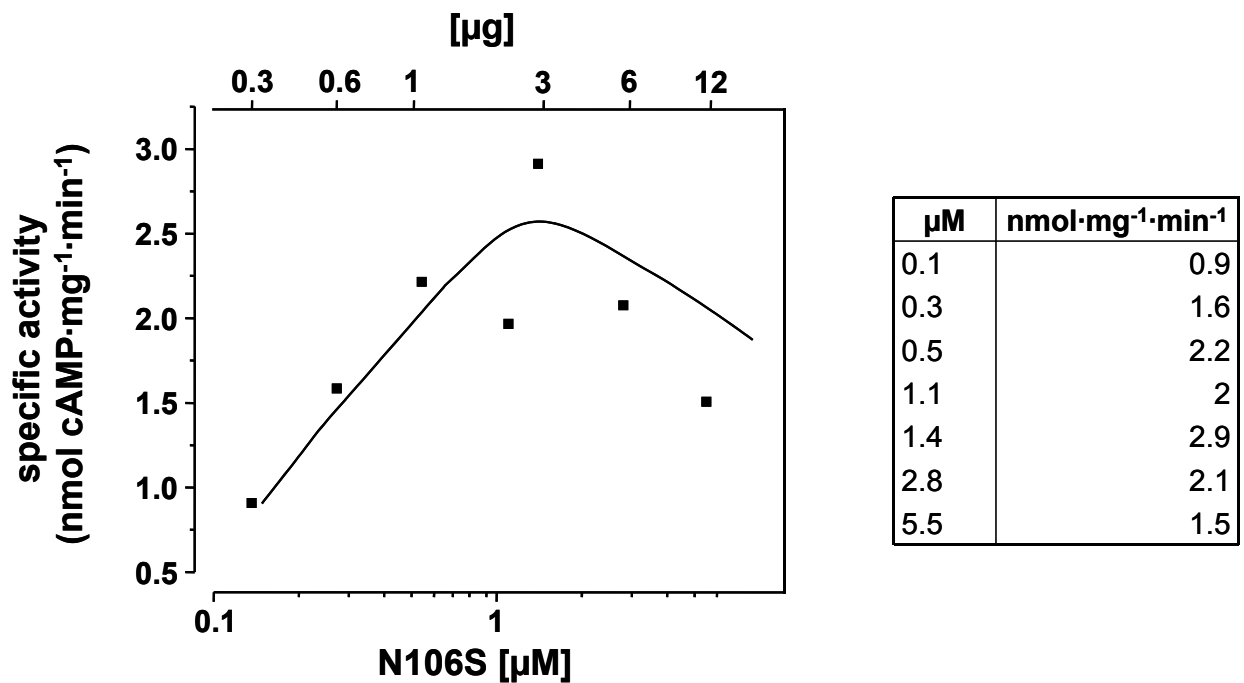
**Fig. 4.32:** a) 15% SDS-PAGE analysis of N106S. Lanes 1 and 2 correspond to the pellet (20  $\mu\text{g}$ ) and supernatant (8  $\mu\text{g}$ ) of empty pQE30 vector in BL21 cells. Lanes 3 and 4 correspond to pellet (20  $\mu\text{g}$ ) and supernatant (20  $\mu\text{g}$ ) of N106S. Lane 5 corresponds to the purified mutant (3  $\mu\text{g}$ ). b) Western blot from 15 % SDS-PAGE of 2  $\mu\text{g}$  dialyzed N106S analyzed with antibodies anti-KD0386. Time of exposure was 5 s.

N106S showed an AC residual activity of 43% with respect of the wild type. The GC activity corresponded to 8% of its AC activity (Table 4.16).

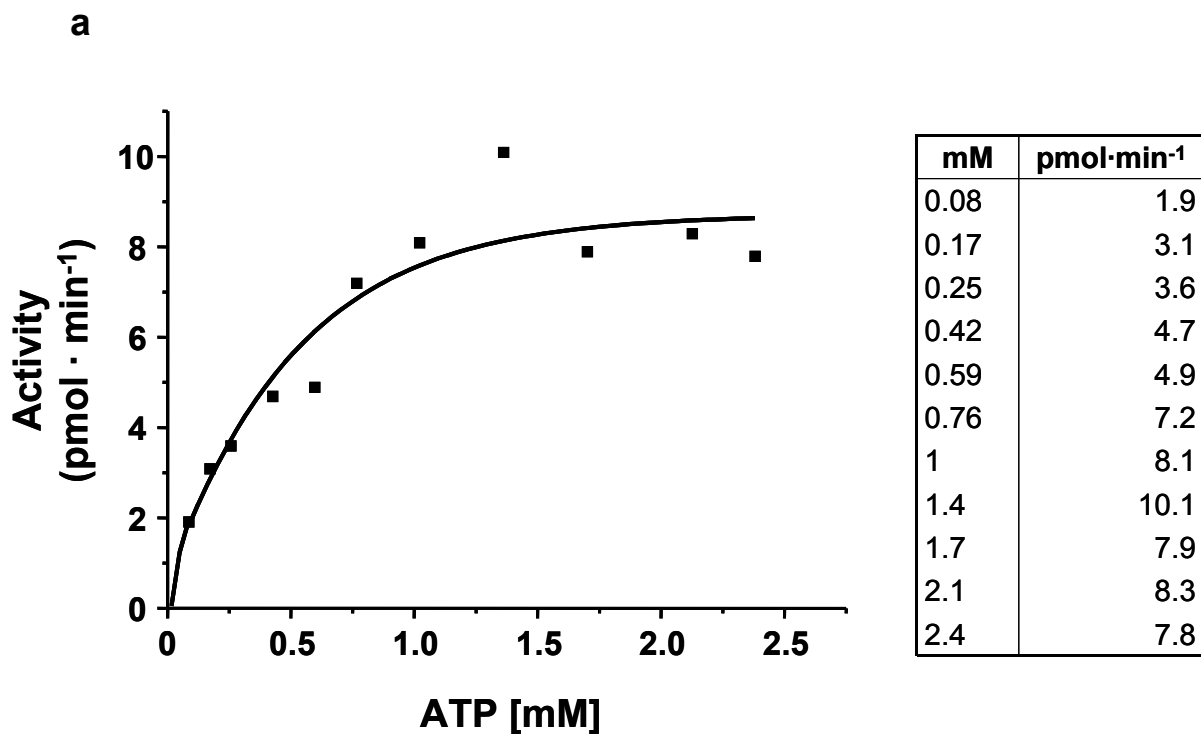
Protein [ $\mu\text{M}$ ]	AC activity $\text{nmol} \cdot \text{mg}^{-1} \cdot \text{min}^{-1}$ (wild type)	% activity of the wild type	GC specific activity ( $\text{nmol} \cdot \text{mg}^{-1} \cdot \text{min}^{-1}$ )	% GC vs. AC activity
2.4	2.1 (5.4)	38.9	0.2	9.5
3.8	1.7 (3.7)	46	0.1	5.9

**Table 4.16:** AC and GC activities of N106S. Wild-type AC activity at the same assay conditions are in parentheses. Assay conditions were: 850  $\mu\text{M}$  ATP or GTP, 20 min, 30°C, buffer MOPS pH 7.5.

Protein and substrate dependence of N106S were investigated. Like wild type, the mutant N106S AC activity increased with increasing protein concentrations (figure 4.33). That indicates dimerization already observed in Western blot (see above). The graphically derived apparent  $K_d$  value is 0.3  $\mu\text{M}$  (2-fold wild type). The enzyme kinetics of N106S showed a  $K_m$  value of 337  $\mu\text{M}$  and  $V_{\text{max}}$  of 9.3 pmol/min (figure 4.34). The Hill coefficient of 0.9 indicated no cooperativity.



**Fig. 4.33:** Protein dependence of N106S with ATP as a substrate. Assay conditions: 850  $\mu\text{M}$  ATP, 5 mM  $\text{Mn}^{2+}$ , MOPS pH 7.5, 30 °C, 20 min. Protein concentrations were from 136 nM to 5.5  $\mu\text{M}$ . An  $\text{EC}_{50}$  value of 0.34  $\mu\text{M}$  could be derived from a graphical analysis.



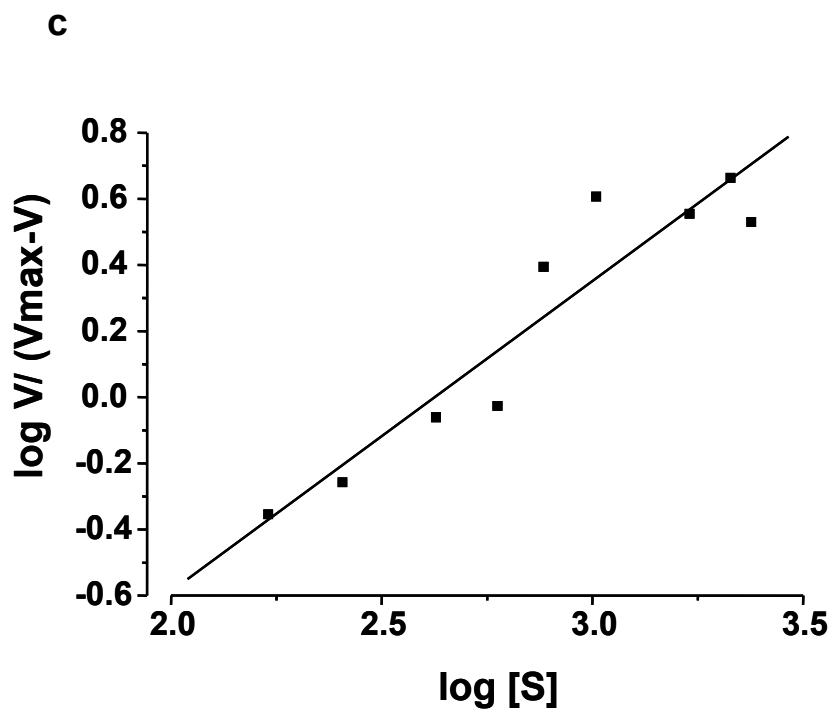
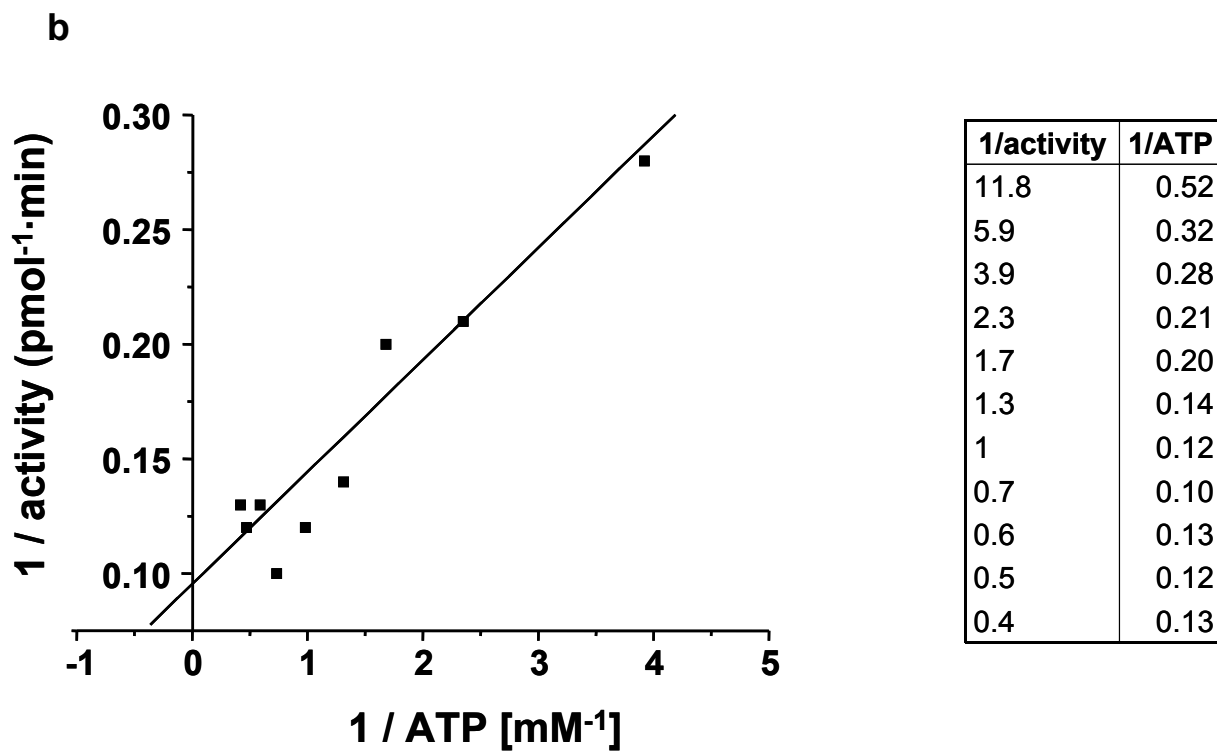


**Fig. 4.34:** a) Michaelis-Menten kinetic for ATP as a substrate. Assays were conducted at 1.4  $\mu\text{M}$  of protein, MOPS pH 7.5, 30°C, 5 mM  $\text{Mn}^{2+}$  and 10 min; **b)** corresponding Lineweaver-Burk linear fit; **c)** corresponding Hill-Plot ( $R^2= 0.9229$ ;  $y= 0.92213x - 2.42055$ ). **b** and **c)** the two smallest values were not drawn for graph clarity but taken for  $K_M$  and  $V_{\text{max}}$  calculation.  $V$ = activity ( $\text{pmol}\cdot\text{min}^{-1}$ );  $[S]$ = ATP.



#### 4.2.2.9 Expression and characterization of an N-terminally elongated AC domain

This protein corresponds to the Rv0386 AC domain elongated at the N-terminus with 7 amino acids (MRLSGAG) and is also called AC domain MT0399 (see 3.6.3.7 and 3.6.3.8 on chapter 3 for details). Purpose of its characterization was to determine its utility for crystallization experiments. Protein was expressed with N-terminal as well as with C-terminal His-tag in BL21 cells (5 h, 60  $\mu$ M IPTG, RT), purified and dialyzed as usual. Recoveries of 0.6 mg of N-terminally His-tagged protein (from 3 x 600 ml culture) and 0.3 mg of C-terminally His-tagged protein (from 400 ml culture) were obtained. Expression and purification steps were controlled by SDS-PAGE (Fig. 4.35).

Both proteins showed an AC activity of 30% of the wild type. The GC activities correspond to 27% of the AC activity for N-His tag MT0399 and 21% of the AC activity for C-His tag MT0399 (Table 4.17). The proportion AC/GC activity of both proteins is similar to that of wild type indicating no change in the substrate discrimination. Nevertheless the low activities point to a critical role of the N-terminus of the protein for catalysis in Rv0386. Both proteins were used for crystallization experiments but without success.

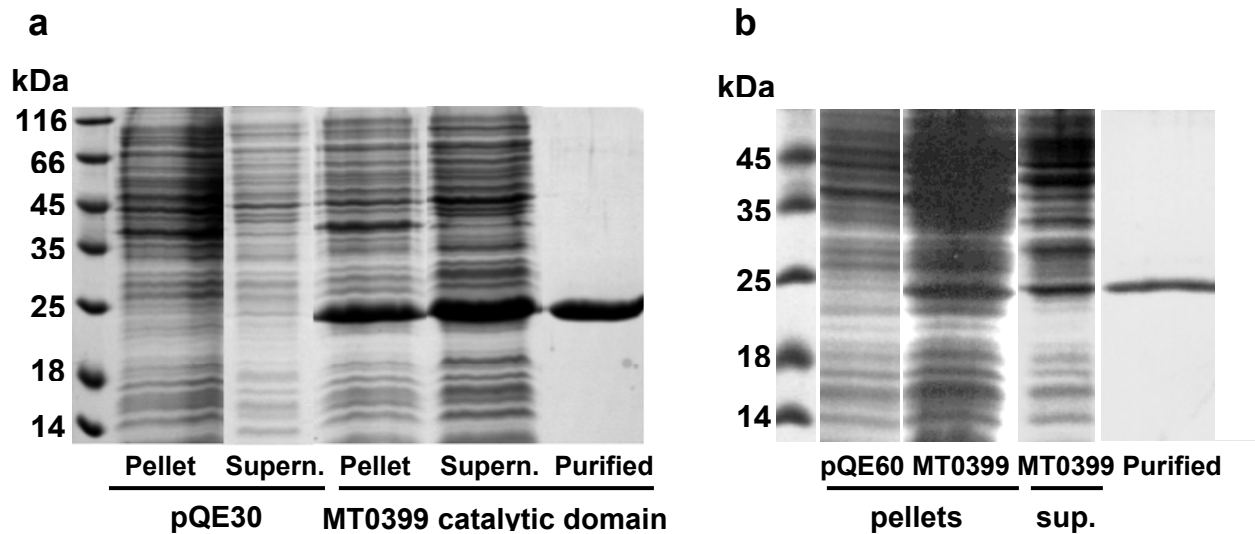


**Fig. 4.35:** 15% SDS-PAGE analysis of the N-terminally elongated AC domain (equivalent to MT0399 AC domain). **a)** Protein with N-terminal His-tag and **b)** with C-terminal His-tag. Empty vectors pQE30 and pQE60 were also expressed as controls. 20  $\mu$ g of pellets and 10-15  $\mu$ g of supernatants were applied. 1-2  $\mu$ g of purified and dialyzed protein were applied.

Protein	[ $\mu\text{M}$ ]	AC activity $\text{nmol} \cdot \text{mg}^{-1} \cdot \text{min}^{-1}$ (wild type)	% AC activity of the wild type	GC activity $\text{nmol} \cdot \text{mg}^{-1} \cdot \text{min}^{-1}$	% GC vs. AC activity
N-His tag	1.4	2.3 (6.7)	34.3	n.d.	-
MT0399	2.4	1.4 (5.4)	25.9	0.4	28.6
	3.8	1.2 (3.7)	32.4	0.3	25
	5.2	1.2 (4.1)	29.2	n.d.	-
C-His tag	1.9	0.9 (4.2)	21.4	0.2	22
MT0399	3.9	1 (3.4)	29.4	0.2	20

**Table 4.17:** AC and GC activities of MT0399 AC domain with N-terminal and C-terminal His-tag. Activities of both proteins were examined in separated assays (AC domain wild type at same assay conditions in parentheses). Assay conditions: 850  $\mu\text{M}$  ATP or GTP, 20 min, 30°C, buffer MOPS pH 7.5. n.d.= not determined.

Protein and substrate dependence of MT0399 with N-His tag were investigated. No apparent  $K_d$  value could be determined (Fig. 4.36). Probably the dimerization of the protein occurred at protein concentrations  $<214$  nM. That could not be further investigated due to the detection limit. The enzyme kinetics of this protein showed a  $K_m$  value of 2.3 mM and  $V_{\text{max}}$  of 13.6 pmol/min (Fig. 4.37). The Hill coefficient of 0.9 pointed to no cooperativity. Such characterizations were not made for MT0399 with C-terminal His-tag.

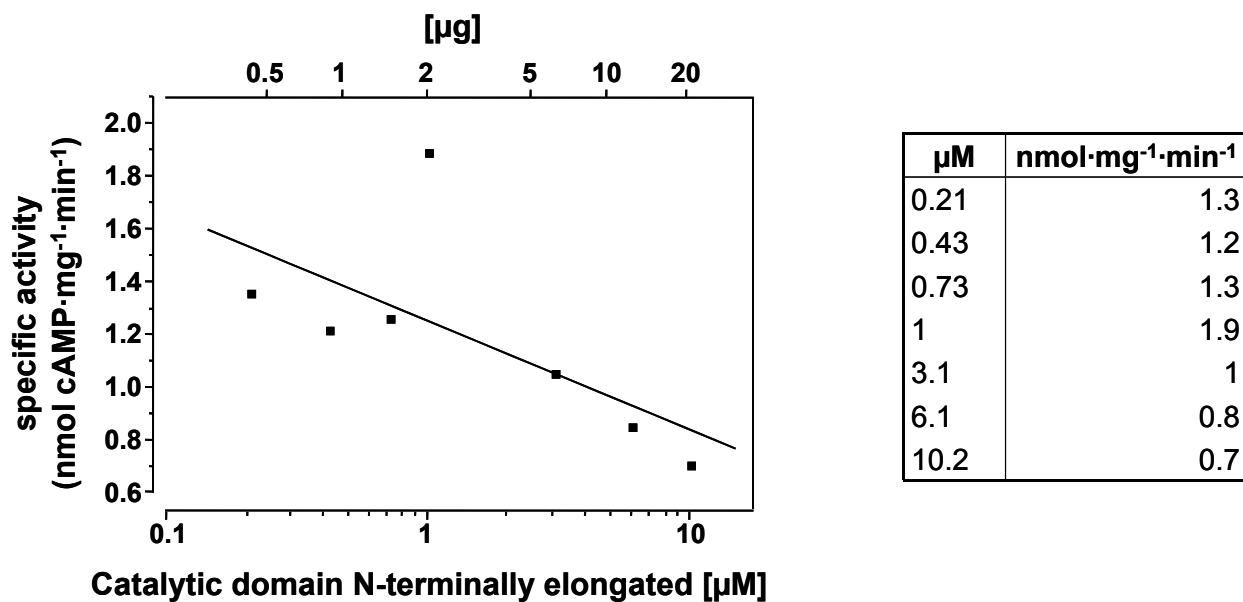
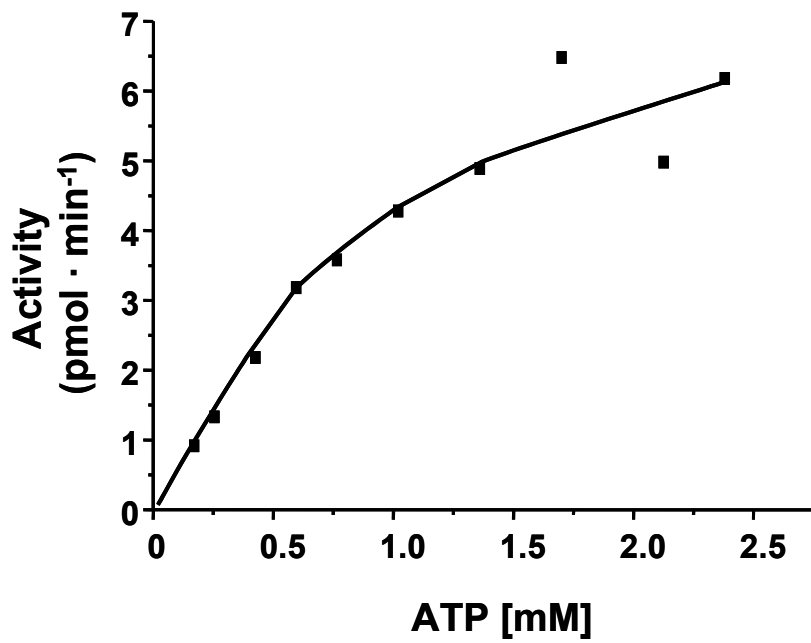


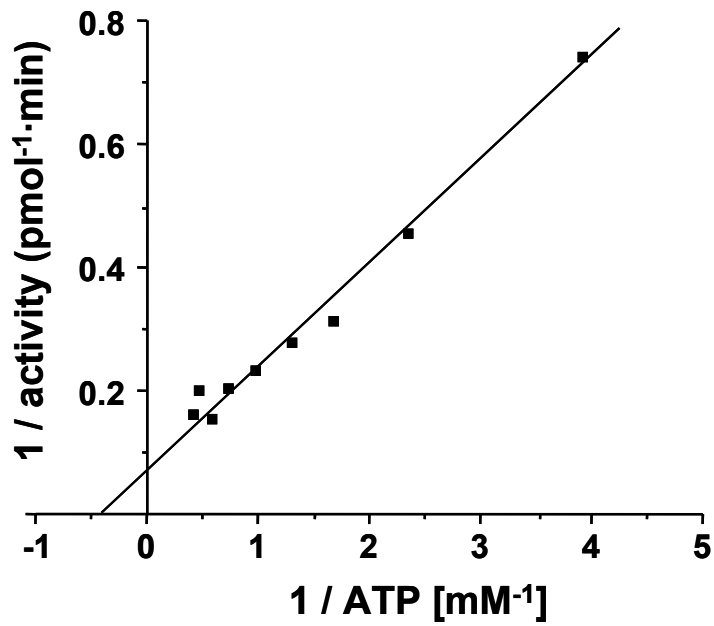
**Fig. 4.36:** Protein dependence of MT0399 (N-His tag) with ATP as a substrate. Assay conditions: 850  $\mu\text{M}$  ATP, 5 mM  $\text{Mn}^{2+}$ , MOPS pH 7.5, 30 °C, 20 min. Protein concentrations tested were from 214 nM to 10.2  $\mu\text{M}$ .

a



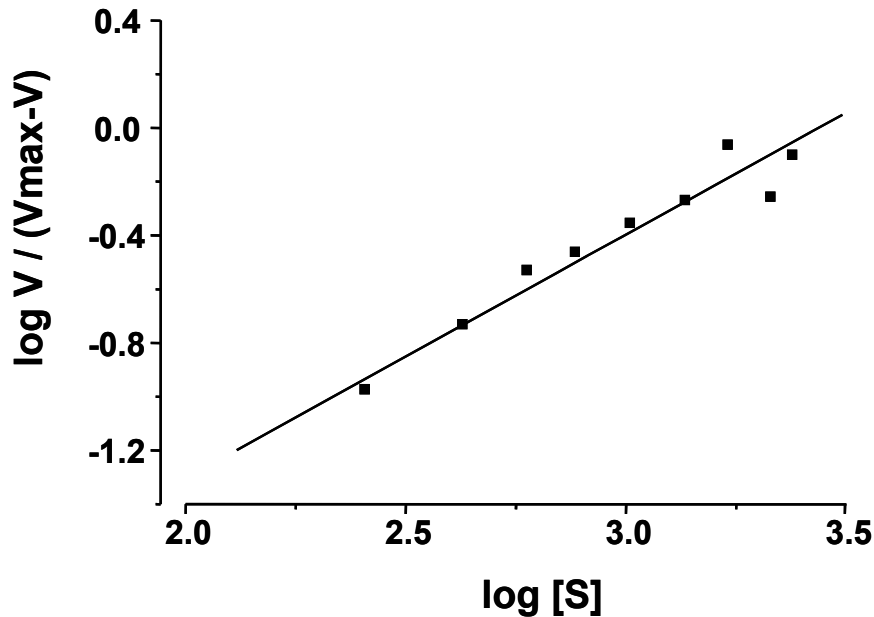
mM	pmol·min <sup>-1</sup>
0.2	0.9
0.25	1.3
0.4	2.2
0.6	3.2
0.8	3.6
1	4.3
1.4	4.9
1.7	6.5
2.1	5
2.4	6.2

b



1/activity	1/ATP
5.9	1.1
4	0.7
2.4	0.4
1.7	0.3
1.3	0.3
1	0.2
0.7	0.2
0.6	0.1
0.5	0.2
0.4	0.2

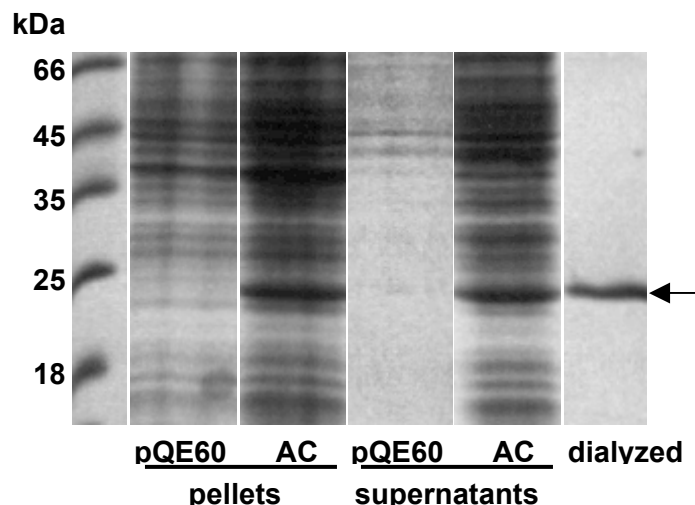
c



**Fig. 4.37:** a) Michaelis-Menten kinetic for ATP as substrate. Assays were conducted at 1.5  $\mu\text{M}$  protein, MOPS pH 7.5, 30°C, 5 mM  $\text{Mn}^{2+}$  and 10 min; b) corresponding Lineweaver-Burk linear fit; c) corresponding Hill-Plot ( $R^2 = 0.9540$ ;  $y = 0.90744x - 3.11893$ ). b and c) the smallest value were not drawn for graph clarity but taken for  $K_M$  and  $V_{\max}$  calculation.  $V =$  activity ( $\text{pmol}\cdot\text{min}^{-1}$ );  $[S] = \text{ATP}$ .

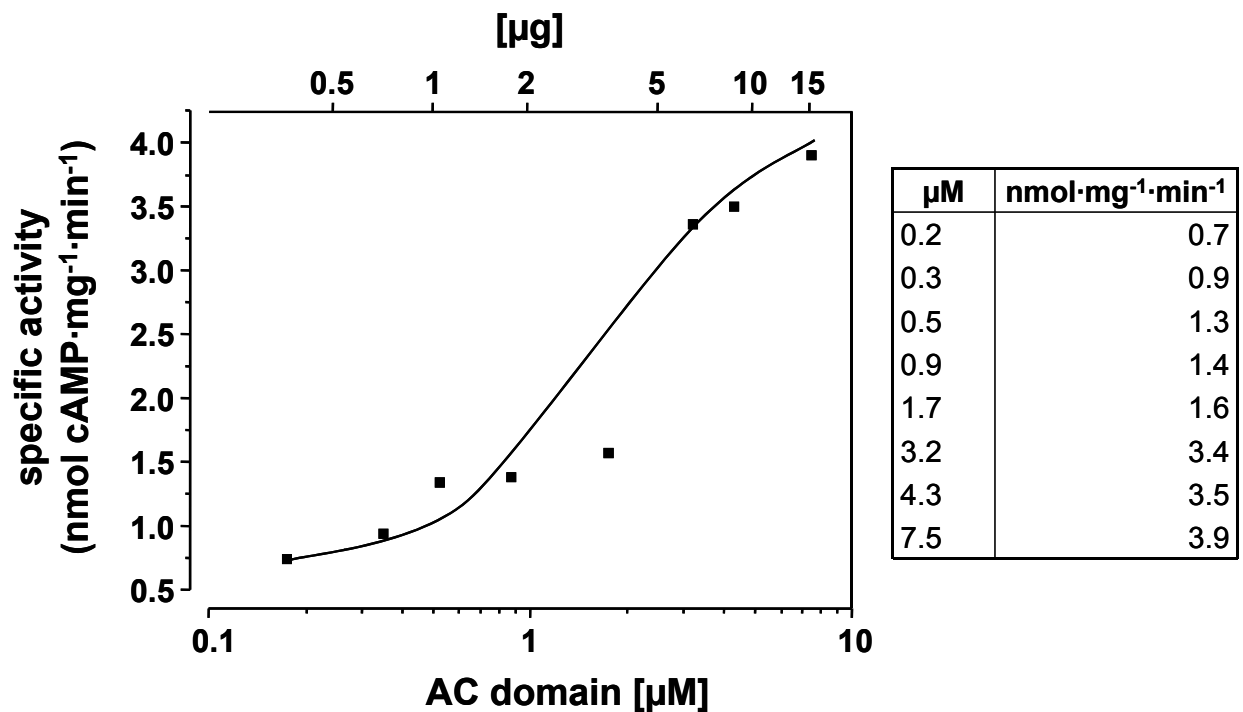
#### 4.2.2.10 Expression and characterization of the C-terminally His-tagged AC domain

The C-terminally His-tagged AC domain of Rv0386 was expressed in BL21 cells (5 h, 60  $\mu\text{M}$  IPTG, RT) with a protein recovery of 0.7 mg pro 400 ml culture after  $\text{Ni}^{2+}$ -NTA-agarose purification (Fig. 4.38). The protein was dialyzed (20% glycerol) and stored at  $-20^\circ\text{C}$ . The calculated molecular weight was 20 kDa including the C-terminal His-tag. This protein showed 81% of the AC activity of the N-terminally His-tagged AC domain.



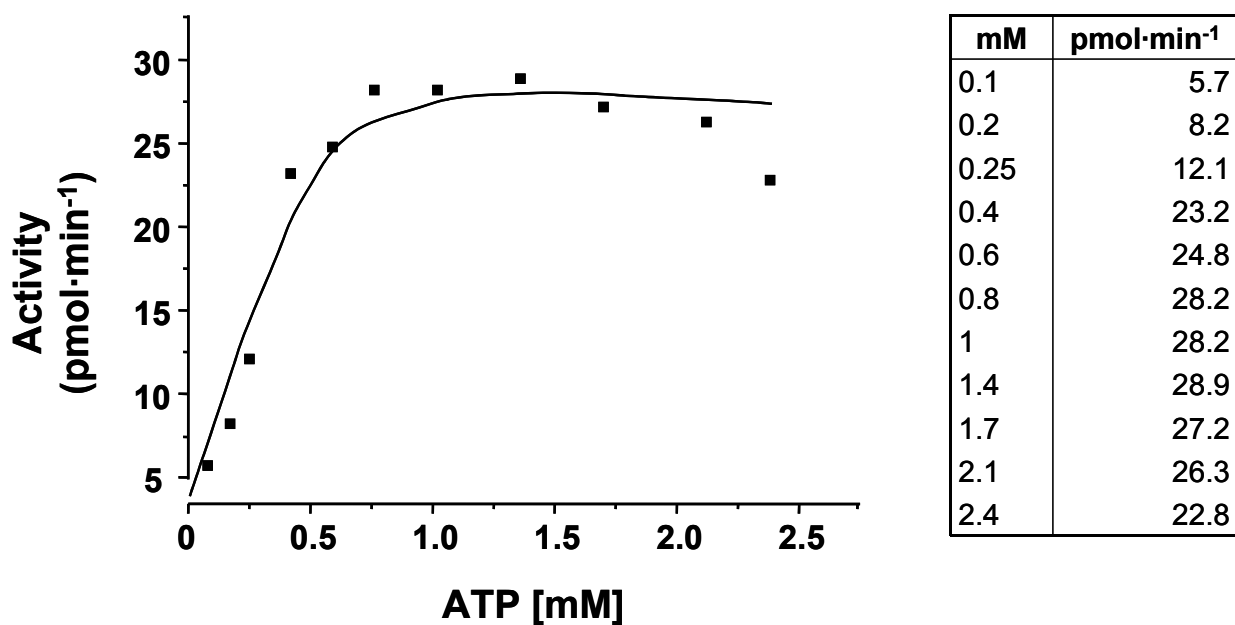
**Fig. 4.38:** 15% SDS-PAGE of the C-terminally His-tagged AC domain. An empty vector control was carried in parallel. 20  $\mu\text{g}$  of pellet proteins were applied. From supernatants, 5  $\mu\text{g}$  of pQE60 and 20  $\mu\text{g}$  of AC domain were applied. After purification and dialysis 2  $\mu\text{g}$  of protein were applied.

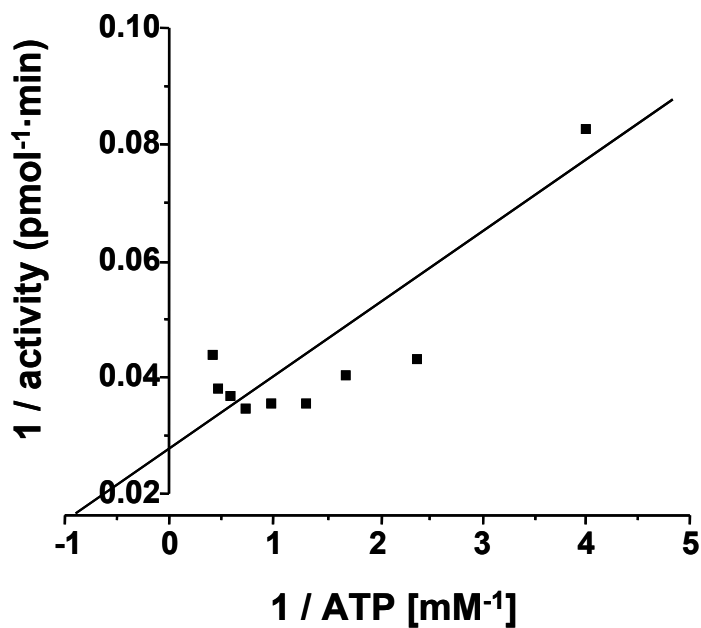
Protein and substrate dependence of the C-terminally His-tagged AC domain were examined. A considerably slowdown of the dimerization process of this protein was observed. The graphically derived apparent  $K_d$  value was 1.5  $\mu\text{M}$  (Fig. 4.39). Surprisingly up to 15  $\mu\text{g}$  protein no reduction in the activity was observed. After kinetic characterization the  $K_m$  value was 454  $\mu\text{M}$  and  $V_{\text{max}}$  was 34.8 pmol of cAMP/min (3.9 nmol of cAMP $\cdot\text{mg}^{-1}\cdot\text{min}^{-1}$ ). The Hill coefficient of 0.9 indicated no cooperativity. A slight inhibition of the activity upon 2 mM ATP was observed (Fig. 4.40).



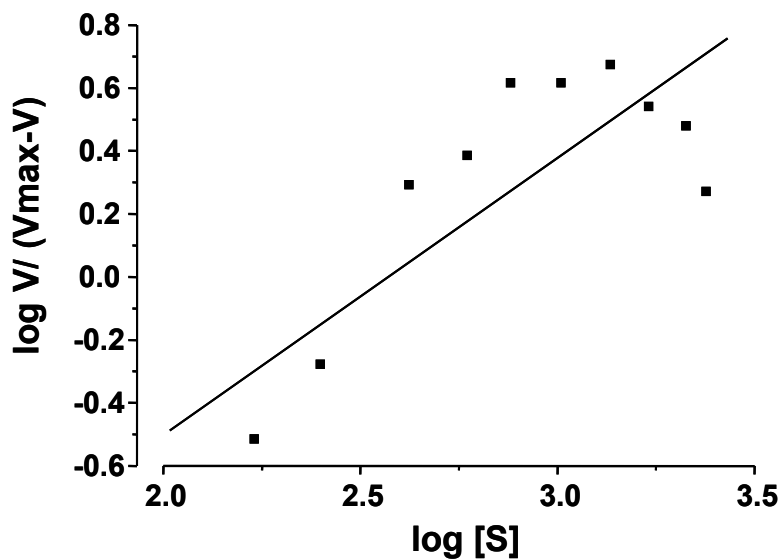
**Fig. 4.39:** Protein dependence of the AC domain with an C-terminal His-tag. Assay conditions: 850  $\mu\text{M}$  ATP, 5 mM  $\text{Mn}^{2+}$ , MOPS pH 7.5, 30°C, 20 min. Protein concentrations tested were from 175 nM to 7.5  $\mu\text{M}$ . An  $\text{EC}_{50}$  value of 1.5  $\mu\text{M}$  could be derived graphically.

a



**b**

1/activity	1/ATP
12.5	0.17
5.9	0.12
4	0.08
2.4	0.04
1.7	0.04
1.3	0.03
1	0.03
0.7	0.03
0.6	0.04
0.5	0.04
0.4	0.04

**c**

**Fig. 4.40:** **a)** Michaelis-Menten kinetic of AC domain with C-terminal His-tag. Assay was conducted at 4.3  $\mu\text{M}$  of protein, MOPS pH 7.5, 30°C, 5 mM  $\text{Mn}^{2+}$  and 10 min; **b)** corresponding Lineweaver-Burk linear fit; **c)** corresponding Hill-Plot ( $R^2= 0.8225$ ;  $y= 0.9085x - 2.3927$ ). **b)** the two smallest values were not drawn for graph clarity but taken for  $K_M$  and  $V_{\text{max}}$  calculation.  $V=$  activity ( $\text{pmol}\cdot\text{min}^{-1}$ ).

#### 4.2.2.11 Expression and AC assay of mutant R7G

This mutant was generated due to a cloning error (see 3.6.3.10 for details). It was expressed in BL21 cells (60  $\mu\text{M}$  IPTG, 4 h, RT), pellet and supernatant were separated, analyzed by SDS-PAGE and tested (Fig. 4.41). AC assay conditions were 75  $\mu\text{M}$  ATP, 37°C, 2 mM  $\text{Mn}^{2+}$ , 10 min, Tris-HCl pH 7.5. Activity of the supernatant fraction (0.6 pmol  $\text{min}^{-1}$ ) was identical to an empty vector control (0.5 pmol  $\text{min}^{-1}$ ). Activity of the pellet was 0.3 pmol  $\text{min}^{-1}$  (control pellet 0.1 pmol  $\text{min}^{-1}$ ). After Ni-NTA-agarose purification the specific activity was 26 pmol  $\text{mg}^{-1} \text{min}^{-1}$  (4  $\mu\text{M}$  protein, 30°C, 75  $\mu\text{M}$  ATP, 10 min, Tris pH 7.5). Under identical conditions the wild type AC showed a specific activity of 460 pmol  $\text{mg}^{-1} \text{min}^{-1}$ . Since the activity of this mutant was rather low it is possible that this N-terminally positioned arginine residue in Rv0386 AC domain is critical for catalysis. For Rv1625c it is reported a significant loss of the activity when two N-terminally located arginine residues i.e. R43 and R44 were mutated to alanine and glycine, respectively (Reddy et al., 2001).

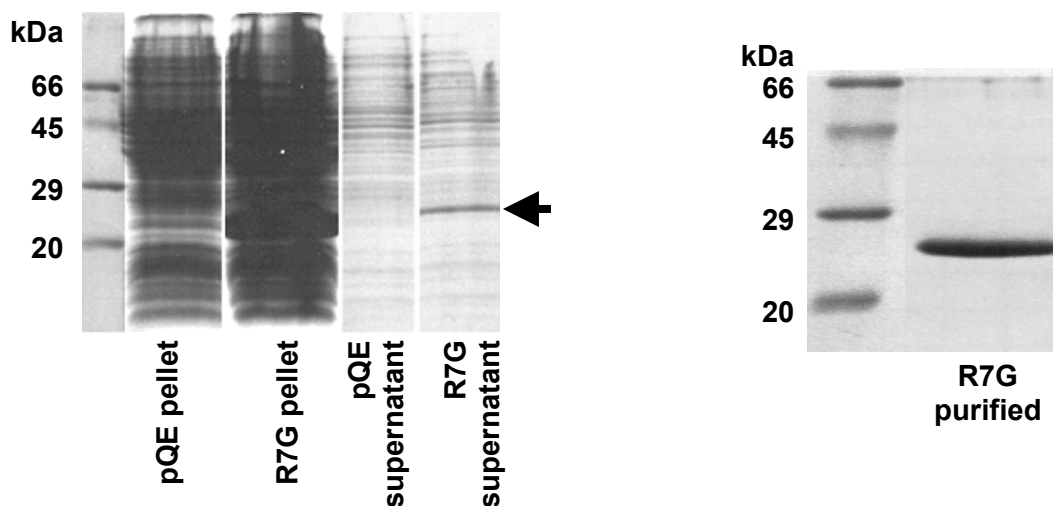


**Fig. 4.41:** 15% SDS-PAGE analysis of the mutant R7G in pellet and supernatant and in eluate after Ni-NTA purification. Applied were about 40  $\mu\text{g}$  protein of pellets and about 20  $\mu\text{g}$  protein of supernatants. About 5  $\mu\text{g}$  of purified R7G were applied.

#### 4.2.2.12 Crystallization of the AC domain

First crystals were obtained with the N-terminally His-tag construct with buffers CS#22 and CS2#1 (Hampton Research kit). Variations of these conditions and of the protein



solution components and concentration were made to optimize size and quality of the crystals (Table 4.18). With the C-terminally His-tagged construct four different conditions corresponding to buffers CS#6, CS2#30, CSL#22 and CSL#25 were found (Table 4.19). See appendix for pictures of the best crystals obtained.

<b>Protein: N-terminally His-tagged Rv0386<sub>(1-175)</sub></b>				
Buffer components	Protein solution components	Protein concentration	Crystal form	Remarks
30% PEG 4000, 0.1 M Tris HCl pH 8.5, 0.2 M sodium acetate (CS#22*)	50 mM Tris HCl pH 8.5, 20% glycerol, 10 mM NaCl, 2 mM $\beta$ -mercaptoethanol	9 mg/ml	Needles (clusters)	After 3 weeks at 12 °C.
10% PEG 6000, 2 M NaCl (CS2#1*)			Cubes (very small)	after 8 days at 12°C
<b>Optimization based on buffer CS2#1*</b>				
10% PEG 6000, 2 M NaCl	50 mM Tris HCl pH 8.5, 10% glycerol, 10 mM NaCl, 2 mM $\beta$ -mercaptoethanol	16 mg/ml	Rectangles 40 x 25 $\mu$ m	after 6 days at 12°C
		30 mg/ml	Rectangles 115 x 30 $\mu$ m	after 2 weeks at 12°C
22 mg/ml + 1.7 mM $\alpha,\beta$ -CH <sub>2</sub> ADP		Rectangles 150 x 35 $\mu$ m		
10% PEG 6000, 2 M NaCl, 1 mM Dibutyryl cAMP		22 mg/ml	Rectangles 200 x 75 $\mu$ m	
12% PEG 6000, 2 M NaCl		30 mg/ml	Rectangles 115 x 30 $\mu$ m	after 2 weeks at 12°C
10% PEG 5000, 2 M NaCl		16 mg/ml	Rectangles 50 x 20 $\mu$ m	after 8 days at 12°C
10% PEG 4000, 2 M NaCl			Rectangles 200 x 175 $\mu$ m	
10% PEG 3350, 2 M NaCl			Rectangles 200 x 175 $\mu$ m	

**Table 4.18:** Summary of conditions in which crystals of N-terminally His-tagged Rv0386<sub>(1-175)</sub> were grown. \* Name according to the Crystal Screen Buffer Kit of Hampton Research (CS= crystal screen, CS2= crystal screen 2, CSL= crystal screen lite).

Protein: C-terminally His-tagged Rv0386 <sub>(1-175)</sub>					
Buffer name	Buffer components	Protein solution components	Protein conc.	Crystal form	Remarks
CS#6*	30% PEG 4000, 0.1 M Tris HCl pH 8.5, 0.2 M MgCl <sub>2</sub>	50 mM Tris HCl pH 8.5, 5 % glycerol, 2 mM β-mercaptoethanol, 10 mM NaCl, incubated 12-14 h at 0°C with 1 mM ATP	9 mg/ml	Needles (clusters)	after 10 days at 16 °C
CS2#30	10 % PEG 6000, 0.1 M Hepes pH 7.5, 5% MPD			Needles 40 x 5 μm	
CSL#22	15% PEG 4000, 0.1 M Tris HCl pH 8.5, 0.2 M sodium acetate			Half-moon shaped 50 x 50 μm	after 24 h at 16 °C
CSL#25	0.5 M sodium acetate, 0.1 M imidazole pH 6.5			Needles** 40 x 5 μm	

**Table 4.19:** Summary of conditions in which crystals of N-terminally His-tagged Rv0386<sub>(1-175)</sub> were grown. \* Name according to the Crystal Screen Buffer Kit of Hampton Research (CS= crystal screen, CS2= crystal screen 2, CSL= crystal screen lite). \*\* Diffraction-quality crystals; see preliminary data in appendix.

## 4.2.3 Expression of Rv0386 holoenzyme

### 4.2.3.1 Expression in BL21 (DE3) [pREP4] cells

After expression (60 μM IPTG, 5 h, RT) cells were sonicated, pellet and supernatant were separated (14000 x g; 30 min; 4°C) and tested for AC activity. BL21 with empty vector served as a control (Fig. 4.42a). The expected MW including His-tag was 117 kDa. The holoenzyme was in the pellet (presumably inclusion bodies). For better lysis a French Press was used (20,000 psi). Pellet and supernatant were separated as usual, protein purified with Ni-NTA-agarose (Fig. 4.42b) and tested. Only degradation products (because AC activity was detectable) were found in the eluate after purification.

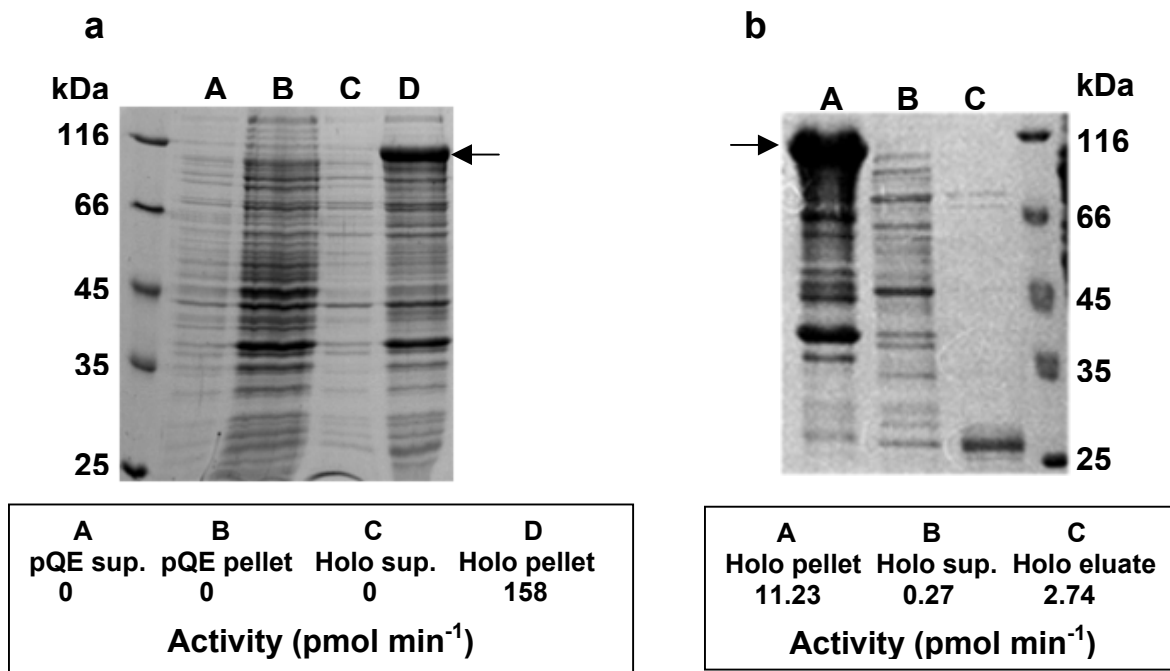


**Fig. 4.42:** 12.5% SDS-PAGE of the holoenzyme Rv0386 using (a) sonification and (b) French Press for lysis. (a) Applied were: about 1.5  $\mu\text{g}$  protein of supernatants, 4  $\mu\text{g}$  of pQE30 pellet and 7  $\mu\text{g}$  of holoenzyme pellet. Activities correspond to: 5  $\mu\text{g}$  protein of supernatants, 32  $\mu\text{g}$  of pQE30 pellet and 55  $\mu\text{g}$  of holoenzyme pellet. (b) Applied were: 8  $\mu\text{g}$  of pellet, 5  $\mu\text{g}$  of supernatant and 1  $\mu\text{g}$  of purified protein. Activities correspond to 10.8  $\mu\text{g}$  protein. Specific activity of the purified protein (0.9  $\mu\text{M}$ ) was 254  $\text{pmol cAMP}\cdot\text{mg}^{-1}\cdot\text{min}^{-1}$  (assay conditions: 75  $\mu\text{M}$  ATP, 10 min, 30°C, 2 mM  $\text{Mn}^{2+}$ , Tris-HCl pH 7.5).

Incubation with DNase (30 min, 0°C, 20  $\mu\text{g}/\text{ml}$ ) direct after cell lysis with French Press was performed in case that the holoenzyme bound to the DNA. Pellet and supernatant were as usual separated and the supernatant was further purified with Ni-NTA-agarose (Fig. 4.43). An increment of soluble holoenzyme in the supernatant was not observed.

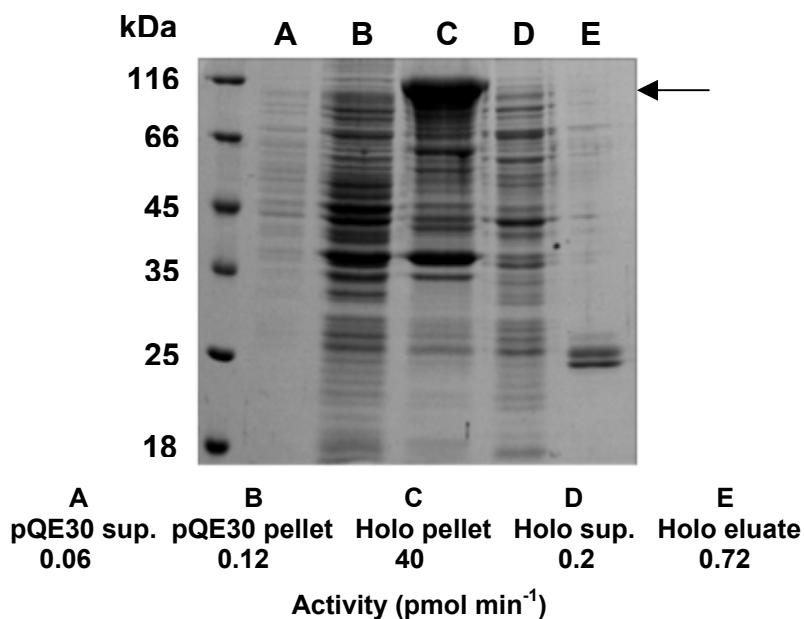


**Fig. 4.43:** 12.5% SDS-PAGE analysis. Applied were : 24  $\mu\text{g}$  of pellet proteins, 5  $\mu\text{g}$  of supernatant and 1  $\mu\text{g}$  of eluate. AC activities correspond to 2  $\mu\text{g}$  pQE30 supernatant, 54  $\mu\text{g}$  pQE30 pellet, 72  $\mu\text{g}$  holoenzyme pellet, 40  $\mu\text{g}$  holoenzyme supernatant and 4  $\mu\text{g}$  (0.3  $\mu\text{M}$ ) of eluate. Specific activity of the purified protein is 181  $\text{pmol cAMP}\cdot\text{mg}^{-1}\cdot\text{min}^{-1}$ . Assay conditions: 75  $\mu\text{M}$  ATP, 10 min, 2 mM  $\text{Mn}^{2+}$ , Tris/HCl pH 7.5, 30°C, 60 mM imidazole (from purified samples).

Furthermore protease inhibitors (Complete tablets) with and without EDTA (1 mM) were added to the lysis buffer before French Press lysis. Pellets and supernatants were separated and analyzed by SDS-PAGE together with the eluates after protein purification (Fig. 4.44). In both cases intact holoenzyme could be recovered in the eluates.

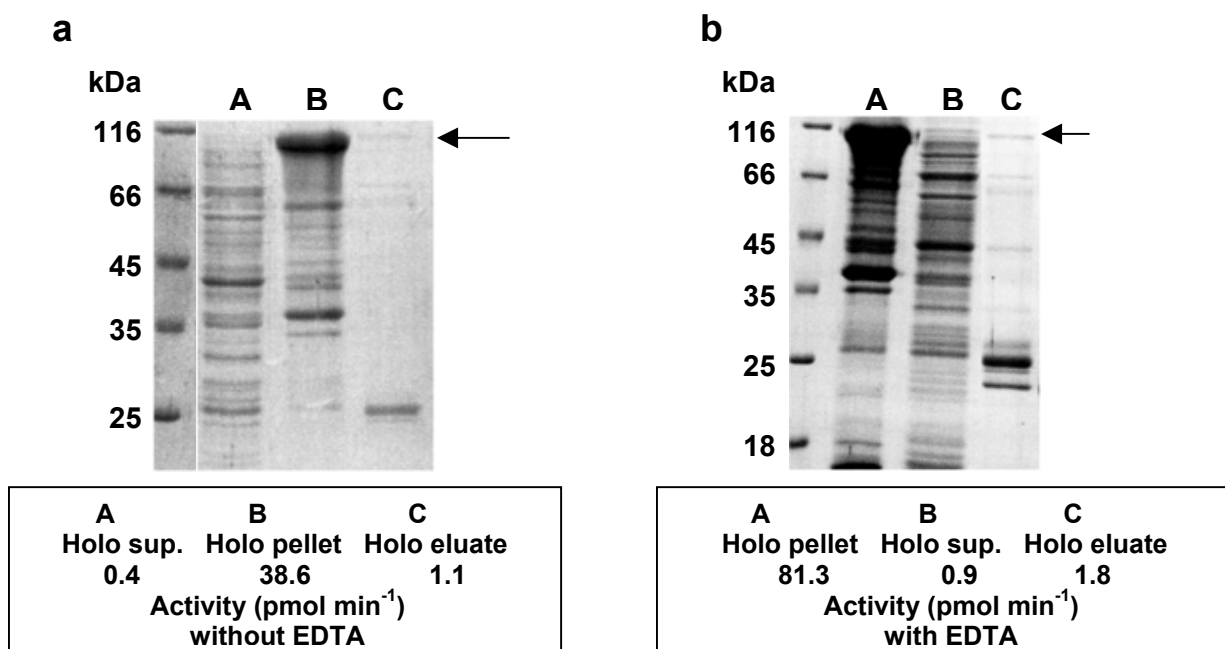


**Fig. 4.44:** 12.5% SDS-PAGE analysis after addition of (a) protease inhibitors only or (b) together with EDTA. Applied were 20  $\mu\text{g}$  pellets, 15  $\mu\text{g}$  supernatants and 1.5  $\mu\text{g}$  eluates. AC activities are from (a) 50  $\mu\text{g}$  pellet proteins, 35  $\mu\text{g}$  supernatant, 4.8  $\mu\text{g}$  eluate (0.4  $\mu\text{M}$ ; 235  $\text{pmol cAMP}\cdot\text{mg}^{-1}\cdot\text{min}^{-1}$ ) and (b) 90  $\mu\text{g}$  pellet proteins, 52  $\mu\text{g}$  supernatant, 6.8  $\mu\text{g}$  eluate (0.6  $\mu\text{M}$ ; 262  $\text{pmol cAMP}\cdot\text{mg}^{-1}\cdot\text{min}^{-1}$ ). Assay conditions: 75  $\mu\text{M}$  ATP, 30°C, 2 mM  $\text{Mn}^{2+}$ , Tris/HCl pH 7.5, 10 min, 60 mM imidazole (from purified samples).

Expression of the holoenzyme with and without IPTG induction (60  $\mu\text{M}$ , 3 h, RT) was investigated. Cell lysis was with addition of protease inhibitors and French Press, pellet and supernatant were separated as usual and the holoenzyme was further purified with Ni-NTA-agarose (Fig. 4.45). The majority of the expressed holoenzyme was found in the

pellet. From the expression without IPTG a little more soluble protein could be purified, but presumably IPTG induction is not directly responsible for the formation of inclusion bodies.

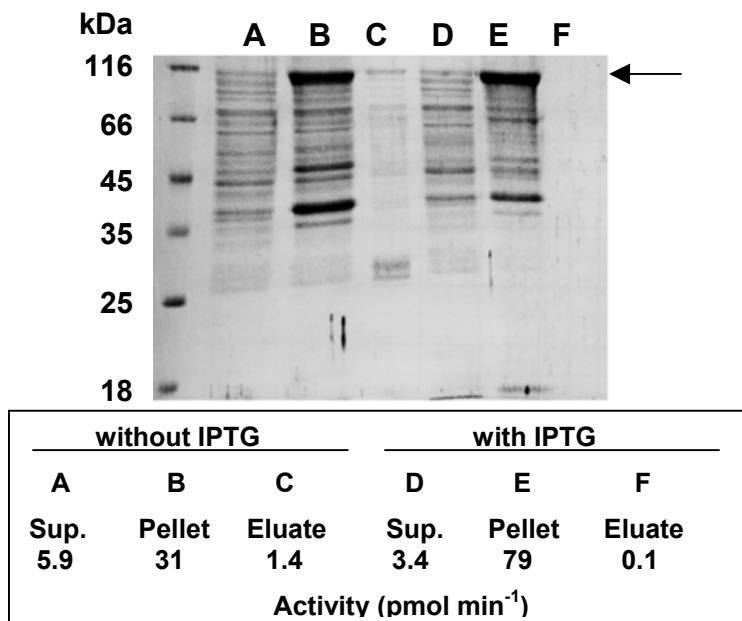


**Fig. 4.45:** 12.5 % SDS-PAGE of the holoenzyme expression with and without IPTG induction. Applied were: about 4  $\mu\text{g}$  of pellet and supernatant proteins together with 0.5  $\mu\text{g}$  of eluates. AC activities were from 80  $\mu\text{g}$  supernatants, 54  $\mu\text{g}$  pellet  $-$ IPTG, 90  $\mu\text{g}$  pellet  $+$ IPTG, 3.2  $\mu\text{g}$  eluate  $-$ IPTG (0.3  $\mu\text{M}$ ; 443  $\text{pmol}\cdot\text{mg}^{-1}\cdot\text{min}^{-1}$ ) and 0.8  $\mu\text{g}$  eluate  $+$ IPTG (68 nM; 174  $\text{pmol}\cdot\text{mg}^{-1}\cdot\text{min}^{-1}$ ). Assay conditions: 100  $\mu\text{M}$  ATP, 30°C, 10 min, 2 mM  $\text{Mn}^{2+}$ , MOPS pH 7.5, 60 mM imidazole (from purified samples).

#### 4.2.3.2 Membrane preparations and attempts of solubilization

A methodology normally used for solubilizing membrane proteins by addition of detergents was used for the holoenzyme (see chapter 3, purification of insoluble proteins). Detergents polidocanol (1%; Table 4.20; Fig. 4.46) and CHAPS (2%; Fig. 4.47 and 4.48) solubilized good quantities of intact holoenzyme. Other detergents like SDS and Nonidet P-40 were of no use for the solubilization (Fig. 4.47). Degradation products were present in all cases.

SAMPLE		SDS-PAGE	AC-TEST	
		µg protein	µg protein	Activity (pmol min <sup>-1</sup> )
A	Pellet after centrifugation at 3000 g	100	412	185
B	Supernatant after centrifugation at 3000 g	-	74	7.4
C	Supernatant after centrifug. At 100,000 g	14	54	0.7
D	Pellet after incubation with detergent	12	49	15.3
E	Supernatant after 2 <sup>nd</sup> centrifug. 100,000 g	12	48	0.6
F	Pellet after 2 <sup>nd</sup> centrifug, at 100.000 g	62	249	113.5
G	Wash fraction of Ni-NTA purification	4	16	0
H	Eluate after Ni-NTA purification	3	16	4.3

**Table 4.20:** Solubilization and purification of the holoenzyme using 1% Polidocanol. Samples of each step of the process were analyzed by SDS-PAGE and AC-test. Assay conditions: 75 µM ATP, 30°C, 10 min, MOPS pH 7.5. Eluate after purification showed a specific activity of 274 pmol·mg<sup>-1</sup>·min<sup>-1</sup> for 16 µg protein (7.6 µM).

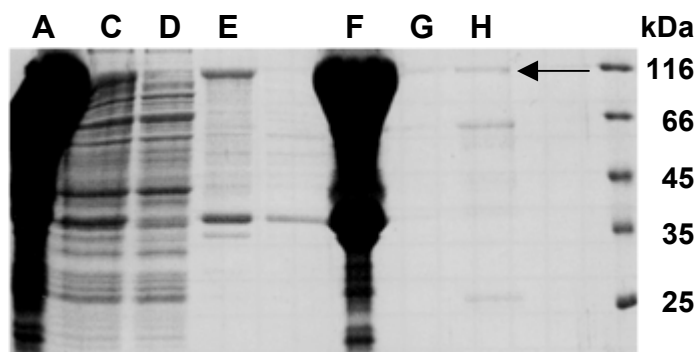


**Fig. 4.46:** 12.5% SDS-PAGE analysis of the solubilization with 1 % Polidocanol. Sample and protein amounts applied on each lane are specified above in table 4.17.

To investigate the solubilization with 2% CHAPS, 1% TRITON X-100, 1% SDS and 1% NONIDET P-40, pellets before incubation with the detergent and the Ni-NTA-purification eluates were analyzed by Western blot (antibodies anti-RGS-His<sub>4</sub>). For CHAPS and TRITON, the presence of more degradation products in the eluates than in the pellets was noticeable. With SDS it was impossible to purify detectable amounts of protein.

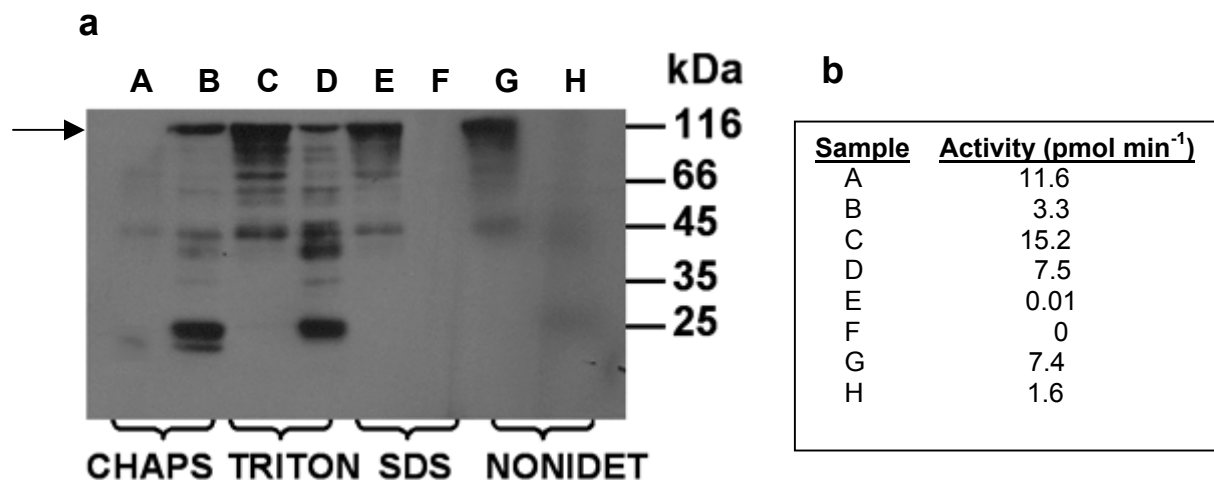


**Fig. 4.47:** **a)** Western blot analysis of the pellets (33,000 x g) before incubation with detergent (lanes A, C, E and G each about 4  $\mu$ g of protein) and of the Ni-NTA-purification eluates (lanes B, D, F and H each 0.2-1  $\mu$ g of protein). Samples were analyzed with antibodies anti-RGS-His<sub>4</sub> diluted 1:2000. Time of exposure: 5 s. **b)** AC-test of the blotted samples: 75  $\mu$ M ATP, MOPS pH 7.5, 30 °C, 10 min, with ATP-regenerating system. Specific activities of the eluates were: 555 (CHAPS), 1871 (Triton), 0 (SDS) and 311 (Nonidet) pmol mg<sup>-1</sup> min<sup>-1</sup>.

Solubilization with CHAPS (2%) was examined in detail. Cell pellets were processed as usual. 8-15  $\mu$ l of each step were analyzed by Western blot (no determination of protein concentration was made; Fig. 4.48). Degradation products of the holoenzyme were detected in most of the samples with exception of the supernatant after the second centrifugation step at 33,000 x g. A protein concentration of 80 ng was calculated for it by Western blot through a calibration curve (catalytic domain as a standard, anti-RGS-His<sub>4</sub>). An AC-test using 320 ng protein showed an activity of 0.9 pmol min<sup>-1</sup> (assay conditions: 500  $\mu$ M ATP, MOPS pH 7.5, 30 °C, 4 min, with ATP-regenerating system). It corresponds to a specific activity of 2.9 nmol mg<sup>-1</sup> min<sup>-1</sup>.

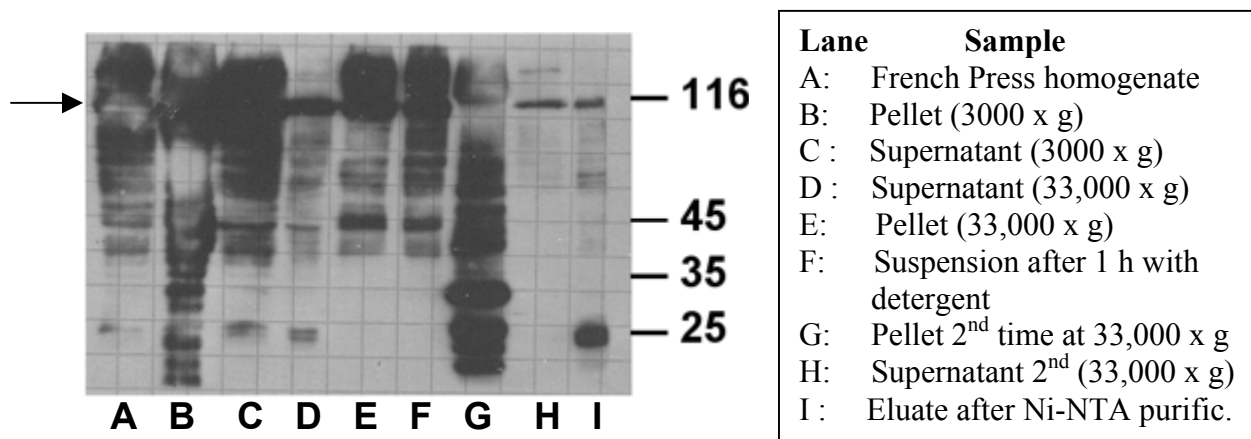


**Fig. 4.48:** Western blot analysis of the solubilization with 2% CHAPS. Antibodies anti-RGS-His<sub>4</sub> were used. Time of exposure was 60 s. 8  $\mu$ l of pellet samples as well as 15  $\mu$ l of supernatant and eluate samples were applied.

#### 4.2.3.3 Expression in BL21 STAR and ROSETTA cells

##### 4.2.3.3.1 Expression in BL21 STAR (DE3) [pREP4] cells

Expression was performed with and without IPTG induction (30  $\mu$ M, O/N, 15°C). Cells were sonificated in presence of protease inhibitors, lysates were incubated with lysozyme and DNase, pellets and supernatants were separated as usual and protein was purified with Ni-NTA agarose (Fig. 4.49). From 3 x 600 ml of uninduced culture, 20  $\mu$ g purified protein were obtained and from an induced culture 12  $\mu$ g protein. AC activities of pellets, supernatants and eluates were measured (Table 4.21). Differences between holoenzyme expression with or without induction with IPTG were not observed. In both cases eluates after purification showed degradation products.

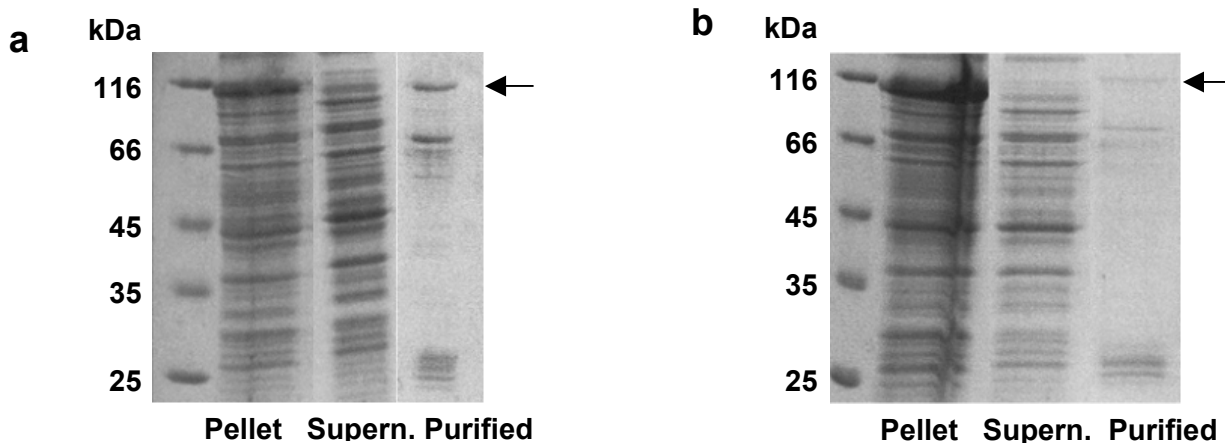


**Fig. 4.49:** 12.5% SDS-PAGE analysis of the expression in BL21 STAR cells. **a)** Cells were not induced; applied: 20  $\mu$ g pellet, 15  $\mu$ g supernatant and 1  $\mu$ g eluate. **b)** Cells induced with 30  $\mu$ M IPTG; applied: 20  $\mu$ g pellet, 9  $\mu$ g supernatant and 0.6  $\mu$ g eluate.



Sample	Protein ( $\mu\text{g}$ )	Activity ( $\text{pmol}\cdot\text{min}^{-1}$ )	Specific activity ( $\text{nmol}\cdot\text{mg}^{-1}\cdot\text{min}^{-1}$ )
Pellet	40.3	59	1.4
Supernatant uninduced	14.8	0.7	0.05
Eluate	2	7.3	3.7
Pellet	35.6	77	2.2
Supernatant +30 $\mu\text{M}$ IPTG	8.6	0.2	0.02
Eluate	1.2	6.7	5.6

**Table 4.21:** AC activities of pellets, supernatants and eluates of expression in BL21 STAR cells. Specific activities of eluates:  $3.7 \text{ nmol}\cdot\text{mg}^{-1}\cdot\text{min}^{-1}$  without induction and  $5.6 \text{ nmol}\cdot\text{mg}^{-1}\cdot\text{min}^{-1}$  with induction (30  $\mu\text{M}$  IPTG). Assay conditions: 500  $\mu\text{M}$  ATP, 10 min, 30°C, 5 mM  $\text{Mn}^{2+}$  and MOPS pH 7.5. Detection limit was  $20 \text{ pmol}\cdot\text{mg}^{-1}\cdot\text{min}^{-1}$ .

An expression was carried out (60  $\mu\text{M}$  IPTG, 16°C, 21 h). Cells were lysed with French Press with prior addition of protease inhibitors (Complete EDTA-free), and the cell homogenate was incubated with lysozyme and DNase. Pellet and supernatant were separated as usual and protein was purified from with Ni-NTA-agarose (19 h binding). From 3 x 600 ml culture 0.4 mg protein could be purified. Analysis by SDS-PAGE (Fig. 4.50), AC assay (Table 4.22) and Western blot of the pellet, supernatant and eluate were performed (Fig. 4.51).

Sample	Activity ( $\text{pmol}\cdot\text{min}^{-1}$ )	Specific activity ( $\text{nmol}\cdot\text{mg}^{-1}\cdot\text{min}^{-1}$ )
Pellet	21	4.3
Supernatant	1.1	0.2
Eluate	31	6.3

**Table 4.22:** AC activities from expression in BL21 STAR cells. Protein amount tested of each sample was 5  $\mu\text{g}$ . Specific activity of the purified protein:  $6.3 \text{ nmol}\cdot\text{mg}^{-1}\cdot\text{min}^{-1}$ . Assay conditions: 500  $\mu\text{M}$  ATP, 10 min, 30 °C, 5 mM  $\text{Mn}^{2+}$  and MOPS pH 7.5.

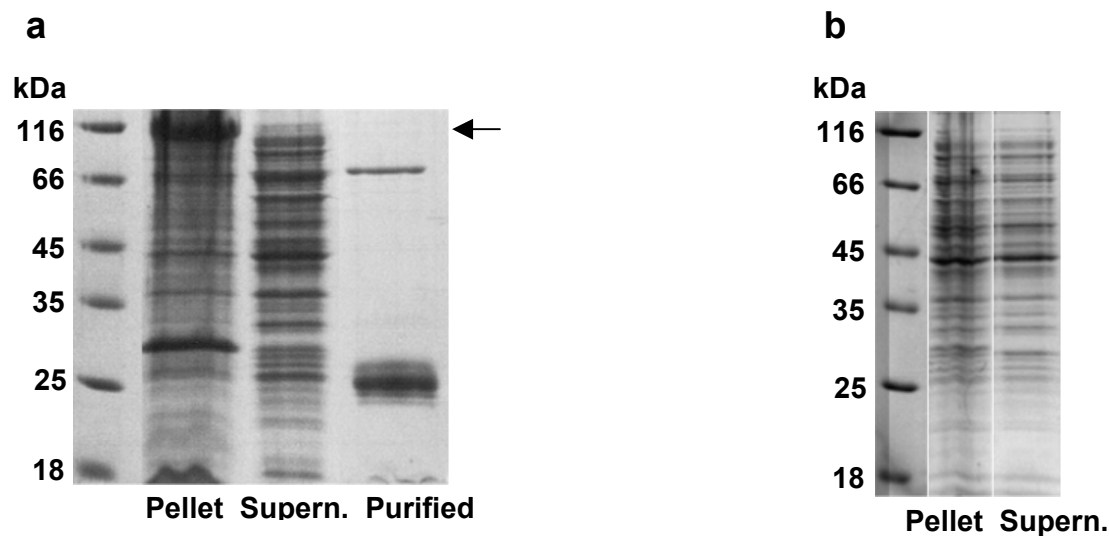


**Fig. 4.50:** 12.5% SDS-PAGE analysis of (a) expression of holoenzyme in BL21 STAR cells; applied were: 20  $\mu\text{g}$  protein of pellet and supernatant and 3.2  $\mu\text{g}$  of eluate and (b) expression of empty vector pQE30; applied were: 10  $\mu\text{g}$  of pellet and supernatant.

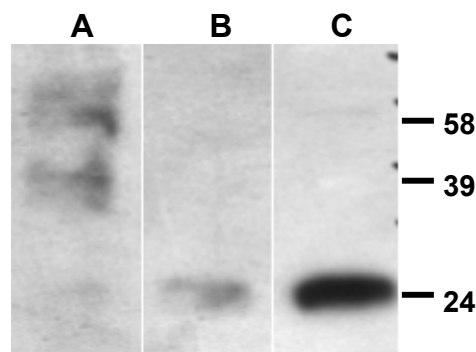


**Fig. 4.51:** Western Blot analysis of the expression in BL21 STAR cells. Lanes A and B correspond to the proteins of the pellet (5  $\mu\text{g}$ ) and eluate (1.4  $\mu\text{g}$ ) respectively, analyzed with anti-KD0386. Lane C corresponds to the eluate analyzed with anti-DB0386 (antibodies against the DNA-binding domain). Time of exposure: 15 s. Molecular weight of the signals were calculated with the marker peqGold.

After SDS-PAGE and Western blot analysis a band of approximately 25 kDa was identified as the main degradation product of the holoenzyme after purification. A considerable amount of non-degraded protein could be purified after expression in STAR cells when cell lysis was performed with sonification, but with the unavoidable presence of degradation products.

#### 4.2.3.3.2 Expression in BL21 ROSETTA [pREP4] cells

Expression was carried out (12 h, 12°C, 60 μM IPTG), cells were lysed with French Press with prior addition of protease inhibitors (Complete EDTA free), cell homogenate was incubated with lysozyme and DNase, pellet and supernatant were separated as usual and the protein was purified with Ni-NTA agarose (19 h binding). SDS-PAGE analysis (Fig. 4.52), AC assay (Table 4.23) and Western blot (Fig. 4.53) were performed.

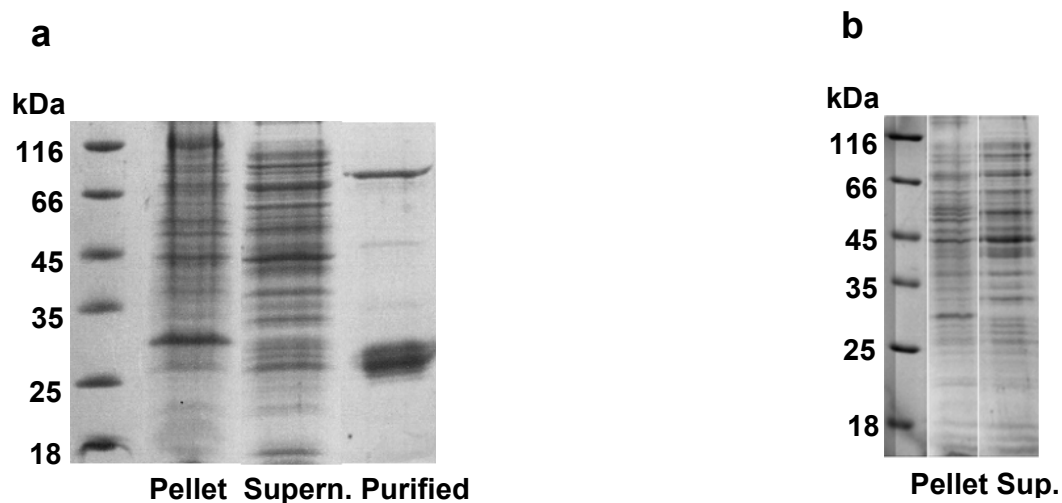


**Fig. 4.52:** 12.5% SDS-PAGE analysis of expression in BL21 ROSETTA cells of (a) the holoenzyme; applied were: 20 μg protein of pellet and supernatant and 3.8 μg of eluate and (b) the empty vector pQE30; applied were: 10 μg protein of pellet and supernatant.

Sample	Activity (pmol·min <sup>-1</sup> )
Pellet	13.2
Supernatant	0.8
Eluate	23.8

**Table 4.23:** AC activity of the holoenzyme expressed in BL21 ROSETTA cells. Protein amount tested was 5 μg of each sample. Specific activity of the purified protein: 4.8 nmol·mg<sup>-1</sup>·min<sup>-1</sup>. Assay conditions: 500 μM ATP, 10 min, 30 °C, MOPS pH 7.5.

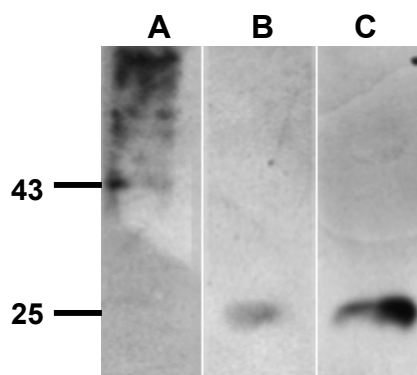


**Fig. 4.53:** Western Blot of the holoenzyme expressed in ROSETTA cells. Lanes A and B: pellet (5 µg) and eluate (1.2 µg) analyzed with anti-KD0386. Lane C correspond to the eluate analyzed with anti-DB0386 (antibodies against the DNA-binding domain, see below). Time of exposure: 15s.

#### 4.2.3.4 Anion exchange chromatography of the purified holoenzyme

The holoenzyme was expressed in BL21 STAR cells (1.2 L culture, 12°C, 15 h, 60 µM IPTG). Cell lysis was with protease inhibitors (Complete tablets, EDTA free) and French Press, lysates were incubated with lysozyme and DNase, after centrifugation (33,000 x g, 1 h) protein purification was carried out as usual, 20% glycerol was added. Sample for chromatography was 800 µl of Ni-NTA eluate (about 280 µg protein; Fig. 4.54a). Chromatography was described in chapter 3 more exact. A 40 µL sample of fractions with UV absorption was tested. An SDS-PAGE analysis and Western Blot (Fig. 4.55) were performed only for those fractions which showed AC activity.

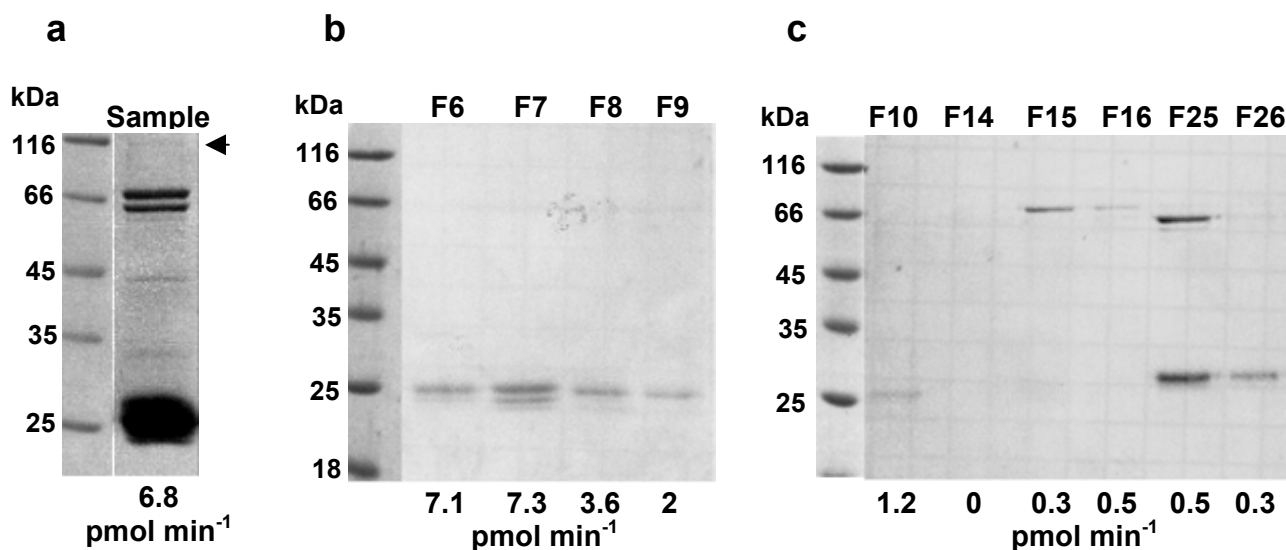


**Fig. 4.54:** a) 12.5% SDS-PAGE analysis of the Ni-NTA eluate sample applied for chromatography; b and c) fractions collected with 100mM NaCl (6 to10), 200 mM NaCl (14 to16) and 300 mM NaCl (25 and 26). Activities in AC-test (850 µM ATP, 30 °C, MOPS pH 7.5, 5 mM MnCl<sub>2</sub>, 20 min) are shown below.

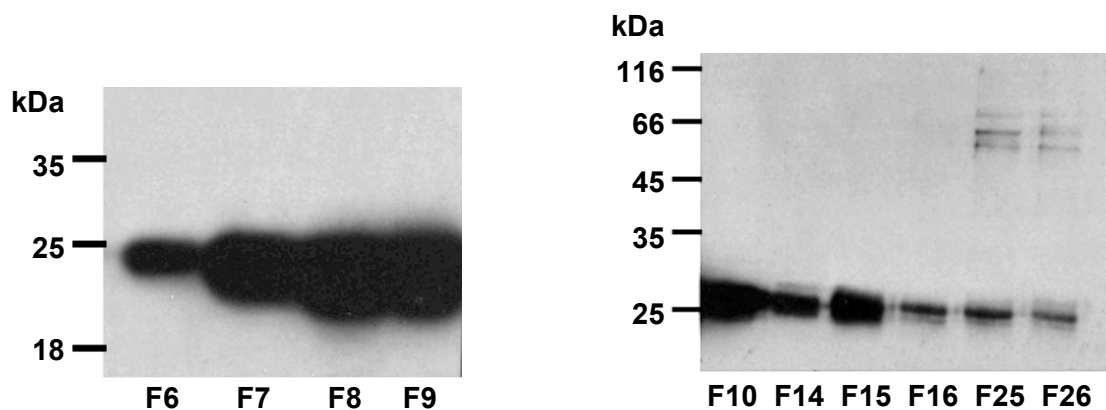


**Fig. 4.55:** Western blot analysis of the fractions analyzed in figure 4.54. Antibodies anti-KD0386 diluted 1:10000 were used. Time of exposure was 60 s.

All fractions which showed AC activity contained a degradation product of approximately 25 kDa containing the AC catalytic domain of Rv0386. Another degradation product of about 60 kDa contained also the catalytic domain but had low activity presumably because of the high NaCl concentrations (fractions 25 and 26, 300 mM NaCl).

#### 4.2.3.6 Determination of Rv0386 orthologs in *M. bovis* BCG and *M. smegmatis*

*Mycobacterium bovis* and *Mycobacterium smegmatis* cell cultures (about 3 days old) were obtained from Priv. Doz. Dr. Peter Sander (Institut für Medizinische Mikrobiologie, Universität Zürich). 50 ml cultures were centrifuged (5,000 x g, 10 min). Pellets were frozen with liquid nitrogen, then suspended in 3 ml of 50 mM Tris-HCl pH 7.5 and lysed with French Press. Cell homogenates (1 ml) were centrifuged (20,000 x g, 30 min), supernatants were separated from pellets, and pellets were suspended in 100 µl of 50 mM Tris-HCl pH 7.5. Samples were analyzed by Western blot with specific antibodies anti-KD0386 and anti-DB0386. The presence of an ortholog of Rv0386 was shown for *M. bovis* (detected in the soluble fraction only) but not in *M. smegmatis* (Fig. 4.56). These results are in line with genomic data which indicate the presence of a Rv0386 ortholog in *M. bovis*, but not in *M. smegmatis*. With anti-KD0386 additionally to the ~116 kDa band detected, other more intense protein signals could be detected, maybe corresponding to other cyclases which cross-reacted with the antibodies. With the antibodies anti-DB0386 only a protein of about 64 kDa was detected, possibly another protein of *M. bovis* with a similar DNA-binding domain.

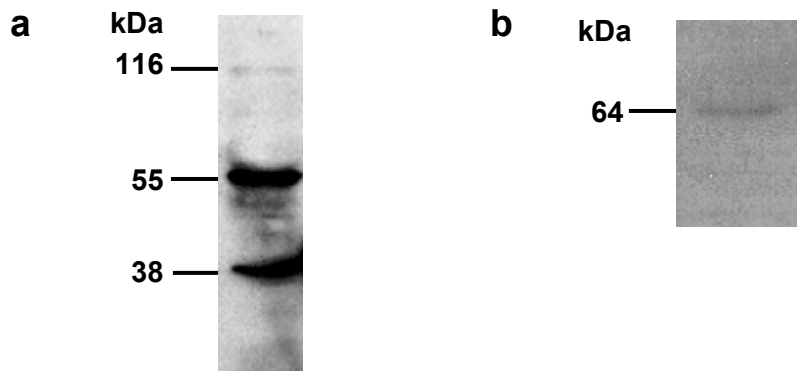


**Fig. 4.56:** Western blot analysis of the supernatant proteins found in *M. bovis* BCG with specific antibodies anti-KD0386 (a) and anti-DB0386 (b). 11 and 7  $\mu$ g protein were applied in a and b respectively. Antibodies anti-KD0386 were diluted 1:10000 and the anti-DB0386 1:5000. Time of exposure was 60 s (a) and 90 s (b). Molecular weight of the proteins detected were calculated with the help of the protein marker pEqGold.

#### 4.2.4 Expression of the putative ATPase domain of Rv0386

This domain (351 aa, 39 kDa) was expressed in BL21 cells (30  $\mu$ M IPTG, 25°C, 3 h). Cells were sonicated, pellet and supernatant were separated and analyzed by SDS-PAGE (Fig. 4.57a). After Ni-NTA purification the yield of protein was 0.1 mg protein from 400 ml culture. Most of the protein was found in the pellet and after Ni-NTA purification the protein could be detected only by Western blot (Fig. 4.57b). Molecular weight of this protein is about 39 kDa (including N-terminal His-tag).

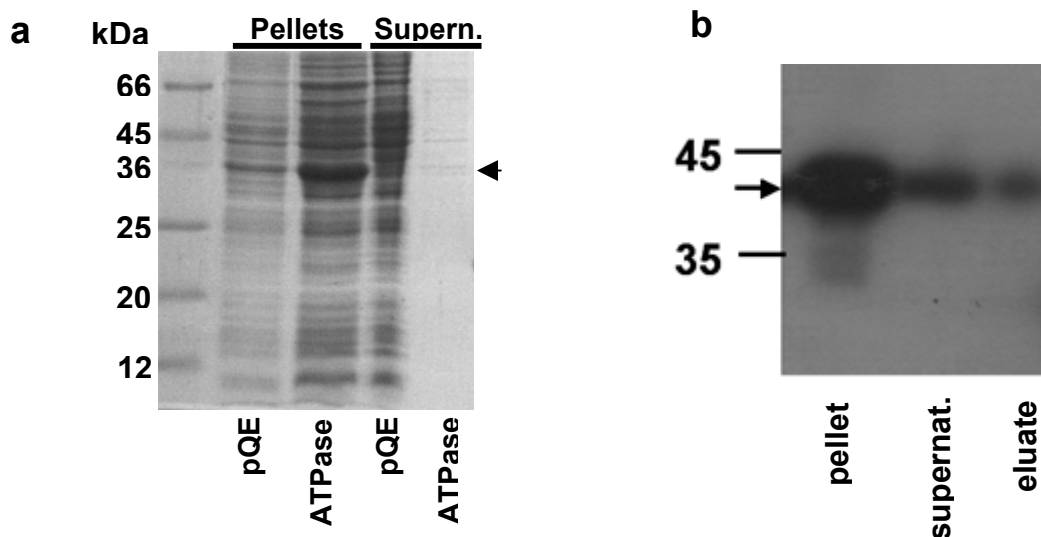


**Fig. 4.57:** a) 15% SDS-PAGE analysis of empty vector pQE30 and ATPase domain expressed in BL21 cells (Coomassie staining). Applied were: 20  $\mu$ g of pellets and pQE30 supernatant and 8  $\mu$ g of ATPase supernatant. b) Western blot of pellet, supernatant and eluate from Ni<sup>2+</sup>-NTA of the ATPase domain with anti-RGS-His<sub>4</sub>. Applied were: 2  $\mu$ g of pellet and supernatant and 1  $\mu$ g of purified protein. Time of exposure: 5 seconds.

The ATPase domain was also expressed in BL21 STAR cells (6  $\mu$ M IPTG, 20°C, 3 h). Cells were sonificated, pellet and supernatant were separated and analyzed by SDS-PAGE (Fig. 4.58a). For protein purification and Western blot analysis a second expression was carried out (30  $\mu$ M IPTG, 22°C, 3.5 h). A sample of pellet and supernatant was separated and the rest of the supernatant was purified as usual. From 600 ml culture it was impossible to determine protein with BIORAD in the Ni-NTA eluate. All samples were analyzed by Western blot (Fig. 4.58b). Since only small amounts of ATPase domain were soluble, no ATPase tests were attempted.

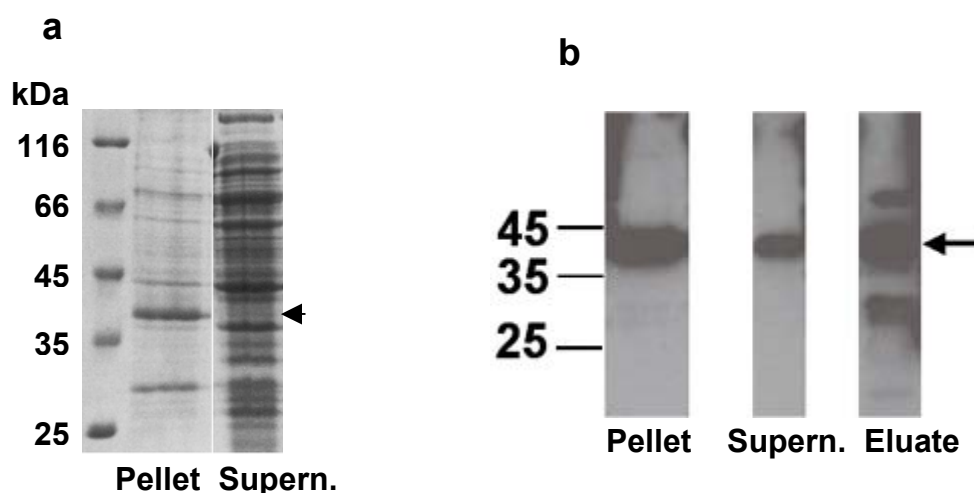


**Fig. 4.58:** **a)** 12.5% SDS-PAGE analysis of the ATPase domain in BL21 STAR cells. About 20  $\mu$ g protein of both pellet and supernatant were applied. **b)** Western blot analysis. Pellet (1.2  $\mu$ g), supernatant (0.5  $\mu$ g) and 15  $\mu$ l eluate after Ni-NTA purification were analyzed with anti-RGS-His<sub>4</sub>. Time of exposure: 15 s.

#### 4.2.5 Expression of the putative transcription factor domain of Rv0386

This domain (929 aa, 100 kDa including His-tag) was expressed in BL21 and BL21 STAR cells (60  $\mu$ M IPTG, 23 °C, 3 h) and analyzed by SDS-PAGE (Fig. 4.59). Only the pellet of BL21 STAR cells showed an overexpressed protein compared with the control.

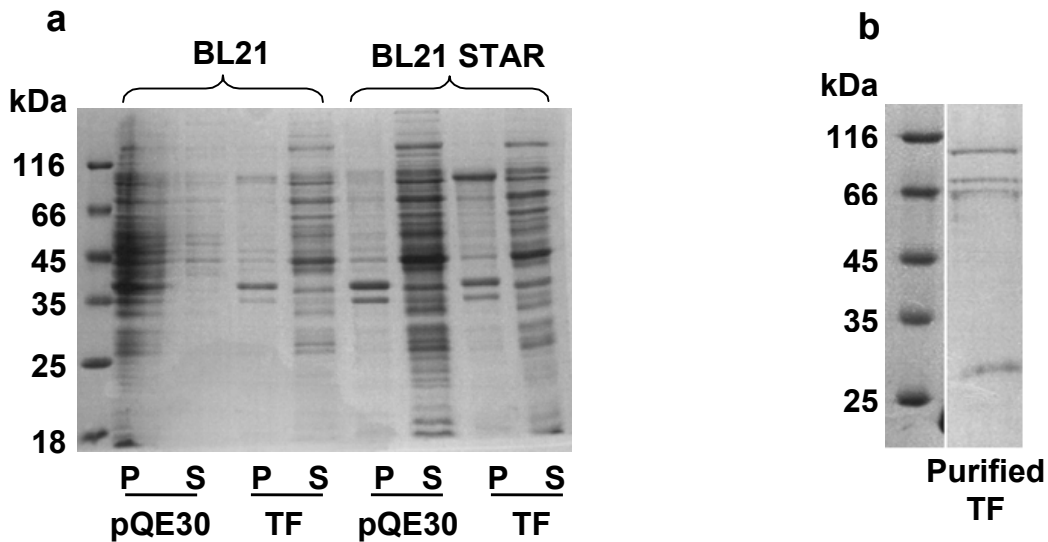


**Fig. 4.59:** 12.5% SDS-PAGE analysis of **a)** empty pQE30 and transcription factor (TF) domain expressed in BL21 and BL21 STAR cells. Applied were: 15-20  $\mu$ g of pQE30 pellet (BL21), pQE30 supernatant (STAR) and TF supernatants (BL21 and STAR); 8-12  $\mu$ g of pQE30 and TF pellets (STAR), pQE30 supernatant and TF pellet (BL21). **b)** TF domain purified with Ni-NTA-agarose after expression in STAR cells. 15  $\mu$ l of the eluate were applied. P=pellets and S=supernatants.

For Western blot analysis expression was carried out again (30  $\mu$ M IPTG, 3 h, 22  $^{\circ}$ C). Cells were sonificated (with protease inhibitors and lysozyme). Pellet, supernatant and eluate after Ni-NTA-agarose purification were analyzed by Western blot. The presence of degradation products in pellets and eluates was observed.

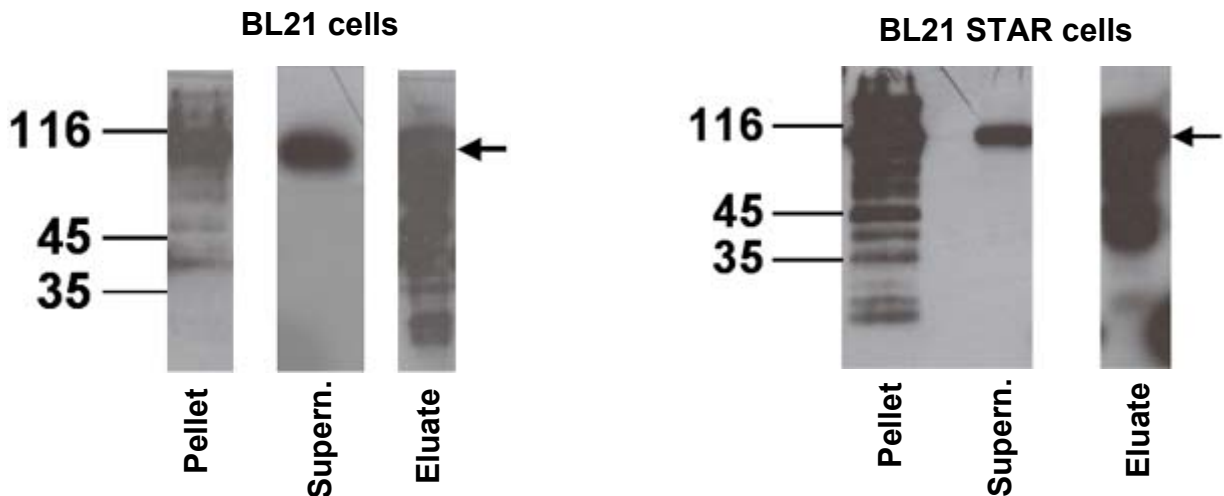


**Fig. 4.60:** Western blot of the transcription factor domain expressed in BL21 and BL21 STAR cells. Applied were: about 1  $\mu$ g of pellets, 0.5  $\mu$ g of supernatants and 15  $\mu$ l of the Ni-NTA-agarose eluate. Antibodies anti-RGS-His<sub>4</sub> were used. Time of exposure: 15 s.



#### 4.2.6 Expression of the putative DNA-binding domain of Rv0386

This domain (103 aa, 12 kDa including His-tag) was expressed in BL21 cells (4 h, 25°C, 60 µM IPTG). Pellet, supernatant and eluate after Ni-NTA purification were analyzed by SDS-PAGE and Western blot (Fig. 4.61 a, b, c). This protein tended to dimerize and multimerize.

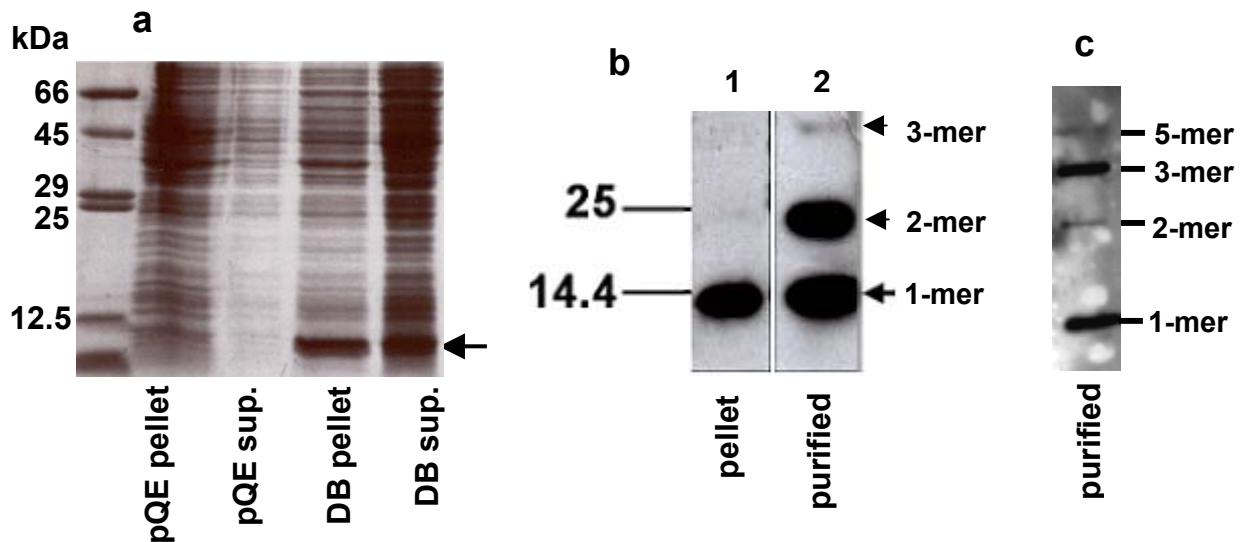


**Fig.4.61:** (a) 15% SDS-PAGE analysis of the DNA-binding domain (DB) expressed in BL21 cells (pQE30 empty vector as a control). (b) Western blot of 0.3 µg of pellet and eluate from Ni-NTA analyzed with anti-RGS-His<sub>4</sub> antibodies. Time of exposure: 15 seconds. (c) Western blot of the purified DB domain (1 µg) after dialysis with phosphate buffer and concentration. Time of exposure: 30 s. Protein of lane **b2** was purified without DNase and that of lane **c** with addition of it.

#### 4.2.6.7 Sensitivity and specificity of the antibodies anti-DB0386

A protein sample with a concentration of 1-2 µg/µl (Fig. 4.62a) was used by BioGenes to produce affinity purified antibodies against the DNA-binding domain of Rv0386 (see chapter 3). The reactivity of the antibodies from two immunized rabbits was tested against different concentrations of DNA-binding domain by Dot Blot (Fig. 4.62b). With an antibody dilution of 1:10 000 it was possible to detect 10 ng protein (rabbit 5081).

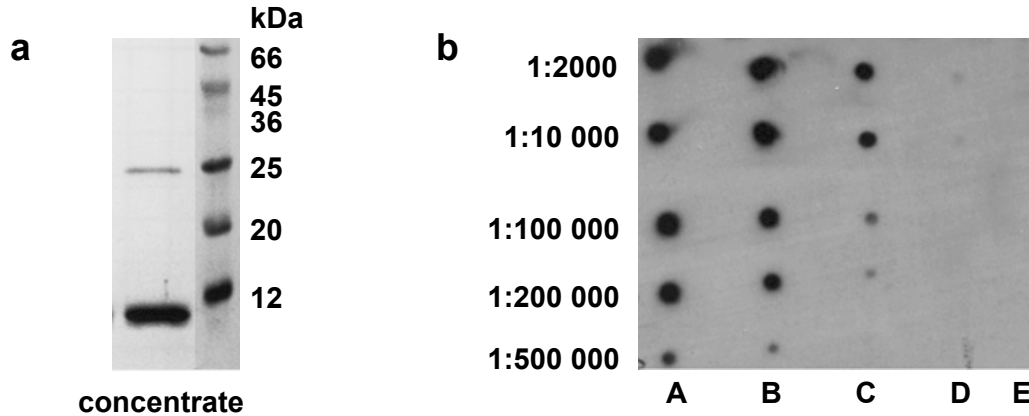


**Fig. 4.62:** (a) 15% SDS-PAGE analysis of the protein used for production of anti-DB0386. 2  $\mu$ g protein were applied. (b) Dot Blot. 5 different antibody dilutions (1:2000 to 1:500,000) as well as protein concentrations were used for testing purified antibodies from rabbit 5081. Protein concentrations were: 300 ng (A), 100 ng (B), 10 ng (C), 1 ng (D) and 0.1 ng (E). Time of exposure: 30 s.

With anti-DB0386 it was possible to detect cross-reactivity with proteins of the three *E. coli* strains used for expression within this work (Fig. 4.63). These proteins have a MW (derived from standards on the blotted membrane) of 68 and 25 kDa and presumably contain a DNA-binding domain very similar to that of Rv0386. Based on these results, this antibody seems to recognize many DNA-binding proteins of *E. coli* and probably also of *M. tuberculosis*. Its utility for immunodetection of Rv0386 might be only possible simultaneously with antibody anti-KD0386.

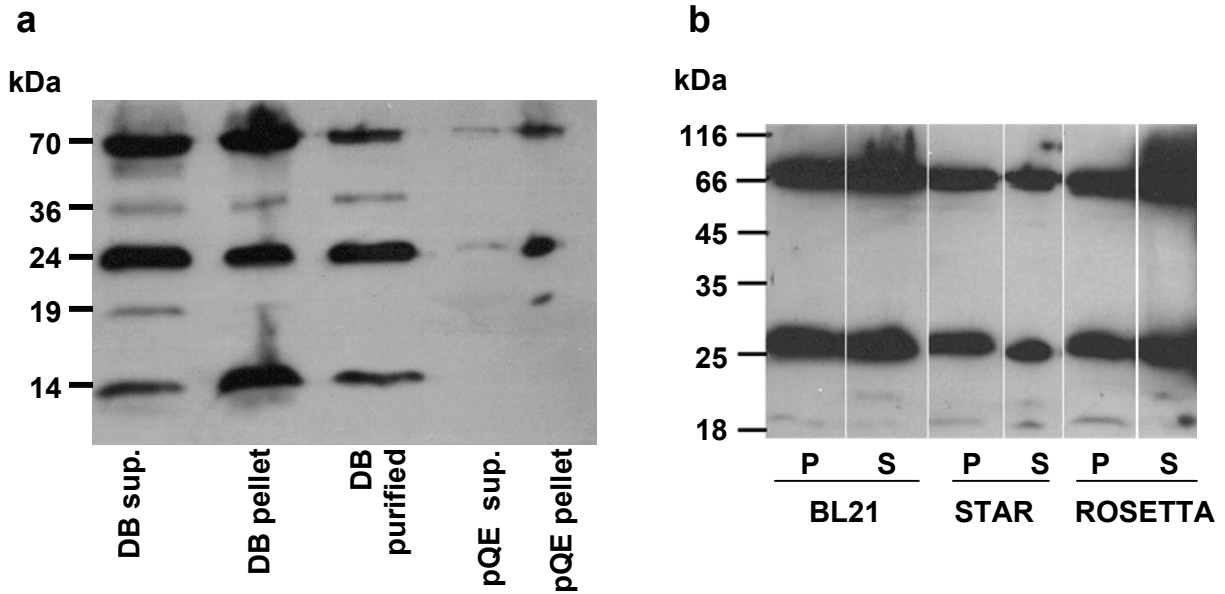


**Fig. 4.63:** (a) Western blot of the expressed DNA-binding domain and empty vector pQE30 in BL21 cells. Antibodies anti-DB0386 1:5000 were used. Time of exposure: 30 s. Molecular weights were calculated with a marker. Applied were: 20  $\mu$ g of DB supernatant, pellet and pQE30 pellet. From pQE30 and DB purified, 3 and 1  $\mu$ g respectively were applied. (b) Western blot of expression of empty vector pQE30 in BL21, STAR and ROSETTA cells analyzed with antibodies anti-DB0386 (diluted 1:10000). 10  $\mu$ g protein were applied in each lane. Time of exposure was 60 s.

## 5 Discussion

### 5.1 Chimeras of mycobacterial Rv1625c mutants with soluble mammalian and *Paramecium* cyclases

As a complementary study to the already published data regarding the expression and characterization of Rv1625c (Guo et al., 2001), additional point mutants N372A, N372T and D300S were generated here. The idea was to check a) whether a threonine might be able to take over the function of an asparagine in transition state stabilization and b) whether a serine might substitute for aspartate in substrate definition. This was not the case. The mutants were essentially inactive. This was further proof that the six canonical amino acids identified in mammalian ACs as critical for catalysis and conserved in Rv1625c, are also absolutely essential in the latter.

Since soluble mammalian AC domains C1 and C2 from different isoforms have shown a restored catalytic activity when mixed i.e. IC1/IIC2 (Tang and Gilman, 1995; Whisnant et al., 1996; Yan et al., 1996), VC1/IIC2 (Désaubry et al., 1996; Dessauer et al., 1997; Sunahara et al., 1997; Tesmer et al., 1997) and IXC1/IIC2 (Hoffmann, 1999), the possibility to get active chimeras by mixing mycobacterial soluble catalytic domains with mammalian ones was enticing. The mycobacterial Rv1625c inactive mutant D300A lacking its metal binding function and consequently their mammalian-like C1-domain function, were barely able to reconstitute enzymatic activity when mixed with mammalian IC1, VC1, VIIC1 or IXC1 domains. Similarly inactive mutants R376A, N372T and N372A having no mammalian-like C2-function were not really capable to complement inactive mammalian IIC2 and IXC2 domains.

The observed specific AC activity of these chimeras was very small, actually tiny compared to Rv1625 wild type. This fact indicates that although the substrate binding and some catalysis may have taken place, no complementation of the C1/C2 domains occurred. One explanation could be the differences of dimerization epitopes between Rv1625c and mammalian ACs, e.g. the “arm region” (proposed in Linder et al., 2002) where the motif KWQ is replaced by RFF in Rv1625c. This KWQ motif is invariant in ACs I-VIII and specially the residue Q (Q<sub>584</sub> in AC type V from rabbit) was identified as crucial on the dimerization interface (Zhang et al., 1997; Sunahara et al., 1998; Tucker et al., 1998). Although recent studies showed that in the chimera VC1a/IIC2 the KWQ

motif is not involved in substrate binding (Tesmer et al., 1999), it could be possible that its direct participation depends on the cyclase isoform. The lack of the KWQ motif in Rv1625c and also the conformational changes due to the mutations in the mycobacterial monomers could explain the lack of a robust reconstitution.

Surprisingly, the C2-positioned domain from the *Paramecium* GC and its triple mutant ParaGC-C2KWQ reconstituted a soluble AC when mixed with mammalian IIC2 domain (Linder et al., 2000) and with the mycobacterial mutant D300A. The topological inversion of the cytosolic domains in the *Paramecium* GC and the fact that the KWQ motif is an AC-specific stabilizing motif of the dimerization between C1 and C2, was in agreement with Linder et al. (2000). The C2-positioned *Paramecium* GC domain contributed the metal binding function while IIC2 or D300A contributed the substrate specificity function upon mixing. Additionally, the mutant ParaGC-C2KWQ stabilized and/or enhanced the interaction of the C1 and C2 equivalent domains since the specific activity of ParaGC-C2KWQ/IIC2 was about 3-fold higher than ParaGC-C2/IIC2. That was not the case with the chimera ParaGC-C2KWQ/D300A which was equally active as the ParaGC-C2/D300A dimer. Dimerization of the chimera ParaGC-C2/D300A was substrate dependent, no activity with  $Mg^{2+}$  was supported, the diterpene forskolin did not stimulate and P-site inhibitors did not inhibit. It seems that the individual catalysis and regulation properties possess enough structural complementarity to allow formation of a functional chimera. Kinetic characterization of ParaGC-C2/D300A showed an ATP affinity ( $K_m=201\ \mu M$ ) similar to that of Rv1625c AC domain ( $K_m=150\ \mu M$ ; Guo et al., 2001) with about a 70-fold reduced  $V_{max}$  ( $29.5\ \text{nmol cAMP}\cdot\text{mg}^{-1}\cdot\text{min}^{-1}$ ).

An open question concerning the Rv1625c AC was why was it not stimulated by forskolin, a character shared among all but type IX of the mammalian ACs. The alignments in chapter 4 (Fig. 4.1 a, b) clearly indicate the amino acid differences which may be responsible for this lack of a forskolin effect on Rv1625c. While in mammalian ACs the binding of forskolin is shared between C1 and C2 domains (the C1 domain provides a threonine and C2 a serine, e.g., T<sub>426</sub> in ACI-C1 and S<sub>927</sub> in ACII-C2), in the mycobacterial AC Rv1625c those residues are substituted by an asparagine (N372) and an aspartate (D300), respectively, both directly implicated in catalysis. Rv1625c acts as a homodimer with two ATP binding sites in contrast to the mammalian ACs in which one site has evolved to bind forskolin instead of ATP. Therefore, it was speculated that the

mutants N372T and D300S may reconstitute an active heterodimer with a single ATP-binding site and a forskolin-binding site.

Somewhat surprisingly mutants N372T and D300S subserving C1 and C2 functions, respectively, did complement each other quite well to form an active enzyme (Table 4.6, Fig. 4.10). A forskolin stimulation, however, was not observed. This is evidence that those two amino acids implicated in forskolin stimulation are required but not sufficient to confer diterpene sensitivity. Obviously, the binding pocket for forskolin at the C1/C2 interface is more elaborate and probably requires additional structural features absent in Rv1625c. Similarly, chimeras N372T/IIC2 and N372T/IXC2 were not activated by addition of forskolin. The observed weak effects were solely due to the solvent DMSO. Reconstitution experiments with the mutants N372T, N372A and D300S were carried out. Chimeras of these mutants did not show  $Mg^{2+}$  supported activity in agreement with the observations for the wild type (Guo et al., 2001). By titration of N372T, N372A and R376A with increasing amounts of D300A or D300S it was determined that they folded correctly and are capable of forming productive heterodimeric complexes in analogy to a mammalian C1-C2 arrangement. Nevertheless, the apparent dissociation constants derived from the titration curves showed lower affinity of the monomers to each other in comparison with the wild type (Guo et al., 2001). Conformational changes due to mutations may explain this effect on the dimerization of these chimeras.

## 5.2 Adenylyl cyclase catalytic domain of Rv0386

The gene product of Rv0386 was not originally predicted as an AC but denoted as a transcriptional regulator containing an ATP/GTP-binding site motif A, a luxR family signature and an helix-turn-helix motif. After a functional classification of nucleotide cyclase superfamilies in *M. tuberculosis* through computational methods and phylogenetic analysis, the cyclase homology domain (CHD) of Rv0386 was described as a cytoplasmic class III AC with similarity to CHDs detected in other Gram-positive bacteria, e.g. in *Streptomyces* (McCue et al., 2000). Following subclassification of class III ACs, Rv0386 was assigned to class IIIc ACs in which the frequency of substitutions in the six canonical catalytic residues is remarkably high (Linder and Schultz, 2003). In the CHD of Rv0386 a substrate-defining glutamine and an asparagine instead of the canonical lysine and aspartate were found. Since enzymatic activities have been

demonstrated for unorthodox cyclases having variations in the canonical residues and since all known subclass IIIc enzymes appear to function as homodimers (Linder and Schultz, 2003), two major questions were addressed: Has AC Rv0386 an AC activity in spite of the changes of both amino acids involved in defining the substrate specificity? And if active, is AC Rv0386 functioning as a homodimer like mammalian-type AC Rv1625c?

The recombinant CHD Rv0386<sub>(1-175)</sub> was used for answering these questions. This AC was capable of converting ATP to cAMP, using Mn<sup>2+</sup> as a cofactor. Yet it displayed a rather low activity (4.8 nmol of cAMP·mg<sup>-1</sup>·min<sup>-1</sup>), corresponding to only 1/400 to 1/250 of AC activities characterized in other mycobacterial ACs, e.g. Rv1625c (Guo et al., 2001) and Rv1264 (Linder et al., 2002). Most surprisingly, Rv0386<sub>(1-175)</sub> had also a 30% GC side activity strictly dependent on Mn<sup>2+</sup> as divalent cation cofactor. No AC nor GC activities were detectable with Mg<sup>2+</sup> as a cofactor. A preference for Mn<sup>2+</sup> was also shown for Rv1625c and Rv1264 (Guo et al., 2001, Linder et al., 2002). It was reported that macrophages are able to import Mn<sup>2+</sup> providing a suitable environment for resident *M. tuberculosis*. The mycobacterial gene product Rv0924c was recently reported to be a homologue of the macrophage Nramp Mn<sup>2+</sup> transporter protein (Agranoff et al., 1999; Reddy et al., 2001). The kinetic properties of Rv0386<sub>(1-175)</sub> such as temperature optimum of 30-37°C, activation energy of 76 kJ/mol and pH optimum of 8.3 were within the usual range reported for the mammalian AC catalysts. No activation by forskolin and no inhibition by the P-site inhibitor 2'd3'-AMP were observed, as expected. Substances like  $\alpha,\beta$ -CH<sub>2</sub>-ADP (ADP-analog) and cordycepin 5'-triphosphate (ATP-analog) inhibited AC activity as did cAMP derivatives like monobutyryl cAMP and dibutyryl cAMP. Dimerization of the catalytic domain of Rv0386 was demonstrated by the fact that AC specific activity increased almost 5-fold by increasing protein concentration and an apparent association constant of 0.1  $\mu$ M was derived indicating a high affinity of the monomers to each other. That was further substantiated by western blotting, where with the specific antibody anti-KD0386, the presence of monomers, dimers, tetramers together with higher multimers was observed. Using GTP as a substrate, the specific activity increased only 3-fold upon increasing protein concentration and the calculated apparent association constant was 0.9  $\mu$ M. The fact that the dimerization process occurs slower with GTP than with ATP points to an important role played by the substrate during the formation of the

homodimeric catalytic complex. AC kinetic parameters were  $K_m = 417 \mu\text{M}$  and  $V_{\text{max}} = 4.8 \text{ nmol of cAMP}\cdot\text{mg}^{-1}\cdot\text{min}^{-1}$ . For GC activity  $K_m$  and  $V_{\text{max}}$  values of  $299 \mu\text{M}$  and  $1.6 \text{ nmol of cAMP}\cdot\text{mg}^{-1}\cdot\text{min}^{-1}$  were obtained.

To determine if the amino acid residues Q<sub>57</sub> and N<sub>106</sub> which deviate from the canonical K and D, are critical for catalysis in Rv0386, they were mutated to A. Residual AC specific activities of less than 2% for mutants Q57A and N106A demonstrated the important role played by Q and N when recognizing ATP as a substrate. GC residual activities of these mutants were also lower showing that the same residues are involved in recognizing GTP as a substrate. Whether the AC activity of Rv0386 is so low because of the substituted canonical K and D residues was examined with the mutants Q57K, N106D and Q57K/N106D. A reduction of more than 90% of the AC activity was observed by these three mutants. The GC activity was also affected as expected. Interestingly, comparison of the AC and GC activities of the mutants showed a significant reduction in the substrate discrimination for mutants Q57K/N106D and N106A. These results strongly argue that completely different substrate-specifying mechanisms exist in Rv0386 in comparison with canonical class III ACs.

Through an alignment of the sequences of the AC domain of Rv0386 and the *Paramecium* GC (see appendix and alignment in section 4.2.2.8, chapter 4) the substitution of Q<sub>57</sub> and N<sub>106</sub> (Rv0386) by E<sub>1681</sub> and S<sub>1748</sub> (in ParaGC) was identified. Assuming that E<sub>56</sub> (Rv0386) might functionally correspond to E<sub>1681</sub> of ParaGC, the mutation of N<sub>106</sub> to S was examined for its substrate specificity. This mutant had no increased GC activity, on the contrary it was reduced >80%. The AC activity of N106S was also reduced but to a lesser extent. Considering that the AC activity of Rv0386 is lower in comparison with the mycobacterial AC's Rv1625c and Rv1264, its low but detectable GC activity points to a certain plasticity of the substrate-defining mechanism. A hypothetical substrate binding mechanism for AC Rv0386 is shown in figure 5.1. This way of binding of ATP or GTP is drawn according to the mode of binding of cAMP or cGMP within the phosphodiesterase (PDE) superfamily based on the X-ray structure of the catalytic domain of PDE 4B2B (Xu et al., 2000).



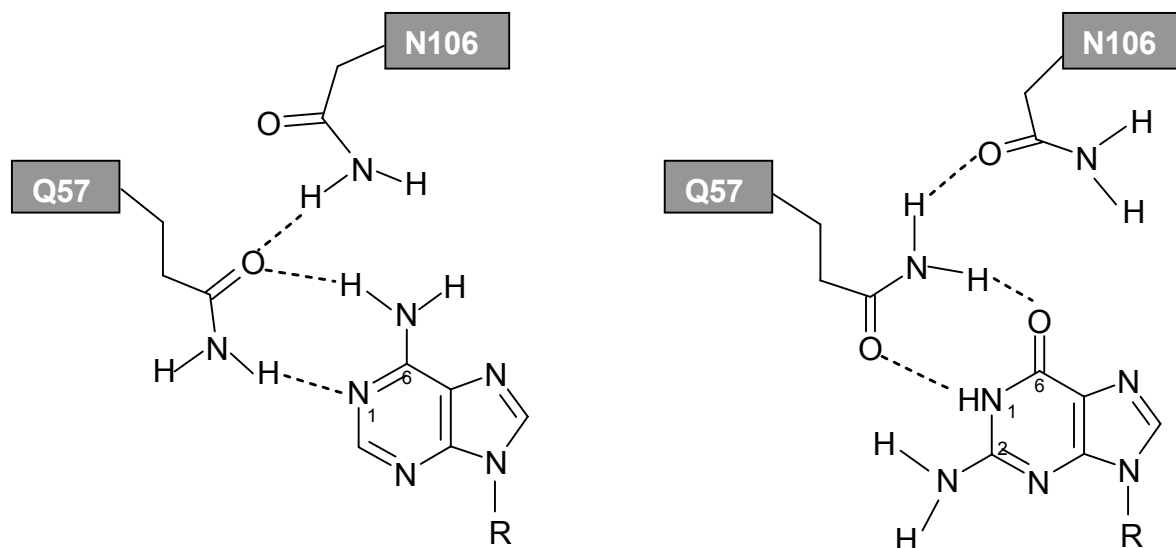


**Fig. 5.1:** Hypothetical substrate recognition mechanism proposed for Rv0386 as adenylyl cyclase (left) and as guanylyl cyclase (right). See explanation in the text.

According to the model of cAMP binding in PDE4, the side chain of a glutamine residue present in the active site forms hydrogen bonds with the N<sub>1</sub> and N<sup>6</sup> groups of adenine, but this glutamine could also accommodate the N<sub>1</sub> and O<sup>6</sup> groups of guanine in cGMP-binding by rotation of its amide group by 180° (Xu et al., 2000). Compared with that, in Rv0386 Q<sub>57</sub> could be responsible for the dual specificity and N<sub>106</sub> could form a hydrogen bond with Q<sub>57</sub> affecting the correct orientation of the substrate towards the transition state. In PDE4 this role is taken by a tyrosine side chain. Unfortunately, the low AC and GC activities of mutants Q57K, Q57A, N106D, N106A and Q57K/N106D did not permit kinetic studies to determine if their diminished turnover was due to reduced substrate-affinity, conformational changes affecting the transition state or both. However, the kinetic parameters obtained for N106S using ATP as a substrate somewhat support the hypothetical substrate-binding mechanism proposed above. Since N106S showed a reduced V<sub>max</sub> but not reduced K<sub>m</sub> in comparison with the catalytic domain of the wild type, it is clear that N<sub>106</sub> is less important for coupling the substrate than for positioning it. Such an argument was previously made for the *Anabaena* AC *cyaB1*, where a threonine functionally replaced the substrate-specifying aspartate and its mutation to alanine resulted also in a V<sub>max</sub>- but not a K<sub>m</sub>-change (Kanacher et al., 2002). Unfortunately, it was not possible to make a kinetic study for N106S to determine its specificity for GTP as a substrate because of its low GC activity. Finally, when the

differences in length of the respective side chains between Q and K, and N and D are considered, the variation in length of the “arm region” or “dimerization region” in Rv0386 (see chapter 1 for explanation and alignments in appendix) compared with this sequence segment in mammalian ACs (8 vs. 14 residues, respectively) could be also responsible for the changes in the fine structure of the purine-binding pocket in Rv0386 as a result of a conformational adjustment and compensation. Within this arm region, the triad KWQ (in mammalian ACs) or LVR (in *Paramecium* GC) is found. Particularly, the Q of this triad was claimed to assist K and D in adenine binding (Tesmer et al., 1997; Sunahara et al., 1998) while its correspondent R in the *Paramecium* GC is supposed to assist the E and S in guanine binding (Linder and Schultz, 2002; see fig. 4.1 for sequence alignments). On the contrary, structural data concerning substrate binding of the AC VC1a/IIC2 chimera showed that the KWQ motif appeared uninvolved (Tesmer et al., 1999). In any case this motif stabilizes AC-specifically the dimerization and its residues are absent in the shortened arm region of Rv0386. The unexpected reduction in the GC activity upon mutation of N<sub>106</sub> to S highlights again the different substrate-specifying mechanism in Rv0386.

The effect on the catalytic properties of Rv0386<sub>(1-175)</sub> by modifications of its N-terminal region was also remarkable. Mutant R7G showed only 6% residual activity and the Rv0386 catalytic domain-equivalent of MT0399 (with 7 amino acid residues elongation before the M<sub>1</sub> of Rv0386) showed only 30% residual activity. Kinetic parameters of R7G were not investigated but the N-terminally elongated catalytic domain showed a 5-fold reduction in ATP-affinity ( $K_m = 2.3$  mM) in comparison with Rv0386<sub>(1-175)</sub> ( $K_m = 417$   $\mu$ M). Notably, small C-terminal modifications of Rv0386<sub>(1-175)</sub> like changing the His-tag to the C-terminal position were well tolerated and did not modify the substrate affinity ( $K_m = 454$   $\mu$ M) and caused only an insignificant reduction (20%) in the specific activity, but compromising significantly the dimerization process.

It can be concluded that amino acid additions or charge changes in the N-terminal end of Rv0386 considerably affected the substrate binding and/or catalysis, maybe because of important conformational changes. These results together with the mutational studies show how important the determination of the three-dimensional structure of the unorthodox catalytic domain of Rv0386 might be to establish the individual architecture of its purine-binding pocket. Within the scope of this study, crystals of the AC catalytic

domain of Rv0386 were obtained. N-terminal as well as C-terminal His-tagged Rv0386<sub>(1-175)</sub> were successfully used for these purposes. Using the vapor diffusion method, a wide variety of crystallization conditions and crystal forms were found for these proteins. Until now diffraction-quality crystals were obtained only with the C-terminal His-tagged catalytic domain. Since Rv0386<sub>(1-175)</sub> has a high crystallization potential, optimization experiments are continuing in collaboration with the Biochemie-Zentrum in Heidelberg.

### 5.3 Holoenzyme Rv0386

Rv0386 seems to be a very interesting enzyme in terms of its multi-domain composition, the possible evolutionary origin of its modular architecture and, of course, its demonstrated unorthodox activity as an AC. In Rv0386, the N-terminally located cyclase homology domain is succeeded by a putative transcription factor domain comprising an ATPase domain and a HTH-DNA-binding domain.

The Rv0386 holoenzyme could be expressed in three different *E. coli* strains (BL21, BL21 STAR and BL21 ROSETTA all with pREP4 plasmid), but it ended up mostly in inclusion bodies. Small amounts of full length protein remained in the soluble fraction and could be purified using Ni-NTA-agarose including all kinds of degradation products, possibly originating during the purification process. It is likely that the protein was degraded instead of prematurely terminated, since the full length protein was still present in the insoluble material (inclusion bodies). It was attempted to optimize expression varying external conditions (time, temperature, concentration of the inducer) or using special host strains for improvement of mRNA stability (STAR cells) or enhancing the expression of proteins containing rare codons (ROSETTA cells). The use of protease inhibitors and detergents for protein solubilization after cell lysis were also tried. DNase was added after cell disruption in case that protein was bound to DNA through its DNA-binding domain. These steps did not improve recovery of the holoenzyme. The conditions found to be best for obtaining more soluble protein and less degradation products were expression in BL21 STAR cells without induction with IPTG (expression at 15°C for 16 h) and addition of lysozyme and DNase after cell disruption. The protein obtained under these conditions showed an AC activity of 3.7 nmol of cAMP·mg<sup>-1</sup>·min<sup>-1</sup>. Unfortunately, the eluate contained at least five additional main degradation products which, if containing AC catalytic domain, could also contribute to

the AC activity observed. Therefore, it is impossible to make any conclusions or comparisons between the AC activity of the holoenzyme and the AC domain.

With the antibodies anti-KD0386 and anti-DB0386 it was possible to identify the principal degradation products of Rv0386. Identified with anti-KD0386 were products of 25-28 kDa, 40-45 kDa and 60-70 kDa as main bands. With anti-DB0386, a main product of about 25 kDa was detected. There were also degradation products observed on the SDS-PAGE gels that were not detected either with anti-KD0386 nor with anti-DB0386, probably corresponding to holoenzyme fragments that did not contain the AC catalytic domain nor the DNA-binding domain. It could be speculated that the folding of the holoenzyme Rv0386 was defective and that the most probable sites for rupture were interdomain, mainly after the AC catalytic domain. Until now for most studied transcription factor proteins, binding of their cognate signals destabilized them for proteolysis (sometimes autoproteolysis) (Little et al., 1980; Becker et al., 1999), but recently it was also reported that the transcription factor TraR of *Agrobacterium tumefaciens* must bind its inducing ligand (N-3-oxooctanoyl-L-homoserine lactone) to acquire its native conformation and protease resistance when expressing in *E. coli* cells. This TraR signaling ligand is critical for the folding of nascent protein into its mature tertiary structure (Zhu and Winans, 2001). Both aspects could be the reason why Rv0386 full length protein was found mainly degraded. Either an *E. coli* signaling molecule is inducing proteolysis of Rv0386 in some manner or a particular ligand for Rv0386 could exist in *M. tuberculosis* and not in *E. coli* expression cells, which could be responsible for attaining the Rv0386 native conformation and conferring resistance to cellular proteolysis only when synthesized in the presence of this signal molecule.

The *in vivo* expression of Rv0386 was shown using *Mycobacterium bovis* cell cultures (BCG strain), which is reported to contain a homologous protein denoted as Mb0393 (Garnier et al., 2003). A very slight signal of the holoenzyme could be detected with the help of antibodies anti-KD0386 in the soluble cellular fraction. Since the antibodies anti-KD0386 were able to recognize 10 of the other 14 class III AC's present in *M. tuberculosis* (probably because of the high conformation similarity between their cyclase homology domains), the detection of two additional stronger signals (about 55 and 38 kDa) with these antibodies in the soluble fraction of *M. bovis* cells could be explained as the recognition of other cyclases. It is possible to suggest that Rv0386 as a

transcription factor could show variable expression levels and was expressed in very low amounts when the *M. bovis* cells were disrupted for analysis. With the antibodies anti-DB0386 only a signal of about 64 kDa could be detected, maybe because of the recognition of other transcription factors with similar HTH-DNA-binding domains. Nevertheless, the possibility that Rv0386 could also suffer interdomain proteolysis *in vivo* should not be neglected.

The putative transcription factor-, ATPase and DNA-binding domains of Rv0386 could also be expressed in *E. coli* as individual proteins. The purification of reasonable amounts of the transcription factor domain was however impossible. The ATPase domain was found in its majority in the insoluble fraction and only a very low amount could be purified. That is the reason why no further experiments were made. On the contrary, the DNA-binding domain could be purified in sufficient amounts to produce specific antibodies. Through Western blot it was possible to determine the high tendency of dimerization of this domain. However, antibodies anti-DB0386 were also capable of detecting *E. coli* proteins (28 and 68 kDa, approximately), probably transcription factors with a similar conformation to the DNA-binding domain as Rv0386.

The role that could be played by Rv0386 as a transcription factor in *M. tuberculosis* remains unclear. The consequences and advantages gained by joining an adenylyl cyclase domain with a transcription factor containing an ATPase motif responsible for ATP binding and hydrolysis remain unexplained. Certainly, the vast regulation possibilities of Rv0386 as an AC and as a transcription regulator *in vivo* must be the reason why this multimeric signaling unit could evolutionarily arise.

## 5.4 Remaining questions

Since Rv0386 has evolved to use specific variant residues in an altered catalytic mechanism and of unsuspected regulation possibilities by joining this AC domain with a transcriptional regulator, two main questions remain open after this work: Is it possible to elucidate the structure of the AC domain for an understanding of its catalytic properties observed until now through biochemical analysis? And what is the role that Rv0386 plays *in vivo* as a transcription factor? Anyhow, the first of these questions is hopefully going to be answered soon, since the first crystallization attempts of the Rv0386 AC domain were started successfully.

## 6 Summary

I report on two class III ACs of *Mycobacterium tuberculosis* which possess very different structural as well as catalytic characteristics: the mammalian-like membrane-anchored Rv1625c and the transcription-factor-attached Rv0386. As a complementary study to published data (Guo et al., 2001), additional point mutations were made which demonstrated the essential role of the six canonical amino acids for catalysis in Rv1625c. The cytosolic mutants of Rv1625c N372A, N372T and D300S were used to investigate dimerization with mammalian AC catalytic units. Rv1625c engineered to contain forskolin binding amino acids cannot be stimulated by the diterpene. The similarities in conformation and mechanisms of catalysis between ACs and GCs was confirmed through the formation of functional chimeras between *Mycobacterium* Rv1625c and a guanylyl cyclase of *Paramecium*. The versatility of the class III cyclase homology domains concerning their modular architectures and mechanisms of catalysis was demonstrated with the biochemical characterization of Rv0386. This enzyme has a substrate-defining mechanism distinctly different of that of mammalian ACs. In addition by using ATP as well as GTP as a substrate it is a unique AC isoform unknown so far. Mutational studies of the Rv0386 AC domain proved the essential role that is played by a glutamine and an asparagine instead of the canonical lysine and aspartate for recognition of ATP and GTP as substrates. Diffraction-quality crystals of this AC domain were obtained as a first step to decipher the molecular and structural particularities of its catalytic function. Sequence comparisons identified an ATPase, a HTH DNA-binding and a transcription factor domain in Rv0386. How these domains affect AC activity in a concerted regulatory mechanism remains a pressing question for future studies.

## 7 Zusammenfassung

Im Rahmen der vorliegenden Arbeit wurden zwei Klasse III ACn aus *Mycobacterium tuberculosis* mit unterschiedlicher strukturellen und katalytischen Eigenschaften untersucht: die Mammalia-ähnliche Rv1625c und die an einen Transkriptionsfaktor gebundene Rv0386. Als ergänzende Studien zu bereits publizierten Daten (Guo et al., 2001), wurden zur Überprüfung der wesentlichen Rolle der sechs kanonischen Aminosäuren, die bei Mammalia-ACn in der Katalyse beteiligt sind und die in Rv1625c konserviert und auch katalytisch relevant sind, zusätzliche Punktmutationen durchgeführt und getestet. Die Rv1625c Mutanten N372A, N372T und D300S, die einzeln inaktiv sind, wurden für Rekonstitutionsversuchen benutzt wobei die Bildung katalytisch aktiver Homodimere in Rv1625c nachgewiesen wurde. Punktmutationen in Rv1625c, die Forskolin-bindende Aminosäuren in Säugercyclasen betreffen, erfahren dennoch keine Stimulierbarkeit durch das Diterpen. Die Ähnlichkeiten in Struktur und katalytischem Mechanismus zwischen ACn und GCn wurden hier bestätigt, da Chimären zwischen *Mycobacterium* Rv1625c und einer Guanylatcyclase aus *Paramecium* aktive katalytische Zentren gebildet haben. Die Vielseitigkeit der Klasse-III Cyclase Homologie Domänen hinsichtlich ihres modularen Aufbaus und ihres katalytischen Mechanismus wurde hier durch die biochemische Charakterisierung von Rv0386 nachgewiesen. Dieses Enzym zeigte einen Mechanismus zur Erkennung des Substrates, der sich von dem der Mammalia-ACn deutlich unterscheidet. Dieser ermöglicht die Erkennung sowohl von ATP als auch GTP als Substrat und ist eine Eigenschaft, die bis jetzt in keiner anderen AC Isoform beobachtet wurde. Mutationen der AC Domäne beweisen die essentielle Rolle, die Glutamin und Asparagine statt dem kanonischen Lysin und Aspartat bei der Erkennung der Substrate ATP und GTP in Rv0386 spielen. Der Erhalt der ersten diffraktionsfähigen Kristalle der AC Domäne innerhalb dieser Arbeit ist ein erster Schritt zur Erkenntnis der Besonderheiten ihrer katalytischen Funktion. Die Suche nach Sequenz Ähnlichkeiten zeigte, dass Rv0386 zusätzlich zu der AC Domäne aus ATPase-, HTH DNA-bindungs- und Transkriptionsfaktor-Domänen besteht. Noch zu beantworten bleibt die Frage, wie die regulatorische Verbindung zwischen der AC Domäne und dem Transkriptionsregulator AC Aktivität und weitere unbekannte Regulationsmechanismen beeinflusst.

## 8 Appendix

### 8.1 DNA and protein sequences of Rv0386

DNA and protein sequences of Rv0386 (Sanger Institute MTV036.21 or Swiss-Prot/TrEMBL accession number O53720).

														bp	aa	
ATG	AGC	AAG	TTG	CTG	CCA	CGG	GGC	ACA	GTG	ACA	TTG	CTG	TTG	GCC	45	
M	S	K	L	L	P	R	G	T	V	T	L	L	L	A		15
GAC	GTC	GAG	GGA	TCC	ACC	TGG	CTG	TGG	GAG	ACC	CAT	CCA	GAC	GAC	90	
D	V	E	G	S	T	W	L	W	E	T	H	P	D	D		30
ATG	GGT	GCT	GCC	GTG	GCG	CGC	CTC	GAC	AAA	GCC	GTG	TCT	GGT	GTG	135	
M	G	A	A	V	A	R	L	D	K	A	V	S	G	V		45
ATT	GCC	GCC	CAT	GAC	GGC	GTA	CGC	CCA	GTC	GAG	CAG	GGT	GAG	GGT	180	
I	A	A	H	D	G	V	R	P	V	E	Q	G	E	G		60
GAT	AGC	TTT	GTC	CTC	GCG	TTC	GCC	TGC	GCG	TCG	GAT	GCC	GTG	GCC	225	
D	S	F	V	L	A	F	A	C	A	S	D	A	V	A		75
GCC	GCG	TTG	GAC	TTG	CAG	CGA	GCG	CGG	CTC	GCA	CCG	ATC	CGG	TTG	270	
A	A	L	D	L	Q	R	A	R	L	A	P	I	R	L		90
CGC	ATA	GGC	GTG	CAC	ACC	GGG	GAG	GTC	GCG	CTC	CGC	GAC	GAA	GGC	315	
R	I	G	V	H	T	G	E	V	A	L	R	D	E	G		105
AAC	TAT	GCC	GGT	CCG	ACC	ATC	AAC	CGG	ACC	GCG	CGC	CTG	CGT	GAC	360	
N	Y	A	G	P	T	I	N	R	T	A	R	L	R	D		120
TTG	GCG	CAT	GGG	GGC	CAG	ACG	GTG	CTC	TCG	GGC	GTG	ACC	GAA	AGC	405	
L	A	H	G	G	Q	T	V	L	S	G	V	T	E	S		135
CTG	GTC	ATC	GAT	CGC	CTC	CCG	GAC	AAA	GCA	TGG	CTG	GTT	GAC	CTG	450	
L	V	I	D	R	L	P	D	K	A	W	L	V	D	L		150
GGG	ACG	CAC	GCG	CTG	CGG	GAT	CTG	TCG	CGT	CCG	GAG	CGG	GTA	ATG	495	
G	T	H	A	L	R	D	L	S	R	P	E	R	V	M		165
CAG	CTG	TGT	CAT	CCC	GAA	TTG	CGT	ATC	GAT	TTC	CCG	CCG	CTG	CGG	540	
Q	L	C	H	P	E	L	R	I	D	F	P	P	L	R		180
GTG	GCC	AAT	GAC	GAT	GTG	GCC	CAT	GGT	CTT	CCG	GTG	CAC	CTG	ACG	585	
V	A	N	D	D	V	A	H	G	L	P	V	H	L	T		195
CGT	TTT	GTG	GGG	CGC	GGC	GCG	CAG	ATC	ACC	GAG	GTG	CAC	CGG	TTG	630	
R	F	V	G	R	G	A	Q	I	T	E	V	H	R	L		210
GTG	ACC	GAT	AAC	CGG	TTG	GTG	ACC	CTG	ACC	GGC	GCC	GGC	GGC	GTG	675	
V	T	D	N	R	L	V	T	L	T	G	A	G	G	V		225
GGC	AAG	ACA	CGG	CTG	GCG	GCG	CAG	CTC	GCG	GCG	CAG	ATC	GCC	GGT	720	
G	K	T	R	L	A	A	Q	L	A	A	Q	I	A	G		240
GAG	TTC	GGT	GCG	GCG	TGG	TTC	GTG	GAT	CTG	GCG	CCG	ATC	ACG	GAC	765	
E	F	G	R	A	W	F	V	D	L	A	P	I	T	D		255
CCC	GAC	TTG	GTG	CCG	GTC	ACG	GTG	GCG	GGC	GCG	CTG	GGA	CTG	CAC	810	
P	D	L	V	P	V	T	V	A	G	A	L	G	L	H		270
GAC	CAG	CCG	GGC	CGC	TCC	ACG	ACG	GAC	ACC	GTG	CTG	CGC	TTT	CTT	855	
D	Q	P	G	R	S	T	T	D	T	V	L	R	F	L		285
GGC	GGG	CGT	CCA	GCC	CTG	GTG	GTG	CTG	GAT	AAC	TGC	GAG	CAC	CTG	900	
G	G	R	P	A	L	V	V	L	D	N	C	E	H	L		300
CTG	GAT	GCG	ACG	GCG	GCC	TTG	GTG	TTA	GCG	CTG	GTG	AAA	GCG	TGC	945	
L	D	A	T	A	A	L	V	L	A	L	V	K	A	C		315
CGG	GGG	GTG	AGG	TTG	CTG	GCA	ACT	TGT	CGT	GAG	CCG	CTC	CGG	GTC	990	
R	G	V	R	L	L	A	T	C	R	E	P	L	R	V		330
GAG	GGT	GAG	GTG	AGC	TAC	CGG	GTG	CCG	TCG	CTG	TCA	CTG	AGC	GAT	1035	
E	G	E	V	S	Y	R	V	P	S	L	S	L	S	D		345



GAA	GCC	GTT	GAG	ATG	TTT	TGC	TAC	CGG	GCT	CAG	CGA	GTC	CGG	CCG	1080	
E	A	V	E	M	F	C	Y	R	A	Q	R	V	R	P	360	
GAC	TTT	CGC	CTC	ACC	GAC	GAC	AAC	TCC	GCC	GCA	GTG	ACC	GAG	ATC	1125	
D	F	R	L	T	D	D	N	S	A	A	V	T	E	I	375	
TGC	AAA	CGG	CTG	GAC	GGT	TTG	CCG	CTG	GCG	ATC	GAG	CTG	GCG	GCT	1170	
C	K	R	L	D	G	L	P	L	A	I	E	L	A	A	390	
GCG	CGG	CTG	CGG	TCG	ATG	ACG	CTT	GAC	GAG	ATC	ATC	GAT	GGC	TTG	1215	
A	R	L	R	S	M	T	L	D	E	I	I	D	G	L	405	
CGT	GAC	CGG	TTC	SCG	CTG	TTG	ACC	GGC	GGT	GCG	CGC	ACG	GCC	GCG	1260	
R	D	R	F	A	L	L	T	G	G	A	R	T	A	A	420	
CAC	CGG	CAG	CAG	ACG	CTG	TGG	GCC	TCG	GTG	GAT	TGG	TCG	TAC	ACG	1305	
H	R	Q	Q	T	L	W	A	S	V	D	W	S	Y	T	435	
CTA	TTG	ACC	GAG	CCG	GAA	CGT	ACC	TTG	TTT	CGC	CGG	CTT	GCG	GTG	1350	
L	L	T	E	P	E	R	T	L	F	R	R	L	A	V	450	
TTT	GTG	GGT	TGC	TTT	TTT	GTC	GAC	GAC	GCA	CAG	GCG	GTT	GCC	TGC	1395	
F	V	G	C	F	F	V	D	D	A	Q	A	V	A	C	465	
AGC	GGC	GAT	GTG	CAG	CGC	TAC	CAG	GTC	CTT	GAC	GAG	ATC	ACC	CTG	1440	
S	G	D	V	Q	R	Y	Q	V	L	D	E	I	T	L	480	
CTG	GTC	GAC	AAG	TCA	CTG	GTG	ATG	GCC	GAC	GAC	AAC	AGC	GGC	CGG	1485	
L	V	D	K	S	L	V	M	A	D	D	N	S	G	R	495	
ACG	TGC	TAT	CGG	TTA	TGC	GAG	ACG	ATG	CGC	CAC	TAC	GCG	TTG	GAA	1530	
T	C	Y	R	L	C	E	T	M	R	H	Y	A	L	E	510	
AAA	CTC	TCC	GAG	GCT	GGC	GAG	GTG	GAC	GCC	GTG	TTT	GCG	CGG	CAC	1575	
K	L	S	E	A	G	E	V	D	A	V	F	A	R	H	525	
CGT	GAC	TAC	TAC	ACG	GCG	CTG	GCT	GCC	AGG	GTC	GAC	AAT	CCC	GGA	1620	
R	D	Y	Y	T	A	L	A	A	R	V	D	N	P	G	540	
CCC	TCC	GAT	TAT	TCG	CAC	TGC	CTC	GAC	CAA	GCC	GAA	ACC	GAG	ATC	1665	
P	S	D	Y	S	H	C	L	D	Q	A	E	T	E	I	555	
GAC	AAC	CTA	CGT	GCC	GCC	TTT	GTG	TGG	AAC	CGG	GAA	AAT	TCC	GAC	1710	
D	N	L	R	A	A	F	V	W	N	R	E	N	S	D	570	
ACC	GAG	GGC	GCC	TTG	GCG	CTG	GCG	TCC	TCC	CTG	TTG	CGG	GTA	TGG	1755	
T	E	G	A	L	A	L	A	S	S	L	L	R	V	W	585	
ATG	ACG	CGG	GGG	CGC	ATC	CAG	GAG	GGG	CGC	GCC	TGG	TTT	GAC	AGC	1800	
M	T	R	G	R	I	Q	E	G	R	A	W	F	D	S	600	
ATT	CTT	GCC	GAC	GAG	AAT	GCG	CGT	CAT	CTC	GAG	GTG	GCG	GCC	GCG	1845	
I	L	A	D	E	N	A	R	H	L	E	V	A	A	A	615	
GTG	CGC	GCC	CGG	GCA	TTG	GCC	GAC	AAG	GCC	CTG	CTC	GAC	ATC	TTC	1890	
V	R	A	R	A	L	A	D	K	A	L	L	D	I	F	630	
GTC	GAC	GCC	GCC	GCC	GGT	ATG	GAG	CAG	GCC	CAA	CAG	GCT	TTG	GTG	1935	
V	D	A	A	A	G	M	E	Q	A	Q	Q	A	L	V	645	
ATC	GCG	CGC	GAG	GTC	GAT	GAA	CCG	GCG	CTG	CTG	TCC	CGG	GCG	CTC	1980	
I	A	R	E	V	D	E	P	A	L	L	S	R	A	L	660	
ACG	GCC	TGC	GGC	TTG	ATC	GCG	GTA	GCG	GTA	GCT	CGC	GCC	GAT	GCG	2025	
T	A	C	G	L	I	A	V	A	V	A	R	A	D	A	675	
GCC	GCG	TCT	TAT	TTC	GCC	GAG	GCG	ATC	GAC	CTG	GCA	CGA	GCG	GTA	2070	
A	A	S	Y	F	A	E	A	I	D	L	A	R	A	V	690	
GAC	GAC	CGG	TGG	AGG	CTG	GCC	CAG	ATC	CTT	ACC	TTT	CAG	GCG	GTC	2115	
D	D	R	W	R	L	A	Q	I	L	T	F	Q	A	V	705	
GAT	GCG	GTC	GTG	GCG	GGT	GAC	CCG	GTC	GCG	GCA	CGC	CCG	GCC	GCC	2160	
D	A	V	V	A	G	D	P	V	A	A	R	P	A	A	720	
CAA	GAG	GCA	CGC	GAG	CTG	GCT	GCC	GCG	ATC	GGT	GAC	CAC	TCC	AAT	2205	
Q	E	A	R	E	L	A	A	A	I	G	D	H	S	N	735	
GCG	CTG	TGG	TGC	CGC	TGG	TGT	CTC	GGC	TAC	GCC	CAG	CTG	ATG	CGG	2250	
A	L	W	C	R	W	C	L	G	Y	A	Q	L	M	R	750	
GGG	GAG	CTG	GCC	GCG	GCC	GCC	GCC	CAA	TTC	GGC	GAG	GTG	GTG	GAC	2295	
G	E	L	A	A	A	A	A	Q	F	G	E	V	V	D	765	
GAG	GCC	GAG	GCG	TCT	CAG	GAA	GTG	CTG	CAC	AAG	GCC	AAC	AGC	CTG	2340	

E	A	E	A	S	Q	E	V	L	H	K	A	N	S	L	780
CAG	GGC	CTG	GCC	TTC	GCG	CTC	GCC	TAC	CAG	GGT	GAA	TTG	AGT	GCG	2385
Q	G	L	A	F	A	L	A	Y	Q	G	E	L	S	A	795
GCT	AGG	GCG	GCG	GCC	GAC	GCC	GCT	CTC	GAG	GCC	GCC	GAG	CTG	GGC	2430
A	R	A	A	A	D	A	A	L	E	A	A	E	L	G	810
GAG	TAC	TTC	GCG	GGT	ATG	GGC	TAC	TCG	GCG	TTG	ACC	ACG	GCC	GCG	2475
E	Y	F	A	G	M	G	Y	S	A	L	T	T	A	A	825
TTG	GCC	GCC	GGC	GAC	GTG	CAG	ACG	GCT	CAA	CAT	GCC	AGC	GAG	GCG	2520
L	A	A	G	D	V	Q	T	A	Q	H	A	S	E	A	840
GCC	TGG	CGG	AAC	TTG	AGT	TTG	TCG	CTG	CCC	CTC	TCG	GCA	GCG	GTG	2565
A	W	R	N	L	S	L	A	L	P	L	S	A	A	V	855
CAG	CGC	GCG	TTC	AAT	GCC	CAG	GCT	GCA	CTG	GCT	GGT	GGT	GAC	CTT	2610
Q	R	A	F	N	A	Q	A	A	L	A	G	G	D	L	870
AGC	GCA	GCG	CGT	CGT	TGG	TGT	GAC	GAT	GCC	GTG	CAG	TCA	ATG	ACC	2655
S	A	A	R	R	W	C	D	D	A	V	Q	S	M	T	885
GGC	CAT	CAT	CTG	GCG	ATG	GCG	CTG	GCG	ACT	CGC	GCC	AGG	ATC	GCG	2700
G	H	H	L	A	M	A	L	A	T	R	A	R	I	A	900
GTC	GCC	GAG	GGC	AAG	CGG	GAA	GAA	GCC	GAA	CGC	GAC	GCG	CAT	AAG	2745
V	A	E	G	K	R	E	E	A	E	R	D	A	H	K	915
GCG	CTC	GCG	TGC	GCG	GCC	GAG	AGC	GGG	GCA	CAC	CTG	GAT	CTC	CCC	2790
A	L	A	C	A	A	E	S	G	A	H	L	D	L	P	930
GAC	GTG	CTC	GAA	TGC	CTT	GCC	GGC	CTG	GCC	AGC	GAC	GCC	GGC	ACC	2835
D	V	L	E	C	L	A	G	L	A	S	D	A	G	T	945
CAC	CAT	GCG	GCG	GCA	CGA	CTC	TTC	GGC	GCC	GCC	GAG	GCT	ATC	CGA	2880
H	H	A	A	A	R	L	F	G	A	A	E	A	I	R	960
CAG	CAG	ATC	GGC	TCG	GTC	CGC	TTC	GCG	ATT	TAC	CGT	TCG	GAC	TAT	2925
Q	Q	I	G	S	V	R	F	A	I	Y	R	S	D	Y	975
GTG	CAG	TCG	GTG	ACG	GCT	CTG	CGA	GAT	GCG	ATG	GGG	GAG	AAA	GAC	2970
V	Q	S	V	T	A	L	R	D	A	M	G	E	K	D	990
TTC	GAC	GCT	GCA	TGG	GCC	GAA	GGT	GCC	GCG	TTG	TCG	ATC	AAG	GAG	3015
F	D	A	A	W	A	E	G	A	A	L	S	I	K	E	1005
ACG	ATC	GCC	TAT	GCG	CAA	CGT	GGC	CAC	TCC	TGG	CGC	AAA	CGA	CCG	3060
T	I	A	Y	A	Q	R	G	H	S	W	R	K	R	P	1020
GCC	ACC	GGT	TGG	GAA	TCG	CTT	ACT	CCG	ACC	GAG	ATT	GAC	GTC	GTG	3105
A	T	G	W	E	S	L	T	P	T	E	I	D	V	V	1035
CGA	CTG	GTT	GGC	GAG	GGA	CTG	GCC	AAC	AAG	GAC	ATC	GCG	ACG	CGG	3150
R	L	V	G	E	G	L	A	N	K	D	I	A	T	R	1050
CTT	TTC	GTC	TCA	CCG	CGA	ACA	GTG	CAA	ACG	CAC	CTG	ACG	CAC	GTC	3195
L	F	V	S	P	R	T	V	Q	T	H	L	T	H	V	1065
TAC	ACC	AAA	CTC	GGC	TTC	ACC	TCG	CGA	CTG	CAA	CTC	GCT	CAA	GCG	3240
Y	T	K	L	G	F	T	S	R	L	Q	L	A	Q	A	1080
GCC	GCC	CGC	CGT	ACC	TGA										3258
A	A	R	R	T	.										1085

## 8.2 Results of the Protein-Protein BLAST Search

At NCBI a Protein-Protein BLAST search (blastp) with the full length Rv0386 and its AC, ATPase, Transcription factor and DNA-binding domains was made (Nov-26-2003; <http://www.ncbi.nlm.nih.gov/BLAST/>; Altschul et al., 1997). The 5 best hits are here reported.

Database: All non-redundant GenBank CDS translations+PDB+SwissProt+PIR+PRF

## 8.2.1 Blastp of the full length Rv0386

Sequences producing significant alignments:			Score	E
			(bits)	Value
gi 15609625 ref NP_217004.1	hypothetical protein Rv2488c [...		890	0.0
gi 31792554 ref NP_855047.1	PROBABLE TRANSCRIPTIONAL REGUL...		759	0.0
gi 15840308 ref NP_335345.1	transcriptional regulator, Lux...		688	0.0
gi 15840309 ref NP_335346.1	hypothetical protein [Mycobact...		223	2e-56
gi 29832482 ref NP_827116.1	putative multi-domain regulato...		219	2e-55

## 8.2.2 Blastp of the adenylyl cyclase domain

Sequences producing significant alignments:			Score	E
			(bits)	Value
gi 31791563 ref NP_854056.1	PROBABLE TRANSCRIPTIONAL REGUL...		300	9e-81
gi 15607527 ref NP_214900.1	hypothetical protein Rv0386 [M...		300	1e-80
gi 15839770 ref NP_334807.1	transcriptional regulator, Lux...		299	1e-80
gi 15840309 ref NP_335346.1	hypothetical protein [Mycobact...		191	5e-48
gi 15842015 ref NP_337052.1	transcriptional regulator, Lux...		178	4e-44

## 8.2.3 Blastp of the ATPase domain

Sequences producing significant alignments:			Score	E
			(bits)	Value
gi 15609625 ref NP_217004.1	hypothetical protein Rv2488c [...		228	8e-59
gi 31792554 ref NP_855047.1	PROBABLE TRANSCRIPTIONAL REGUL...		219	3e-56
gi 15840814 ref NP_335851.1	transcriptional regulator, Lux...		217	1e-55
gi 15608030 ref NP_215405.1	hypothetical protein Rv0890c [...		197	1e-49
gi 15840308 ref NP_335345.1	transcriptional regulator, Lux...		197	1e-49

## 8.2.4 Blastp of the transcription factor domain

Sequences producing significant alignments:			Score	E
			(bits)	Value
gi 15839770 ref NP_334807.1	transcriptional regulator, Lux...		1428	0.0
gi 15607527 ref NP_214900.1	hypothetical protein Rv0386 [M...		1428	0.0
gi 31791563 ref NP_854056.1	PROBABLE TRANSCRIPTIONAL REGUL...		1411	0.0
gi 15842015 ref NP_337052.1	transcriptional regulator, Lux...		728	0.0
gi 15609625 ref NP_217004.1	hypothetical protein Rv2488c [...		727	0.0

## 8.2.5 Blastp of the DNA-binding domain

Sequences producing significant alignments:			Score	E
			(bits)	Value
gi 15839770 ref NP_334807.1	transcriptional regulator, Lux...		162	1e-39
gi 15607527 ref NP_214900.1	hypothetical protein Rv0386 [M...		162	1e-39
gi 31791563 ref NP_854056.1	PROBABLE TRANSCRIPTIONAL REGUL...		148	2e-35
gi 15840308 ref NP_335345.1	transcriptional regulator, Lux...		127	4e-29
gi 15608030 ref NP_215405.1	hypothetical protein Rv0890c [...		127	5e-29

### 8.3 Sequence alignments of Rv0386

The sequence of the AC domain of Rv0386 was aligned with mammalian AC's, mycobacterial Rv1625c and *Paramecium* GC sequences for identification of variations in amino acids that are critical for AC and GC catalysis and for presence or absence of other features like the "arm region". The sequences of the other individual domains of Rv0386 were aligned with those proteins who showed the highest similarity after BLAST Search.

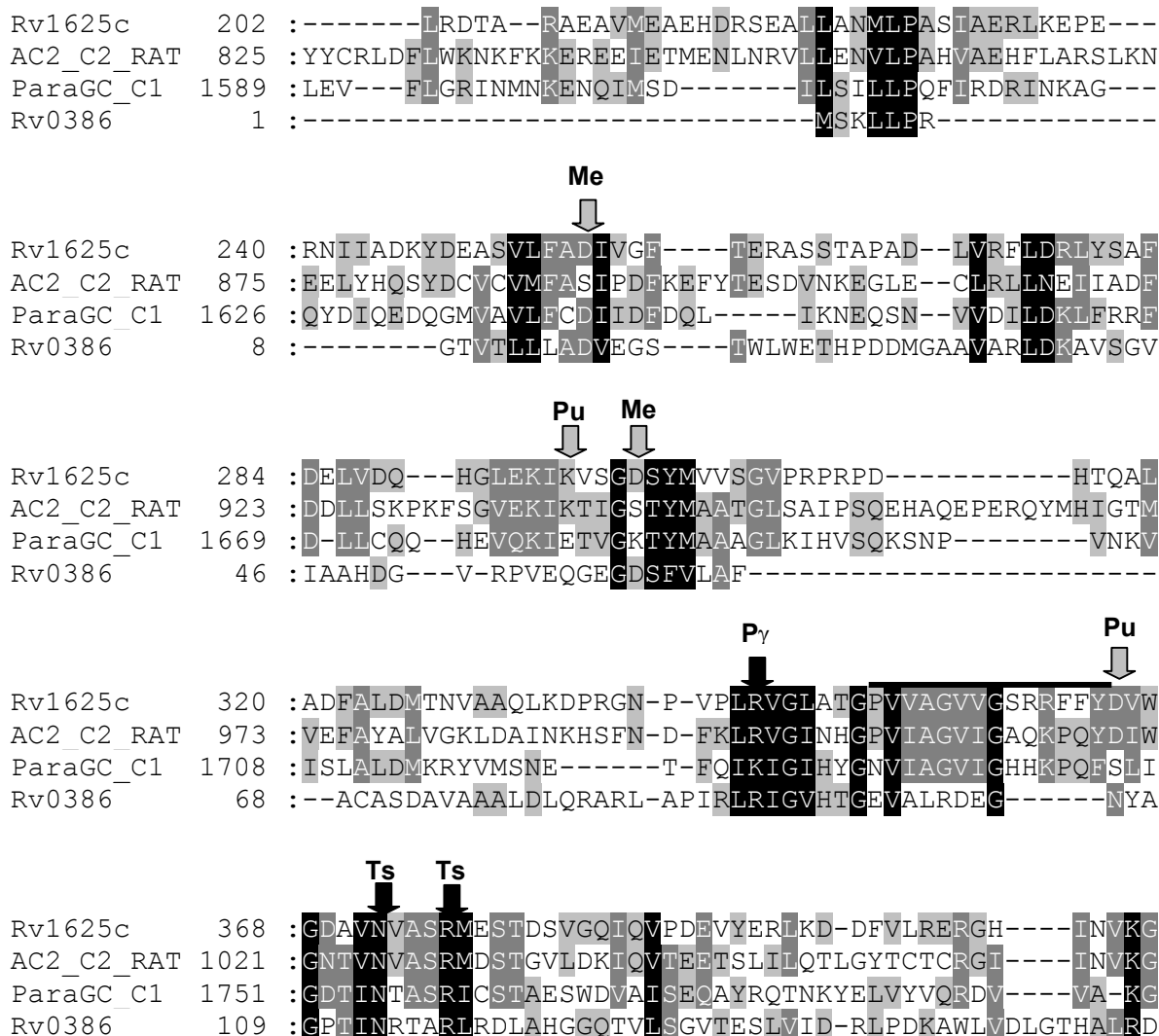


**Fig. 8.1:** Complete alignment of the AC domain of Rv0386 with the mycobacterial Rv1625c AC domain, the mammalian C2 cytosolic domain (rat) and the C1 region of the *Paramecium* GC. Shown are the purine-binding sites (Pu), the transition state-stabilizing sites (Ts), the  $\gamma$ -phosphate-binding site (Py), the metal binding sites (Me) and the "arm or dimerization region" (represented with a top bar).

```

Rv0386 179 : -LRVANDDVAHGIPVHLTRFVGRGAQITEVHRL---VTDNR----LVTLT
AfsR 258 : PGRAPSDGRKGNIRPRLTTFVGREPELDALRSE---LPGAR----LVTLT
Apaf-1 109 : --YVRTVLCEGGVPQRPVVFVTRKKLVNAIQQKLSKLGKGEF---GWVTIH
I2C-1 153 : ---KQETRTPSTSLVDDSGIFGRKNEIENLVGRLLSMDTKRKNLAVVPIV
L6tr 220 : --DIWSHISKENILETDELVGIDDHITAVLEK-LSLDSSEN--VTMVGLY
RPM1 156 : ---WVNNISESSLFFSENSLVGIDAPKGKLI GRLLSPEPQR---IVVAVV

```

```

Rv0386 221 : GAGGVGKTRLAAQLAAQ--IAGEFGRAWFVDIAPITDPLVPVTVAGALG
AfsR 301 : GPGSGKTRLAEEAAAG--LD---QAWLVELAPLDRPEAVPGAIVNALG
Apaf-1 154 : GMAGCGKSVLAAEAVRDHSLLEGCFPGGVHWVSVGKQDKSGLLMKLNLC
I2C-1 200 : GMGGMGKTTLAKAVYNDERVQKHFGLTAWFCVSEAYDAFRITKGLLQEIIG
L6tr 265 : GMGGIGKTTTAKAVYN--KISSCFDCCCFIDNIRETQEKDGVVVIQKKLV
RPM1 200 : GMGGSKTTLSANIFKSQSVRRHFESYAWVTISKSYVIEDVFRMTI KEF-
      ▲      ▲▲▲

```

```

Rv0386 269 : ---LHD-----Q-PGR---STTDTVLRFLGGRPALVVLDNCEHLL
AfsR 345 : ---LRETV---ILTGD RPAGQ-DDPVALLVEYCAPRSQLLVLDNCEHVI
Apaf-1 204 : TRLDQDESFSQRILPLNIEEAKD---RLRIILMLRKHPRSLIILDDVWDSW
I2C-1 250 : STD LKADDNLNQLQVKLKADDNLNQLQVKLKEKLNKGRFLVVLDVWVNDN
L6tr 313 : SEILRIDS--GSVGFNNDSSG-----RKTIKERVS RFKILVVLDVDEKF
RPM1 249 : ---YKEAD--TQIPAE LYS LG-YRELVEKLV EYLQSKRYIVVLDVVTTG

```

```

Rv0386 302 : D-ATAALVLA LVKACRGVRLIATCREPLRVEGE-----VSYRVPSLSLS
AfsR 387 : G-AAARLVETLLTRCPGLTVLATSREPLGVPGE-----SVRPVEPLTQ-
Apaf-1 250 : -----VLKAFDSQCQIILLTTRD-KSVTDSVMGPKYVVPV ESSLGK-
I2C-1 300 : YPEWDDL RNLFLQGDIGSKIIVTTRK-ESVALM---MDSGAIYMGILSS-
L6tr 356 : --KFEDMLGSPKDFISQSRFIIITSRS-MRVLGTLNENQCKLYE VGSMSK-
RPM1 293 : --LWREISIALPDGIYGSRVMMTTRD-MNVASF PYGIGSTKHEIELLKE-

```

```

Rv0386 345 : DEAVEMFCYRAQVRPDFRLTDDNSAAVTEITCKRLDGLPLAIE LAAARLR
AfsR 429 : EQAQRLEFTARAGAVRPDADAVLRDEEAVAEICRRLDGLPLAIE LAAARLR
Apaf-1 289 : EKGLEILSLFVNMMKK-----ADLPEQAHSIIKECKGSPLV VSLIGALL-
I2C-1 345 : EDSWALFKRHSLEHK-DPKEHPEFEVVGKQIADKCKGLPLAL KALAGMLR
L6tr 402 : PRSLELFSKHAFKKN---TPPSYYETLANDVVDTTAGLPLTLK VIGSLL-
RPM1 339 : DEAWVLF SNKAFPASLEQCRTQNLEPIARKLVERCOGLPLA IASLGSMMS

```

**Fig. 8.2:** Alignment of the ATPase domain of Rv0386 with representative proteins containing also an ATP/GTP-binding motif A (P-loop or Walker A box with a consensus sequence [AG]-x(4)-G-K-[ST]; represented here through black triangles) and disease resistance genes signatures (represented with top bars). Aligned were: AfsR (P25941), Apaf-1 (O14727), I2C-1 (O24015), L6tr (Q40254) and RPM1 (Q39214). The Swiss-Prot/TrEMBL accession numbers are in parentheses.

**a**

```

BVGA_BORPER 149 : LSNRELTVLQLLAQQGMSNKDIADSMFLSNKTVSTYKTRLLQKLNATSLVE
FIMZ_ECOLI 150 : LSNREVTILRYLVSGLSNKEIADKLLLSNKTVSAHKSNIYGKLGHSIVE
FIMZ_SALTY 150 : LSNREVTVLRVLANGMSNKEIAEQLLLSNKTISAHKANIFSKLGLHSIVE
NARP_HAEIN 149 : LTDREMGVLRQIATGLSNKQIAAQLFISEETVKVHIRNLLRKLNVHSRVA
YXJL_BACSU 157 : FTKRELEVLQQMAYGIRNEDIAEKLFVSESTVKTHVHRTLQKCNAQDRTO
SCO3008 189 : LTDRELEVLKLVATGMNNRDIAKELFISENTVKNHVRNILEKLQLHSRME
Rv0890c 821 : LTPTERDVVRLVSEGLSNKDIKRLFVSPRTVQTHLTHVYAKLGLPSRVQ
Rv0386 1027 : LTPTEIDVVRLVGEGLANKDIATRLFVSPRTVQTHLTHVYTKLGFTSRLQ

```

▲ ▲ ▲▲ ▲ ▲ ▲▲ ▲▲ ▲

**b**

```

narL 1 : SNQEPATILLI DDHPMLRTGVKQLISMAPDITVVGEEASNGE-----QG
uhpA 1 : ----MITVALI DDHLIVRSGFAQLLGLPDLQVVAEFGSGR-----EA
Rv0386 867 : GGDLSAARRWCDDAVQSMTGHHLAMALATRARI AVAEGKREEAERDAHKA

```

```

narL 44 : TELAESLDPDIILLDLNMPGMNGLETLDKIREKSLSGRIVVFSVSNHEED
uhpA 40 : LAGLPGRGVQVCICDISMPDISGLELLSQLP-KGMA--TIVLSVHDSPAL
Rv0386 917 : LACAESGAHLIDLDPV-LECLAGLASDAGTHHAAARLFGAAEAIRQQIGS

```

```

narL 94 : VVTALKRGADGYLLKDMEPEDLLKALHQAAAGEMVLSEALTPVLAASLRA
uhpA 87 : VEQALNAGARGFLSKRCSPELIAAVHTVATGGCYL----TPDIAVKLAA
Rv0386 966 : VRFAIYRSYVQSVTALRDAMGEKDFDAAWAEGAA LSIKETIAYAQRGHS

```

```

narL 144 : NRATTERDVNQ LTPRERDILKLI AQGLPNKMIARRLDITESTVKVHVHKHM
uhpA 133 : GRQ--D----PLTKRERQVAEKLAQGMVKEIAAELGLSPKTVHVRANL
Rv0386 1016 : WRKR PATGWES LTPTEIDVVRLVGEGLANKDIATRLFVSPRTVQTHLTHV

```

```

narL 194 : LKKMKLKS RVEAAVWVHQERIF
uhpA 177 : LEKLGVSNDVEIAHRMFDGW--
Rv0386 1066 : YTKLGFTSRLQLAQAARRT--

```

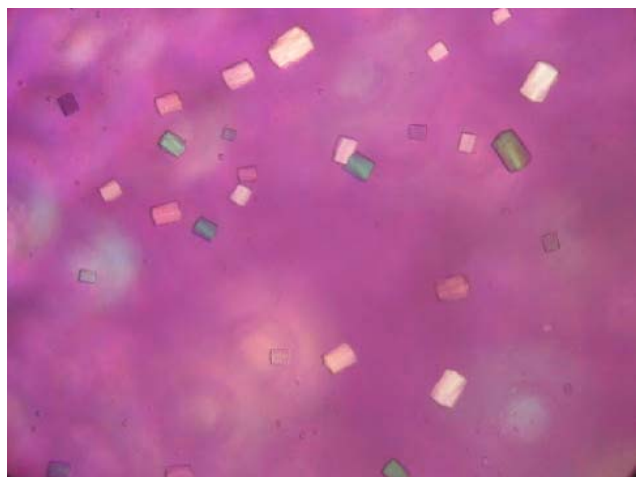
**Fig. 8.3:** a) Alignment of the DNA-binding domain of Rv0386 with representative proteins containing a Helix-Turn-Helix DNA-binding signature (top bar). The consensus sequence of this signature is represented here with black triangles. Aligned were: BVGA (P16574), FIMZ (P26319), NarP from *Haemophilus influenzae*, YXJL from *Bacillus subtilis*, SCO3008 from *Streptomyces coelicolor* and Rv0890c from *M. tuberculosis*. b) Detailed alignment with narL (P10957) and uhpA (P27667) showing the DNA-binding motif and other conserved regions. Swiss-Prot/TrEMBL accession numbers are in parentheses.

## 8.4 Crystal pictures

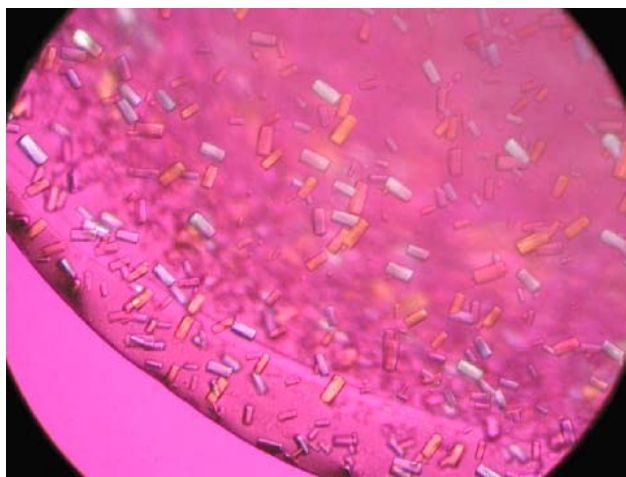
Representative pictures of some of the crystals obtained with the catalytic domain of Rv0386 within this work. First diffraction-data obtained is also shown.

### 8.4.1 Crystals of the AC domain of Rv0386 with N-terminal His-tag

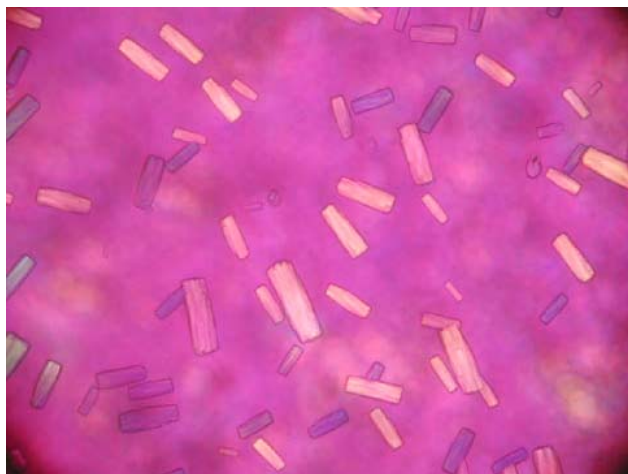
**a**



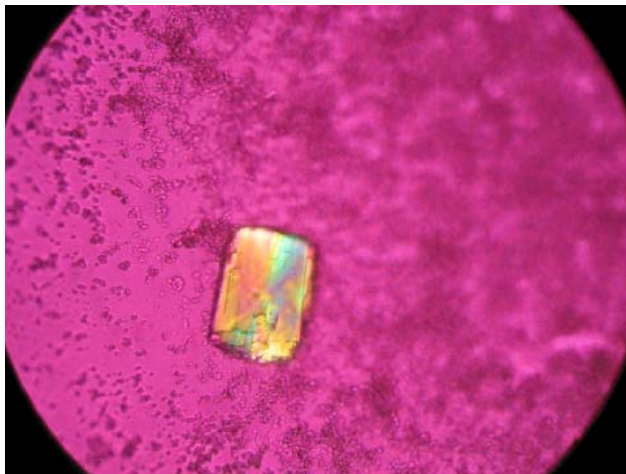
**b**

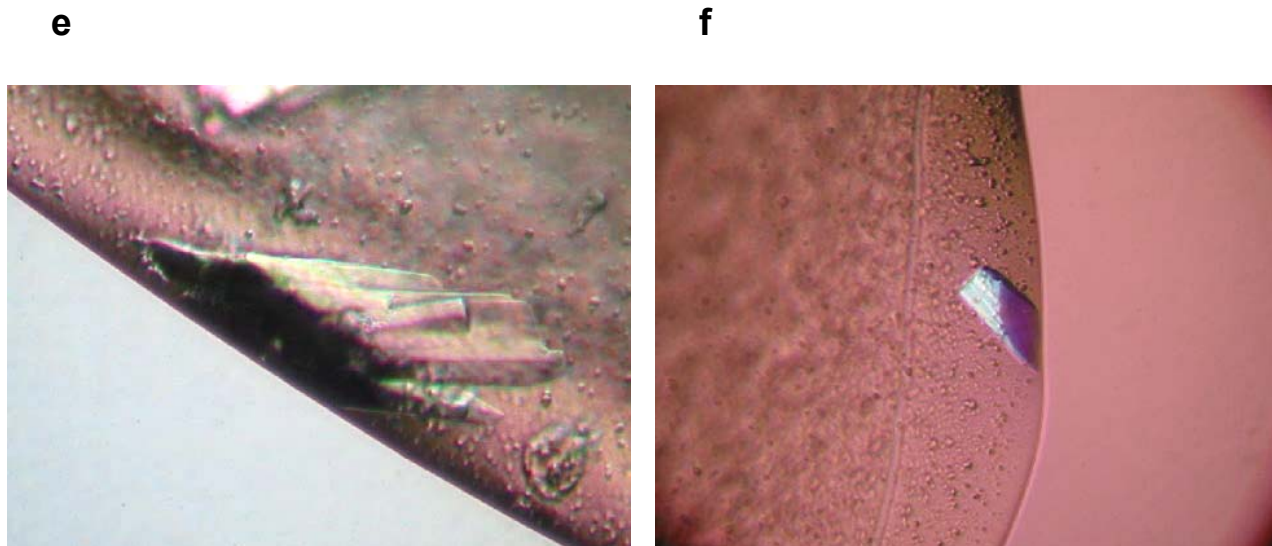


**c**



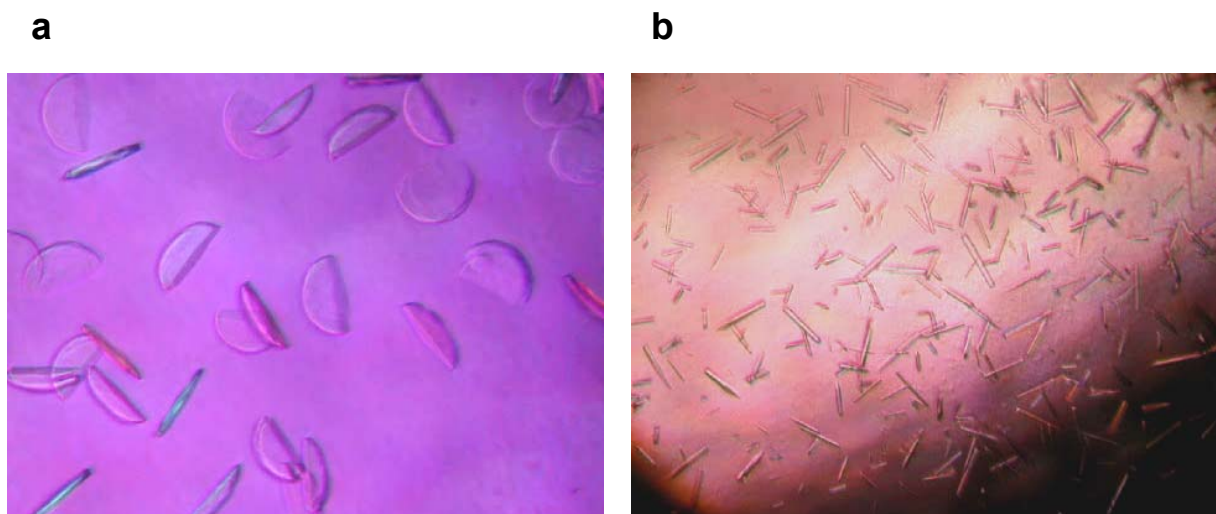
**d**





**Fig. 8.4:** Crystals obtained with the N-terminal His-tagged AC domain dialyzed after Ni-NTA-purification in 50 mM Tris-HCl pH 8.5, 10 mM NaCl, 2 mM  $\beta$ -mercaptoethanol and 10% glycerol. Precipitant solution was 10 % PEG 6000 + 2 M NaCl (a,b,e and f); 12 % PEG 6000 + 2 M NaCl (c) and 10 % PEG 4000 + 2 M NaCl (d). Incubation temperatures were: 16 °C (a and d) and 12 °C (b,c,e and f). Protein concentrations used were: a) 16  $\mu$ g/ $\mu$ l; b) 25  $\mu$ g/ $\mu$ l; c) 20  $\mu$ g/ $\mu$ l ; d) 12  $\mu$ g/ $\mu$ l ; e and f) 22  $\mu$ g/ $\mu$ l. Approximate size of the crystals: a) 15x17  $\mu$ m and 50x50  $\mu$ m; b) 50x20  $\mu$ m; c) 25x75  $\mu$ m and 90x30  $\mu$ m; d) 175x125  $\mu$ m; e) 150x75  $\mu$ m and f) 150x50  $\mu$ m.

#### 8.4.2 Crystals of the AC domain of Rv0386 with C-terminal His-tag





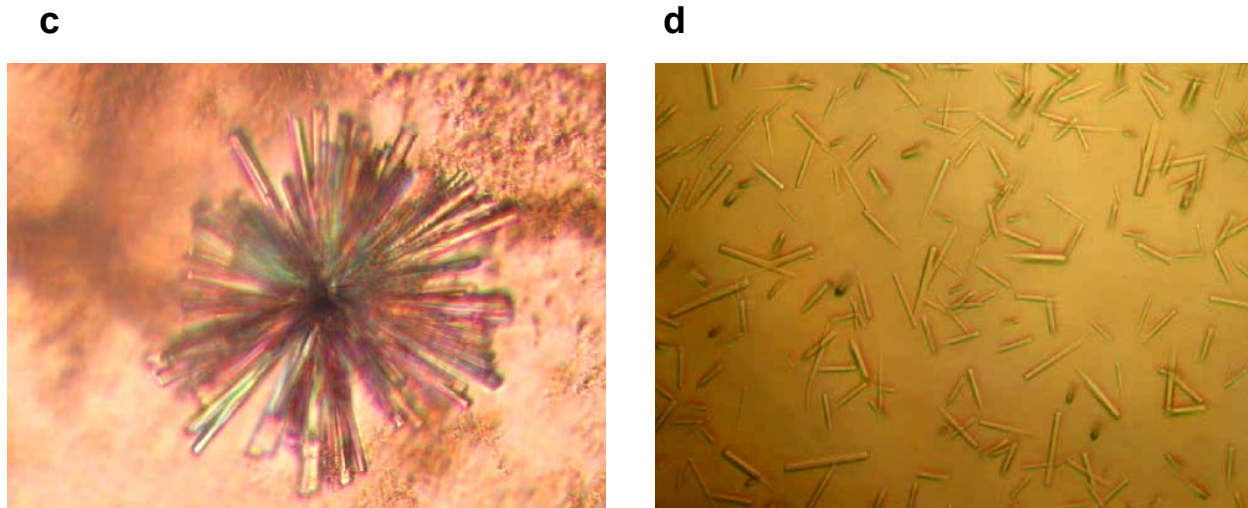


**Fig. 8.5:** Crystals obtained with the C-terminal His-tagged AC domain dialyzed after Ni-NTA-purification in 50 mM Tris-HCl pH 8.5, 10 mM NaCl, 2 mM  $\beta$ -mercaptoethanol and 5% glycerol. Protein concentration was 9.8  $\mu$ g/ $\mu$ l. Protein was 14 h incubated with 1 mM ATP at 0  $^{\circ}$ C. Incubation temperature was 16  $^{\circ}$ C. Precipitant solutions were: a) 15 % PEG 4000 + 0.1 M Tris HCl pH 8.5 + 0.2 M sodium acetate; b) 10 % PEG 6000 + 0.1 M Hepes pH 7.5 + 5 % MPD; c) 30 % PEG 4000 + 0.1 M Tris HCl pH 8.5 + 0.2 M magnesium chloride; d) 0.5 M sodium acetate + 0.1 M imidazole pH 6.5. First diffraction data could be obtained with the crystals of picture d (see data below).

Shell limit	Lower Angstrom	Upper Angstrom	Average I	Average error	Norm. stat.	Linear Chi**2	Square R-fac	R-fac
	25.00	15.81	37.3	6.6	3.1	1.000	0.105	0.078
	15.81	13.13	38.2	7.6	3.9	1.000	0.138	0.122
	13.13	11.66	53.9	11.0	6.7	1.000	0.117	0.106
	11.66	10.69	79.9	11.6	8.9	0.999	0.096	0.087
	10.69	9.97	63.4	9.9	7.1	1.000	0.109	0.110
	9.97	9.42	58.7	8.7	6.0	1.000	0.120	0.106
	9.42	8.97	49.3	13.8	8.7	1.001	0.160	0.148
	8.97	8.59	50.3	15.1	10.2	1.000	0.197	0.196
	8.59	8.28	32.3	11.3	6.9	1.000	0.226	0.174
	8.28	<b>8.00</b>	22.5	16.8	10.3	1.001	0.382	0.335
All reflections			49.0	11.3	7.2	1.000	0.146	0.128
finishing up after 8 cycles - overall R 14.6 percent - crystal q2-1 calculating ...								
=====								
dataset: q2-1.tru logfile: q2-1.truncate-log								
=====								
unit cell: 82.941 82.941 277.636 90.000 90.000 90.000								
space group = 75								
starting resolution = 24.77								
<b>finishing resolution = 8.00</b>								
number of amino acids in AU = 1600								
fraction of unit cell occupied by atoms = 53.1%								
solvent content = 46.9%								
=====								

**Fig. 8.6:** Preliminary diffraction data of the crystals of figure 8.5 d collected on the ID13 Micro Focus Beam Line (ESRF-Grenoble, France). Dr. Ivo Tews and Dr. Felix Findeisen from Biochemie Zentrum Heidelberg made the measurements.

## 9 References

- Agranoff, D., Monahan, I.M., Mangan, J.A., Butcher, P.D. and Krishna, S. (1999) *Mycobacterium tuberculosis* expresses a novel pH-dependent divalent cation transporter belonging to the Nramp family. *J. Exp. Med.*, **190**, 717-724.
- Altschul, S.F., Madden, T.L., Schaffer, A.A., Zhang, Z., Miller, W. and Lipman, D.J. (1997) Gapped BLAST and PSI-BLAST: a new generation of protein database search programs. *Nucleic Acids Res.*, **25**, 3389-3402.
- Aravind, L. and Koonin, E.V. (1999) DNA polymerase  $\beta$ -like nucleotidyltransferase superfamily: identification of three new families, classification and evolutionary history. *Nucleic Acids Research*, **27**, 1609-1618.
- Artymiuk, P.J., Poirrette, A.R., Rice, D.W. and Willet, P. (1997) A polymerase I palm in adenylyl cyclase?. *Nature*, **388**, 33-34.
- Baillie, L. and Read, T.D. (2001) *Bacillus anthracis*, a bug with attitude!. *Curr. Opin. Microbiol.*, **4**, 78-81.
- Bârzu, O. and Danchin, A. (1994) Adenylyl Cyclases: A Heterogeneous Class of ATP-Utilizing Enzymes. *Progress in Nucleic Acid Research and Molecular Biology*, **49**, 241-283.
- Becker, G., Klauck, E. and Hengge-Aronis, R. (1999) Regulation of RpoS proteolysis in *Escherichia coli*: The response regulator RssB is a recognition factor that interacts with the turnover element in RpoS. *Proc. Natl. Acad. Sci. USA*, **96**, 6439-6444.
- Brendel, V., Bucher, P., Nourbakhsh, I., Blaisdell, B.E. and Karlin, S. (1992) Methods and algorithms for statistical analysis of protein sequences. *Proc. Natl. Acad. Sci. USA*, **89**, 2002-2006.
- Cole, S.T. et al. (1998) Deciphering the biology of *Mycobacterium tuberculosis* from the complete genome sequence. *Nature*, **393**, 537-544.
- Danchin, A. (1993) Phylogeny of adenylyl cyclases. *Adv. Second Messenger Phosphoprotein Res.*, **27**, 109-162.
- Danchin, A., Pidoux, J., Krin, E., Thompson, C.J. and Ullmann, A. (1993) The adenylate cyclase catalytic domain of *Streptomyces coelicolor* is carboxy-terminal. *FEMS Microbiol. Lett.*, **114**, 145-151.
- Désaubry, L., Shoshani, I. and Johnson, R.A. (1996) 2', 5'-dideoxyadenosine 3'-polyphosphates are potent inhibitors of adenylyl cyclases. *J. Biol. Chem.*, **271**, 2380-2382.

- Dessauer, C.W., Scully, T.T. and Gilman, A.G. (1997) Interactions of forskolin and ATP with the cytosolic domains of mammalian adenylyl cyclase. *J. Biol. Chem.*, **272**, 22272-22277.
- Fleischmann, R.D., Alland, D., Eisen, J.A., Carpenter, L., White, O., Peterson, J., DeBoy, R., Dodson, R., Gwinn, M., Haft, D., Hickey, E., Kolonay, J.F., Nelson, W.C., Umayan, L.A., Ermolaeva, M., Salzberg, S.L., Delcher, A., Utterback, T., Weidman, J., Khouri, H., Gill, J., Mikula, A., Bishai, W., Jacobs, Jr W.R. Jr., Venter, J.C. and Fraser, C.M. (2002) Whole-genome comparison of *Mycobacterium tuberculosis* clinical and laboratory strains. *J. Bacteriol.*, **184**, 5479-5490.
- Gamielien, J., Ptitsyn, A. and Hide, W. (2002) Eukaryotic genes in *Mycobacterium tuberculosis* could have a role in pathogenesis and immunomodulation. *Trends Genet.*, **18**, 5-8.
- Garnier, T., Eiglmeier, K., Camus, J.C., Medina, N., Mansoor, H., Pryor, M., Duthoy, S., Grondin, S., Lacroix, C., Monsempe, C., Simon, S., Harris, B., Atkin, R., Doggett, J., Mayes, R., Keating, L., Wheeler, P.R., Parkhill, J., Barrell, B.G., Cole, S.T., Gordon, S.V. and Hewinson, G. (2003) The complete genome sequence of *Mycobacterium bovis*. *Online publication at the NCBI Website*.
- Guo, Y.L., Seebacher, T., Kurz, U., Linder, J.U. and Schultz, J.E. (2001) Adenylyl cyclase Rv1625c of *Mycobacterium tuberculosis*: a progenitor of mammalian adenylyl cyclases. *EMBO*, **20**, 3667-3675.
- Hoffmann, T.R. (1999) Membranständige Guanylatcyclasen aus *Paramecium* und *Tetrahymena*: Klonierung und bakterielle Expression der katalytischen Bereiche. Dissertation der Universität Tübingen.
- Hurley, J.H. (1998) The adenylyl and guanylyl cyclase superfamily. *Current Opinion in Structural Biology*, **8**, 770-777.
- Hurley, J.H. (1999) Structure, mechanism and regulation of mammalian adenylyl cyclase. *J. Biol. Chem.*, **274**, 7599-7602.
- Johnson, R.A. and Shoshani, I. (1990) Kinetics of "P"-site-mediated inhibition of adenylyl cyclase and the requirements for substrate. *J. Biol. Chem.*, **265**, 11595-11600.
- Kanacher, T., Schultz, A., Linder, J.U. and Schultz, J.E. (2002) A GAF-domain-regulated adenylyl cyclase from *Anabaena* is a self-activating cAMP switch. *EMBO*, **21**, 3672-3680.
- Kanacher, T. (2003) Die Adenylatcyclase CyaB1 aus *Anabaena* sp.PCC7120 ist ein cAMP-sensitives Protein. Dissertation der Universität Tübingen.

- Kasahara, M., Yashiro, K., Sakamoto, T. and Ohmori, M. (1997) The *Spirulina platensis* adenylate cyclase gene, *cyaC*, encodes a novel signal transduction protein. *Plant Cell Physiol.*, **38**, 828-836.
- Ladant, D. and Ullman, A. (1999) *Bordetella pertussis* adenylate cyclase: a toxin with multiple talents. *Trends Microbiol.*, **7**, 172-176.
- Linder, J.U., Engel, P., Reimer, A., Krüger, T., Plattner, H., Schultz, A. and Schultz, J.E. (1999) Guanylyl cyclases with the topology of mammalian adenylyl cyclases and an N-terminal P-type ATPase-like domain in *Paramecium*, *Tetrahymena* and *Plasmodium*. *EMBO J.*, **18**, 4222-4232.
- Linder, J.U., Hoffmann, T., Kurz, U. and Schultz, J.E. (2000) A guanylyl cyclase from *Paramecium* with 22 transmembrane spans. *J. Biol. Chem.*, **275**, 11235-11240.
- Linder, J.U., Schultz, A. and Schultz, J.E. (2002) Adenylyl cyclase Rv1264 from *Mycobacterium tuberculosis* has an autoinhibitory N-terminal domain. *J. Biol. Chem.*, **277**, 15271-15276.
- Linder, J.U. and Schultz, J.E. (2003) The class III adenylyl cyclases: multi-purpose signalling modules. *Cellular Signalling*, **15**, 1081-1089.
- Little, J.W., Esmiston, S.H., Pacelli, L.Z. and Mount, D.W. (1980) Cleavage of the *Escherichia coli* *lexA* protein by the *recA* protease. *Proc. Natl. Acad. Sci. USA*, **77**, 3225-3280.
- Lowrie, D.B., Jackett, P.S. and Ratcliffe, N.A. (1975) *Mycobacterium microti* may protect itself from intracellular destruction by releasing cyclic AMP into phagosomes. *Nature*, **254**, 600-602.
- McCue, L.A., McDonough, K.A. and Lawrence, C.E. (2000) Functional classification of cNMP-binding proteins and nucleotide cyclases with implications for novel regulatory pathways in *Mycobacterium tuberculosis*. *Genome Res.*, **10**, 204-219.
- Peters, E.P., Wilderspin, A.F., Wood, S.P., Zvelebil, M.J., Sezer, O. and Danchin, A. (1991) A pyruvate-stimulated adenylate cyclase has a sequence related to the *fes/fps* oncogenes and to eukaryotic cyclases. *Mol. Microbiol.*, **5**, 1175-1181.
- Rechsteiner, M. and Rogers, S.W. (1996) PEST sequences and regulation by proteolysis. *TIBS*, **21**, 267-271.
- Reddy, S.K., Kamireddi, M., Dhanireddy, K., Young, L., Davis, A. and Reddy, P.T. (2001) Eukaryotic-like adenylyl cyclases in *Mycobacterium tuberculosis* H37Rv. *J. Biol. Chem.*, **276**, 35141-35149.
- Roelofs, J. and Van Haastert, P.J.M. (2002) Deducing the origin of soluble adenylyl cyclase, a gene lost in multiple lineages. *Molecular Biology and Evolution*, **19**, 2239-2246.

- Salomon, Y., Londos, C. and Rodbell, M. (1974) A highly sensitive adenylate cyclase assay. *Anal. Biochem.*, **58**, 541-548.
- Shenoy, A.R., Srinivasan, N. and Visweswariah, S.S. (2002) The ascent of nucleotide cyclases: conservation and evolution of a theme. *J. Biosci.*, **27**, 85-91.
- Steinlen, S. (1988) Guanylatcyclase in Präparationen olfaktorischer Cilien aus Ratte und Schwein. Diplomarbeit der Fakultät für Chemie und Pharmazie der Universität Tübingen.
- Sunahara, R.K., Dessauer, C.W. and Gilman, A.G. (1996) Complexity and diversity of mammalian adenylyl cyclases. *Annu. Rev. Pharmacol. Toxicol.*, **36**, 461-480.
- Sunahara, R.K., Dessauer, C.W., Whisnant, R.E., Kleuss, C. and Gilman, A.G. (1997) Interaction of G<sub>s</sub>α with the cytosolic domains of mammalian adenylyl cyclase. *J. Biol. Chem.*, **272**, 22265-22271.
- Sunahara, R.K., Beuve, A., Tesmer, J.J.G., Sprang, S.R., Garbers, D.L. and Gilman, A.G. (1998) Exchange of substrate and inhibitor specificities between adenylyl and guanylyl cyclases. *J. Biol. Chem.*, **273**, 16332-16338.
- Tang, W.J. and Gilman, A.G. (1995) Construction of a soluble adenylyl cyclase activated by G<sub>s</sub>α and forskolin. *Science*, **268**, 1769-1772.
- Tang, W.J. and Hurley, J.H. (1998) Catalytic mechanism and regulation of mammalian adenylyl cyclases. *Mol. Pharm.*, **54**, 231-240.
- Taussig, R. and Gilman, A.G. (1995) Mammalian membrane-bound adenylyl cyclases. *J. Biol. Chem.*, **270**, 1-4.
- Tesmer, J.J.G., Sunahara, R.K., Gilman, A.G. and Sprang, S.R. (1997) Crystal structure of the catalytic domains of adenylyl cyclase in a complex with G<sub>s</sub>α·GTPγS. *Science*, **278**, 1907-1916.
- Tesmer, J.J.G., Sunahara, R.K., Johnson, R.A., Gosselin, G., Gilman, A.G. and Sprang, S.R. (1999) Two-metal-ion catalysis in adenylyl cyclase. *Science*, **285**, 756-760.
- Tesmer, J.J.G., Dessauer, C.W., Sunahara, R.K., Murray, L.D., Johnson, R.A., Gilman, A.G. and Sprang, S.R. (2000) Molecular basis for P-site inhibition of adenylyl cyclase. *Biochemistry*, **39**, 14464-14471.
- Towbin, H., Staehelin, T. and Gordon, J. (1979) Electrophoretic transfer of proteins from polyacrylamide gels to nitrocellulose sheets: procedure and some applications. *Proc. Natl. Acad. Sci. USA*, **76**, 4350-4354.

- Tucker, C.L., Hurley, J.H., Miller, T.R. and Hurley, J.B. (1998) Two amino acid substitutions convert a guanylyl cyclase, RetGC-1, into an adenylyl cyclase. *Proc. Natl. Acad. Sci. U.S.A.*, **95**, 5993-5997.
- Weber, J.H. (2003) Klonierung und Charakterisierung einer Adenylatcyclase aus *Plasmodium falciparum*. Dissertation der Universität Tübingen.
- Whisnant, R.E., Gilman, A.G. and Dessauer, C.W. (1996) Interaction of the two cytosolic domains of mammalian adenylyl cyclase. *Proc. Natl. Acad. Sci. U.S.A.*, **93**, 6621-6625.
- Xu, R.X., Hassell, A.M., Vanderwall, D., Lambert, M.H., Holmes, W.D., Luther, M.A., Rocque, W.J., Milburn, M.V., Zhao, Y., Ke, H. and Nolte, R.T. (2000) Atomic structure of PDE4: Insights into phosphodiesterase mechanism and specificity. *Science*, **288**, 1822-1825.
- Yan, S.Z., Hahn, D., Huang, Z.H. and Tang, W.J. (1996) Two cytoplasmic domains of mammalian adenylyl cyclase form a Gs $\alpha$ - and forskolin-activated enzyme in vitro. *J. Biol. Chem.*, **271**, 10941-10945.
- Yan, S.Z., Huang, Z.H., Shaw, R.S. and Tang, W.J. (1997) The conserved asparagine and arginine are essential for catalysis of mammalian adenylyl cyclase. *J. Biol. Chem.*, **272**, 12342-12349.
- Yan, S.Z., Huang, Z.H., Andrews, R.K. and Tang, W.J. (1998) Conversion of forskolin-insensitive to forskolin-sensitive (mouse-type IX) adenylyl cyclase. *Mol. Pharmacol.*, **53**, 182-187.
- Young, D.B. (2001) A post-genomic perspective. *Nature Medicine*, **7**, 11-13.
- Zhang, G., Liu, Y., Ruoho, A.E. and Hurley, J.H. (1997) Structure of the adenylyl cyclase catalytic core. *Nature*, **386**, 247-253.
- Zhu, J. and Winans, S.C. (2001) The quorum-sensing transcriptional regulator TraR requires its cognate signaling ligand for protein folding, protease resistance, and dimerization. *Proc. Natl. Acad. Sci. USA*, **98**, 1507-1512.

Meine akademischen Lehrer neben Herrn Prof. Dr. J. E. Schultz waren die Damen und Herren:

Robinson, V.A.	Pharmakologie, Biopharmazie, Toxikologie, Diplomarbeit; Puebla, México.
Anaya, C.	Organische Chemie; Puebla, México.
Garcés, J.	Biochemie; Puebla, México.
Parra, L.	Biologie und Biophysikalische Chemie; Puebla, México.
Piquer, A.	Pharmakologie und Medikamentenanalyse; Puebla, México.
Quiroz, M.A.	Physikalische Chemie und Instrumentalanalyse; Puebla, México.
Reyna, S.	Biochemie, Mikrobiologie und Immunologie; Puebla, México.
Roth, H.	Pharmazeutische Chemie; Puebla, México.
Sánchez, E.	Chemie der natürlichen Produkte; Puebla, México.

## Lebenslauf

### Persönliche Daten

Name: Lucila Isabel Castro Pastrana

Geburtstag: 22.06.1975

Geburtsort: Puebla, Puebla, México.

### Ausbildung

1981-1991 Grundschule und Gymnasium, Puebla, México.

1991-1994 Abitur, Puebla, México.

1994-1999 Lizenziatstudium in Pharmabiochemie (Schwerpunkt Pharmazie) an der Universität de las Américas-Puebla (UDLA-P), México.

1999-2000 Laborpraktikum Betreuung bei der Chemie und Biologie Abteilung der Universität de las Américas-Puebla, México.

2000-2004 CONACYT-DAAD Stipendiatin zur Promotion an der Fakultät für Chemie und Pharmazie der Universität Tübingen. Der experimentelle Teil dieser Arbeit wurde im Zeitraum von März 2001 bis November 2003 unter der Anleitung von Prof. Dr. J. E. Schultz durchgeführt.



## Curriculum vitae

Lucila Isabel Castro Pastrana

Born on the 22<sup>nd</sup> of June, 1975, in Puebla, Puebla, México.

School: 1981-1991 in Puebla (México)

High School: 1991-1994 in Puebla (México)

University: 1994-1999 Under-graduate studies at the Department of Chemistry and Biology at the University de las Américas-Puebla (UDLA-P), México; studies in chemistry, biology and pharmacy.  
1999-2000 Laboratory assistant at the Department of Chemistry and Biology at the UDLA-P, México  
2000-2004 PhD Thesis in pharmaceutical biochemistry (CONACYT-DAAD grantee) at the University of Tübingen, Faculty of Chemistry and Pharmacy.